Title	Real-time Thermal Sensation Prediction Incorporating Individual Differences via Thermal Comfort Models and Physiological Responses
Author(s)	Biswas, Biplob Kanti
Degree Grantor	北海道大学
Degree Name	博士(工学)
Dissertation Number	甲第16624号
Issue Date	2025-09-25
DOI	https://doi.org/10.14943/doctoral.k16624
Doc URL	https://hdl.handle.net/2115/98234
Type	doctoral thesis
File Information	Biplob_Kanti_Biswas.pdf, 全文

Real-time Thermal Sensation Prediction Incorporating Individual Differences via Thermal Comfort Models and Physiological Responses

温熱快適性モデルと生理反応を用いた個人差を考慮したリアルタイム温冷感予測

by

Biplob Kanti BISWAS

ビプロブ　カンティ　ビスワス

A thesis submitted in partial fulfillment of the requirements for the Doctorate Degree of Engineering

Division of Human Environmental Systems

Graduate School of Engineering, Hokkaido University

September 2025

List of Publication

1. B.K. Biswas, K. Ishii, K. Okamoto, Y. Watanabe, J. Li, Y. Tan, A. Dempoya, S.-I. Lee, T. Iwamura, S. Konoshita, Investigating real-time thermal sensation predictions using predicted mean vote and local skin temperature analysis via infrared thermography as a nonintrusive tool, Energy and Buildings (2025) 115763.

2. B.K. Biswas, K. Ishii, Y. Watanabe, J. Li, Y. Tan, A. Dempoya, S.-I. Lee, T. Iwamura, S. Konoshita, H. Wakabayashi, Predicting individual variability in thermal sensation, PMV predictions, and local skin temperature differences using infrared thermography, Building and Environment 269 (2025) 112477.

3. B.K. Biswas, K. Ishii, Y. Watanabe, J. Li, Y. Tan, A. Dempoya, S. Takeuchi, S.-I. Lee, T. Iwamura, S. Konoshita, H. Wakabayashi, Association of thermal perceptions, metabolic rate, clothing and local skin temperature in people with cold constitution in air-conditioned office environments. Journal of Physiological Anthropology (Under review).

Table of Contents

List of Figures

List of Tables

List of Abbreviations

$A_{cov,\ 0}$	Body surface area not covered by the clothing, as a percentage of total body surface are (%)
$A_{cov,\ 1}$	Body surface area covered by the clothing, as a percentage of total body surface area (%)
A_{du}	Body surface area (m^2)
A_r/A_{DU}	Fraction of the skin surface in the radiative heat exchange
ABW	Activity-based working
AI	Artificial intelligence
ASHRAE	American society of heating, refrigerating and air-conditioning engineers
ASG	Activated sweat glands
AVAs	Arteriovenous anastomoses
BAT	Brown adipose tissue
BMI	Body mass index (kg/m^2)
BMR	Basal metabolic rate (W)
BSA	Body surface area (m^2)
BVP	Blood volume pulse
$Corr,\ I_a$	Correction factor for resultant insulation provided by the boundary air layer
CC	Cold constitution
D_{max}	The maximum operational range distance of IRT (m)
D	Diameter of the globe (m)
ECG	Electrocardiography
EDA	Electrodermal activity
EDV	Endothelium-dependent vasodilation
EE	Energy expenditure ($W{\cdot}h\ /\ O_2$)
f_{cl}	Clothing area factor
h_c	Convective heat transfer coefficient ($W/m^2{\cdot}K$)
h_r	Radiative heat transfer coefficient ($W/m^2{\cdot}K$)
H_b	Body height (cm)
HR_0	Heart rate at rest (beats/min)

HR_m	Mean heart rate (beats/min)
HR_{max}	Maximum heart rate (beats/min)
H	Height of the object (m)
H	Dry heat loss (W/m^2)
HR	Heart rate (beats/min)
HVAC	Heating, ventilation, and air conditioning
I_a	Insulation provided by the boundary air layer (m^2·K/W)
$I_{a,r}$	Resultant insulation provided by the boundary air layer (m^2·K/W)
I_{cl}	Clothing insulation (m^2·K/W)
I_{clu}	Clothing insulation for every individual garment (clo or m^2·K/W)
I_{cl}_q	Clothing insulation obtained from the questionnaire survey (clo or m^2·K/W)
$I_{cl}\_t_{cl}$	Clothing insulation obtained from clothing temperature (clo or m^2·K/W)
$I_{cl}\_t_{cl}\,(M\_{1.2})$	Clothing insulation obtained from clothing temperature and common metabolic rate for sedentary activities (clo or m^2·K/W)
$I_{cl}\_t_{cl}\,(M\_{hr})$	Clothing insulation obtained from clothing temperature and heart rate (clo or m^2·K/W)
$I_{cl}\_t_{cl}\,(M\_{bmr})$	Clothing insulation obtained from clothing temperature and basal metabolic rate and physical activity ratio (clo or m^2·K/W)
$I_{cl}\_t_{cl},\ t_{sk}$	Clothing insulation obtained from clothing temperature and skin temperature (clo or m^2·K/W)
I_T	Total clothing insulation (m^2·K/W)
$I_{T,r}$	Resultant total clothing insulation (m^2·K/W)
IR	Infrared
IRT	Infrared thermography
L	Thermal load (W)
LDF	laser doppler flowmetry
m_{clo}	Clothing mass (without shoes) (kg)
M_o	Resting metabolic rate (W)
M	Metabolic rate (MET or W/m^2)
$M\_{1.2}$	Common metabolic rate for sedentary activities (1.2 MET)
M_{bmr}	Metabolic rate obtained from basal metabolic rate and physical activity ratio (MET or W/m^2)
M_{hr}	Metabolic rate obtained from heart rate (MET or W/m^2)
ML	Machine learning
MWC	Maximum working capacity (W)

NA	Noradrenaline
NCC	Non cold constitution
NO	Nitric oxide
NST	Non-shivering thermogenesis
p_a	Water vapor pressure in ambient air (P_a)
$PMV(M\_{1.2}, I_{cl}\_q)$	Predicted mean vote calculated from common metabolic rate for sedentary activities and clothing insulation obtained from questionnaire survey
$PMV(M\_{1.2}, I_{cl}\_t_{cl})$	Predicted mean vote calculated from common metabolic rate for sedentary activities and clothing insulation obtained from clothing temperature
$PMV(M\_{1.2}, I_{cl}\_t_{cl}, t_{sk})$	Predicted mean vote calculated from common metabolic rate for sedentary activities and clothing insulation obtained from clothing temperature and skin temperature
$PMV(M\_{bmr}, I_{cl}\_q)$	Predicted mean vote calculated from basal metabolic rate and physical activity ratio and clothing insulation obtained from questionnaire survey
$PMV(M\_{bmr}, I_{cl}\_t_{cl})$	Predicted mean vote calculated from basal metabolic rate and physical activity ratio and clothing insulation obtained from clothing temperature
$PMV(M\_{bmr}, I_{cl}\_t_{cl}, t_{sk})$	Predicted mean vote calculated from basal metabolic rate and physical activity ratio and clothing insulation obtained from clothing temperature and skin temperature
$PMV(M\_{hr}, I_{cl}\_q)$	Predicted mean vote calculated from heart rate and clothing insulation obtained from questionnaire survey
$PMV(M_{hr}, I_{cl}\_t_{cl})$	Predicted mean vote calculated from heart rate and clothing insulation obtained from clothing temperature
$PMV(M\_{hr}, I_{cl}\_t_{cl}, t_{sk})$	Predicted mean vote calculated from common metabolic rate for sedentary activities and clothing insulation obtained from clothing temperature and skin temperature
PAR	Physical activity ratio
PET	physiological equivalent temperature (°C)
PMV	Predicted mean vote
PPG	Photoplethysmography
RH	Relative humidity (%)
RM	Heart rate increase per unit of metabolic rate
RMSE	Root mean square error
RQ	Respiratory quotient

SD	Standard deviation
*SET**	Standard effective temperature (°C)
SGO	Sweat output per gland
SM	Skeletal muscle
SR	Sweating rate (L/h)
SL	Satisfaction level
t_a	Air temperature (°C)
t_{arm}	Arm skin temperature (°C)
t_{calf}	Calf skin temperature (°C)
t_{cheek}	Cheek skin temperature (°C)
t_{chin}	Chin skin temperature (°C)
t_{chest}	Chest skin temperature (°C)
t_{cl}	Clothing temperature (°C)
$t_{dorsal\ finger}$	Dorsal finger skin temperature (°C)
$t_{dorsal\ hand}$	Dorsal hand skin temperature (°C)
$t_{eye\ canthus}$	Eye canthus skin temperature (°C)
$t_{forehead}$	Forehead skin temperature (°C)
t_g	Globe temperature (°C)
$t_{palmar\ finger}$	Palmar finger skin temperature (°C)
$t_{palmar\ hand}$	Palmar hand skin temperature (°C)
t_{neck}	Neck skin temperature (°C)
t_{nose}	Nose skin temperature (°C)
t_{thai}	Thai skin temperature (°C)
t_r	Mean radiant temperature (°C)
t_{sk}	Skin temperature (°C)
t_{sk_r}	Skin temperature calculated by Ramanathan proposed equation (°C)
TC	Thermal comfort
TISEM	Thermographic imaging in sports and exercise medicine
TNZ	Thermoneutral zone
TP	Thermal preference
TSV	Thermal sensation vote
UTCI	Universal thermal climate index (°C)
Vco_2	Carbon dioxide consumption rate (lO_2 / h)
Vo_2	Oxygen consumption rate (lO_2 / h)

v_a	Air velocity (m/s)
W	Rate of mechanical work (W/m^2)
W_b	Body mass (kg)
W_{bl}	Lean body mass (kg)
$WBGT$	Wet bulb globe temperature (°C)
WHO	World health organization
$\Delta t_{proximal\ -\ distal}$	Temperature differences between proximal and distal body parts (°C)
$\Delta t_{eye\ canthus\ -\ nose}$	Temperature differences between eye canthus and nose skin (°C)
$\Delta t_{eye\ canthus\ -\ palmar\ finger}$	Temperature differences between eye canthus and palmar finger skin (°C)
$\Delta t_{forehead\ -\ nose}$	Temperature differences between forehead and nose skin (°C)
$\Delta t_{forehead\ -\ palmar\ finger}$	Temperature differences between forehead and palmar finger (°C)
$\Delta t_{palmar\ hand\ -\ palmar\ finger}$	Temperature differences between palmar hand and palmar finger (°C)
$\Delta t_{dorsal\ hand\ -palmar\ finger}$	Temperature differences between dorsal hand and dorsal finger (°C)
ε	Emissivity of the globe (usually 1.00 for a black globe)
α	Horizontal viewing angles of IRT camera (°)
β	Vertical viewing angles of IRT camera (°)
x_1	Horizontal pixels of IRT camera
y_1	Vertical pixels of IRT camera
$\lvert TSV - PMV \rvert$	Absolute mean differences between thermal sensation vote and predicted mean vote

CHAPTER 1: General introduction

1.1 Human thermal comfort

According to American society of heating, refrigerating and air-conditioning engineers (ASHRAE) Standard [1], thermal comfort is defined as the condition of mind which expresses satisfaction with the adjacent thermal environment. This definition highlights the fact that comfort is not only determined by measurable environmental variables. Instead, it also relies immensely on how individuals perceive and interpret these conditions by their physiological and psychological responses [2]. These perceptions are shaped by a complex interaction of both physiological and psychological factors.

In evaluating thermal comfort, several quantifiable environmental parameters such as air temperature (t_a), relative humidity (RH), air velocity (v_a), and mean radiant temperature (t_r) are typically considered. t_a influence the sensation of warmth or coolness, RH affects the evaporation of sweat and the perception of moisture in the air, v_a is the reason behind heat loss through convection and evaporation process and t_r signifies the mean temperature of surrounding surfaces that can emit or absorb radiant heat. While these environmental variables provide an objective outline for assessing the thermal environment, though it is not sufficient enough to determine whether an individual feels thermally comfortable or not. Beyond these quantifiable factors, thermal comfort is profoundly molded by individual factors such as metabolism, clothing insulation, individual differences, acclimatization and behavioral adaptations.

Therefore, thermal comfort is most precisely understood as a dynamic interaction between the external physical environment and the internal subjective responses of individuals. It is a combination between objective conditions and subjective perception. Subsequently, thermal comfort can be defined by a multidimensional phenomenon requiring both environmental control and user-centered design strategies to ensure individual comfort [3].

1.2 Influence of the thermal comfort

In contemporary society, a large number of people spend more than one third of their day in office environments as part of their standard work routines. Given this context an extended exposure, the thermal environments of these indoor spaces play a vital role in shaping individuals' physical comfort, mental well-being, and overall work efficiency [4, 5]. Indoor climate is a crucial determinant of the occupants' overall comfort experience and their levels of satisfaction [6].

Moreover, it is remarkable that various aspects of cognitive performance such as attention, problem-solving ability, and decision-making are closely interlinked to the thermal environment. It influences not only comfort feelings, but they also influence how effectively they can perform their tasks throughout the day. When indoor condition is not suitable, individuals may experience discomfort, fatigue, or loss of focus, what can negatively affect overall productivity and intensity [7]. In contrast, when indoor thermal conditions are optimized to meet human comfort standards, it can raise alertness, efficiency, and improved outcomes. A thermally comfortable space not only supports physical ease but also enhances mental engagement, leading to better overall performance outcomes and increased individual satisfaction.

1.3 Factors associated with thermal comfort

Well-designed indoor environments that carefully consider key thermal comfort parameters such as t_a, RH, v_a and t_r can extensively enhance inhabitants' overall satisfaction, health, and well-being [8]. By retaining a balanced and stable thermal environment, these spaces can reduce discomfort level, prevent thermal stress, and uphold both psychological and physiological comfort [9]. Such balanced thermal environment not only improves the immediate experience of the space, but it also contributes to long-term advantages in terms of productivity, awareness, and engagement [10]. In addition to environmental conditions, personal factors such as metabolic rate (M) and clothing insulation (I_{cl}) play a crucial role in shaping an individual's thermal experience [3, 11]. In the well-known heat balance equation, both environmental and personal factors are taken into account to assess individual's thermal state [1]. These variables collectively determine the heat exchange between the environment and the human body, eventually influencing thermal comfort and physiological responses.

To address this issue, as maintaining indoor thermal conditions within a neutral range, many modern indoor spaces rely on centralized heating, ventilation, and air conditioning (HVAC) systems. The aim is to achieve a thermal balance where most of the occupants experience a neutral thermal sensation, neither too warm nor too cold. By achieving this thermal balance, HVAC systems aim to create an environment where most individuals experience thermal neutrality. Beyond physical comfort, maintaining optimal thermal conditions also upholds enhanced cognitive function, concentration, and overall productivity [12]. This ensures thermal regulation is a crucial component in the design and operation of indoor spaces.

1.4 Challenges in assessing thermal comfort

Thermal sensation represents an individual's perception of thermal comfort, and it is not a static parameter rather than inherently dynamic. It can vary by the course of time based on various physical or cognitive activities with the activity pattern and duration [13]. For instance, during or after physical activities, M increases and it causes raise body temperature [14]. This phenomenon changes the thermal sensation to a warmer direction. Conversely, sedentary activities or resting condition can reduce body heat generation [15], potentially can lead to a cooler thermal sensation. I_{cl} is another significant factor that directly influences the heat distribution between the human body and its surrounding environment. Due to its thermal resistance properties, clothing significantly affects the body's ability to retain or dissipate heat, thereby performing a critical role in determining individual's thermal comfort [16].

Even when individual's physical activity level and pattern remain persistent, adaptation to the thermal environments can significantly modulate their thermal sensation [17]. Additionally, seasonal variation can have an adaptive impact on thermal sensation [18]. People can gradually adjust to different thermal environments as the seasons change. Individuals may become more tolerant to heat during summer while in winter, they can be more comfortable in cooler conditions. It should be noted that thermal sensation is inherently dynamic because of adaptation and altered activities [19-21].

Furthermore, considering the above-mentioned issues, to ensure comfort for all it is essential to assess the thermal sensation in real-time. Real-time assessment provides continuous feedback on individuals' thermal perceptions, and it can serve as a fundamental parameter for making necessary adjustment to the thermal environment in order to achieve thermal comfort for all. This dynamic approach can enable the maintenance of an optimal comfort environment across diverse user preferences as well as changing environmental factors.

Another important factor that influences thermal sensation is individual differences. It is essential to acknowledge that different individuals can perceive the same thermal environment in different ways [22, 23]. Even under identical environmental conditions, people may perceive varying levels of comfort or discomfort. This deviation arises not only from environmental factors but also influenced by individual characteristics that impact thermal perception. As a result, a standardized thermal setting may not effectively meet the comfort needs of all occupants. This phenomenon is largely because of individual differences such as morphological factors like body height, weight, and body mass index (*BMI*) and also demographic aspects like age and gender. Despite the common variables, "cold constitution" is another aspect, where individuals associated with cold constitution tends to feel colder comparing with other individuals [24].

Therefore, addressing thermal adaptations, individual differences and real-time thermal assessment is essential for accurately evaluating thermal comfort.

1.5 Research objectives

Taking these aspects into account, the research was structured around three fundamental studies. The first one is to figure out a simplistic and more accurate approach to assess thermal sensation by predicted mean vote (*PMV*) model, what can be applicable in real-time. The second one is to understand the importance of addressing individual differences in thermal assessment while designing a comfortable environment for all. And the third one is to address the physiological responses in different climatic conditions and develop a model to predict real-time thermal sensation based on physiological responses.

In the first study *PMV* model was used because it is widely renowned mathematical model which considers environmental factors (t_a, RH, v_a and t_r) with individual factors (M and I_{cl}) to assess thermal sensation [8, 11]. The model's outputs are also comparable with actual Thermal sensation votes (TSV), to validate its prediction accuracy. In addition, in this study M was examined as a key parameter representing the body's internal heat generation. I_{cl} was investigated as an indicator of behavioral thermoregulation in response to environmental conditions. In the second and the third study, skin temperature (t_{sk}) were analyzed as a physiological response to the thermal environment which can be predicted by infrared camera as a non-invasive tool. It was observed that peripheral skin temperature highly influence thermal sensation and thermal comfort [25]. The skin surface functions as a sensory interface with the thermal environment, transmitting signals related to warmth or coldness to the central nervous system for thermoregulatory processing. In response to these sensations, human body regulates heat dissipation or heat retention through mechanisms like vasodilation and vasoconstriction, which modulate blood flow to the skin [26] and it effect t_{sk}. In hot conditions, increased blood flow at distal body parts elevates t_{sk} to facilitate heat dissipation, whereas in cold conditions, reduced blood flow causes lower t_{sk}, to conserve body heat. Normally t_{sk} at the distal parts changes more frequently due to environmental changes, while proximal parts t_{sk} remain mostly remain unchanged for less vasoconstriction. Several studies reported that, the proximal to distal skin temperature gradient remains a valid indicator of vasoconstriction [27] and it have strong correlation with skin blood flow [28, 29].

Considering the abovementioned physiological thermoregulation, temperature differences between proximal and distal body parts ($\Delta t_{proximal\ -\ distal}$) were also analyzed as a parameter of physiological response to the thermal environment.

The studies can be highlighted as:

Study 1: Investigating real-time thermal sensation prediction, using predicted mean vote (*PMV*).

The aim of this study was to figure out a real-time thermal sensation assessment technique. This study explores the potentiality of improving *PMV* accuracy by integrating individual factors via IRT as a non-intrusive tool. The following hypotheses were formulated:

a) The use of standardized uniform values for individual factors such as M and I_{cl} can produce significant error in the prediction of *PMV* while compared to TSV responses.

b) Individualized assessment of M and I_{cl} can significantly enhance the accuracy of *PMV* predictions in relation to TSV.

c) IRT can serve as a reliable, non-intrusive tool for precise prediction of *PMV*, thereby this *PMV* can make better correlation with actual TSV.

In this study infrared thermography (IRT) was used as a nonintrusive tool to predict t_{sk} and clothing temperature (t_{cl}) to calculate *PMV*. Additionally, several methods were used to calculate M. Finally different *PMV* predictions were compared with TSV to figure out the appropriate and reliable real-time thermal sensation prediction.

Study 2: Predicting individual variability in thermal sensations, predicted mean vote (*PMV*) and predicted percentage of dissatisfied (*PPD*) and local skin (t_{sk}) temperature differences.

The aim of this study was to investigate individual differences in morphological characteristics, thermal perceptions and thermoregulatory responses by examining local t_{sk} variations. The differences were analyzed across *BMI* differences, gender variances, and association of cold constitution, in order to understand how the factors influence thermal sensations and physiological responses. The following hypotheses were established in this study:

a) There are significant relationships among *BMI*, gender and cold constitution according to thermal perceptions and demographical characteristics.

b) There are significant differences in thermal perceptions across groups differentiated by *BMI* categories, gender and association with cold constitution.

c) Personal factors like M and I_{cl} are associated with TSV, also vary significantly with *BMI*, gender and cold constitution.

d) Physiological responses such as local t_{sk} and temperature gradient $\Delta t_{proximal\ -\ distal}$ differ significantly among groups based on *BMI*, gender and cold constitution, and are significantly associated with corresponding TSV responses.

Study 3: Assessing physiological responses to develop a real-time thermal sensation prediction model.

The aim of this study was to figure out the physiological responses in wide range of climatic conditions and their association with the thermal sensation. In this study a new predicting model to predict thermal sensation was developed based on physiological responses. This study was guided by the following hypotheses:

a) There are significant relationships between physiological responses with different environmental conditions.

b) Physiological responses and environmental conditions are significantly associated with TSV.

c) Physiological responses, such as local t_{sk} and the temperature gradient $\Delta t_{proximal\ -\ distal}$ can reliably predict TSV independently.

1.6 Significance of this research

In today's world, thermal comfort is highly significant to perform daily activities effectively. Particularly in indoor environments such as classrooms and offices which demand persistent concentration, awareness, and mental focus. Therefore, confirming a thermally comfortable environment is fundamental not only for productivity but also for overall well-being.

A major challenge in such kind of indoor settings is that occupants in that conditions typically have limited ability to modify their thermal surroundings. Unlike in more flexible environments, persons in classrooms or offices cannot always adjust their clothing, open or close windows, control shading devices, or liberally manipulate heating or cooling apparatus. While consolidated HVAC systems provide in that spaces can only ensure a general thermally comfort environment, however they often fail to address the diverse comfort demands of all inhabitants. Moreover, it was observed that maintaining uniform thermal settings for everyone can also lead to excessive and unnecessary energy consumption.

To address this issue, it is important to develop real-time thermal sensation assessment models that can consider individual differences such as morphological characteristics, gender, and activity intensity. This approach supports the use of personalized thermal comfort systems (e.g., local heating or cooling devices) that allow occupants to fine-tune their immediate thermal environment without altering the centralized HVAC settings. As a result, energy usage can be optimized centrally, and it can enhance individual comfort and assist elevated cognitive performance and well-being.

This study aims to contribute to the creation of more adaptive and user-friendly activity-based working (ABW) environments by offering insights into real-time thermal sensation assessment techniques with individual diversities. The outcomes will help the improvement of adjusting inclusive indoor thermal environments that recognize individual difference and promote thermal comfort, satisfactory well-being, and higher efficiency for all occupants.

1.7 Organization of the dissertation

The structure of this dissertation is outlined as follows:

Chapter 1: General introduction

This chapter introduces the fundamental aspects of the research work, outlining the background, identifying research questions and existing challenges, defining the research objectives and hypotheses that underpin the study.

Chapter 2: Literature review

This chapter presents a comprehensive review of the literature related to thermal comfort and thermal sensation. It covers human bodies thermoregulation process, approaches to evaluate thermal comfort and sensation, thermal comfort assessment models, discussion on current advancements in thermal comfort assessment and highlights the role of individual differences in influencing thermal perception.

Chapter 3: Investigating real-time thermal sensation prediction, using predicted mean vote (*PMV*) (Study 1)

Drawing on the first empirical study, this chapter focuses on *PMV* model, for real-time thermal sensation assessment. It evaluates the accuracy and practicality of various techniques, with particular attention to the integration of infrared thermography.

Chapter 4: Predicting individual variability in thermal sensations, predicted mean vote (*PMV*) and predicted percentage of dissatisfied (*PPD*) and local skin (t_{sk}) temperature differences (Study 2)

This chapter investigates the impact of physical, physiological and behavioural differences on thermal sensation. It also explores the interrelationships among these individual characteristics and their influence on thermal comfort responses.

Chapter 5: Assessing physiological responses to develop a real-time thermal sensation prediction model (Study 3)

This chapter investigates the physiological responses in different climatic conditions and their association with thermal sensations. It also proposes a model to assess thermal sensation in real time based on physiological responses.

Chapter 6: Summary and future perspective

The final chapter summarizes the key findings of the research, discusses the implications in practical scenarios, and outlines potential directions for future research in the domain of personalized thermal comfort assessment.

CHAPTER 2: Literature review

2.1 Thermal environment

Thermal environment encompasses a range of various environmental factors, including t_a, RH, t_r and v_a. As Parsons [13] explains, challenge for every person is to effectively interact with his or her local environmental factors to achieve thermal comfort. Human body responds to these environmental variables in a dynamic interactive way, what can lead to discomfort if the response is inappropriate. Environmental factors such as t_a, RH, t_r and v_a determine whether a person feels hot, cold, or thermally comfortable.

Among them, perhaps t_a is the most immediate and noticeable environmental factor. It refers to the temperature of the air, surrounding the body, which affects the exchange of heat between the body and the environment. It also influences thermal sensation and thermal comfort by governing the convective heat exchange between the skin and the air. When the air temperature is lower than the skin temperature, the body loses heat, when it is warmer, the body gains heat. This balance plays a significant role in the sensation of warmness or coolness, making air temperature a fundamental factor in determining thermal comfort.

RH, indicates the amount of water vapor present in the air relative to its capacity at a given temperature. It affects the body's ability to regulate heat through evaporative heat loss, in the form of sweating. When the humidity is high, or sweating is less, evaporative heat loss from the skin is limited. Conversely, low humidity can lead to excessive evaporation, causing dry skin and discomfort. Therefore, maintaining a satisfactory level of humidity is essential, particularly in hot and humid or cold and dry climates.

t_r refers to the average temperature of all surrounding surfaces. It significantly influences radiative heat exchange between the body and the environment. Even when the t_a is within a comfortable range, a hot surface can cause overheating, or a cold surface can cause the body to lose heat through radiation. t_r is essential to control in order to prevent unwanted heat gain or heat loss.

v_a represents the air movement around the body. It plays a significant role by influencing both convective and evaporative heat loss. In warm conditions, higher air movement enhances heat loss from the skin and improves sweat evaporation. In contrast, in cold conditions, higher air velocity can accelerate heat loss, which often creates discomfort. Thus, air velocity effect on thermal comfort significantly.

Combined with the metabolic heat production by human activity and clothing worn by a person, these four environmental factors form the six fundamental factors that define human thermal environments [8, 11, 13].

2.2 Thermal sensation and thermal comfort

Thermal sensation and thermal comfort are fundamental aspects of human responses to thermal stimuli, each reflecting interconnected dimensions of how individuals perceive and evaluate their thermal environment. According to Nakamura et al. [30], these responses are prompted from the adjoining thermal environment by specific thermal inputs that are processed through sensory pathways, leading to conscious awareness of comfort or discomfort. While, thermal comfort echoes a more integrative and evaluative process, thermal sensation is a more immediate and instantaneous response to the thermal stimuli.

Thermal sensation refers to the immediate and conscious perception of environmental condition, such as feeling hot, warm, neutral, cool, or cold. Berglund [31] and Gagge [32] emphasized that the thermal sensation is derived from a complex integration of sensory signals. These include direct thermal and moisture sensations through the skin surface, the internal temperature of the core body, and the physiological effort required to regulate the body heat through autonomic thermoregulation such as sweating in hot condition, shivering in cold condition and vasomotor response controlling skin blood flow in thermoneutral condition. Essentially, the human mind constantly assesses these sensory inputs to determine whether the body is in thermal equilibrium or requires thermoregulatory action to balance with the environment. De Dear and Brager [2] highlighted that perception plays a crucial role in determining thermal comfort status or levels. Two individuals exposed to the same identical thermal conditions may testify different comfort levels due to their physiological and psychological adaptation, expectations, activity level, or cultural factors.

Thermal comfort refers a subjective state in which an individual feels that the surrounding thermal environment is satisfactory or acceptable. Parsons [13] defined comfort as a desirable human condition and a comfortable environment where people would require no change. As defined by ASHRAE [1], this perception is not determined solely by the physical environment but is influenced by an sophisticated interaction of human's physical, physiological, psychological, and behavioural characteristics. For instance, factors such as t_a, t_r, v_a, and RH, interact with personal factors including M, I_{cl}, and adaptations to shape individual's overall comfort understanding.

In addition to thermal sensation and thermal comfort, researchers also employ parameters such as thermal preference (TP) and thermal dissatisfaction level (DL) to evaluate an individual's thermal experience more comprehensively. TP refers to a person's desire for a warmer, cooler, or unchanged environment, while DL estimates how far the current thermal conditions are from a person's ideal thermoneutral state. These parameters are included in guidelines in international standards such as ISO 28802 [33] and typically assessed through subjective surveys or interviews.

Furthermore, individual differences also play a significant role in thermal perceptions. Morphological characteristics such as age, gender, body size, body mass, fat, muscle mass, clothing insulation, and physical activity level can significantly influence personal experiences of thermal sensation, thermal comfort and preference under the same environmental condition [34].

To understand thermal sensation, thermal comfort and other thermal experiences requires a holistic approach that incorporates environmental conditions, morphological character, physiological responses, psychological awareness and individual variability. This comprehensive evaluation is fundamental for fabricating thermally comfortable indoor environments, especially in workplaces and public facilities.

2.3 Human thermoregulation

While thermal sensation and thermal comfort reflects how the body perceives its thermal environment, then thermoregulation refers to the physiological processes that maintain the body's core temperature stable, despite external environmental change. Thermal sensation, thermal comfort and thermoregulation are deeply interlinked, as comfort perception often arises from the body's effort to regulate temperature, while thermal sensation evokes the thermoregulation.

Human thermoregulation is the physiological process that maintains the core body temperature within a narrow, optimal range (36.5~37.5°C) [13], despite changes in environmental conditions. Fig. 2.1 shows a conceptual distribution of body temperature in cold and hot environment, where core body temperature is always maintained at same level, whereas distal body parts are more influenced by the surrounding environment and tend to become cooler in cold conditions.

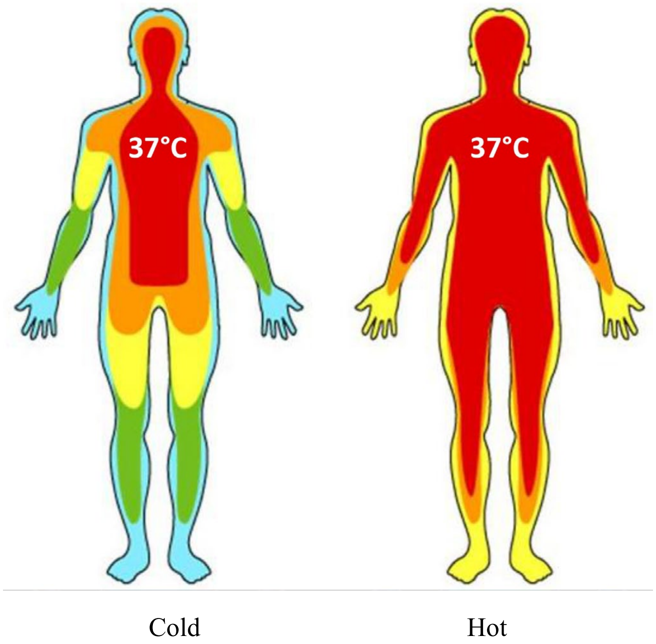

Fig. 2.1. Distribution of body temperature in cold and hot environment

This precise regulation is vital because internal body functions depend on stable internal temperatures to operate efficiently. This thermoregulation is a combination of mechanisms that detect environmental changes and initiate appropriate responses to either conserve or dissipate heat. Internal heat production which is known as metabolic heat production also plays an integral part of the thermoregulatory system. As the body performs various activities such as resting or exercising, body produce energy, and a significant portion of this energy is released as heat. This heat raises the core body temperature, and thermoregulation mechanisms respond to maintain a stable core body temperature. Fig. 2.2 shows the balance of heat production and heat loss to maintain the core body temperature.

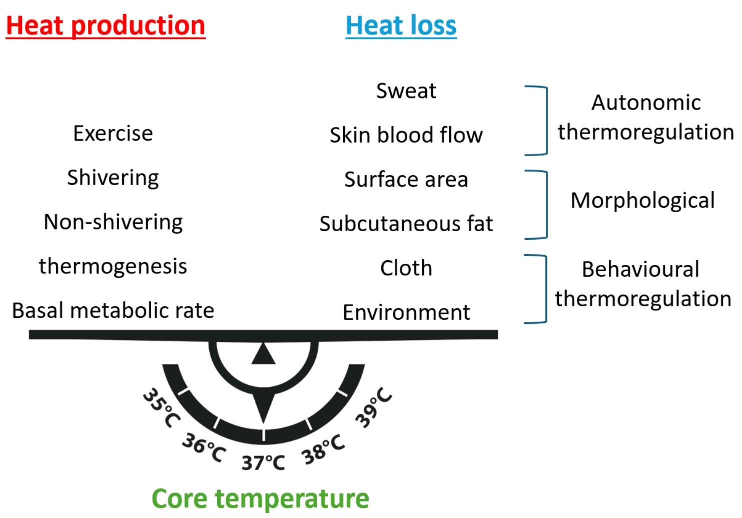

Fig. 2.2. Balance of heat production and heat loss to maintain the core body temperature.

When the condition is thermoneutral, body temperature is controlled by adjusting heat loss through changes in blood flow, which effect skin temperature. Scholars reported that skin temperature varies significantly in response to changes in environmental factors [35], and it shows a strong correlation with thermal sensation and thermal comfort [36, 37]. Fig. 2.3 shows relationship between thermoregulatory responses to the ambient temperature. In thermoneutral zone (TNZ), body regulates heat loss through mechanisms like vasodilation and vasoconstriction, which modulate blood flow to the skin surface to manage heat retention or loss [26]. In TNZ, the environmental temperature range allows the resting metabolic rate to remain at its minimum. The lower and upper limits of thermoneutral zone, the temperature are known as metabolic regulatory zone (below lower critical temperature threshold) and sudomotor regulatory zone (above upper critical temperature threshold) [38]. TNZ differs according to insulation, posture and basal metabolic rate [39].

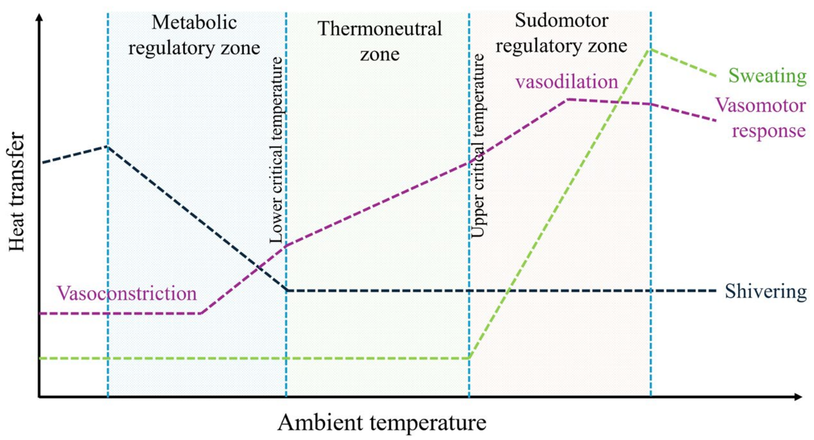

Fig. 2.3. Relationship between thermoregulatory responses to the ambient temperature. (Modified from Taylor et al., 2008 [40])

In human thermoregulation, blood flow is a fundamental element, playing a critical role in maintaining core temperature by facilitating heat exchange between the body's core and the environment. Beyond meeting the metabolic demands of cutaneous tissues, blood flow also helps to regulate heat transfer from the body's core to the periphery. Under resting conditions in TNZ, skin blood flow averages approximately 350 mL/min, accounting for about 5–10% of the cardiac output (volume of total blood circulation in a minute). Because blood has a high volume-specific heat capacity (3.85 kJ/L·°C) and a typical 4°C temperature gradient exists between the body core and skin in thermoneutral conditions, metabolic heat is continuously transported to the skin for dissipation [40]. Indeed, during rest within the thermoneutral zone, core body thermal homeostasis can be maintained solely through adjustments in skin blood flow.

Changes in skin blood flow are the body's first act in thermoregulation, particularly in conserving heat. Exposure to cold triggers cutaneous vasoconstriction (narrowing of vessels), reducing blood flow to the skin and subsequently lowering skin temperature. This action decreases the temperature gradient between the skin and the environment, thereby reducing heat loss. In hot conditions, changes in skin blood flow are the body's first response to promote heat loss. Heat exposure triggers cutaneous vasodilation (widening of vessels), increasing blood flow to the skin and raising skin temperature. This widens the temperature gradient between the skin and the environment, allowing more heat to escape.

In acral (non-hairy, ventral) skin regions including the nose, ears, lips, palms, and soles, blood flow is modulated primarily through adrenergic vasoconstrictor fibers. Under thermoneutral conditions, sympathetic constrictor tone is strong, resulting in very low blood flow to these areas. Upon body cooling, vasoconstriction in these regions becomes nearly maximal, while heating reduces sympathetic tone, leading to passive vasodilation [41] and an increase in blood flow.

In non-acral (hairy, dorsal) skin areas are regulated by two sympathetic pathways: an adrenergic vasoconstrictor system and a separate active vasodilator system. While the vasoconstrictor pathway is present throughout the skin, 80–90% of the increase in skin blood flow during heat stress is mediated by active vasodilation [40].

Cutaneous vascular system regulates the blood vessel diameter, to manage blood flow and heat dissipation. It is controlled by the vasomotor centre, which sends sympathetic signals to vascular smooth muscle for vasoconstriction or vasodilation based on environmental condition. Vasoconstriction is triggered by sympathetic stimulation and helps conserve heat by reducing skin blood flow. Vasodilation occurs through reduced sympathetic vasoconstrictor activity for enhancing skin blood flow to release heat [42].

Anatomically, the cutaneous vascular system consists of two key components capillaries and arteriovenous anastomoses (AVAs). Fig. 2.4 shows a schematic drawing of cutaneous vascular system at finger area. Compared to ordinal capillaries, AVAs allow a significantly greater volume of blood flow and play a more prominent role in thermoregulation. AVAs is typically located acral skin at distal body parts such as finger, toe and nose. AVAs have greater sensitivity to the sympathetic nervous system [43] and have direct connections between small arteries and veins, bypassing the capillary bed [44]. The length of AVAs is typically from 200 to 500 μm, inner diameter from 10 to 150 μm, and the thickness of the wall from 40 to 60 μm, with an inner layer of smooth muscle cells which enables them to close the vessels completely in cold conditions [45]. When the ambient temperature is at the lower edge of the thermoneutral zone, all AVAs remained closed [45]. This leads to a reduction in blood flow to the skin in distal regions of the body, resulting in lower skin temperatures in those areas especially at finger, toe and nose. While proximal body temperatures where AVAs are absent, such as forehead temperature remain relatively constant within the thermoneutral zone. Only distal body parts temperatures exhibit greater variability in response to ambient conditions [46, 47], especially areas with high AVAs. It was observed that the temperature difference between proximal and distal body regions increases as the ambient temperature decreases within the thermoneutral zone [38]. Researchers have also identified the temperature gradient between proximal and distal body regions as an key indicator of peripheral vasoconstriction [27, 28]. In the field of thermal physiology laser doppler flowmetry (LDF) is considered the standard for directly measuring microvascular skin blood flow. It is limited by its requirement for expensive special device and sensor contact with the skin. For this reason, researchers have tested whether proximal-distal skin temperature gradients can serve as a surrogate indicator of skin blood flow and peripheral vasomotor activity. House and Tipton analysed [28], forearm to finger skin temperature gradient as a surrogate measure of vasomotor control during cold exposure, in comparison with skin blood flow measured using LDF. Mekjavic et al. reported temperature gradient between eye canthus and fingertip can reflect vasomotor activity [27, 48]. Krauchi et al. also found that a gradual decrease in proximal-distal temperature gradient was observed before sleep onset, which may serve as an indicator of heat loss response prior to sleep [29].

Fig. 2.5 shows a conceptual local skin temperature variations in different ambient temperature. It was observed that the local skin temperature of proximal body parts, such as the forehead, remains relatively stable, whereas the skin temperature of distal body parts, such as the feet and fingers, drops in cold conditions due to vasoconstriction [46].

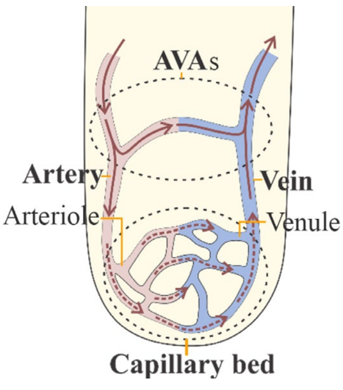

Fig. 2.4. Schematic drawing of cutaneous vascular system at finger. (Modified from Zhang, 2021 [49])

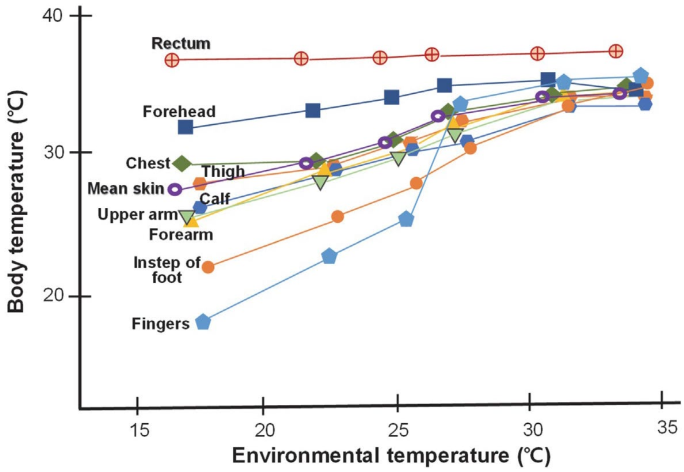

Fig. 2.5. Local skin temperature variations in different ambient temperature. (Modified from Fukazawa, 2012 [46])

In cold conditions, vasoconstriction and reduced blood flow to the skin lead to a decrease in skin temperature. It reduces the temperature difference between the skin and the environment, helping the body to limit heat loss. Further, when the ambient temperature drops below the low critical temperature threshold, the body initiates heat production through non-shivering thermogenesis (NST) [50]. When cold-induced thermogenesis occurs, it defined as NST threshold. This process involves increased heat production in tissues like brown adipose tissue (BAT), skeletal muscle (SM) and internal organs [51]. When the condition gets more cold, shivering thermogenesis is generated in the SM to produce additional heat and preserve a stable core temperature [52]. This process involves involuntary rhythmic contractions of SM, which generate heat through increased metabolic activity in the muscle tissue. The threshold at which shivering begins known as shivering threshold.

Conversely, when ambient temperature rises, vasodilation and increased blood flow to the skin elevate skin temperature to promote heat loss. Cutaneous vascular system including blood vessels and AVAs at some limited areas plays a crucial role in regulating heat loss. In more hotter condition once the body's temperature research the threshold of sweating, body begins to sweat to promote rapid heat loss through evaporative cooling [13]. Sweating decreases the skin temperature by evaporating perspiration from the skin surface once it reaches the heat of vaporization [38].

In addition, several morphological characteristics also influence on regulating heat exchange between the body and the environment. For example, body mass is positively associated with heat production, as individuals with greater body mass generally exhibit higher resting metabolic rates and greater internal heat generation. A large body surface area promotes greater heat loss, as more surface is exposed to the environment, increasing the potential for heat exchange through radiation, convection, and evaporation. In a consequence surface area to volume ratio influences heat exchange. When an individual has a relatively large surface area to volume ratio (SA/volume), heat loss is quicker to the surrounding environment, which is beneficial in hot condition. In animal studies, Bergmann reported that, animals in colder climates tend to have larger body mass causing reduced SA/volume, resulting minimized heat loss per unit heat production [53]. Similarly, Allen observed that, animals in colder regions tend to have shorter limbs, which have a higher SA/volume than the trunk [54]. Shorter limbs reduce convective and radiative heat loss per unit mass, and therefore advantageous for surviving in colder climates. In case of humans, body insulation such as subcutaneous fat layer and clothing insulations slow down the heat exchange with the thermal environment. Furthermore, skin thickness, surface colour, and skin water vapor permeability also impact on the heat exchange.

2.4 Approaches to evaluate thermal comfort

In present thermal comfort assessment, two fundamental approaches are widely used to evaluate thermal comfort: the rational (or heat balance) approach and the adaptive approach. Each method is grounded based on different types of data and theoretical frameworks.

2.4.1 Rational or heat balance approach

The rational approach is based on maintaining thermal equilibrium between the heat produced by the human body and the heat loss to the environment. The process can be explained as heat balance equation, as follows,

$$M - W = q_{sk} + q_{res} + S$$
$$= (K + C + R + E_{sk}) + (C_{res} + E_{res}) + (S_{sk} + S_{cr}) \quad [1] \qquad \text{(Equation 2.1)}$$

Where,

M is rate of metabolic heat production [W/m²]

W is rate of mechanical work accomplished [W/m²]

q_{sk} is total rate of heat loss from skin [W/m²]

q_{res} is total rate of heat loss through respiration [W/m²]

K is conductive heat loss from the skin [W/m²]

C is convective heat loss from the skin [W/m²]

R is radiative heat loss from the skin [W/m²]

E_{sk} is total rate of evaporative heat loss from skin [W/m²]

C_{res} is rate of convective heat loss from respiration [W/m²]

E_{res} is rate of evaporative heat loss from respiration [W/m²]

S_{sk} is rate of heat storage in skin component [W/m²]

S_{cr} is rate of heat storage in core component [W/m²]

When the S or (S_{sk} + S_{cr}) is "0", it can be said that heat production and heat loss is balanced. In hot environments, individuals need to lose excess body heat to maintain comfort, while in cold environments, retaining body heat becomes essential to achieve comfort. Heat balance equation states that, for a person to be thermally comfortable, heat production (metabolism + external work) must equal heat loss (via convection, radiation, evaporation, etc.), as a result the heat retained by the body should be zero.

2.4.2 Adaptive thermal comfort approach

Adaptive approach recognizes occupants are not passive recipients of environmental stimuli but actively interact with it and can adapt as per their necessity. It is based on the adaptive principle, which posits that when discomfort arises due to environmental changes, people react in ways that aim to restore their comfort [34]. It is a continuous process shaped by existing environmental conditions, past experiences, and the occupant's prospects. This approach assumes that individuals actively respond to changes in their thermal environment by adjusting personal factors and physiological responses to the surrounding to restore thermal comfort. Significantly, when occupants have the adaptive opportunities to make such adjustments, it considerably enhances their overall satisfaction. Adaptive models acknowledge that thermal comfort is influenced by a wide range of variables [2, 34, 55] and this model can be classified into three major categories as behavioral adaptation, psychological adaptation and physiological adaptation.

2.4.2.1 Behavioral adaptation

Behavioral adaptation, the most significant visible adaptation, involves physical actions taken to adjust thermal stability. It includes a wide range of conscious and unconscious actions occupants implement to maintain thermal comfort. When the heat exchange between the human body and the surrounding thermal environment becomes out of proportion, occupants act to restore comfort by adjusting clothing, using heating or cooling devices, or consuming hot or cold beverages. These actions are influenced by both indoor conditions and outdoor climatic variables [56-58]. These behaviours fall into three subcategories [59], personal adjustments (e.g., removing or adding a layer or multiple of clothing, drinking hot or cold beverages), technological responses (e.g., turning on a fan or air conditioner or heater or cooler) and cultural practices (e.g., taking a siesta during hot summer day).

2.4.2.2 Psychological adaptation

Psychological adaptation mentions how cognitive and cultural factors, such as expectations and habituations shape the thermal perceptions [60-62]. Psychological adaptation is less visible and difficult to measure its impact directly compared to the other types. Psychological adaptation comprises of naturalness, expectations, experience (short-term and long-term), time of exposure, perceived control and environmental stimulation, as it is hard to quantify these effects on thermal comfort [63]. Cumulative result of past thermal experiences play a benchmark for future comfort valuations. Experience is linked to memory and appears to influence changes in people's thermal expectations from one day to the next.

In addition, psychologically occupants may experience less discomfort from an undesirable external stimulus in a given thermal environment if they perceive they have some degree of control over it [64]. Considering the concept, Liu et al. mentioned some significant positive correlations among occupants perception of controlling environment with their thermal comfort and satisfaction [65]. Tochihara et al. found linguistic heat acclimatization among populations from different climatic zones reflects psychological adaptation, where repeated exposure to heat alters thermal perception and the use of thermal sensation terminology for expressing thermal comfort [66]. This indicates a cognitive shift in comfort expectations, shaped by environmental, cultural, and experiential factors.

2.4.2.3 Physiological adaptation

Physiological adaptation like acclimatization or acclimation, what expresses human adaptation on a particular environment for a long time or repeated short time, enables individual to perform better and reduce stress [44]. Repeated exposer to heat or cold, whether natural environment or controlled environment enhance humans' ability to tolerate heat or cold stress more. Through such adaptations, physiological responses including skin temperature, skin blood flow, heart rate, shivering, sweating, can be modulated to better cope with thermal challenges [67]. To preserve thermal comfort, human body engrosses a range of physiological adaptation mechanisms, all aims at balancing internal heat production with heat exchange between human and environment. For example, some laboratory study reported habituation by repeated cold exposure, enhance BAT activity and non-shivering thermogenesis (NST) to produce more heat [68]. Shor-term heat acclimations include reductions in core body temperature thresholds for initiating heat loss response, such as increased sweat rate and improved vasodilation [69, 70]. On the other hand, long-term heat acclimatized individuals such as populations living in tropical region have been shown to have elevated resting core temperature, lower sweat rate with higher sweat glands density and better heat tolerance to maintain lower core temperature during heat exposure [71]. It was observed that heat-acclimatized individuals tend to have a higher core body temperature and lower distal body temperature at rest. This creates a larger temperature gradient between the core and distal regions, which facilitates more heat transfer via blood circulation from core to skin and more efficient heat dissipation during heat exposure even with the lower sweat rate [72, 73].

Therefore, physiological adaptation involves changes in response to thermal stimuli based on prior encounters. Repeated exposure to specific thermal environments can lead to physiological adaptation characterized by reduced thermal sensitivity and a recalibration of thermoregulatory set points.

2.5 Thermal comfort assessment models

Numerous indices have been developed throughout the years [74] . Among them some of the indices are well recognised by the international standards like ASHRAE or ISO. Some of them are well recognized in the application sectors, though all of them have decent advantages to usage with some limitations. Among them wet bulb globe temperature (*WBGT*), UTCI universal thermal climate index (*UTCI*), standard effective temperature (*SET**), predicted mean vote and predicted percentage of dissatisfied (*PMV-PPD*) and physiological equivalent temperature (*PET*) are well known for their diversified benefits [75]. Out of these models, the *PMV-PPD* model is the most commonly used mathematical model to predict thermal sensation and thermal comfort for large group of people.

2.5.1 Predicted mean vote and predicted percentage of dissatisfied (*PMV-PPD*)

PMV-PPD model was developed by Fanger [3], estimates the average thermal sensation of a large group of individuals exposed to a particular environmental. It is grounded in the principle of human heat balance, where thermal comfort is achieved when the internal heat production of the body is in an equilibrium condition with the heat exchange between the body and the surrounding environment. *PMV* scale ranges from -3 through 0 to +3, indicating cold (-3), cool (-2), slightly cool (-1), neutral (0), slightly warm (+1), warm (+2) and hot (+3).

When the comfort equation is satisfied, *PMV* will be 0, for a large group of people. Franger [3] assumed that thermal sensation at a given activity level is a function of thermal load (L). L is the difference between internal heat production and the heat loss to the actual environment. In comfort condition L will be zero (L = S = 0), then body is neither storing nor losing excess heat, and thermal neutrality is expected.

PMV predicts the level of thermal sensation by considering combinations of environmental variables (t_a, t_r, v_a, and RH), and personal factors (I_{cl} and M) [1, 3, 8, 11]. Alongside *PMV*, Fanger introduced the *PPD*, which estimates the proportion of occupants likely to feel thermally uncomfortable under specific conditions. *PMV* can be calculated by the following equation,

$$PMV = \{0.303 \times \exp(-0.036 \times M) + 0.028\} \times L \qquad \text{(Equation 2.2)}$$

Here, $L = M - W - E_d - E_{sw} - E_{res} - C_{res} - R - C$ (Equation 2.3)

$$\begin{aligned} PMV = {} & [0.303 \times \exp(-0.036 \times M) + 0.028] \times \{(M - W) \\ & - 3.05 \times 10^{-3} \times [5733 - 6.99 \times (M - W) - p_a] \\ & - 0.42 \times [(M - W) - 58.15] \\ & - 1.7 \times 10^{-5} \times M \times (5867 - p_a) \\ & - 0.0014 \times M \times (34 - t_a) \\ & - 3.96 \times 10^{-8} \times f_{cl} \times [(t_{cl} + 273)^4 - (t_r + 273)^4] \\ & - f_{cl} \times h_c \times (t_{cl} - t_a) \end{aligned} \qquad \text{(Equation 2.4)}$$

Here,

$[3.05 \times 10^{-3} \times [5733 - 6.99 \times (M - W) - p_a]]$, represents evaporative heat loss by diffusion, E_d

$[0.42 \times [(M - W) - 58.15]]$, represents evaporative heat loss by sweating, E_{sw}

$[1.7 \times 10^{-5} \times M \times (5867 - p_a)]$, represents evaporative heat loss by respiration, E_{res}

$[0.0014 \times M \times (34 - t_a)]$, represents convective heat loss by respiration, C_{res}

$[3.96 \times 10^{-8} \times f_{cl} \times [(t_{cl} + 273)^4 - (t_r + 273)^4]]$, represents radiative heat loss, R

$[f_{cl} \times h_c \times (t_{cl} - t_a)]$, represents convective heat loss, C

Where,

M is the metabolic rate of the human body [W/m^2],

W is the rate of mechanical work [W/m^2],

t_a is the air temperature [°C],

t_r is the mean radiant temperature [°C],

f_{cl} is the clothing area factor,

t_{cl} is the mean temperature of the outer surface of the clothed body [°C],

h_c is the convective heat transfer coefficient [W/(m^2·K)], and

p_a is the water vapor pressure in ambient air [P_a].

And *PPD* can be calculated as a function of PMV using the following equation,

$$PPD = 100\text{-}95 \times \exp(-0.03353 \times PMV^4 - 0.2179 \times PMV^2)\ [\%] \qquad \text{(Equation 2.5)}$$

Although the *PMV-PPD* model is the most widely used method for assessing thermal sensation, its accuracy is highly sensitive to the precision of input data, as its outcomes depend directly on the exact values provided. Especially M and I_{cl} estimation is crucial, because they vary by individual to individual, whereas environmental factors are mostly same for every individual in a particular moment in a given condition. Misinterpretation can occur when input variables are incomplete, which can result in inaccurate predictions [76].

Fig 2.6 represents the relation of *PMV* and *PPD*. While the *PMV* is in a range between -0.5 to 0.5, *PPD* shows less than 10% population is thermally dissatisfied. According to Fanger [3], ASHRAE [1] and ISO [11], this range was considered as a thermally acceptable comfort zone.

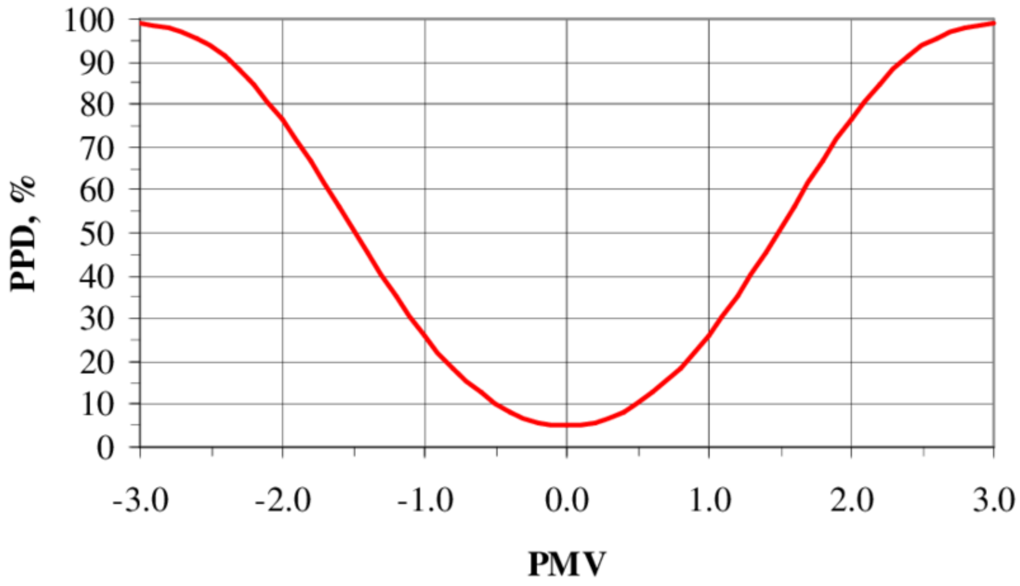

Fig. 2.6. Predicted percentage of dissatisfied *(PPD)* as function of predicted mean vote *(PMV)* [1].

2.5.1.1 Estimating clothing insulation (I_{cl})

There are several methods, what can be used to estimate clothing insulation. According to ISO [77]. Most popular methods are listed below.

2.5.1.1.1 Traditional clothing insulation estimation in static condition

Traditionally clothing insulation is estimated from questionnaire survey or personal enquiry, where participants' total clothing insulation is estimated based on individual unit garment using the following formula.

$$I_{cl} = 0.161 + 0.835\Sigma I_{clu} \ [\mathrm{m^2{\cdot}K/W}], \qquad \text{(Equation 2.6)}$$

Here, I_{clu} is the effective thermal insulation of the individual garments making up the ensemble. Table 2.1 shows some regular clothing and clothing insulation in clo (1 clo = 0.155 $m^2{\cdot}K/W$).

Table 2.1. Regular clothing and clothing insulation.

Individual Clothing Item	I_{cl} [clo]	Individual Clothing Item	I_{cl} [clo]	Individual Clothing Item	I_{cl} [clo]
Underwear		Shirts		Pants	
Bra	0.01	Blouse	0.13	Shorts	0.06
Briefs	0.04	Short-sleeve shirt	0.19	Thin long pants	0.15
T-shirt	0.08	Long-sleeve shirt	0.25	Thick long pants	0.24
Socks	I_{cl} [clo]	Suits etc.	I_{cl} [clo]	Skirts & others	I_{cl} [clo]
Ankle socks	0.02	Thin jacket	0.36	Thin skirt	0.14
Sneakers	0.02	Thick jacket	0.44	Thick skirt	0.23
Stockings	0.02	V-neck Cardigan	0.23	Long-sleeve shirt dress	0.32

From the recommendation of ISO 9920, the most common individual garment I_{clu} can be found (Annex B, Table B). The I_{clu} values are based on the list obtained by the previous measurements using standing thermal manikin.

However, these values are related to the thickness of the cloth, and in reality, the thickness is greatly varied even across the same clothing brands. This method shows the limitation of considering the air layer insulation between clothing layers [77].

2.5.1.1.2 Clothing insulation estimation from clothing mass and covering the body surface in static condition

It is also recommended by ISO to determine the clothing insulation of an ensemble using the following empirically determined relationship based on clothing weight and body covering percentage.

$$I_{cl} = 0.919 + 0.255 \times m_{clo} - 0.00874 \times A_{cov,\,0} - 0.00510 \times A_{cov,\,1} \quad [\mathrm{m^2 \cdot K/W}], \qquad \text{(Equation 2.7)}$$

Here,

m_{clo} is clothing mass (without shoes) [kg],

$A_{cov,\,0}$ is body surface area not covered by the clothing, as a percentage of total body surface are, and

$A_{cov,\,1}$ is body surface area covered by the clothing, as a percentage of total body surface are.

Though in practical scenarios, it’s very difficult to measure $A_{cov,\,0}$ and $A_{cov,\,1}$ accurately.

2.5.1.1.3 Clothing insulation estimation from clothing temperature, metabolic rate and environmental conditions in static condition

According to ISO 9920 [77], clothing insulation can be measured from clothing temperature, M, clothing area factor and environmental conditions by the following equation ,

$I_{cl} = (35.7-0.028\times(M-W)-t_{cl})/\{3.98\times10^{-8}\times f_{cl}\times[(t_{cl}+273)^4-(t_r+273)^4]+f_c\times h_c\times(t_{cl}-t_a)\}$ [m^2·K/W],

(Equation 2.8)

Here $f_{cl} = A_{cl} / A_{du}$ (Equation 2.9)

$A_{du} = 0.007184 \times W_b^{0.425} \times H_b^{0.725}$ [m^2], (Equation 2.10)

$h_c = 2.38\times |t_{sk} - t_a|^{0.25}$ or $3.5 + 5.2\ v_a$ or $8.7 \times v_a^{0.6}$ (greatest value among these three), (Equation 2.11)

Where,
A_{cl} is outer surface area of a clothed person [m^2],
A_{du} is nude body surface area calculated by DuBois method [m^2],
t_{sk} is mean temperature [°C],
t_{cl} is clothing temperature [°C],
v_a is air velocity [m/s],
W_b is the body mass [kg], and
H_b is the body height [cm]

This formula estimates clothing insulation as the thermal resistance between skin and the environment, by using the temperature gradient between skin temperature and clothing surface temperature and the rate of heat transfer from the clothing to the air and surroundings. In addition, f_{cl} quantifies how much extra surface area is created by clothing, comparing nude body surface area, which in turn effects on heat transfer. However, estimating f_{cl} is challenging in real time. In addition, increase of heat exchange surface area due to clothing also includes the insulating effect of the air trapped between the clothing and the skin, which is difficult to quantify precisely.

2.5.1.1.4 Clothing insulation estimation from skin temperature and clothing temperature in static condition

Clothing insulation can be measured from skin temperature and clothing temperature by the following equation,

$I_{cl} = (t_{sk} - t_{cl})/H$ [m^2·K/W], (Equation 2.12)

Here, $H = (t_{cl} - t_o)/(h_c + h_r)$, (Equation 2.13)

$t_o = (h_r \times t_r + h_c \times t_a)/(h_c + h_r)$ [°C], (Equation 2.14)

$h_r = 5.67 \times 10^{-8} \times \varepsilon \times (A_r / A_{du}) \times [\{(t_{cl} + 273)^4 - (t_r + 273)^4\} / (t_{cl} - t_r)]$, (Equation 2.15)

where,

t_o is the operative temperature [°C],

H is the dry heat loss from skin to the atmosphere [W/m^2], and

h_r is the radiative heat transfer coefficient [W/(m^2·K)].

And A_r / A_{du} is the fraction of the skin surface in the radiative heat exchange based on human posture [77].

This model also estimates clothing insulation as the thermal resistance between skin and the environment, by using the temperature gradient between skin temperature and clothing surface temperature and the rate of dry heat loss through convection and radiation. It doesn't consider the evaporative heat loss and it requires direct input of mean skin temperature under the cloth surface and the cloth surface temperature.

2.5.1.1.5 Clothing insulation estimation in dynamic condition

The physical activity and air velocity, modify the insulation characteristics of clothing and its adjacent air layer. Both wind and body movement reduce the insulation. The corrected clothing insulation can be estimated by the followings,

For a clothed person in normal clothing,

$I_{T,r} = I_T \times Corr, I_T$

$= I_T \times \exp[-0.281 \times (v_{ar} - 0.15) + 0.44 \times (v_{ar} - 0.15)^2 - 0.492 \times v_w + 0.176 \times v_w^2]$ [m^2·K/W]

(Equation 2.16)

Here, $v_{ar} = v_a + v_w$ [m/s] (Equation 2.17)

Where,

$I_{T,r}$ is the resultant total clothing insulation [W/(m^2·K)],

I_T is the total clothing insulation [W/(m^2·K)],

$Corr, I_T$ is the correction factor for total clothing insulation,

v_{ar} is the air velocity relative to the person [m/s],

v_w is the walking speed [m/s],

For a nude person in normal clothing,

$I_{a,r} = I_a \times Corr, I_a$

$= I_a \times \exp [-0.533 \times (v_{ar} -0.15) + 0.069 \times (v_{ar} -0.15)^2 - 0.462 \times v_w + 0.201 \times v_w^2]$ [m^2·K/W]

(Equation 2.18)

Where,

$I_{a,r}$ is the resultant insulation provided by the boundary air layer [W/(m^2·K)],

I_a is the insulation provided by the boundary air layer [W/(m^2·K)],

Corr, I_a is the correction factor for resultant insulation provided by the boundary air layer.

And the resultant dynamic clothing insulation is determined by,

$I_{cl,r} = I_{T,r} - (I_{a,r} / f_{cl})$ [m^2·K/W] (Equation 2.19)

This estimation of clothing insulation is more complex and it's better to use in a dynamic environment while the individual is active with some movement.

Considering the various approaches available for predicting I_{cl}, measuring the clothing weight and covered-uncovered body surface in regular working environment is impractical. Last estimation process is mostly focused on dynamic environment. Considering all, in a static condition, mostly for sedentary activities and real time measurement in mind, clothing insulations can be measured by the remaining three methods, traditional clothing insulation estimation, estimation from clothing temperature, metabolic rate and environmental conditions and estimation from skin temperature and clothing temperature.

2.5.1.2 Estimating metabolic rate (*M*)

Metabolic heat production is the key factor associated with heat transfer and thermal comfort. There are several methods to estimate *M*. According to ISO 8996 [15], there are four levels of the metabolic rate assessment, by screening, observation, analysis and expertise, as follows. Additionally some researchers estimated metabolic rate from basal metabolic rate considering physical characteristics [78].

2.5.1.2.1 Estimation by activities

Metabolic heat production can be classified according to the activity. However, it can be considered as a rough estimation and have error prediction. In this estimation metabolic rate is classified into five categories, resting, low, moderate, high and very high. The metabolic rate can be collected from ISO 8996 [15]. There are five categories of metabolic rate according to ISO 8996. Table 2.2 shows classification of metabolic rate by categories.

Table 2.2. Classification of metabolic rate by category.

Class	Range of metabolic rates	Examples
resting	100 ~ 125 W	Resting, sitting at ease
low metabolic rate	125 ~ 235 W	Sedentary activities, standing light activities, hand and arm work, light arm and leg work, machining work with low power tools, casual walking (2 km/h)
moderate metabolic rate	235 ~ 360 W	Sustained hand and arm work, arm and leg work, arm and trunk work, welding, hoeing, picking fruits and vegetables, pushing or pulling lightweight carts, bricklaying, intermittent handling of moderately heavy material, walking (2.5 ~ 5 km/h)
high metabolic rate	360 ~ 465 W	Intense arm and trunk work with hand tools or machines, carrying heavy material, shovelling, pushing or pulling heavy loaded hand carts, chipping casting, concrete block laying, sledgehammer work, walking (5.5~ 7 km/h)
very high metabolic rate	above 465 W	Intense activity at fast to maximum pace, running, working with an axe, walking (above 7 km/ h)

2.5.1.2.2 Estimation by observation

ISO 8996 [15] gives several equations for different kind of activities.

For metabolic rate at rest for a seated subject can be roughly estimated using the following equation,

$M_0 = 60 \times A_{du}$ (male) or $55 \times A_{du}$ (female) [W] (Equation 2.20)

Where,

M_0 is the resting metabolic rate [W]

For metabolic rate for activities with displacements,

For walking at velocities,

< 6km/h, $M = (0.5 + 0.37 \times v_w + 0.2\times v_w \times G) \times (w_b \times L)$ [W], (Equation 2.21)

For running at velocities,

≥ 6km/h, $M = (0.5 + 0.75 \times v_w + 0.1\times v_w \times G) \times (w_b \times L)$ [W], (Equation 2.22)

Where,

L is the load carried by the person [kg], and

G is ground slope [%].

For going up stairs,

$M = (0.42 + 0.61 \times v_v) \times (w_b \times L) = (0.42 + N_{steps}/10) \times (w_b \times L)$ [W] (Equation 2.23)

For going downstairs,

$M = (0.42 + 0.21 \times v_v) \times (w_b \times L) = (0.42 + N_{steps}/28) \times (w_b \times L)$ [W] (Equation 2.24)

For going up ladders,

$M = (2.78 + 1.04 \times v_v) \times (w_b \times L) = (2.78 + N_{rungs}/4) \times (w_b \times L)$ [W] (Equation 2.25)

For going down ladders,

$M = (1.98 + 0.17 \times v_v) \times (w_b \times L) = (1.98 + N_{rungs}/23) \times (w_b \times L)$ [W] (Equation 2.26)

Where,

V_v is the vertical speed [m/min],

N_{steps} is the number of steps of stairs of height = 17 cm per min (1 m/min = 5.88 steps/min),

N_{rungs} is the number of rungs of ladders of height = 25 cm per min (1 m/min = 4 rungs/min),

For metabolic rate for activities without displacements,

ISO 8996 [15] provides some standard metabolic rates while lifting or lowering loads, seated subject as a function of work intensity and body segments involved and also according to body postures.

2.5.1.2.3 Estimation from heart rate

In the case of pure dynamic work using major muscle groups, with no static, muscular, thermal and mental loads, metabolic rate can be estimated by heat rate (HR), while working. In that case HR shows a linear relationship with *M*. Since *M* is the rate of energy expenditure in the human body, HR can be used as a physiological indicator of oxygen consumption for estimating the metabolic rate during physical activity, especially under steady-state conditions.

From the heart rate *M* can be estimated by the following,

$M = M_0 + (HR_m - HR_0)/RM$ [W], (Equation 2.27)

$RM = (HR_{max} - HR_o)/(MWC - M_o)$, (Equation 2.28)

$HR_{max} = 208 - 0.7 \times Age$ [beats/min], (Equation 2.29)

$MWC = (19.45 - 0.133 \times Age) \times W_{bl}$ (male) or $(17.51 - 0.150 \times Age) \times W_{bl}$ (female) [W], (Equation 2.30)

$W_{bl} = (1.08 - W_b/(80 \times H_b^2)) \times W_b$ (male) or $(0.86 - W_b/(107.5 \times H_b^2)) \times W_b$ (male) [kg], (Equation 2.31)

Where,

HR_m is the mean heart rate during the activity for assessing the M [beats/min],

HR_0 is the heart rate at rest [beats/min],

HR_{max} is the maximum heart rate [beats/min],

MWC is the maximum working capacity [W],

W_{bl} is the lean body mass [kg], and

RM is the heart rate increase per unit of metabolic rate.

This equation demonstrates that metabolic rate can be estimated by adding resting metabolism to the heart rate increase during activity, scaled by the heart rate-metabolism relationship. Here, in HR_0 measurement, the subject should be at rest in a neutral environment for at least 5 minutes.

2.5.1.2.4 Estimation from oxygen consumption rate

Since very small amount of oxygen can be stored in the human body, it is continuously taken up from the atmosphere by respiration. Muscle can work for a short time without being directly provided with oxygen (anaerobic work) but for longer periods of work oxidative metabolism is the major energy source.

To predict *M*, oxygen consumption and carbon dioxide production are measured from expired gas by analysing the volume of air exhaled and the concentrations of O_2 and CO_2 in that air. These values are used to calculate energy expenditure (EE) through indirect calorimetry. The respiratory quotient (*RQ*), defined as Vco_2 / Vo_2, is essential in this calculation. The energy source for the metabolic heat production is mixture of the fat, glucose and protein. When fat is burned as 100% of the energy source, *RQ* = 0.7; when 100% of glucose is burned, then *RQ* = 1.0. Since different energy substrates yield different amounts of energy per litter of oxygen consumption, *RQ* should be considered to estimate *EE*. Metabolic rate can be evaluated by the following equations,

$M = EE \times Vo_2$ [W] (Equation 2.32)

Here,

$EE = (0.23 \times RQ + 0.77) \times 5.88$ [W·h / lO_2] (Equation 2.33)

$RQ = Vco_2 / Vo_2$

Here,

RQ is the respiratory quotient,

Vo_2 is oxygen consumption rate [lO_2 / h],

Vco_2 is carbon dioxide consumption rate [lO_2 / h],

EE is the energetic equivalent in watt ours per litre of oxygen [W·h / lO_2]

2.5.1.2.5 Estimation from morphological characteristics

Considering morphological characteristics, a method was adopted to predict *M* based on the basal metabolic rate (*BMR)* and physical activity ratio (*PAR)* [78]. *BMR* represents the energy needed to maintain vital physiological functions while awake, at rest, in a supine position and in a fasted state [79]. *PAR* is defined as a value that represents the energy cost of a specific activity compared to *BMR* [80, 81]. The metabolic rate derived from individual morphological characteristics can be estimated as follows:

$M = (BMR \times PAR)/BSA$ [W/m^2], (Equation 2.34)

Here,

$BMR = \{0.0481 \times W_b + 2.34 \times H_b - 0.0138 \times Age - 0.4235 \times Gender\} \times 11.574$ [W], (Equation 2.35)

$BSA = 0.008883 \times W_b^{0.444} \times (H_b \times 100)^{0.663}$ [m^2], [82] (Equation 2.36)

where *Age* is measured in years, and *Gender* is assigned a value of 1 for males and 2 for females.

The above formula of *BMR* was specifically developed using data from Asian population [83].

Furthermore, the *PAR* values were derived from previous studies focused on Asian participants [81, 84]. Table 2.3 shows the *PAR* values for desk work.

Table 2.3. Physical activity ratio (*PAR*) values for desk work activities as per body mass index (*BMI*).

BMI (kg/m^2)	Male	Female
BMI < 18.5	1.35	1.33
18.5 < *BMI* < 24.9	1.32	1.34
BMI > 25	1.38	1.36

Considering the various approaches available for predicting *M,* in real working environment conditions, metabolic rate prediction by HR, from morphology or general estimation by activities are practical options to estimate *M*.

2.5.2 Comparison of the most popular thermal comfort assessment models

Beside *PMV* prediction model there are several popular models to predict thermal comfort. In Table 2.4, a comparison among most popular thermal comfort indices such as *WBGT, PMV, SET**, *PET* and *UTCI* has drawn [75, 85].

Considering the comparison of thermal comfort assessment models, *PMV- PPD* model is most relevant to predict thermal comfort for a large number of populations. The reasons behind it were that the *PMV* includes both environmental factors and personal factors to assess thermal comfort. In addition, in thermally neutral or mild hot or cold condition, no extreme physiological responses like sweating or shivering was rare to the participants, this model is most suitable for comfort assessment. Besides that, *PMV's* estimation of thermal sensation is easily comparable with actual thermal sensation vote (TSV) recommended by ISO [33].

2.6 Thermal comfort and thermal sensation assessment approach

To assess the thermal comfort and thermal sensation assessment, traditional questionnaire survey or personal inquiry is the real authentic way. However, considering real working environment, wearable devices also used to assess thermal comfort by addressing physiological responses to the thermal environment. In recent time with the advancement of technologies and availability of cameras or thermal cameras with the introduction of artificial intelligence (AI) and machine learning (ML), now comfort assessment is forwarding to non-invasive measurements.

Table 2.4. Comparison among *WBGT, PMV, SET**, *PET* and *UTCI*.

Thermal comfort assessment model	***WBGT*** (wet-bulb globe temperature)	***PMV*** (predicted mean vote)	***SET**** (standard effective temperature)	***PET*** (physiological equivalent temperature)	***UTCI*** (universal thermal climate index)
Usages	Occupational heat stress Prediction	Indoor comfort prediction	Thermal comfort & thermal stress prediction	Outdoor thermal comfort and urban climate	Thermal comfort & thermal stress prediction
Originated from	US military (1950s)	Fanger, 1970 [3]	Gagge et al., 1986 [86]	Höppe, 1999 [87]	Bröde et al. 2012 [88]
Basic conception of heat transfer and thermoregulation	Empirical heat balance	Steady-state heat balance	2-node model	2-node model, Munich Energy-balance Model for Individuals	Multi-node thermoregulatio n model [89]
Consideration of: Environmental factors	t_a, RH , t_r, v_a	t_a, RH , t_r, v_a	t_a, RH , t_r, v_a	t_a, RH , t_r, v_a	t_a, RH , t_r, v_a
Consideration of: Personal factors	None	M, I_{cl}	M, I_{cl}	M, I_{cl}	M, I_{cl}
Consideration of: Physiological Responses	None	None	sweating, vasomotor control	Core & skin temperature	Core and skin temperature, sweating, shivering, skin wettedness and blood flow
Outcomes	°C (empirical index)	Dimensionless (-3 to +3)	°C (equivalent temp)	°C (equivalent air temp)	°C (equivalent air temp)
Thermal Comfort Range	< 25°C (no heat stress)	-0.5< PMV< 0.5	23°C ~ 26°C typical comfort	18°C ~ 23°C (no thermal stress)	9°C ~ 26°C (comfort zone)
Limitations	No consideration of personal factors [90]	Only valid in steady-state condition [76]	Complex calculation [91], limited for light activities [92]	Assumes fixed morphological character [93]	Mostly designed for outdoor, observed great sensitivity for v_a [85]

2.6.1 Traditional approach

Thermal comfort and thermal sensation are subjective perceptions. It is true that from physiological characteristics it is possible to estimate the body state, however comfort and sensation is shaped by different parameters including psychological and physiological state. In generally questionnaire survey or interview is the real way to investigate the personal thermal comfort and thermal sensation [11, 33]. In recent days, questioner assessment through computer application or online survey is popular than printed questionnaire survey. Even though it is time consuming and a single survey reflects only the thermal comfort or thermal sensation at that specific moment in time. For a continuous thermal comfort assessment, it is mostly impractical.

2.6.2 Technological approach to detect physiological responses by wearable devices or sensors

In resent technological updates and availability of modern sensors, to estimate thermal comfort and thermal perceptions, technical approaches are quite familiar to detect physiological responses. Wearable devices are increasingly capable of monitoring a wide range of physiological responses of human body to the thermal environment [94]. These devices leverage diverse sensor technologies in combination with advanced algorithms to derive both primary signals and physiological considerations. The physiological signals that can be captured through these devices, and their relevance to thermal comfort research are shown below:

2.6.2.1 Heart rate (HR)

HR signals provide critical insights into cardiovascular function and stress levels. Heart activity can be monitored using two main technologies. This kind of device is used to measure the number of heart beats per minute, known as bpm [95]. This data provides insights into the cardiovascular activity of an individual. HR measurement typically follows two main techniques: electrocardiography (ECG) or photoplethysmography (PPG). ECG detects the electrical signals formed during cardiac activity. Electrodes are placed on the chest or other body parts to record the electrical impulses that trigger heart contractions. PPG is often used in wrist-worn devices, and work by emanating usually infrared light into the skin and measuring the amount of light either absorbed or reflected by the blood vessels. Blood flow changes during the cardiac cycle alter light absorption, which is then converted into heart rate data. PPG is an optoelectronic method that assesses blood volume pulse (BVP). This measure the amount of blood flowing through tissues, by measuring changes in light absorption and reflection at the skin surface using a light source (typically a LED) and a photodetector [96].

2.6.2.2 Skin response

Skin is the primary interface between the body and environment. Skin plays a vital role in the thermoregulation process through sweat glands and cutaneous blood vessels. To observe the thermoregulatory response to the surrounding thermal environment, two primary parameters of skin activity can be measured. At first electrodermal activity (EDA) is also known as galvanic skin response or skin conductivity. EDA is a measure of continuous changes in the skin electroconductivity due to the modification of sweat gland activity. When people are under stress, sympathetic nerve activation increases sweat gland activity. It causes an increase in moisture on the skin and, consequently, its electroconductivity [97]. And another skin response is skin temperature. Skin temperature can be measured using technologies such as resistance thermometers, thermistor, infrared thermometers, or thermocouples [98, 99]. Skin temperature changes due to vasomotor control, influenced by thermal environment. Skin surface senses temperature changes in environment and send signals to the central nervous system to regulate heat transfer through blood flow adjustments (vasodilation and vasoconstriction), affecting skin temperature changes. This temperature change in skin is the physiological responses induced by environmental changes.

2.6.3 Technological approach to detect physiological responses by non-invasive (non-contact) measurements

In recent times researchers are increasingly trying to integrate comfort assessment with AI and ML technologies. Some sensors used in AI and ML are often embedded in wearable accessories like goggles and watches to reduce discomfort due to attached sensors. In parallel, non-invasive measurement techniques using image or video processing have been investigated. Currently, three main research directions are emerging [100]. The first one is using infrared camera technology, what can detect physiological response through skin temperature. The second one is known as Eulerian Video Magnification techniques to standard cameras for detecting human thermal physiological signals. And the third stream is the use of skeleton key point models with standard cameras to analyze body posture associated with thermal comfort or discomfort.

2.6.3.1 Infrared camera

Initially applied in fields like medical diagnostics, and face recognition as well as skin temperature monitoring. Other parameters like skin electrical potential, skin electrical resistance, RR, clothing temperature and HR can also be detected and analyzed by infrared images [101].

Radiant energy is emitted across a broad spectrum of wavelengths, with the peak wavelength determined by Wien's displacement law. The law states that as the temperature of an object increases, the wavelength at which it emits the most radiation shifts to shorter wavelengths. Instruments that measure this radiation operate within specific wavelength ranges. For objects with temperatures between −10 °C and 50 °C, measurements are typically conducted in the 9–11 μm spectral range, as this corresponds to the peak of spectral emission [102]. The process of measuring this emitted radiation is known as infrared thermography.

Specific recommendations for infrared thermography such as camera calibration, data collection, and processing are outlined in thermographic imaging in sports and exercise medicine (TISEM) [103] as well as by other researchers [104]. This checklist outlines key methodological requirements for using IRT in research. They emphasized the necessity to report detailed participant data (e.g. activity profile), control extrinsic factors affecting skin temperature (e.g., recent activity, alcohol, sunbathing), and maintain consistent ambient conditions (e.g., temperature, humidity). IRT assessment should avoid external infrared sources and forced air movement, and camera specifications, calibration status, and emissivity settings must be documented. Proper camera positioning, acclimation time, and image recording conditions (e.g., distance, region of interest) are required, as well as clear documentation of thermogram analysis methods. A visual reference of body position with temperature scale is recommended, and skin preparation setups such as drying must be described. It was recommended that the camera should capture measurements at a 90° angle, positioned perpendicular to the front of the subject.

Though using IRT accuracy have some limitations, such as it is highly sensitive to environmental factors like ambient temperature, humidity, and radiant heat, necessitating strict control during data collection [104]. Additionally, the method assumes a constant skin emissivity value typically around 0.98 and variations due to moisture, sweat, or skin characteristics can introduce significant errors [105]. IRT also has limited ability to capture rapid dynamic changes in skin temperature.

Considering the relationship between thermal sensations and physiological responses, some studied found a correlation between thermal sensation and skin temperature predicted by IRT. They observed predictions by thermal cameras have an accuracy between 65–85% [100]. Though thermal sensation can be strongly influenced by individual variation, one technical reason for the low estimation could be the effect of noise in the thermal images. In addition, low-cost cameras' accuracy is still questionable to predict physiological responses like skin temperature.

2.6.3.2 Euler video magnification technology - aided normal camera and skeleton key points model - aided normal camera

This technology amplifies subtle motions and colour changes in video frames that are typically invisible to the naked eye [106]. Euler processing doesn't follow movement directly; instead, it breaks the video into different levels of detail and uses timing analysis to make small changes more visible. The core principle of this method is to analyze the time series of color values at each pixel and amplify variations within a specific frequency band of interest. This system has applied in various fields like monitoring physiological changes like HR, skin color variations, and blood flow.

To capture human poses and movement more accurately, skeleton key points were investigated. Tracking was performed using convolutional pose machines, which apply machine learning to recognize image features and use spatial models that adapt to the image content [107]. This tracking can be used to predict the activity levels and eventually metabolic rate, though the accuracy of this method is still under review [108].

2.7. Thermal comfort and individual differences

Individual differences in thermal sensation and thermal comfort identify the phenomenon where individuals perceive the thermal environment differently even they are exposed to the same thermal environment [23]. Because of the existence of the individual differences, it is hard to make and maintain a thermoneutral environment, which may satisfy every occupant for a long period of time. Rupp et al. [109] classified the sources of individual differences as one is the physiological origins, mainly metabolic heat production differences between individuals, and secondly the cultural and behavioural differences expressed through the clothing insulation. Besides that, there are several physical, physiological and psychological differences, which plays significant role to shape individual differences. Some of the major individual differences are discussed below.

2.7.1 Morphological differences

Variations in human morphology play a significant role in influencing physiological responses and individual perceptions in different thermal environments. For example body mass significantly affects thermal comfort by influencing both heat production and thermal inertia [110]. A large body mass contributes to improved thermal stability by increasing heat production and resistance to the temperature fluctuations. This makes individuals with greater body mass more tolerable to cold environments, as greater body mass helps dissipates heat from the body more slowly.

Body mass mainly consists of both fat and muscle tissue. It was observed that muscle tissue helps to produce more heat than fat during both rest and physical activity. Individuals with greater muscle mass tend to have a higher *M*, leading to increased heat production [14, 111], which may enhance comfort in cold environments, though opposite in hot. Subcutaneous fat thickness acts as an insulation of the body which reducing heat loss in cold environments and thereby improving thermal comfort [112]. However, this insulation can impair heat dissipation in warm condition [54]. As a result, overweight and obese people prefer lower ambient temperature compared to those with normal weight in warm environments [113]. In contrast, in cold condition it was found that heat production is negatively correlated with body fat percentage [114].

Another important morphological characteristic related with the heat exchange is the body surface area (*BSA*). A larger *BSA* relative to body mass results in faster heat loss, making individuals potentially more cold-sensitive. Allen mentioned that animals in colder regions have shorter limbs to minimize heat loss by reducing surface area relative to body mass [54]. Bergmann found that animals in colder climates have larger body size, reducing SA/volume and minimizing heat loss [53].

Body mass index (*BMI*) is another morphological parameter commonly used as an integrative indicator that reflects body height and weight. *BMI* summarizes the interactive effects of internal heat generation, insulation, and heat exchange with the surrounding thermal environment, making it an important factor in thermoregulation. According to world health organization (WHO) [115] *BMI* and the morphological characteristic are divided into underweight to obese scale. Table 2.5 shows the classification of *BMI*.

Table 2.5. Classification according to *BMI*.

BMI (kg/m^2)	Classification
< 18.5	Underweight
18.5 ~ 24.9	Normal range
25.0 ~ 29.9	Overweight
≥ 30.0	Obese
30.0 ~ 34.9	Class I
35.0 ~ 39.9	Class II
≥ 40.0	Class III

In general, a *BMI* of around 22 kg/m^2 is considered as standard value with minimal risk of metabolic disease [116].

From previous research, it was observed that individuals with a lower *BMI* suffered more from thermal discomfort in cold extremities [117]. Study showed that individual with lower *BMI* were comfortable at a little bit higher ambient temperature, while those with greater *BMI* expressed comfort at approximately 1°C lower temperature [118]. In practice, individuals with low or normal *BMI* are more prone to feeling cold, and sometimes compensate by wearing more clothing insulation [119]. Notably, individuals with greater *BMI* shows higher cold tolerance also [120].

Additionally, it was observed that insensible body mass loss is positively correlated with *BMI*. Insensible body mass loss is an important component in body heat exchange [120], and a higher body surface area in individuals with greater *BMI* facilitates increased heat loss through insensible body mass loss. It was observed that higher *BMI* group exhibited significantly greater perceived sweating to increase evaporative heat loss, and higher skin wettedness, compared to the lower *BMI* group above the upper critical temperature threshold.

Individuals with higher *BMI* show better cold tolerance due to greater fat insulation and higher heat production In previous studies it was demonstrated that, in mild cold or neutral condition higher *BMI* individual has higher skin temperatures at the body extremities for the hands and feet [121], resulting from higher heat production and higher blood flow to the extremities. On the other hand, lower *BMI* individuals has lower skin temperatures at the body extremities. This phenomenon represents the vasoconstriction occurrence, especially in lower *BMI* people in the extremities, during neutral or mild cold condition [122].

2.7.2 Gender differences

Gender is one of the major individual differences studied in this thermal comfort studies. Males and females' thermal sensation and thermal comfort differs significantly due to a combination of physiological, morphological, and psychological factors. These variations are induced by morphological characteristics, thermoregulatory functions, subjective perceptions and sex hormonal fluctuations.

Females generally have a higher percentage of subcutaneous fat and lower muscle mass comparing with males [123]. The more subcutaneous fat provides comparatively greater insulation for females, whereas less muscle mass reduces metabolic heat production [124-126]. In addition, females generally exhibit a greater capacity for peripheral heat storage due to higher subcutaneous fat levels, but this is less noticeable in the hands and feet [127]. McArdle et al. found that higher body fat increases body mass relative to surface area, lowering the SA/mass and thereby enhancing insulation against heat loss [128].

While considering the other important physiological aspects, skin temperature is a critical physiological response to the surrounding thermal environment. In general, it was observed that female's skin temperature is lower than males' [118, 129, 130]. Possibly because of higher degree of vasoconstriction in thermoneutral condition, lower blood flow at the extremities reduces skin temperature and this causes higher cold sensations to the female [129, 131, 132]. Cooke et al. found that skin blood flow at hand is lower in females comparing males in cold condition [133]. It also observed that, in mild cold exposure the difference of rectal temperature and the mean skin temperature was greater in the female participants [134]. This clearly highlights that physiological responses, such as greater temperature differences between proximal and distal body parts are more pronounced in females, making them more sensitive to cold in cool or mildly cold conditions. In more severe cold condition females begin shivering at a higher ambient temperature than males to preserve the core body temperature [135].

Above the upper critical temperature threshold, the number of activated sweat glands and/or the sweat output per gland are the reason behind the increase in sweating rate (SR) [136]. It was observed that SR is lower in females than in males during dry and/or humid heat stress. [137]. Men's higher SR supports greater maximum evaporative heat loss capacity in hot conditions. In addition, because of testosterone enhances the sweating response, males had greater sweating responses in hot condition than females [138].

In terms of reproductive hormones, core temperature in females rises during the luteal phase (after ovulation) due to progesterone. In the follicular phase (before ovulation), estrogen is dominant. It tends to lower core body temperature slightly. Many females feel colder, likely due to reduced skin temperature from progesterone-induced vasoconstriction. This cause an increase in the internal threshold temperature for vasodilation as well as sweating and the body extremities remain colder [139].

Because of the physiological characteristics and morphological differences, it was observed that males tend to feel more comfortable than females at both high and low temperature extremes [140]. In contrast, females generally prefer slightly warmer environments for thermal comfort, with preferred temperatures approximately 1.0 to 2.5 °C higher than those preferred by males [130, 141-143]. Females are also more sensitive to mild cold temperatures [130, 144]. Remarkably, females' overall thermal sensation is strongly influenced by their local thermal sensation, particularly at the extremities [131]. Furthermore, field studies on thermal comfort based on gender differences also found that females had higher levels of thermal dissatisfaction than males [141, 145], and their comfort range tends to be narrower [146, 147].

Beside this, another individual factor, strongly influencing thermal comfort is I_{cl}. It was observed that dress norms and adaptive behaviours differ in gender. Women may wear more skin-exposing clothing, even sometime disproportionate clothing insulation between the upper body and lower body. This also effects on thermal perceptions. In addition, it was found that females prefer heavier clothing than males [148] , it can be because of fashion trends which results higher clothing insulation for females.

2.7.3 Cold constitution differences

In the domain of thermal comfort research, one particularly unique and culturally significant concept is known as cold constitution, or "*hie-sho*" in Japanese. This concept was rooted in traditional East Asian medicine and cultural health beliefs [149]. The term "*hie-sho*" describes a heightened sensitivity to cold that affects a substantial portion of the population [150]. Unlike clinical thermoregulatory disorders, cold constitution is often viewed as a subclinical, chronic condition marked by subjective discomfort and determined cold sensations, especially in the body extremities.

Although *hie-sho* has traditionally been described in non-biomedical terms, research were conducted to uncover the physiological mechanisms underlying this phenomenon. One of the most notable characteristics of individuals with cold constitution found is an altered blood flow regulatory system. Specifically, people having a cold constitution exhibit heightened adrenergic sensitivity, which influences cutaneous vasoconstriction in distal body segments such as the hands and feet during cold exposure [151, 152]. This extreme vasoconstriction impairs blood circulation to the peripheral body and causes reduced skin temperature, resulting in extra cold sensitivity. Researchers also found, low skin temperature in cold sensitive individuals because of poor peripheral blood circulation [152]. In females with a cold constitution, it was observed that, peripheral skin vasoconstriction can occur even under thermoneutral conditions [153]. Yamazaki found that cold sensitive subjects keep a specific blood flow-controlling system in the peripheral pathway that is categorized by higher adrenergic sensitivity for greater cutaneous vasoconstriction in the distal body during cold exposure [154]. The finger temperature, and the HR of individuals having cold constitution were found significantly lower than those who have no cold constitution [155].

Numerous studies have demonstrated that individuals with cold constitution showed greater thermal discomfort under cold or thermoneutral conditions. For instance, Nagashima et al. [155] found that cold-sensitive individuals presented higher cold sensation because of greater sensitivity of adreno-receptor. They perceived cold sensations even when exposed to a thermoneutral environment.

Cold constitution phenomenon is more commonly reported among women [154, 156]. Hormonal differences, lower *BMR*, varying body composition and lifestyle been proposed as contributing factors. Women who are associated with cold constitution often feel discomfort due to a severe cold sensation in cold environments, have general malaise (such as sleeplessness, weariness, and lowered concentration), and a tendency to fall ill frequently [157].

Thus, individuals with and without cold constitution showed differences in both their morphological characteristics and physiological responses to the thermal environment.

CHAPTER 3: Investigating real-time thermal sensation prediction, using predicted mean vote (*PMV*)

3.1 Introduction

Thermal comfort is a subjective perception of the surrounding thermal environment [1, 34]. It includes both physiological and psychological responses to the adjacent thermal conditions. Thermal comfort encompassing subjective measures of temperature and moisture sensed by the skin, core body, and the physiological effort required to maintain thermal balance [32]. Environmental parameters such as t_a, *RH*, v_a and t_r are the primary influencers of thermal perception [3, 11]. In addition to environmental factors, personal factors like *M* and I_{cl} are the key elements which significantly shape an individual's thermal experience [11].

In modern society, people spend over 80% of their time in indoor conditions [158]. These indoor thermal environments play a significant role in their thermal comfort and well-being [159]. Maintaining a favorable indoor thermal environment can ensure occupants' good health and thermal satisfaction. It can also enhance productivity, concentration, awareness, and overall work performances [12, 160, 161]. Despite ongoing efforts by designers to design thermoneutral environments, maintaining consistent thermal comfort for a large number of populations remains a big challenge, particularly in spaces occupied by varying inhabitant activities [13, 59, 162]. This complexity is further compounded by the dynamic nature of consistent environmental changes as well as human adaptations [163]. In modern buildings, HVAC systems' aim is to maintain a thermoneutral condition [164, 165], yet the system does not take into account of occupants' morphology, wearing, activity level, and behavioral adaptations. Consequently, thermal neutrality cannot be uniformly applied through all individuals. Additionally, thermal perception is not only variable between individuals to individuals, but also fluctuates within the same individual over a span of time [13, 166]. This variability necessitates real-time thermal comfort assessment to ensure comfort for every individual.

Traditionally, questionnaire surveys or interviews are the most reliable thermal comfort assessments technique [33, 167]. This method is valid, although mostly impractical for continuous examining in real-world environments. To overcome these limitations, several mathematical models have been developed by different researchers through thermal comfort analysis. Among them *PMV* model is the most widely used mathematical model [1, 3, 11]. *PMV* estimates thermal comfort considering the human body's heat balance and it also incorporates both environmental and personal factors. *PMV* depends on four environmental parameters: t_a, *RH*, v_a and t_r. It also counts individual aspects such as *M* and I_{cl}. Because its prediction scale aligns closely with real subjective TSV, it is the most popular model to evaluate thermal sensation for a group of people [168, 169].

However, while *PMV* relies on swiftly measurable environmental variables, it also depends on estimates of *M* and I_{cl}, which are quite challenging to determine accurately in real working conditions. That's the reason, where in most cases these personal parameters are assumed as fixed values across all individuals [15, 77]. This leads to significant discrepancies between *PMV* and actual TSV [170, 171]. Consequently, *PMV* model is primarily static in the sense that it used to predict the average thermal sensation of a large group of individuals [172]. To support personalized thermal comfort, particularly in ABW contexts, it is essential to identify individual factors in real time [173].

In this scenario, recent technological advancements offer promising tools and techniques to assess real-time thermal comfort. For instance, IRT can estimate surface temperatures based on emitted infrared radiation, what enables real-time analysis of I_{cl} in a non-invasive manner [174, 175]. It opens the window to estimate I_{cl} in real-time for every individual in a short period of time. In parallel, another individual factor *M* can be estimated via heart rate (HR) [15] or estimated by combining basal metabolic rate (*BMR*), which is estimated from morphological characteristics and physical activity ratio (*PAR*) [78].

3.2 Aim of the study

Building on this foundation, the present study aims to develop and evaluate practical approaches for real-time prediction of thermal sensation. Specifically, this study evaluates various methods to predict *M*, I_{cl}, and consequently *PMV*, using IRT without reliance on intrusive measurements or static assumptions. These methods offer a simplified alternative to conventional comfort assessment models by focusing on real-time thermal comfort assessment. The overarching goal is to enhance the accuracy and simplicity in thermal comfort assessments in dynamic indoor environments.

3.3 Methods

3.3.1 Participants

This research was conducted in university classrooms at the Hokkaido University, in Sapporo Japan. In this study 88 students in summer, 100 in autumn, and 68 in winter participate. The research was conducted under regular classroom conditions across these three seasons to ensure comprehensive data collection. Table 3.1 represents the morphological characteristics of the students participated in the experiment. All participants provided their written consent after being informed about the research procedures. The research protocol was checked and approved by the IRB in the Faculty of Engineering, Hokkaido University (No. R5-8). All the participants were healthy individuals, predominantly within the normal weight range based on their *BMI* and were free to choose their wearing during the experiment.

3.3.2 Research protocol

To consider diversified climatic conditions, the experiments were conducted in summer (2024/7/26 – 2024/8/11), autumn (2023/10/14 – 2023/11/01), and winter (2023/12/09 – 2023/12/17). The experiments were conducted in two shifts. In morning from 10 am to 12 pm and in afternoon 1 pm to 3 pm.

Classrooms conditions were maintained as their typical setups. It was naturally ventilated and air-conditioned classroom in summer, naturally ventilated in autumn, and heated in winter. The experimental protocol is shown on Fig. 3.1. It lasted approximately 105 min in every session. The experiment was started with the collection of participants' morphological data, including age, sex, height, and weight through a detailed questionnaire survey. After that there was a 60 min stabilization period to adapt the thermal environment. After the stabilization, participants were asked to complete their thermal voting and recorded their clothing ensembles to obtain reference values of TSV and I_{cl}, respectively. Following the phase, armpit temperature was measured using a thermometer (OMRON MC-688), it was considered as a proxy for core body temperature (t_{cr}). Participants' HR were continuously recorded by a wearable wristwatch equipped with heart rate sensor (M430, Polar, Finland). At the end of the experiment, IRT images were captured via an infrared camera (R500EX-S, Nippon Avio, Japan) to estimate t_{cl} and local t_{sk} to evaluate I_{cl}. Throughout the experiment, environmental parameter t_a, RH, v_a, and globe temperature (t_g) were recorded.

Table 3.1. Morphological characteristics and armpit temperature of the participants, in summer, autumn and winter.

Morphology	Summer	Autumn	Winter
Number of participants	88	100	68
Gender (Male : Female)	36 : 52	53 : 47	36 : 32
Age (year)	21.1 ± 2.3	22.1 ± 1.8	21.9 ± 2.0
Height (cm)	163.8 ± 7.4	165.4 ± 9.2	165 ± 8.9
Weight (kg)	54.7 ± 9.3	57.4 ± 10.5	56.3 ± 9.3
BMI (kg/m^2)	20.3 ± 2.3	20.8 ± 2.3	20.5 ± 2.1
BSA (m^2)	1.5 ± 0.2	1.6 ± 0.2	1.6 ± 0.2
t_{cr} (°C) (armpit temperature)	36.63 ± 0.27	36.53 ± 0.33	36.59 ± 0.27

BMI: body mass index, *BSA*: body surface area, t_{cr}: core body temperature.

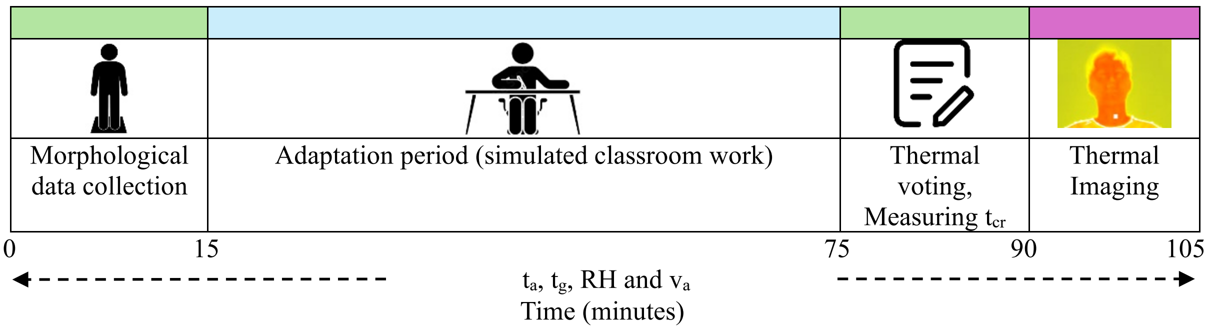

Fig. 3.1. Research protocol in Hokkaido University during summer, autumn and winter.

3.3.3 Environmental data

The classroom setup, including the environmental logger's placement and sensors used in the experiment, is illustrated in Fig. 3.2 and Fig. 3.3. Four fundamental environmental parameters t_a, t_g, *RH*, and v_a were continuously measured throughout the experiment to predict the *PMV*. Using a thermistor sensor, t_a was measured and recorded at 1-s intervals with a data logger (NR543R, Nikkiso-Thermo, Japan). Same thermistor and data logger were used to measure t_g, with a combination of a Bernon type 150 mm black globe (Sibata, Japan), where the thermistor was positioned at the center of the black globe. During the *RH* measurement, it was recorded at 1-s intervals using a humidity recorder (RS-14WB, Espec, Japan) equipped with a humidity sensor (RSH-4010, Espec, Japan). For v_a measurements, an anemometer logger (Testo 440, Testo, Germany) was employed with an omnidirectional hot-wire air-flow probe (TUC 0628 0152, Testo, Germany). It was capable of capturing wind velocity from every direction at 1-s intervals. All measurements were taken at a height of 0.6 m. Considering a seated posture, the tentative center of body is closed to 0.6m, and that's the reason of measuring all the data at that height [176]. To cover all spatial coverage, three sets of environmental sensors and data loggers were positioned at the front-left, center, and back-right corner of the classroom. The loggers were turned on 30 min prior to the experiment to allow for environmental stabilization. To consider the spatial thermal variations, environmental data from the nearest data loggers were applied for each individual's *PMV* prediction. After the end of the experiment, all data was stored digitally on the computer. The value of t_r was calculated by,

$$t_r = ((t_g+273.15)^4 + ((1.1 \times 10^8 \times v_a^{0.6}) / (\varepsilon \times D^{0.4})) \times (t_g - t_a))^{0.25} - 273.15 \text{ [°C]}, \quad [176] \qquad \text{(Equation 3.1)}$$

where,

t_g is the globe temperature [°C],

t_a is the air temperature [°C],

v_a is the air velocity [m/s],

ε is the emissivity of the globe (usually 1.00 for a black globe), and

D is the diameter of the globe [m] (in this case, D = 0.15 m).

3.3.4 Questionnaire survey

A questionnaire survey was conducted to assess individual thermal sensations, with the reported TSV values serving as a reference for comparison with *PMV* predictions. The questionnaire was designed following ISO 28802 [33] guidelines. Participants recorded their TSV using a 7-point scale starting from -3 (cold) to 0 (neutral) to 3 (hot) (Fig. 3.4). Additionally, participants marked their clothing ensembles using a checklist, which was later utilized as the reference value for I_{cl}. Fig 3.5 shows the checklist used in this experiment. was All questionnaires were translated into Japanese to ensure accurate comprehension while retaining its original intent.

Fig. 3.2. Regular classroom image during the experiment with data loggers (a), regular classroom plan with data logger's positions (b).

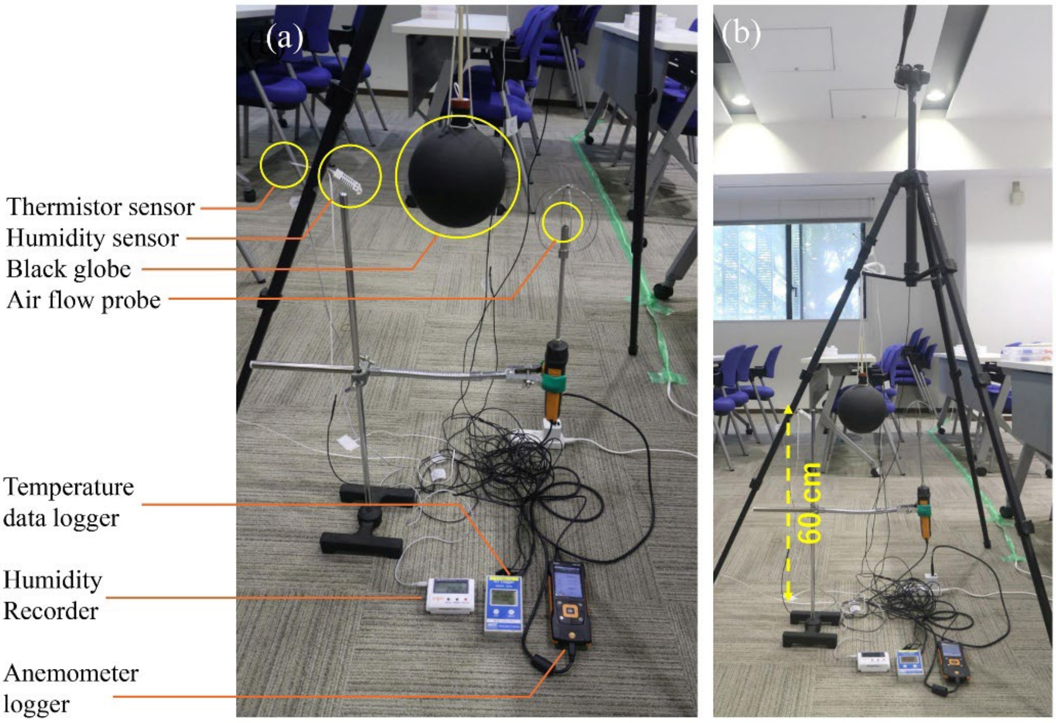

Fig. 3.3. Data logger with sensors (a), data logger setup in classroom (b).

3.3.5 IRT camera setup and prediction process of t_{cl} and t_{sk}

Thermal images were captured using an IRT camera (R500EX-S, Nippon Avio, Japan) with a measurement range of −40°C to 500°C. The accuracy of the camera was ±1°C, and it had a resolution of 640 (Horizontal) × 480 (Vertical) pixels. The camera's viewing angle was 32° (α) × 480° (β). Data collection and processing adhered to the guidelines outlined in Thermographic Imaging in Sports and Exercise Medicine (TISEM) [103].

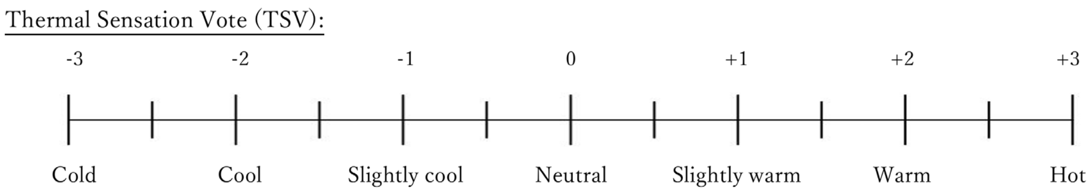

Fig. 3.4. Questionnaire for thermal sensation vote (TSV).

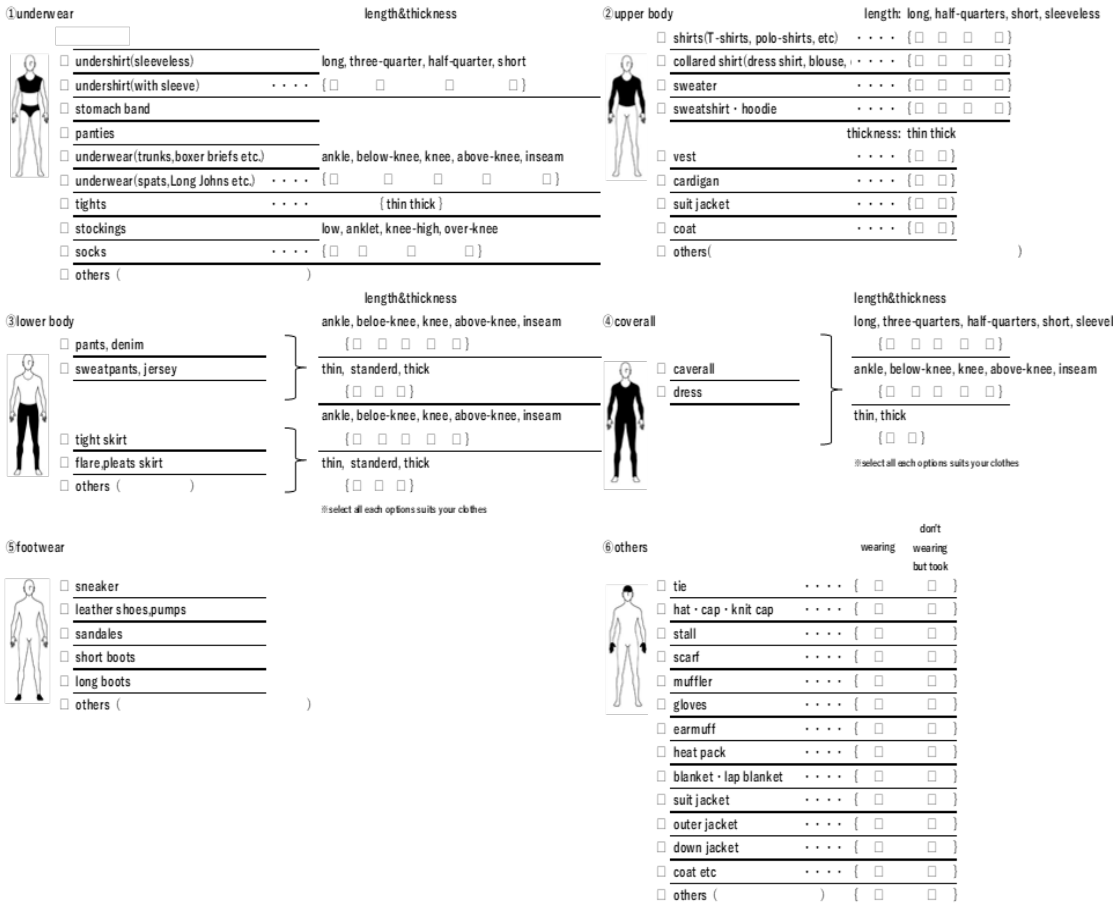
①underwear — length&thickness
□ undershirt(sleeveless) — long, three-quarter, half-quarter, short
□ undershirt(with sleeve) ・・・・ {□ □ □ □}
□ stomach band
□ panties
□ underwear(trunks,boxer briefs etc.) — ankle, below-knee, knee, above-knee, inseam
□ underwear(spats,Long Johns etc.) ・・・・ {□ □ □ □ □}
□ tights ・・・・ { thin thick }
□ stockings — low, anklet, knee-high, over-knee
□ socks ・・・・ {□ □ □ □}
□ others ( )

②upper body — length: long, half-quarters, short, sleeveless
□ shirts(T-shirts, polo-shirts, etc) ・・・・ {□ □ □ □}
□ collared shirt(dress shirt, blouse, ・・・・ {□ □ □ □}
□ sweater ・・・・ {□ □ □ □}
□ sweatshirt・hoodie ・・・・ {□ □ □ □}
thickness: thin thick
□ vest ・・・・ {□ □}
□ cardigan ・・・・ {□ □}
□ suit jacket ・・・・ {□ □}
□ coat ・・・・ {□ □}
□ others( )

③lower body — length&thickness
□ pants, denim
□ sweatpants, jersey
ankle, beloe-knee, knee, above-knee, inseam {□ □ □ □ □}
thin, standerd, thick {□ □ □}
□ tight skirt
□ flare,pleats skirt
□ others ( )
ankle, beloe-knee, knee, above-knee, inseam {□ □ □ □ □}
thin, standerd, thick {□ □ □}
※select all each options suits your clothes

④coverall — length&thickness
□ caverall
□ dress
long, three-quarters, half-quarters, short, sleevel {□ □ □ □ □}
ankle, below-knee, knee, above-knee, inseam {□ □ □ □ □}
thin, thick {□ □}
※select all each options suits your clothes

⑤footwear
□ sneaker
□ leather shoes,pumps
□ sandales
□ short boots
□ long boots
□ others ( )

⑥others — wearing / don't wearing but took
□ tie ・・・・ {□ □}
□ hat・cap・knit cap ・・・・ {□ □}
□ stall ・・・・ {□ □}
□ scarf ・・・・ {□ □}
□ muffler ・・・・ {□ □}
□ gloves ・・・・ {□ □}
□ earmuff ・・・・ {□ □}
□ heat pack ・・・・ {□ □}
□ blanket・lap blanket ・・・・ {□ □}
□ suit jacket ・・・・ {□ □}
□ outer jacket ・・・・ {□ □}
□ down jacket ・・・・ {□ □}
□ coat etc ・・・・ {□ □}
□ others ( ) {□ □}

Fig. 3.5. Questionnaire for clothing assembles.

3.3.5.1 Camera calibration

To confirm temperature accuracy, the camera was calibrated prior to the experiment in a thermally insulated, dark climatic chamber set to a thermoneutral temperature of 25°C. A peltier module coated with black tape (emissivity = 1.00) was used as a black body with known temperatures ranging from 15°C to 35°C in 5°C increments. The actual temperatures were recorded using a thermistor sensor connected to a data logger (NR543R, Nikkiso-Thermo, Japan), and regression analysis was used to compare real and IRT-predicted temperatures. Fig. 3.6 shows the IRT calibration experimental setup with the IRT image analysis. To avoid the effect of the environment on the peltier module, central 50% areas (25mm×25mm) average temperature was considered as the real temperature. After that from the predicted data a correction formula was applied to improve the accuracy of the IRT measurements (Fig. 3.7).

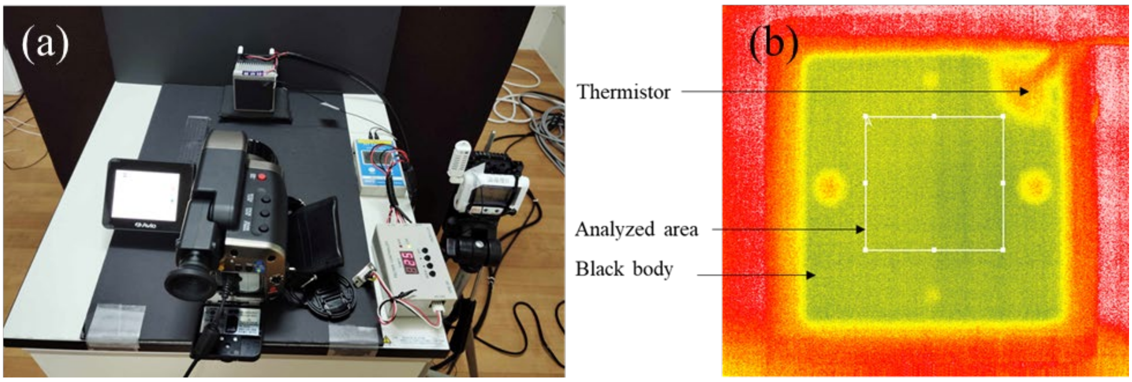

Fig. 3.6. IRT calibration setup (a), IRT taken image of the peltier module as a black body (b).

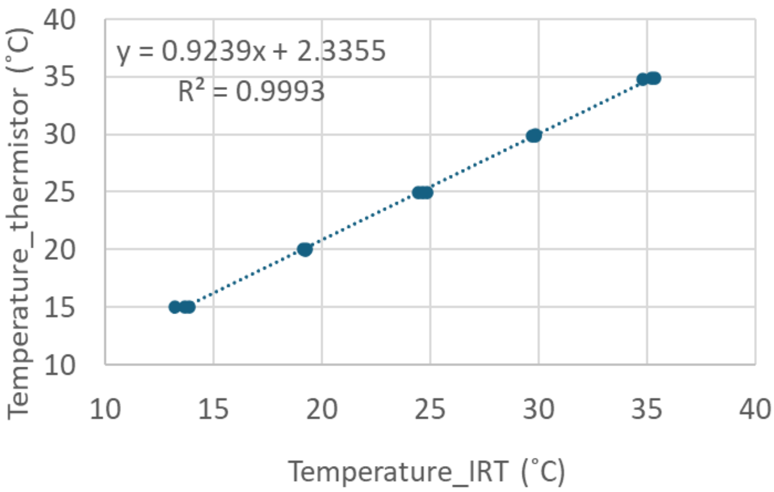

Fig. 3.7. Regression analysis between actual temperature recorded by thermistor and IRT predicted temperature.

3.3.5.2 IRT camera setup

During the experiment, the IRT camera was positioned to reduce the effects of external factors such as direct radiation and airflow. The camera was set at a height of 0.90 m to align with the center of a standing human body and was oriented perpendicularly to the plane of the region being measured. For facial and hand imaging, the camera was adjusted to focus solely on the regions of interest, ensuring higher resolution. The camera's emissivity was set to 0.95.

3.3.5.3 IRT data collection

To stabilize the sensors, the IRT camera was powered on at least 15 min before data collection. Fig. 3.8 represents the IRT camera setup for the thermal image analysis process to predict t_{cl}. For t_{cl} prediction, thermal images of participants' front, and back were taken from a distance of 4 m. Fig. 3.9 represents the IRT camera setup for the thermal image analysis process to predict t_{sk}. The images of the face and hands were taken at 1.5 m (Fig. 3.9). In all cases, the thermal images were captured solely in the region of interest to achieve a higher resolution when detecting that area. The pixel count for the target regions exceeded 18, ensuring a detection probability of over 90% [177]. The maximum operational range distance (D_{max}) for the detection is expressed as,

$D_{max} = [\max (H) / [16 \times \tan \times \{\max(\alpha,\beta)/2\}]] \times \{\max(x_1,y_1)/18\}$, [177] (Equation 3.2)

Where,
H is the height of the object,
α is the horizontal and vertical viewing angles of IRT camera (°),
β is the vertical viewing angles of IRT camera (°),
x_1 is horizontal pixels of IRT camera, and
y_1 is vertical pixels of IRT camera.
In this experiment, the distances used to predict t_{cl} and t_{sk} were within the range required to identify the region [178].

3.3.5.4 IRT data analysis

Thermal data were processed using InfReC Analyzer NS9500 standard, a software specified by the thermal camera manufacturer. To predict t_{cl}, a polygonal line was drawn on the thermal images to mark the edges of clothing insulation on both the front and back sides using the image analysis application. The mean pixel temperature obtained from these two areas were considered as a mean t_{cl}. During local skin temperature prediction, the region of interest was initially predicted and subsequent spot analysis was performed at the key point to identify local t_{sk} on the face and hand regions, following methods used in previous studies [22, 178, 179]. These regions were selected based on the availability of exposed body surfaces suitable for imaging by IRT. The t_{sk} of forehead and dorsal hand were labeled and predicted as $t_{forehead}$ and $t_{dorsal\ hand}$ respectively.

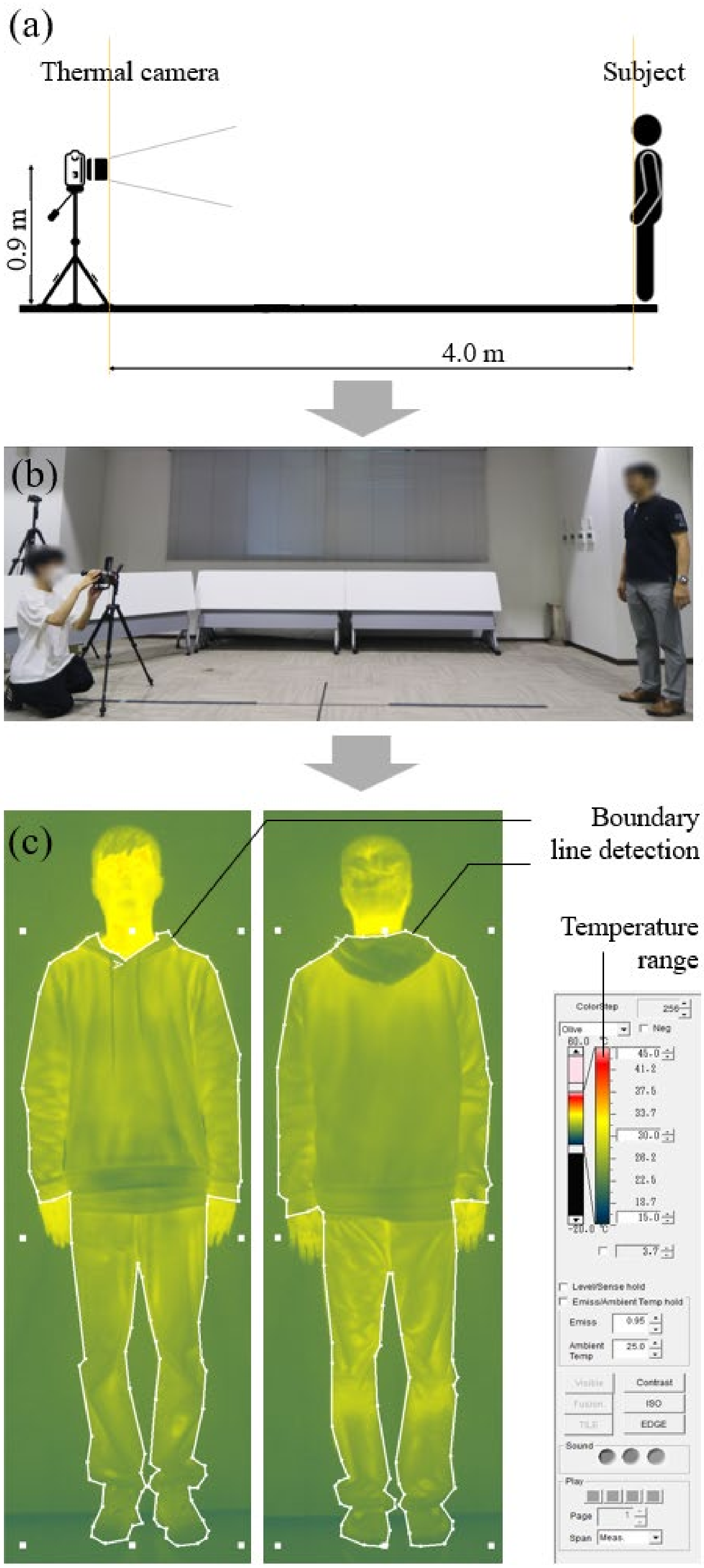

Fig. 3.8. Prediction sequence of estimating t_{cl}: camera setup (a), capturing thermal image (b), front side and back side clothing outline marking and average temperature extraction(c).

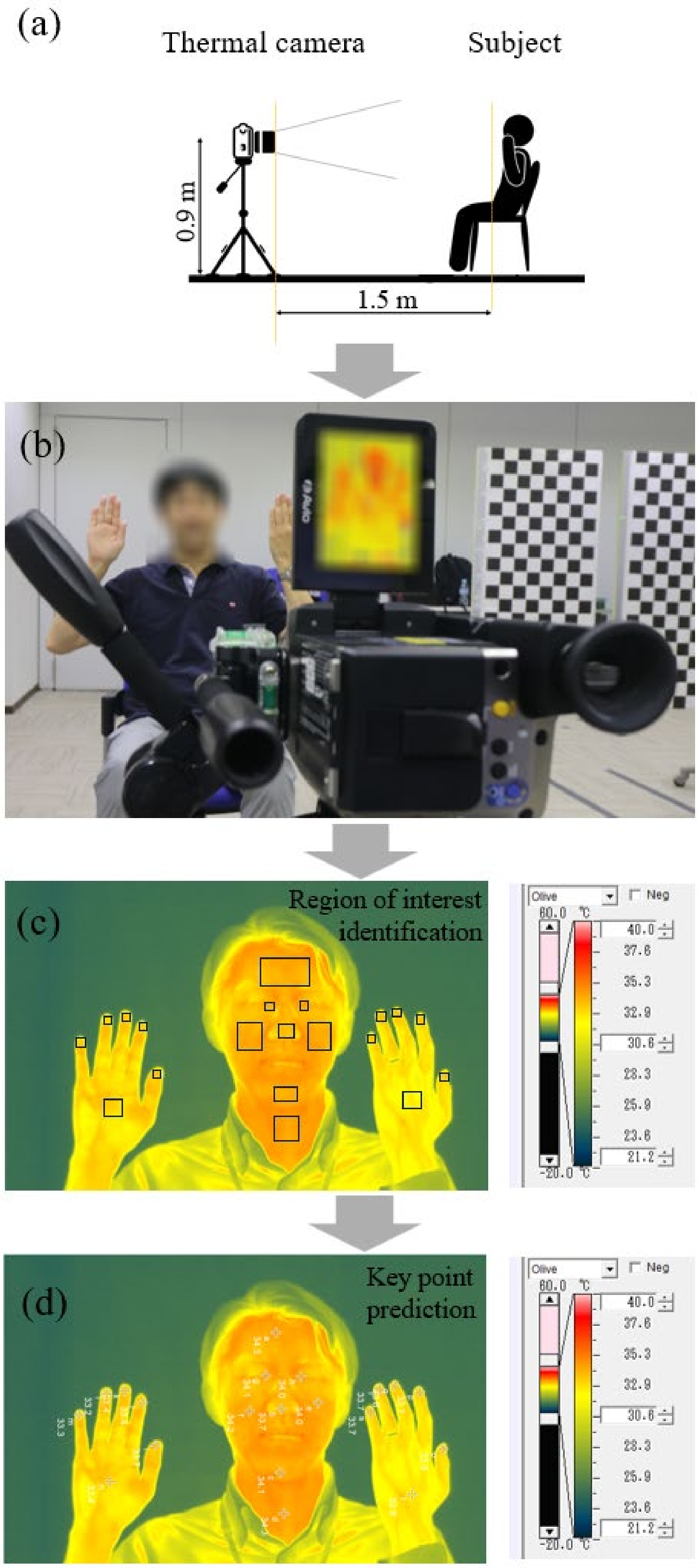

Fig. 3.9. Prediction sequence of estimating local t_{sk}: camera setup (a), capturing thermal image (b), region of interest marking (c), temperature data extraction from the key points (d).

3.3.6 *PMV* prediction

According to ISO 7730 [11], the *PMV* was calculated by the Equation 2.4, explained in Section 2.5.1

It is evident that this equation relies both on environmental factors and individual parameters, such as M and I_{cl}. In this study, three methods were employed to estimate I_{cl}: clothing insulation obtained from the questionnaire survey (I_{cl}_q), I_{cl} from t_{cl} ($I_{cl}\_t_{cl}$), and I_{cl} from t_{cl} and t_{sk} ($I_{cl}\_t_{cl}, t_{sk}$). Similarly, for estimating M, three methods were used: assumed common metabolic rate for sedentary activities ($M\_{1.2}$), M from heart rate (M_{hr}), and M from *BMR* and *PAR* (M_{bmr}). The methodology for each I_{cl} and M estimation is detailed in the following sections. The outcomes of different estimations of I_{cl} and M resulted in nine combinations of *PMV* predictions, and named as: $PMV(M\_{1.2}, I_{cl}\_q)$, $PMV(M\_{1.2}, I_{cl}\_t_{cl})$, $PMV(M\_{1.2}, I_{cl}\_t_{cl}, t_{sk})$, $PMV(M\_{hr}, I_{cl}\_q)$, $PMV(M_{hr}, I_{cl}\_t_{cl})$, $PMV(M\_{hr}, I_{cl}\_t_{cl}, t_{sk})$, $PMV(M\_{bmr}, I_{cl}\_q)$, $PMV(M\_{bmr}, I_{cl}\_t_{cl})$, and $PMV(M\_{bmr}, I_{cl}\_t_{cl}, t_{sk})$.

3.3.6.1 I_{cl} estimation

This study employed three different methods to estimate I_{cl}.

3.3.6.1.1 I_{cl}_q estimation

The values of I_{cl}_q were estimated from the questionnaire survey, where participants' clothing insulation is determined based on individual garment (I_{clu}) using Equation 2.6, explained in Section 2.5.1.1.1 and named as I_{cl}_q.

Here, I_{clu} is the clothing insulation for every individual garment, gathered from a list of the I_{clu} values in ISO 8996 [77].

3.3.6.1.2 $I_{cl}\_ t_{cl}$ estimation

For $I_{cl}\_t_{cl}$ calculation, according to ISO 7730 [11], I_{cl} from t_{cl} was estimated using Equation 2.8 , explained in Section 2.5.1.1.3 and named as $I_{cl}\_ t_{cl}$.

To predict t_{cl}, IRT was used as explained above.

In addition, $I_{cl}\_t_{cl}$ is dependent on M as shown in the equation. Therefore, using $M\_{1.2}$, M_{hr} and M_{bmr} values, three variations of $I_{cl}\_t_{cl}$ were calculated as $I_{cl}\_t_{cl}$ ($M\_{1.2}$), $I_{cl}\_t_{cl}$ (M_{hr}), and $I_{cl}\_t_{cl}$ (M_{bmr}), respectively.

3.3.6.1.3 $I_{cl}\_t_{cl}, t_{sk}$ estimation

For $I_{cl}\_t_{cl}, t_{sk}$, according to ISO 9920 [77], clothing insulation ($I_{cl}\_t_{cl}, t_{sk}$) estimated based on t_{cl} and t_{sk} using Equation 2.12, explained in Section 2.5.1.1.4 and named as $I_{cl}\_t_{cl}, t_{sk}$.

In this estimation process, A_r/A_{DU} is the fraction of the skin surface in the radiative heat exchange and is considered as 0.7 for the seating posture [77].

In this study, the average temperature of $t_{forehead}$ and $t_{dorsal\ hand}$ estimated by IRT was considered as a surrogate measure of the mean t_{sk}.

$$t_{sk} = (t_{forehead} + t_{dorsal\ hand})/2\ [°C], \qquad \text{(Equation 3.3)}$$

The analysis focused only on uncovered body parts to calculate mean t_{sk}. The forehead, being closest to the trunk and exhibiting one of the highest skin temperatures among, and the dorsal hand, a distal extremity affected more by environmental conditions and vasomotor control (showing one of the lowest skin temperatures), were used to calculate mean t_{sk}. The validation of the results was examined by a laboratory experiment, the details of which are presented in the subchapter title "APPENDIX 3.A: Laboratory test, validation of mean t_{sk} estimated from $t_{forehead}$ and $t_{dorsal\ hand}$" at the end of this chapter

3.3.6.2 *M* estimation

In this study *M* was estimated using three different methods.

3.3.6.2.1 $M\_{1.2}$ estimation

$M\_{1.2}$ considers sedentary activities. The common metabolic rate ($M\_{1.2}$) was assumed to be 1.2 MET [180].

3.3.6.2.2 M_{hr} estimation

For M_{hr}, according to ISO 8996 [15], the metabolic rate of a specific activity is derived from the resting metabolic rate, resting heart rate, and mean heart rate. Here, the mean metabolic rate from the heart rate (M_{hr}) was calculated by the Equation 2.27, explained in Section 2.5.1.2.3 and named as M_{hr}.

In this experiment, a wristwatch-type HR monitor (M430, Polar, Finland) was used to record HR at 1-s intervals throughout the experiment for every participant.

3.3.6.2.3 M_{bmr} estimation

For M_{bmr}, to account for individual morphological character, a method was adopted to predict *M* based on the *BMR* and *PAR* [78]. *BMR* represents the energy required for a person to maintain vital physiological functions at rest, in a supine position, during fasting (without breakfast), and while awake [79]. *PAR* is defined as the ratio of energy expended during a specific activity, such as sitting, standing, and desk work, and is expressed in unit time [80, 81]. The metabolic rate derived from individual morphological characteristics (M_{bmr}) can be calculated by Equation 2.34, explained in Section 2.5.1.2.5 and named as M_{bmr}.

For this calculation, the necessary morphological information was collected from the questionnaire survey. Furthermore, the *PAR* values were derived from previous studies [81]. For males with BMI < 18.5

kg/m^2, 18.5 kg/m^2 < BMI < 24.9 kg/m^2 and BMI > 25 kg/m^2, *PAR* values of 1.35, 1.32, and 1.38 were used, respectively, as a desk work activity. For females with BMI < 18.5 kg/m^2, 18.5 kg/m^2 < BMI < 24.9 kg/m^2, and BMI > 25 kg/m^2, *PAR* values of 1.33, 1.34, and 1.36 were considered, respectively, assuming desk work activity.

To compare the $M\_{1.2}$ and *PMV* prediction, M_{hr} and M_{bmr} estimations were converted to MET units (1 MET = 58.2 W/m^2 [11]).

3.3.7 Statistical analysis

In this study, various I_{cl} estimation methods were compared using the paired Student's t-test. The TSV and different *PMV* predictions were compared using the Wilcoxon signed-rank test. Correlations between TSV and a series of *PMV* values were analyzed using Spearman's rank correlation test. Additionally, the absolute mean differences between TSV and *PMV* predictions (|TSV − *PMV*|), and the root mean square error (RMSE) were calculated to evaluate the justification of different estimation methods and the applicability of IRT as a real-time thermal sensation monitoring method. For all statistical analyses, differences were considered significant at $p < 0.05$. The analyses were performed using IBM SPSS Statistics version 20 software.

3.4 Results

This study aimed to investigate various *PMV* predictions to enhance the accuracy and practicality of real-time thermal sensation predictions. It also explores the feasibility of employing IRT for thermal sensation prediction in alternative ways. Table 3.2 presents the environmental conditions recorded during the survey period. It was observed that the temperature differences between autumn and winter were minimal due to the use of heating systems during winter. In contrast, summer temperatures were noticeably higher than those in autumn and winter. Using this environmental data, *PMV* predictions derived from various *M* and I_{cl} estimation methods were compared with TSV.

3.4.1 I_{cl} estimation

Fig. 3.10 presents the comparison between all I_{cl} predictions from different estimation methods. $I_{cl}\_t_{cl}$ ($M\_{1.2}$), $I_{cl}\_t_{cl}$ (M_{hr}), and $I_{cl}\_t_{cl}$ (M_{bmr}) were significantly higher ($p < 0.01$) than I_{cl}_q across all three seasons. Similarly, $I_{cl}\_ t_{cl}, t_{sk}$ was significantly higher ($p < 0.01$) compared to I_{cl}_q in summer and autumn. However, no difference was observed between these parameters in winter.

Table 3.2. Environmental condition during the experiment.

Environmental condition	Summer	Autumn	Winter
t_a (°C)	27.0 ± 1.2	22.3 ± 1.6	21.3 ± 1.3
t_r (°C)	27.3 ± 1.2	22.7 ± 1.9	21.6 ± 1.3
RH (%)	67.7 ± 5.0	47.2 ± 8.8	31.8 ± 12.6
v_a (m/s)	0.13 ± 0.04	0.05 ± 0.01	0.05 ± 0.01

t_a: air temperature, t_r: mean radiant temperature, RH: relative humidity, v_a: air velocity.

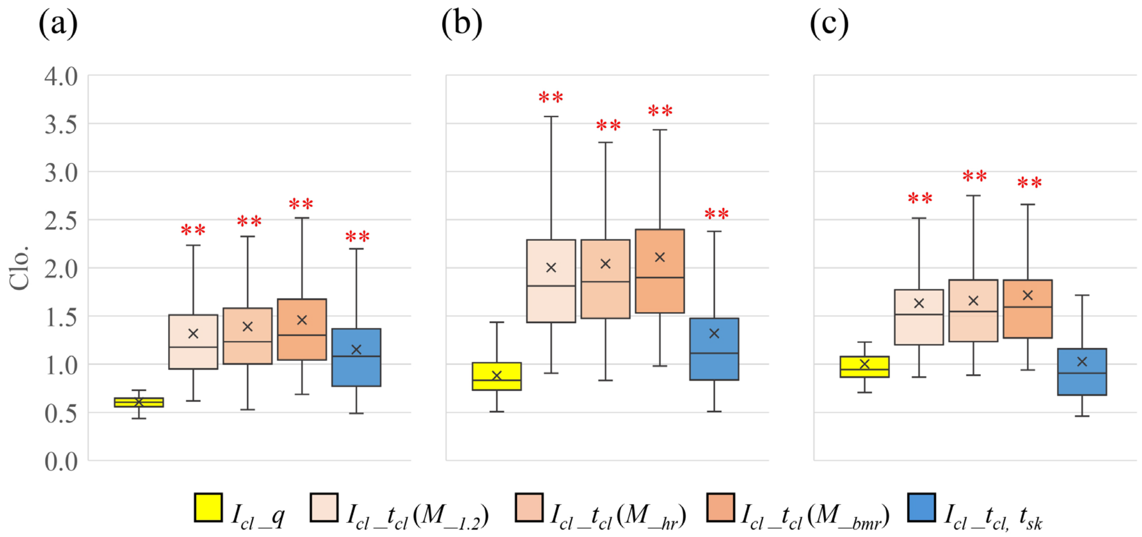

Fig. 3.10. Comparison of clothing insulation (I_{cl}) estimations, among I_{cl}_q, $I_{cl}\_t_{cl}\,(M\_{1.2})$, $I_{cl}\_t_{cl}\,(M\_{hr})$, $I_{cl}\_t_{cl}\,(M\_{bmr})$ and $I_{cl}\_t_{cl},\ t_{sk}$ in summer (a), autumn (b) and winter (c).

**: $p < 0.01$ between I_{cl}_q and I_{cl} estimation.

3.4.2 *M* estimation

According to ASHRAE [180], a generalized metabolic rate of 1.2 MET is typically assumed for sedentary activities such as desk work. This value is commonly accepted due to the lack of real-time investigations. Fig. 3.11 shows the comparison among various M estimations: $M\_{1.2}$, M_{hr} and M_{bmr}, across three seasons. From Fig. 3.11, it was observed that M_{hr} and M_{bmr} predicted mean metabolic rate were comparatively lower than the generalized ISO value of 1.2 MET for sedentary activities [15]. $M\_{1.2}$ showed a wider range of variations in all three seasons. In contrast, M_{bmr} was comparatively in narrower range in all three seasons.

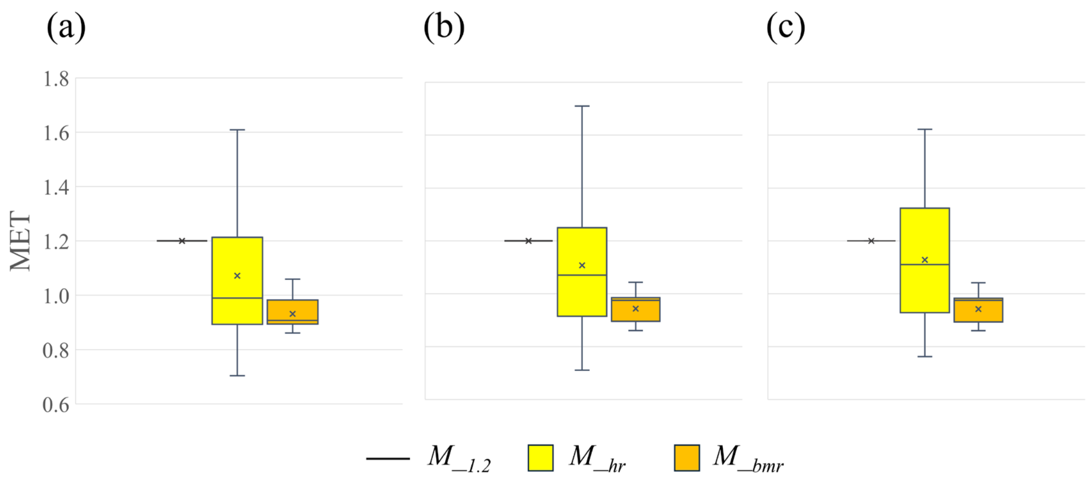

Fig. 3.11. Comparison of metabolic rate (*M*) estimations, among $M_{\_1.2}$, $M_{\_hr}$ and $M_{\_bmr}$ in summer (a), autumn (b) and winter (c).

3.4.3 *PMV* predictions and comparison with the TSV

In this study, nine *PMV* predictions were derived from three types of the *M* estimations and three types of the I_{cl} estimations. As $I_{cl}\_t_{cl}$ estimation depends on the value of three different *M*, $I_{cl}\_t_{cl}$ ($M_{\_1.2}$) with $M_{\_1.2}$, $I_{cl}\_t_{cl}$ ($M_{\_hr}$) with $M_{\_hr}$, and $I_{cl}\_t_{cl}$ ($M_{\_bmr}$) with $M_{\_bmr}$ were used to predict *PMV*($M_{\_1.2}$, $I_{cl}\_t_{cl}$), *PMV*($M_{\_hr}$, $I_{cl}\_t_{cl}$), and *PMV*($M_{\_bmr}$, $I_{cl}\_t_{cl}$), respectively.

Fig. 3.12 compares TSV with *PMV* predictions across three seasons. In summer, most of the *PMV* predictions were significantly higher than the TSV ($p < 0.05$). Only *PMV*($M_{\_hr}$, I_{cl}_q) and *PMV*($M_{\_bmr}$, I_{cl}_q) were significantly lower compared to TSV ($p < 0.01$). In autumn, except for *PMV*($M_{\_hr}$, I_{cl}_q) and *PMV*($M_{\_bmr}$, $I_{cl}\_t_{cl}$, t_{sk}) predictions, all other predictions showed significant differences ($p < 0.01$) compared to TSV. In winter, except for *PMV*($M_{\_1.2}$, $I_{cl}\_t_{cl}$, t_{sk}) and *PMV*($M_{\_hr}$, I_{cl}_q) predictions, all other predictions showed significant differences ($p < 0.05$) compared to TSV. It is worth noting that these results only represent the differences between the mean values of TSV and *PMV* predictions.

Fig. 3.13 shows the correlation between TSV and *PMV* predictions for each season. During summer, the correlation between TSV and *PMV* was low, and only *PMV*($M_{\_hr}$, I_{cl}_q) and *PMV*($M_{\_bmr}$, I_{cl}_q) showed significant positive correlations with TSV ($r = 0.37$, $p < 0.01$). In autumn, significant ($p < 0.01$) moderate correlations were observed for all *PMV* predictions with TSV. Among them, *PMV*($M_{\_bmr}$, $I_{cl}\_t_{cl}$, t_{sk}) and TSV showed the strongest correlations ($r = 0.37$, $p < 0.01$). In winter, *PMV*($M_{\_1.2}$, $I_{cl}\_t_{cl}$) and *PMV*($M_{\_bmr}$, $I_{cl}\_t_{cl}$) did not show significant correlation with TSV. Other predictions showed significant correlations with TSV ($p < 0.05$). Among them, *PMV*($M_{\_bmr}$, $I_{cl}\_t_{cl}$, t_{sk}) showed the maximum positive correlation with TSV ($r = 0.41$, $p < 0.01$).

Table 3.3 provides the absolute mean differences and RMSE between TSV and *PMV* for all three seasons. It was observed that *PMV*($M_{\_1.2}$, $I_{cl}\_t_{cl}$), *PMV*($M_{\_hr}$, $I_{cl}\_t_{cl}$), and *PMV*($M_{\_bmr}$, $I_{cl}\_t_{cl}$) had a relatively higher absolute mean difference and RMSE compared to TSV. $PMV(M_{\_1.2}, I_{cl\_}t_{cl})$, $PMV(M_{\_hr}, I_{cl\_}t_{cl})$, and $PMV(M_{\_bmr}, I_{cl\_}t_{cl})$ resulted from $I_{cl\_}t_{cl}$ clothing insulation estimation. In contrast, $PMV(M_{\_1.2}, I_{cl\_}t_{cl}, t_{sk})$, $PMV(M_{\_hr}, I_{cl\_}t_{cl}, t_{sk})$, and $PMV(M_{\_bmr}, I_{cl\_}t_{cl}, t_{sk})$ showed comparatively better prediction results against TSV, wherein all these three *PMV* predictions resulted from $I_{cl\_}t_{cl}, t_{sk}$ clothing insulation estimation. In addition, when comparing $PMV(M_{\_1.2}, I_{cl\_}t_{cl}, t_{sk})$, $PMV(M_{\_hr}, I_{cl\_}t_{cl}, t_{sk})$, and $PMV(M_{\_bmr}, I_{cl\_}t_{cl}, t_{sk})$ with TSV, the absolute mean difference and RMSE values were similar when compared with $PMV(M_{\_1.2}, I_{cl\_}q)$, $PMV(M_{\_hr}, I_{cl\_}q)$, and $PMV(M_{\_bmr}, I_{cl\_}q)$ with TSV, respectively. $PMV(M_{\_1.2}, I_{cl\_}q)$, $PMV(M_{\_hr}, I_{cl\_}q)$, and $PMV(M_{\_bmr}, I_{cl\_}q)$ resulted from $I_{cl\_}q$ clothing insulation estimation.

3.5 Discussion

This study aimed to predict real-time thermal sensation practically. To achieve this, different *PMV* estimations were compared with TSV. The accuracy of *PMV* predictions greatly depends on four environmental and two personal factors.

3.5.1 I_{cl} estimation

Fig. 3.10 illustrates the I_{cl} predictions using various methods. $I_{cl\_}q$ is most commonly used in estimating I_{cl}, making it the standard method. Despite several limitations, due to the lack of reliable methods for estimating I_{cl} in large populations, the questionnaire method is recommended by ISO 9920 for general I_{cl} estimation [77]. For this reason, in this study, the $I_{cl\_}q$ values derived from the questionnaire assessment were considered as reference values. In this method, the I_{clu} value for each individual garment can be predicted using the ISO 9920 [77] database. However, these values are related to the thickness of the cloth, and in reality, the thickness is greatly varied even across the same clothing brands. Several researchers have also noted the discrepancy between $I_{cl\_}q$ and the actual clothing insulation values obtained from thermal manikin tests [188]. This method shows the limitation of considering the air layer insulation between clothing layers [77]. This could explain the lower estimation in I_{cl} using the $I_{cl\_}q$ method compared to the other two methods. Moreover, this method requires a questionnaire survey in estimating the clothing insulation, making it impractical for real-time applications. Contrastingly, $I_{cl\_}t_{cl}$ and $I_{cl\_}t_{cl}, t_{sk}$ prediction in this study was based on IRT estimation, which could be used as a real-time prediction method. However, $I_{cl\_}t_{cl}$ predictions showed significantly higher values than those of $I_{cl\_}q$ and the estimated values were too high compared to the expected range. This is likely due to the lower estimation of t_{cl} by IRT. Because of the loose fitting of the clothing, and the large air gaps between the clothing layers, as well as between the body surface and clothing contributed to the underestimation of t_{cl}. Moreover, several previous studies reported the IRT's limitation in this context (i.e., the estimation of I_{cl} has a large error when the fitting is loose) [174]. Meanwhile, the estimation of $I_{cl\_}t_{cl}, t_{sk}$ depends on the temperature difference between t_{cl} and t_{sk} as well as on the dry heat loss. Even though it depends on t_{cl}, using t_{sk} as another important parameter may reduce the error in estimation.

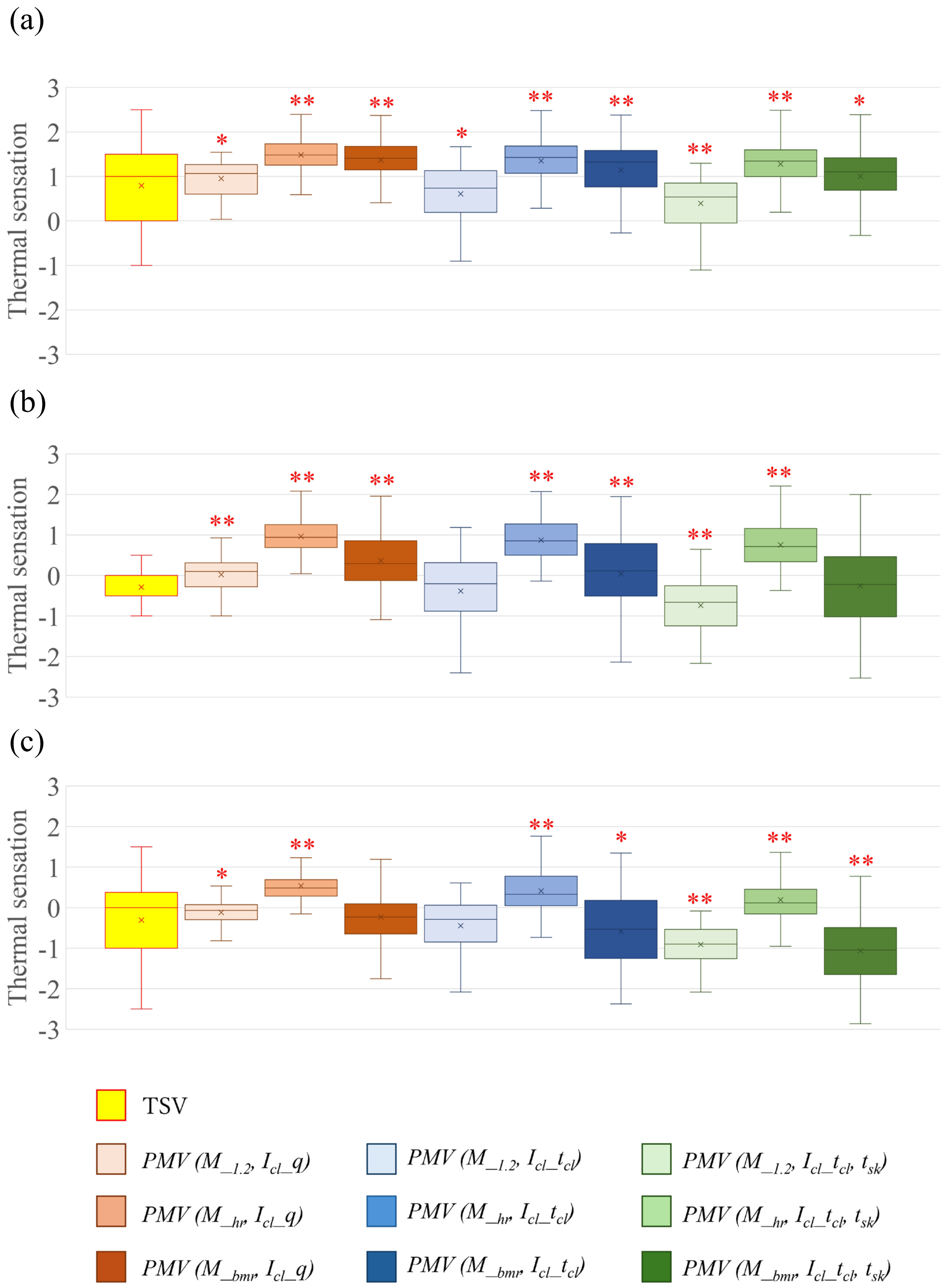

Fig. 3.12. Comparison of TSV with *PMV* predictions in summer (a), autumn (b) and winter (c).

**: $p < 0.01$ between TSV and *PMV* prediction,

*: $p < 0.05$ between TSV and *PMV* prediction.

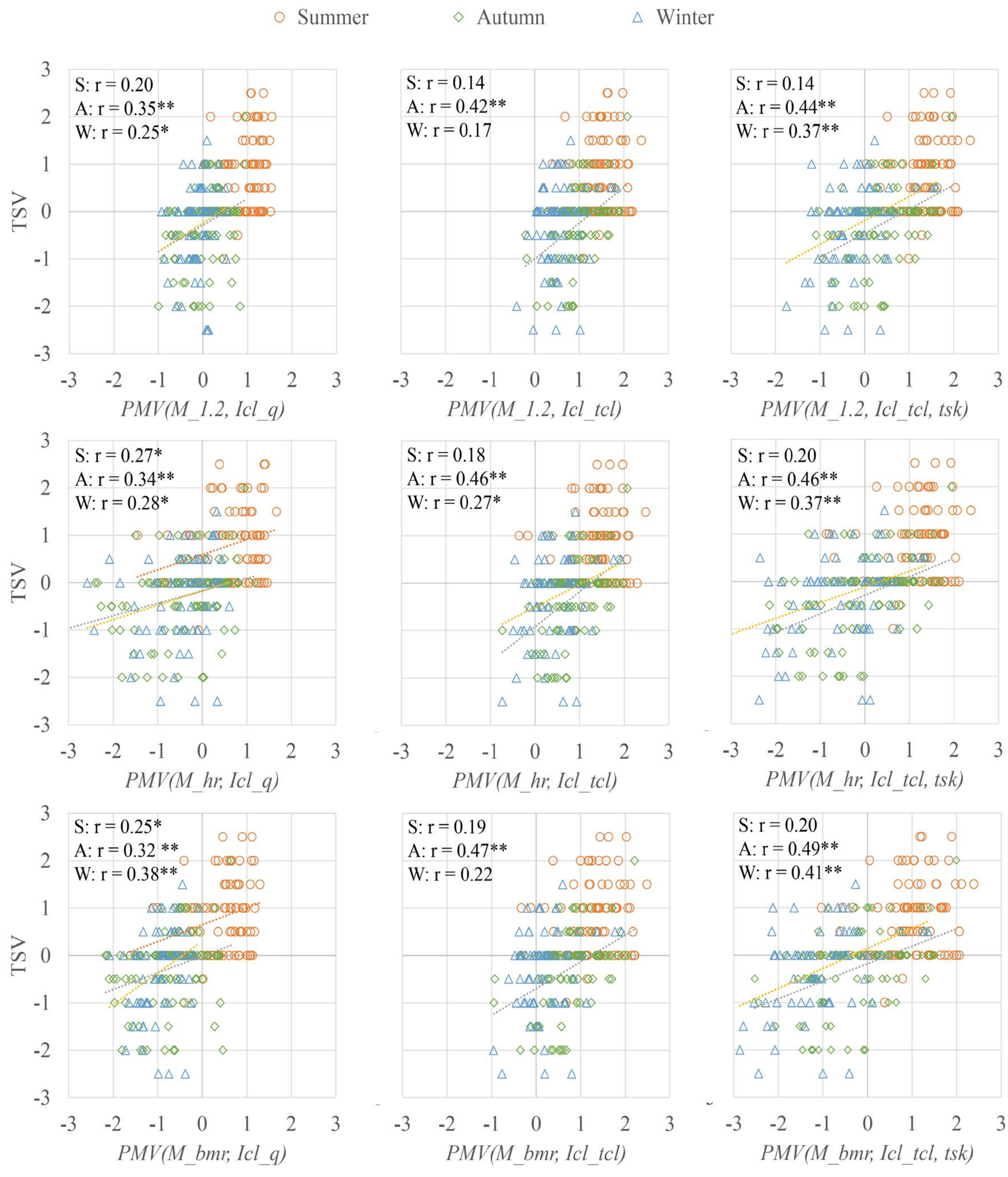

Fig. 3.13. Correlation between TSV with *PMV* in summer, autumn and winter.

(S : Summer, A : Autumn, W : Winter)

**: $p < 0.01$ between TSV and *PMV* prediction,

*: $p < 0.05$ between TSV and *PMV* prediction.

Table 3.3. Comparison between TSV and *PMV* predictions.

Comparison with TSV (Summer)	Absolute mean difference ±SD	RMSE
$PMV\ (M\_{1.2}, I_{cl}\_q)$	0.69 ± 0.43	0.81
$PMV\ (M\_{1.2}, I_{cl}\_t_{cl})$	0.91 ± 0.58	1.08
$PMV\ (M\_{1.2}, I_{cl}\_t_{cl}, t_{sk})$	0.86 ± 0.56	1.02
$PMV\ (M\_{hr}, I_{cl}\_q)$	0.74 ± 0.50	0.89
$PMV\ (M\_{hr}, I_{cl}\_t_{cl})$	0.86 ± 0.55	1.02
$PMV\ (M\_{hr}, I_{cl}\_t_{cl}, t_{sk})$	0.81 ± 0.56	0.98
$PMV\ (M\_{bmr}, I_{cl}\_q)$	0.77 ± 0.53	0.93
$PMV\ (M\_{bmr}, I_{cl}\_t_{cl})$	0.84 ± 0.55	1.00
$PMV\ (M\_{bmr}, I_{cl}\_t_{cl}, t_{sk})$	0.77 ± 0.56	0.96
Comparison with TSV (Autumn)	Absolute mean difference ±SD	RMSE
$PMV\ (M\_{1.2}, I_{cl}\_q)$	0.61 ± 0.56	0.83
$PMV\ (M\_{1.2}, I_{cl}\_t_{cl})$	1.25 ± 0.72	1.43
$PMV\ (M\_{1.2}, I_{cl}\_t_{cl}, t_{sk})$	0.83 ± 0.60	1.02
$PMV\ (M\_{hr}, I_{cl}\_q)$	0.78 ± 0.65	1.01
$PMV\ (M\_{hr}, I_{cl}\_t_{cl})$	1.18 ± 0.67	1.35
$PMV\ (M\_{hr}, I_{cl}\_t_{cl}, t_{sk})$	0.82 ± 0.53	0.97
$PMV\ (M\_{bmr}, I_{cl}\_q)$	0.80 ± 0.56	0.98
$PMV\ (M\_{bmr}, I_{cl}\_t_{cl})$	1.08 ± 0.71	1.29
$PMV\ (M\_{bmr}, I_{cl}\_t_{cl}, t_{sk})$	0.79 ± 0.51	0.94
Comparison with TSV (Winter)	Absolute mean difference ±SD	RMSE
$PMV\ (M\_{1.2}, I_{cl}\_q)$	0.69 ± 0.59	0.90
$PMV\ (M\_{1.2}, I_{cl}\_t_{cl})$	0.98 ± 0.75	1.23
$PMV\ (M\_{1.2}, I_{cl}\_t_{cl}, t_{sk})$	0.68 ± 0.58	0.89
$PMV\ (M\_{hr}, I_{cl}\_q)$	0.77 ± 0.65	1.00
$PMV\ (M\_{hr}, I_{cl}\_t_{cl})$	0.90 ± 0.72	1.15
$PMV\ (M\_{hr}, I_{cl}\_t_{cl}, t_{sk})$	0.88 ± 0.66	1.10
$PMV\ (M\_{bmr}, I_{cl}\_q)$	0.85 ± 0.61	1.04
$PMV\ (M\_{bmr}, I_{cl}\_t_{cl})$	0.81 ± 0.66	1.04
$PMV\ (M\_{bmr}, I_{cl}\_t_{cl}, t_{sk})$	1.01 ± 0.69	1.22

In this method, the temperature difference between t_{sk} and t_{cl} is the fundamental parameter in calculating I_{cl}. Only the clothing insulation layer is responsible for the temperature difference. The calculation of I_{cl} using this method simply relies on the primary heat transfer equation between the outside and inside of the clothing. This explains why $I_{cl}\_t_{cl}, t_{sk}$ showed better prediction against I_{cl}_q than that of $I_{cl}\_t_{cl}$ against I_{cl}_q. However, $I_{cl}\_t_{cl}, t_{sk}$ prediction also have certain limitations due to its reliance on environmental factors. In addition, in hot environments sweat absorption by clothing can lead to inaccurate predictions of clothing temperature. Additionally, the presence of radiation or strong airflow can also reduce the accuracy of clothing temperature predictions

3.5.2 *M* estimation

In Fig. 3.11, $M\_{1.2}$ was higher than M_{hr} and M_{bmr} estimations for all seasons. However, $M\_{1.2}$ is a generalized value for metabolic heat production for sedentary activities, such as desk work, considered by both ISO and ASHRAE. These standards were primarily based on the review article by Passmore and Durnin [181] on energy expenditure measurements where participants were of European and North American descent. In those standards, 1.2 MET was based on 1.8 and 1.6 m^2 body surface area with 70 and 60 kg body mass for man and woman, respectively [182]. Ethnic and geographical backgrounds affect metabolic heat production, leading to variations from standardized ones [183]. The average body surface area and body mass were lower for participants in this study (1.7 ± 0.1 and 1.5 ± 0.1 m^2 body surface area with 62.0 ± 9.3 and 50.8 ± 7.5 kg body mass for man and woman, respectively) compared to those from the study by Passmore and Durnin [181]. Many studies also reported that the resting metabolic rate can be under 1 MET, which is assumed to be equivalent to 58.2 W/m^2 [11, 184, 185]. This potentially explains why $M\_{1.2}$ was higher compared to the other two methods.

In contrast, HR provides a simplified method for estimating *M* using wearable devices. However, when HR is lower than 120 beats/min, the standard does not recommend using it for predicting *M* due to the absence of the dynamic activity [186]. This method requires dynamic activity engaging major muscle groups, with no static muscular, thermal, and mental loads, to evaluate *M* from HR [15]. This likely explains the wide range of differences observed between $M\_{1.2}$ and M_{hr} in this study. In addition M_{hr} includes lots of speculations and assumptions such as M_0, HR_{max}, *MWC,* even in W_{bl} estimation there are some presumptions, which may lead to large errors caused wide result dispersion.

On the other hand, M_{bmr} was estimated based on previous studies where participants were mostly Asian and had similar morphological characteristics as participants in our study [78, 187]. This could account for the consistency in M_{bmr} predictions across all seasons, and it reflects the smaller difference between $M\_{1.2}$ and M_{bmr} (Fig. 3.11). Moreover, M_{bmr} is comparatively easy to estimate based on morphological characteristics, which include minimal measurement error. However, M_{bmr} has a limitation in that it does not account for the individual difference in the physical activity level.

3.5.3 *PMV* prediction

The *PMV* prediction from all models showed significant differences with TSV, which represents the perception of the thermal environment by an individual and depends on many personal considerations such as physical and psychological states [189]. It also varies based on the cultural, climatic, social, and contextual dimensions of comfort awareness [190]. In contrast, *PMV* relies on mathematical prediction, which is dependent on the heat balance between humans and the environment. Many researchers argue about the overestimation of *PMV* with the TSV [118, 168, 191]. In this study, the traditional method was employed $M\_{1.2}$ and I_{cl}_q with four environmental factors to predict $PMV(M\_{1.2}, I_{cl}\_q)$, which was significantly higher compared to TSV across all three seasons. Comparing the *PMV* predictions with TSV, $PMV(M\_{bmr}, I_{cl}\_t_{cl}, t_{sk})$ showed a better agreement with TSV (Fig. 3.12). In addition, $PMV(M\_{bmr}, I_{cl}\_t_{cl}, t_{sk})$ showed better correlation with TSV (Fig. 3.13). These results indicates improved predictions of *M* and I_{cl}, in $PMV(M\_{bmr}, I_{cl}\_t_{cl}, t_{sk})$. However, in summer, the correlation was lower compared to other two seasons, which can be explained as the error in estimating I_{cl}, likely due to the loose fitting of clothing, especially for the female participants. It also indicates the importance of personal factors in predicting thermal sensation. Regardless, based on the absolute mean difference and RMSE between *PMV* and TSV, it was observed that *PMV* greatly differs from the TSV (Table 3.3), suggesting that it was suboptimal. Similarities were evident between this result and those of previous studies [192]. It should be noted that TSV is a subjective judgment, and even though individual factors are precisely determined, it is hard to match *PMV* perfectly with TSV in every case.

3.6 Limitations

Despite these promising findings, our study has some limitations. Notably, the environmental conditions were not widely varied. Due to the selection of typical classroom conditions, the environmental factors remained around within the thermoneutral ranges, even in summer or winter. This limits the applicability of the study's outcomes. Especially in hot conditions, where evaporative heat loss occurs through sweating, predicting skin temperature using IRT may not be as effective as in conditions where dry heat loss is the primary mechanism. Thus, experiments in a wider range of environmental conditions, both in cold and hot environments, may be a future step in this research progression. Similarly, the sample size also exhibited very similar characteristics, in age, height, and weight. Versatile morphological characters can reveal more information regarding the importance of estimating *M* and I_{cl} with individual characteristics. Additionally, behavioral adaptations, such as drinking cold or hot drinks, changing clothing during the experiment, or participant's psychological status, were not considered in this study. These factors also influence thermal sensation and must be considered in future studies. Despite these limitations, this research contributes to the advancements in real-time thermal sensation monitoring process. This study demonstrated that IRT can be utilized to predict thermal sensation in real time to control the HVAC system and optimize the energy consumptions of air conditioning.

3.7 Summary

This study aimed for accurate and simple real-time predictions of thermal sensations. The IRT technology was employed to predict t_{cl}, t_{sk}, and *PMV,* along with the traditional *PMV* prediction method. Additionally, *M* estimation was performed utilizing HR and *BMR* with *PAR,* alongside the generalized *M* as a uniform value. The results demonstrated that IRT could reasonably predict thermal sensation by *PMV* prediction. The major results of this study are as follows:

a) The range of differences between *M* from the HR and 1.2 MET was wider across all seasons, whereas the difference between *M* from the *BMR* and *PAR* with 1.2 MET was narrower; however, the average values of both M_{hr} and M_{bmr} were lower compared to $M\_{1.2}$ in all seasons.

b) The IRT-predicted clothing insulation using t_{cl} was significantly higher compared to the I_{cl}_q in all seasons. However, IRT-predicted I_{cl}, t_{cl}, and t_{sk} showed better estimations against I_{cl}_q.

c) Among the *PMV* predictions based on M_{bmr} and $I_{cl}\_t_{cl}$, t_{sk} showed better correlation with TSV.

The possibility of using IRT to predict *PMV* in real time is validated from these findings. The prediction of I_{cl} via IRT offers a promising alternative for predicting instantaneous thermal sensation estimates in real working environment.

APPENDIX 3.A: Laboratory test, validation of mean t_{sk} estimated from $t_{forehead}$ and $t_{dorsal\ hand}$

3.A.1 Introduction

Mean skin temperature (t_{sk}) is a key physiological parameter that reflects the human response to cold or hot environment and indicates the state of heat exchange between the body and its thermal environment [144]. In general, values for t_{sk} are calculated by summing of multiple local skin temperatures and their corresponding weighting factors. Several calculation methods have been established in the field of physiology, differing mainly by the number of skin temperature measurement sites and their associated weighting factors. Among them Hardy and DuBois's seven-point method (mean t_{sk_hd}) [193] remains one of the commonly used means for assessing thermal comfort which involve forehead, trunk, forearm, hand, thigh, calf and foot local skin temperature. In this method, both covered and non-covered body surface areas by clothing were considered. Another model proposed by Ramanathan (mean t_{sk_r}) [194] is a four point model that includes the chest, upper arm, thigh, and calf regions. Generally, under normal conditions, all four of these areas are typically covered by clothing. Particularly to predict I_{cl}, from the t_{cl} and t_{sk}, mostly t_{sk} represents the mean skin temperature under the clothing.

From a physiological perspective, the forehead, located near the trunk, typically exhibits one of the highest skin temperatures. In contrast, the dorsal hand, located at a distal extremity and more influenced by environmental factors and vasomotor control, mostly shows one of the lowest skin temperatures. From this perspective as well as possibility of easy skin temperature detection by IRT, in this case $t_{forehead}$ and $t_{dorsal\ hand}$ were chosen to estimate mean skin temperature. To confirm the validity of this methos, the average mean skin temperature calculated from that two regions were compared with Hardy and Dubois's seven-point method and Ramanathan's four-point method.

3.A.2 Methods

This research was conducted in July of 2025. The experiment was conducted in a climatic chamber, where environmental condition was fully controlled.

3.A.2.1 Participants

The research protocol was reviewed and approved by the Ethical Review Board for Life Science and Medical Research, Hokkaido University Hospital (No. 生 2024-0238).

In this experiment 22 participants joined either morning or afternoon experimental shift. Their wearing was long-sleeved shirt, long pants and underwear with socks and shoes (around 0.60 clo).

The age of the participants were 22.7 ± 2.2 years old in average. Their height and weight were 172.4 ± 5.3 cm and 61.5 ± 7.9 kg, respectively. Core body temperature was 36.5 ± 0.3 °C (measured orally).

3.A.2.2 Research protocol

Upon arrival at the laboratory, participants changed into pre-selected standardized clothing. Then they entered the climatic chamber and had 30 minutes of adaptation time in experimental condition. In the experiment, the temperature setting was around 26.1 °C. During that time, skin thermistor sensors were attached to the participants. Following the adaptation period, they were seated and involved in sedentary activities for 30 min. Fig. 3.A.1 shows the experimental setup.

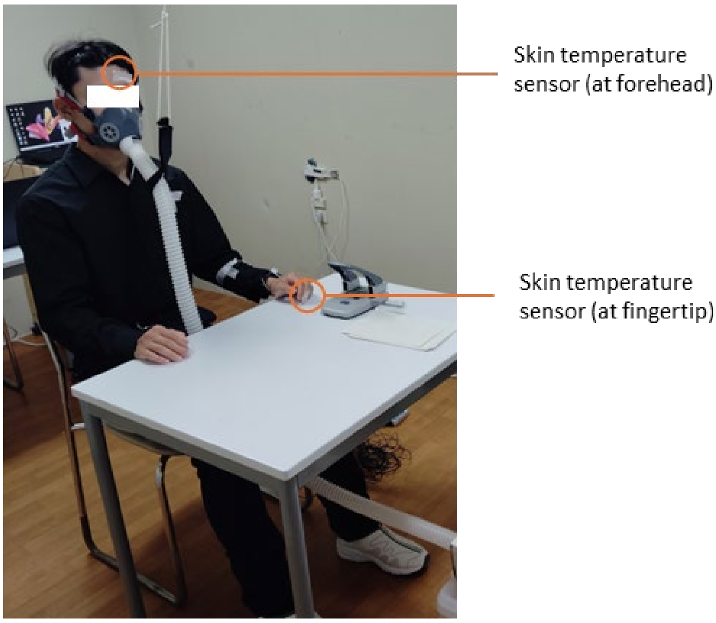

Fig. 3.A.1. Experimental setup for measuring local skin temperatures and environmental conditions.

3. A.2.3 Measurements

During the experiment their local skin temperature of chest (t_{chest}), upper arm ($t_{upper\ arm}$), forearm ($t_{forearm}$), thigh (t_{thigh}), calf (t_{calf}), foot (t_{foot}), $t_{forehead}$ and $t_{dorsal\ hand}$ temperature were recorded by data logger (NR543R, Nikkiso-Thermo, Japan).

Air temperature was measured at a height of 0.6 m using a thermistor sensor connected to a data logger (NR543R, Nikkiso-Thermo, Japan).

3. A.2.4 Prediction of mean t_{sk}

From the experimental data mean t_{sk_hd} were calculated by Hardy and Dubois's proposed equation [193],

$$t_{sk\_hd} = 0.35 \times t_{chest} + 0.19 \times t_{thigh} + 0.14 \times t_{forearm} + 0.13 \times t_{calf} + 0.07 \times t_{forehead} + 0.07 \times t_{foot} + 0.05 \times t_{dorsal\ hand} \quad [°C],$$

(Equation 3.A.1)

Additionally, from the experimental data mean t_{sk_r} were calculated by Ramanathan's proposed equation [194],

$$t_{sk\_r} = 0.3 \times t_{chest} + 0.3 \times t_{upper\ arm} + 0.2 \times t_{thigh} + 0.2 \times t_{calf}\ \ [°C], \qquad \text{(Equation 3.A.2)}$$

And the average temperature of $t_{forehead}$ and $t_{dorsal\ hand}$ estimated as mean $t_{sk,}$ by Equation 3.3, explained at Section 3.3.6.1.3.

3.A.2.5 Statistical analysis

In this study, various mean skin temperature estimations were compared using the paired Student's t-test. For all statistical analyses, differences were considered significant at $p < 0.05$. The analyses were performed using IBM SPSS Statistics version 20 software.

3.A.3 Results

Fig. 3. A.2 shows the comparison of mean t_{sk} calculated from Hardy and Dubois's 7 point method (t_{sk_hd}), Ramanathan's 4 point method (t_{sk_r}) and average temperature of $t_{forehead}$ and $t_{dorsal\ hand}$ estimated as mean t_{sk}, in two conditions.

It was found that t_{sk_hd} was around 0.30°C lower than the average temperature estimated from $t_{forehead}$ and $t_{dorsal\ hand}$, while t_{sk_r} was around 0.38°C lower than the average temperature estimated from $t_{forehead}$ and $t_{dorsal\ hand}$.

3.A.4 Discussion

Even though the significant differences were observed, the absolute mean difference among the three estimations were not so big in margin. There was a significant error observed even in the most renowned two method. Probably larger sample size and/or variation in the environmental conditions can mitigate the differences. In addition, given the inherent variability in skin temperature across body regions due to the difference in vasomotor control, further investigation in variable environmental condition would be better to confirm the validity of this method.

However, at least in the thermoneutral environment with wearing typical cloth, the gap between the standard methods for estimating mean t_{sk} and average of $t_{forehead}$ and $t_{dorsal\ hand}$ appears to be within the acceptable range. Considering the non-invasive practical advantages of $t_{forehead}$ and t_{dorsal} measurements as non-invasive way using IRT, these simplified methods may still provide sufficiently accurate estimates of mean t_{sk}.

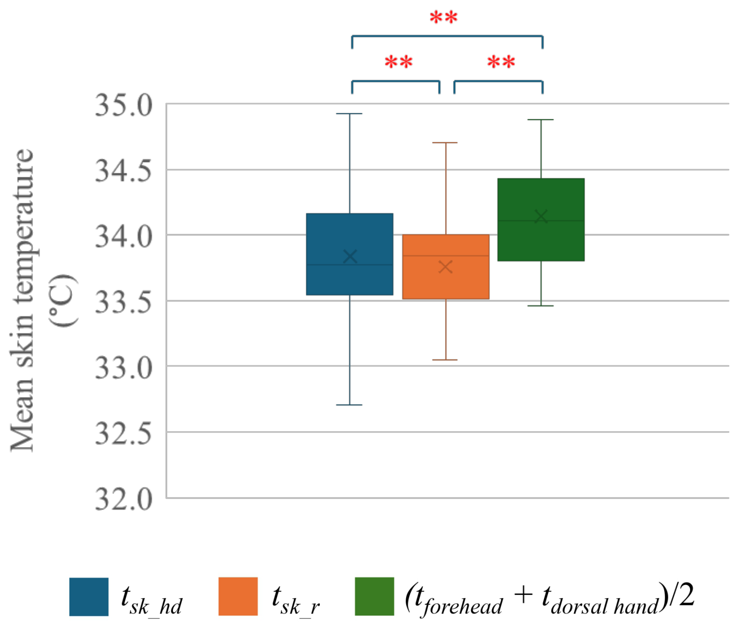

Fig. 3.A.2 Comparison of mean skin temperature (t_{sk}) calculated from Hardy and Dubois's 7 point method (t_{sk_hd}), Ramanathan's 4 point method (t_{sk_r}) and average temperature of $t_{forehead}$ and $t_{dorsal\ hand}$.

3.A.5 Conclusion

From the research outcome it was found that mean skin temperature from $t_{forehead}$ and $t_{dorsal\ hand}$ were in considerable condition. It was also noticed that in any environmental condition, these two local skin temperatures can be easily detectable. Considering the two facts in this research work, average of $t_{forehead}$ and t_{dorsal} was considered as mean skin temperature under the cloth covering body surface.

CHAPTER 4: Predicting individual variability in thermal sensations, predicted mean vote (*PMV*) and predicted percentage of dissatisfied (*PPD*) and local skin (t_{sk}) temperature differences.

4.1 Introduction

Human comfort, specifically thermal comfort is a complex and subjective state of mind that highly reflects an individual's overall satisfaction with their surrounding thermal environment. This description clearly highlights that comfort is not solely dependent on environmental factors but also on how these conditions are perceived by individuals [2]. Consequently, maintaining thermal comfort requires a holistic approach that considers both the physical conditions and the subjective experiences of human being [13].

It is very hard to maintain a common thermoneutral environment to every individual since comfort levels widely varied by numerous contextual factors, such as differences in M, I_{cl}, behavioral adaptation, morphological characteristics and so on [109]. Previous research indicates that thermal comfort is indeed significantly influenced by occupants' individual preferences [6]. The sensation of comfort is highly dependent on a combination of environmental conditions as well as the demographic characteristics of the users [195]. Environmental factors include t_a, RH, t_r, and v_a, while morphological characteristics embrace age, gender, body size as well as clothing, and activity level. Each person's unique combination of these factors influences their individual experience of thermal comfort in a given condition [196]. Chen et al. mentioned strong correlation between comfort vote and the individual factors like M and I_{cl}, [197]. These subjective factors interact in complex ways, meaning that even under the same environmental conditions, individuals can feel varying levels of thermal comfort depending on their distinct characteristics.

Thermal comfort (TC) and thermal sensation can be expressed as the human responses to thermal stimuli, which evoke specific sensory perceptions [30]. Thermal comfort is a subjective assessment of whether the thermal environment is satisfactory or acceptable and it is influenced by physical, physiological, psychological, and many other process [1]. Human mind assess the comfort by integrating direct temperature and moisture sensations from the skin, the temperature of the core body and the necessary effort to balance body temperature [31, 32]. On the other hand thermal sensation is influenced primarily by the activation of thermoreceptors on the skin surface and other sensory pathways that detect changes in the surrounding environment [198]. Thermal sensation refers to the immediate and conscious perception of a thermal environment, such as feeling hot or cold at various levels. Furthermore thermal preference (TP) and thermal dissatisfaction level (DL) are additional parameters used to evaluate the thermal environment [33]. All these evaluations require individual surveys through personal inquiries. Interestingly, individuals' morphological characteristics and activity levels also influences personal experience of thermal comfort, thermal sensation, thermal preference and satisfaction differently under a given condition [34].

Traditionally, subjective survey is considered as the true judgment and can be considered as reference value to assess thermal environment [33]. Though, conducting such surveys in busy working environments presents substantial challenges, largely due to the necessity of obtaining replies from every personnel. Thus, researchers are investigating alternative approaches and technologies, such as mathematical models and sensor-based systems [3, 196], to complement or substitute traditional survey methods.

Following that, to predict thermal sensation, *PMV* is one of the widely used mathematical models, used to predict thermal sensation. *PPD* is calculated based on the *PMV* estimation. According to ASHRAE, most people feel comfortable within a *PMV* range of -0.5 to +0.5 [8]. Additionally in this range, more than 90% of individuals are satisfied with the environmental conditions which is acceptable for setting the thermal environment [11]. According to thermal comfort standards, if the *PPD* value is less than 10%, the environment is considered to provide an acceptable level of thermal comfort for most people [11]. This *PMV* -*PPD* model is developed based on heat balance equation between human and environment [11]. This model consists of four environmental features t_a, t_r, *RH* and v_a, and two human factors, I_{cl} and *M*. Though achieving thermal comfort for everyone requires having some meaningful control over their own thermal conditions as an adaptive approach [6]. To understand these individual requirements, it is essential to understand individual differences in thermal perceptions and physiological responses related to thermal comfort.

In current thermal comfort research, specifically within the context of office environments, morphological variations such as *BMI* emerge as critical factors influencing human thermal perceptions [199]. For example, one of the key factor of *BMI* is body mass, which significantly influence thermal comfort [110]. A higher body mass increases internal heat generation and heat capacity. It is primarily composed of muscle tissue and fat, with muscle playing a key role in heat production and fat layer acts as an insulation of the body which reduces heat loss [200]. This often causing higher *BMI* individuals to feel warmer than their leaner counterparts under the same conditions [201]. Body surface area is another key component that affects heat exchange between human and environment. When an individual has a relatively large surface area compared to their body mass, heat is lost more quickly to the surrounding environment. This accelerated heat loss can increase susceptibility to cold. In contrast, a smaller surface area-to-mass ratio reduces heat loss, which may be beneficial in cold climates but can impair heat dissipation in hot conditions, increasing the risk of overheating. These morphological and physiological distinctions significantly affect individuals experience and respond to their adjoining thermal environments.

Gender differences also play a significant role in shaping thermal comfort. One of the basic reasons for this is the variation in *M* between males and females, with males generally shows higher metabolic heat production due to greater muscle mass and different body composition [202, 203]. This discrepancy can lead to different thermal comfort requirements even under identical environmental conditions. Furthermore, I_{cl} also varies by gender, often influenced by sociocultural norms and fashion trends rather than thermal comfort requirements. Mostly in professional condition, men might wear suits and ties, whereas women may wear heavier garments but non-uniform clothing insulation between upper and lower body [204]. This highly impact on thermal comfort levels. Beyond clothing and metabolism, physiological factors like skin temperature distribution, peripheral blood flow and so on, also differ between genders, contributing different thermal sensitivity and thermoregulatory responses [129, 205, 206]. These intrinsic differences can cause one gender to perceive environmental condition differently, someone may find thermally neutral while the other may find it uncomfortable.

Another individual difference named 'cold constitution', known as 'hie-sho' in Japanese [150], originates from traditional East Asian medicine and culture. This refers to a condition where an individual is substantially sensitive to cold [24]. Individuals with cold constitution have a distinct skin blood flow regulatory system with heightened adrenergic sensitivity, leading to increased cutaneous vasoconstriction in the distal extremities during cold exposure [151]. Certain studies focusing on cold constitution, have reported that people with cold constitution experience greater cold sensations even in the thermoneutral environment recommended by ASHRAE [155, 207]. Cold-sensitive people mostly feel cold sensations, particularly in extremities like hands and feet. This symptom was observed when they were exposed to a cold or even neutral environment and they presented greater vascular sensitivity to sympathetic input. [155]. Inadequate blood flow to the extremities due to vasoconstriction can lead to persistent cold sensations [208]. Considering this, to ensure thermal comfort for a long period of time, it is essential to consider the cold constitution with some behavioural adaptations. Like increasing clothing insulation or ingesting hot liquids, which can influence thermal perception and the body's thermoregulatory response. It is also important to address the cold constitution, while designing personal air conditioning systems rather than just relying on a uniform air conditioning environment for all.

In addition, maintaining a thermoneutral environment is also essential for preserving occupants' performance, productivity, and concentration [7]. Working long-term in an unsatisfactory environment can impair users' motivation to work. Without knowing the corresponds to thermal environment, most of the spaces rely on fixed air conditioning settings to create a decent working environment without accounting for individual thermal preferences. This often leads to widespread discomfort and unnecessary energy consumption [209].

Understanding and integrating morphological characteristics as well as gender difference and cold constitution into thermal comfort standards is necessary for designing thermoneutral environments. That environment can satisfy a diversified population, to ensure optimal thermal comfort for every individual. By doing so, it becomes possible to move toward optimal thermoneutral condition that are inclusive and responsive to individual differences, thereby enhancing comfort, well-being, and productivity in a broader scale.

4.2 Aim of the study

This research aims to investigate the individual variability in thermal perceptions and physiological responses such as skin temperature. Besides these, personal factors like *M* and I_{cl}, as well as *PMV* and *PPD* are also investigated by individual differences, due to seek their significant impact on thermal sensations. To focus on individual differences, subjects were classified based on morphological divergency, gender contrast and association with cold constitution.

Additionally, another focus was to predict the individual differences in real time monitoring. Hence, to predict individual differences and physiological response, a novel method was developed by predicting I_{cl}, t_{cl} and t_{sk} via IRT. Furthermore, to predict *M* a method was adopted considering only morphological differences (gender, age, height, and weight). Finally, estimated *PMV* and t_{sk} (face and hand region) through IRT analysis, were compared with reference value of TSV. This comparison aims to assess the individual differences in thermal perceptions and thermoregulatory responses associated with thermal comfort.

4.3 Methods

4.3.1 Participants

Table 4.1 shows the morphological characteristics of the participants. In this experiment, 89 and 75 volunteers participated during summer and winter, respectively. All participants were informed of the research protocols and gave their written informed consent before participation. They were healthy and joined in the experiment in their office. To identify the individual differences, here three types of group division were made, based on *BMI* difference, gender and association with cold constitution. In *BMI* grouping, 22 kg/m^2 considered as the normal and healthy *BMI* [210] for adults. According to that, less than 22 kg/m^2 named as BMI < 22 group and upper than 22 kg/m^2 named as BMI > 22 group. To identify individuals with cold constitution and non-cold constitution, a questionnaire survey was conducted, and two groups were formed as cold constitution (CC) group and non-cold constitution (NC) group.

In summer and winter corresponding to *BMI* differences, BMI < 22 : BMI > 22 were, 37 : 52 and 28 : 47, corresponding to gender, male : female ratio was 72 : 17 and 61 : 14; and according to cold constitution differences, CC : NC were 29 : 60 and 24 : 51.

The research protocol was reviewed and approved by the IRB in the Faculty of Engineering, Hokkaido University (No. R5-8).

4.3.2 Research protocol

This research was designed as a field experiment to investigate the individual difference of real thermal perception in an office environment at Tokyo in Japan, that was fully air conditioned at the range of thermoneutral condition recommended by ISO 7730 [11], all through the year. The experiment was conducted at the 17th floor of a 54 storied building at it's northern, southern and eastern zone. Average floor area was 3400 m^2 with a partition less office space except wash zone and service zones. The building was constructed by reinforced cement concrete structure with double glass windows and blinds, which could restrict solar heat gain. However, central air conditioning was well-maintained, minimizing the influence of outdoor conditions on the indoor environment. Additionally, the experimental spaces were uniform in terms of use and occupancy load. The field study was conducted during summer (2023/08/30 - 2023/09/05) and winter (2024/02/08 - 2024/02/14) among regular office workers.

This research started with morphological data collection by questionnaire survey, such as age, sex, height and body weight. From there, after 60 minutes of adaptation period with regular office activities, thermal voting was collected by subjective questionnaire. Previous studies indicates that 60 minutes is sufficient for adapting in a new thermal environment [211, 212]. After that time armpit temperature was collected as a substitute of t_{cr}. At last, thermal image was taken by IRT to predict t_{cl}, I_{cl} and t_{sk} to estimate *PMV* and *PPD*.

4.3.3 Environmental data

Four main environmental factors t_a, t_g, *RH* and v_a were recorded throughout the experiment. All the data were recorded at 1-second intervals. Data logger setup with the sensors and loggers are shown in Fig. 4.1. During the experiment, t_a was measured using thermistor sensor and recorded using a data logger (NR543R, Nikkiso-Thermo, Japan). The thermistor sensor probe was placed in open air and was connected with the logger to record the t_a. To predict t_g the same thermistor and logger was used with a Bernon type 150 mm black globe (Sibata, Japan). Here the thermistor was placed at the centre of the globe. *RH* was recorded by humidity recorder (RS-14WB, Espec, Japan), with humidity sensor (RSH-4010, Espec, Japan). For v_a, an anemometer logger (Testo 440, Testo, Germany) was used with an omnidirectional hot-wire air flow probe (–TUC 0628 0152, Testo, Germany) to predict wind velocity from all directions. All the data was collected at a height of 0.6 m, which can be considered as the centre of the body mass while in a sitting position. Before starting of the experiment, three sets of data loggers were placed in three zones of the office space and switched on before 30 minutes prior to the experimental time. Finally, once the experiment was conducted, data was stored as a digital file. Based on the t_g outcomes, t_r was calculated by the Equation 3.1, explained in Section 3.3.3 [176].

To predict the individual *PMV* and *PPD* , the values of t_a, t_r, *RH* and v_a measured at their working area were considered for every individual.

4.3.4 Questionnaire survey

To assess individual thermal sensation, a questionnaire survey was conducted. Questionnaire framework was designed according to ISO 28802 [33] guidelines. For clear understanding, it was translated to Japanese with their original meanings. Participants were asked to vote their TSV on 7-point scale, where -3 to 3 represented by cold, cool, slightly cool, neutral, slightly warm, warm and hot sequentially. Additionally, TC (-3 to +3 represented by very uncomfortable, uncomfortable, slightly uncomfortable, neither, slightly comfortable, comfortable, very comfortable), TP (-3 to 3 represented by much cooler, cooler, slightly cooler, no change, slightly warmer, warmer, much warmer), and DL (1 to 4 represented by satisfied, slightly satisfied, slightly non-satisfied, non-satisfied) were asked to evaluate individual differences. Fig. 4.2 shows a sample of thermal sensation questionnaire survey.

Additionally, to identify individuals with cold constitution and non-cold constitution, a questionnaire survey was conducted. Table 4.2 shows the questionnaire used to assess the subjective symptoms of the cold constitution with the criteria for classifying individuals as having a clod constitution or not. This questionnaire was based on previous research on cold constitutions originally designed by Terasawa [213] and modified by Sakaguchi [214], which included some questions that were not used for the classification. These unused questions were excluded in this study. From the survey, two groups were named as the CC group and the NC group.

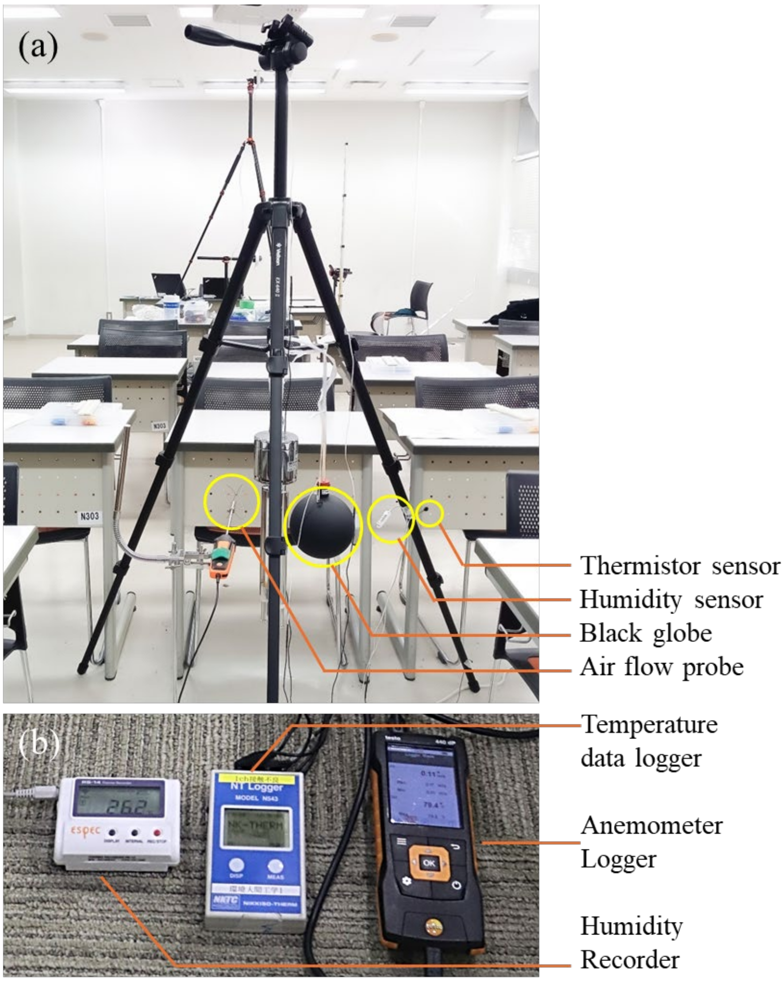

Fig. 4.1. Data logger setup for the environmental data collection (a), different sensors and probes (b), data loggers (c).

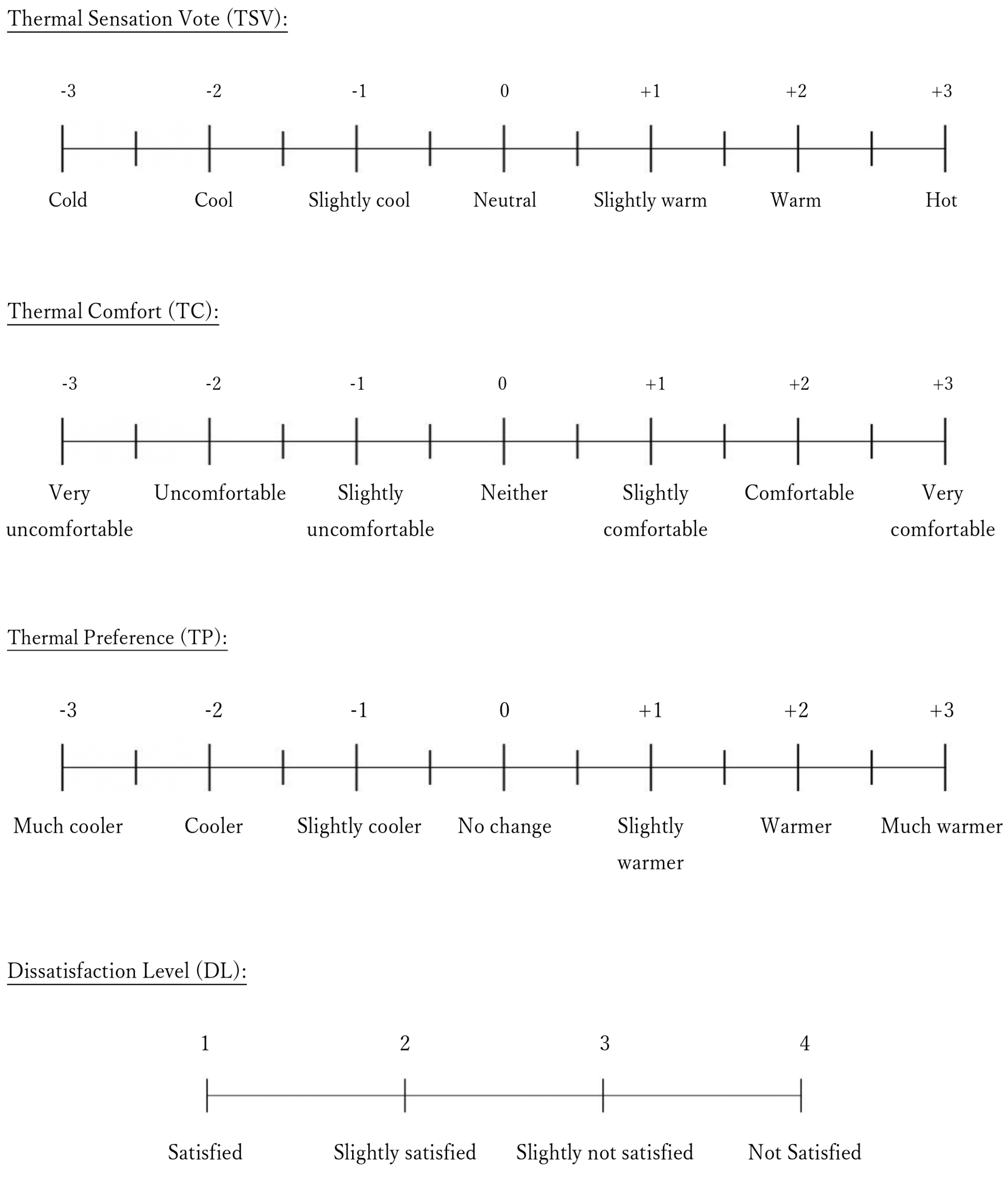

Fig. 4.2. Questionnaire for assessing thermal perceptions.

Table 4.1. Morphological characteristics of the participants.

Morphology	Summer	Winter
Number of participants	89	75
Gender (M : F)	72 : 17	61 : 14
M (BMI < 22 : BMI > 22)	23 : 49	17 : 44
F (BMI < 22 : BMI > 22)	14 : 3	11 : 3
M (CC : NC)	18 : 54	13 : 48
F (CC : NC)	11 : 6	11 : 3
BMI (BMI < 22 : BMI > 22)	37 : 52	28 : 47
BMI < 22 (M : F)	23 : 14	17 : 11
BMI > 22 (M : F)	49 : 3	44 : 3
BMI < 22 (CC : NC)	18: 19	17 : 11
BMI > 22 (CC: NC)	11 : 41	7 : 40
Cold constitution (CC : NC)	29 : 60	24 : 51
CC (M : F)	18 : 11	13 : 11
NC (M : F)	54 : 6	48 : 3
CC (BMI < 22 : BMI > 22)	18 : 11	17 : 7
NC (BMI < 22 : BMI > 22)	19 : 41	11 : 40
Age (year)	36.2 ± 11.9	37.1 ± 11.6
M : F	36.6 ± 12.2 : 34.4 ± 10.7	37.6 ± 11.9 : 34.7 ± 9.9
BMI < 22 : BMI > 22	32.7 ± 11.1 : 38.7± 11.9	33.8 ± 9.6 : 39.0 ± 12.3
CC: NC	36.0 ± 11.6 : 36.3 ± 12.1	36.2 ± 11.1 : 37.5 ± 11.9
Height (cm)	169.3 ± 7.0	168.9 ± 7.0
M : F	171.5 ± 5.6 : 160.1 ± 4.5	171.0 ± 5.1 : 159.3 ± 6.3
BMI < 22 : BMI > 22	167.2 ± 7.6 : 170.9 ± 6.2	166.5 ± 8.1 : 170.3 ± 5.9
CC: NC	167.0 ± 7.5 : 170.5 ± 6.6	165.5 ± 7.2 : 170.5 ± 6.4
Weight (kg)	66.0 ± 11.6	64.9 ± 10.6
M : F	69.4 ± 9.9 : 51.7 ± 6.0	68.0 ± 8.4 : 51.6 ± 8.7
BMI < 22 : BMI > 22	56.3 ± 6.9: 72.9 ± 9.0	54.8 ± 7.5 : 71.0 ± 6.9
CC: NC	59.6 ± 10.3 : 69.1 ± 11.0	57.6 ± 11.1 : 68.4 ± 8.4
Surface area (m^2)	1.76 ± 0.17	1.74 ± 0.16
M : F	1.19 ± 0.19 : 0.83 ± 0.10	1.16 ± 0.16 : 0.82 ± 0.15
BMI < 22 : BMI > 22	0.95 ± 0.16: 1.25 ± 0.19	0.92 ± 0.17 : 1.21 ± 0.14
CC: NC	1.00 ± 0.21 : 1.18 ± 0.22	0.96 ± 0.22 : 1.170.17
Surface area / Weight (m^2/kg)	0.017 ± 0.002	0.017 ± 0.002
M : F	0.017 ± 0.001 : 0.016: 0.001	0.017 ± 0.001 : 0.016 ± 0.001
BMI < 22 : BMI > 22	0.017 ± 0.001 : 0.017 ± 0.001	0.017 ± 0.001 : 0.017 ± 0.001
CC: NC	0.017 ± 0.001 : 0.017 ± 0.001	0.017 ± 0.001 : 0.017 ± 0.001
BMI (kg/m^2)	22.9 ± 3.0	22.7 ± 2.9
M : F	23.5 ± 2.8 : 20.2 ± 2.4	23.2 ± 2.5 : 20.3 ± 3.3
BMI < 22 : BMI > 22	20.1 ± 1.2 : 24.9 ± 2.2	19.7 ± 1.3 : 24.5 ± 1.9
CC: NC	21.3 ± 2.6 : 23.7 ± 2.9	20.9 ± 3.0 : 23.5 ± 2.5

M: male, F: female, *BMI*: body mass index, CC: cold constitution, NC: non-cold constitution.

Table 4.2. Questionnaire on cold constitution.

Cold constitution assessment		
Do you or are you_		
Category "a"	1	Compared to others, I tend to be more sensitive to the cold.
	2	I suffer because my back, hands and feet or some part of my body is cold.
	3	I suffer in air-conditioned rooms because my body feels cold.
	4	Compared to others, my hands and feet are cold.
	5	Even in summer, my hands get cold.
	6	Especially in winter, I sometimes cannot sleep because my feet are cold.
Category "b"	7	I sometimes suffer because my entire body is cold.
	8	I wear thick socks even in the summer because my feet are cold.
	9	Due to cold weather in winter, I always use an electric blanket, mattress or pocket warmer.
	10	I have been suffering from the cold for the last several years.
	11	In winter and on cold days, I urinate more frequently.
	12	Compared to others, my face is more pale.
	13	My hands and feet always feel cold.

This table was modified from a previous study [214].

Criteria for cold constitution:

Answered yes, more than 2 in Category "a" questions or

Answered yes, 1 in Category "a" question + more than 2 in Category "b" questions.

4.3.5 IRT data analysis

To predict I_{cl}, t_{cl} and t_{sk}, IRT was used as a non-intrusive method. In this experiment, thermal images were taken using an IRT camera (R500EX-S, Nippon Avio, Japan), which is well-renowned for its high-resolution imaging capabilities and specific temperature measurement accuracy. The camera was placed at a height of 0.90 m from the ground, considering the camera plane was perpendicular with the body plane at the centre of the body in standing position [178]. For t_{cl} and t_{sk} prediction, same technique and process was followed, described at Section 3.3.5. First the thermal image was taken during the survey, and then regions of interest were mapped in the computer application and finally the required temperature was predicted.

Prior the experiment IRT camera's temperature prediction, the camera's output was calibrated using a thermistor, which measured true known temperature of a black body surface, to ensure the validation of the IRT camera.

4.3.6 *PMV* and *PPD* prediction

According to ISO 7730, *PMV* was calculated by the Equation 2.4, explained in Section 2.5.1. It was mainly calculated from four environmental factors (t_a, t_g, *RH* and v_a) and two personal factors (*M* and I_{cl},).

Additionally, utilizing *PMV* value determined, *PPD* can be calculated by the Equation 2.5, explained in Section 2.5.1.

4.3.7 I_{cl} estimation

According to ISO 7730, there is a relationship between I_{cl} with t_{cl} and t_{sk}, as explained in Section 2.5.1.1.4. In that prediction of I_{cl}, it was estimated based on the ratio of the temperature difference between mean skin temperature under the clothing and clothing surface temperature to the rate of dry heat loss.

In this scenario, IRT was used to predict t_{cl} and t_{sk}. t_{cl} and t_{sk} were estimated by the process explained at Section 3.3.5. Firstly, thermal image was captured by IRT both front and back side and then the average t_{cl} was calculated by the camera application. Average of $t_{forehead}$ and $t_{dorsal\ hand}$ was calculated as t_{sk}. From that I_{cl} was estimated for every individual.

4.3.8 *M* estimation

For the prediction of *M*, a method was adopted based on *BMR* and *PAR* [215]. *BMR* refers to the amount of energy needs to maintain the vital activity of the awake state. It indicates the energy required for our body at rest in supine position, in a fasting situation (without breakfast), and in an awakening condition [79]. *PAR* is the ratio that expresses the energy expended in a particular activity (such as, sitting, standing, and desk work) and relative to an individual's *BMR* [80, 81]. Here *M* was calculated by the equations explained in Section 2.5.1.2.5. It is notable that *BMR* depends on individual morphological differences like age, sex, body height and weight and the adopted formula was derived from studies involving Asian participants. *PAR* also relies on gender and *BMI* and the values of *PAR* used here also derived from studies involving Asian participants.

4.3.9 Local t_{sk} prediction

In this research, non-covered skin surface temperature was examined by IRT analysis. In the face region, skin temperatures of the forehead ($t_{forehead}$), nose (t_{nose}), chin (t_{chin}), neck (t_{neck}), cheek (t_{cheek}) (average of both sides), and inner eye canthus temperature ($t_{eye\ canthus}$) (average of both eyes) were collected by IRT application through spot analysis. In hand region, dorsal hand ($t_{dorsal\ hand}$) dorsal fingertip ($t_{dorsal\ finger}$), palmar hand ($t_{palmar\ hand}$) and palmar fingertip skin temperature ($t_{palmar\ finger}$) were analysed using the same techniques. Additionally, previous researches mentioned $\Delta t_{proximal-distal}$ as a parameter of vasoconstriction [27, 28]. To observe that, $\Delta t_{forehead-nose}$ and $\Delta t_{palm\ hand-palmar\ finger}$ were calculated and analysed.

4.3.10 Statistical analysis

The group differences in TSV, TC, TP and DL were analysed using Mann-Whitney *U* test. Group differences in *I_{cl}, M, PMV, PPD*, t_{sk} and $\Delta t_{proximal-distal}$ predictions were analysed by non-paired Student's *t*-

test. TSV and *PMV* was analysed by Wilcoxon signed ranked test. Correlation between TSV and *PMV*, as well as TSV and t_{sk} was analysed by Spearman rank correlation test. In addition, correlation analysis with *BMI* was analysed by Pearson correlation analysis with I_{cl}, M, t_{sk} and $\Delta t_{proximal-distal}$ (as parametric data) and others with Spearman rank correlation test (as non-parametric data). Correlation analysis with gender and cold constitution were analysed by Spearman rank correlation test. All data are presented as mean ± SD. In all statistical analysis, differences at $p < 0.05$ were considered significant. The analysis was conducted using IBM SPSS statistics version 20, IBM software. Here, gender was also encoded as a binary variable, where males were assigned a value of 0 and females were assigned a value of 1. In addition, cold constitution individuals were coded as 1 and non-cold constitution individuals were coded as 0. This coding scheme was used to facilitate correlation analysis and other statistical procedures that require numerical input.

4.4 Results

This research was carried out in a thermoneutral office environment to signify the differences of thermal sensations between *BMI* variances, gender differences and CC and NC groups via IRT technology. Table 4.3 represents the environmental condition in summer and winter. It was observed that both in summer and winter, the environment was well and uniformly controlled. It is noticeable that, because of the similar environmental condition in two seasons, it was enabled to focus on individual variations.

Here, outcomes can be specified by thermal sensation differences, I_{cl}, M, *PMV* and *PPD*, t_{sk} and $\Delta t_{proximal-distal}$ variations, and comparison between TSV and *PMV* predictions.

Table 4.3. Environmental conditions during the research period.

Environmental condition	Summer	Winter
t_a (°C)	25.09 ± 0.28	25.52 ± 0.50
t_r (°C)	25.62 ± 0.26	25.72 ± 0.61
RH (%)	59.06 ± 1.71	36.10 ± 1.82
v_a (m/s)	0.14 ± 0.00	0.11 ± 0.04
p_a (P_a)	1924.7 ± 38.4	1477.7 ± 65.5
h_c (W/(m^2·K))	4.46 ± 0.07	4.06 ± 0.51
h_r (W/(m^2·K))	5.95 ± 0.02	5.95 ± 0.03

t_a: air temperature, t_r: mean radiant temperature, *RH*: relative humidity, v_a: air velocity, p_a: water vapor pressure in ambient air, h_c: convective heat transfer coefficient, h_r: radiative heat transfer coefficient.

4.4.1 *BMI* differences

4.4.1.1 Morphological differences

Morphological differences are fundamental factors that significantly influence both individual thermal sensation and thermoregulatory responses. It was observed that in the BMI > 22, percentage of females comparing with males were low, as well percentage of cold constitutional individuals comparing with non-cold constitutional individuals were lower. Additionally, the height and weight of BMI > 22 was significantly higher than BMI < 22 ($p < 0.05$) (Table 4.1).

4.4.1.2 Comparison of thermal perceptions

Fig. 4.3 shows the comparison of TSV, TC, TP, and DL between the two BMI groups (BMI < 22 vs. BMI > 22). In summer, the BMI > 22 group showed significantly higher TSV compared to the BMI < 22 group ($p < 0.01$). Additionally, TP in the BMI > 22 group was significantly lower compared to the BMI < 22 group ($p < 0.01$). No significant differences in TC and DL were found between the groups. In winter, no significant differences were observed between these two groups in TSV, TC, TP, and DL.

4.4.1.3 Comparison of I_{cl}

There was no significant difference in I_{cl} between these two groups (Fig. 4.4). However, I_{cl} in winter was significantly higher compared to I_{cl} in summer ($p < 0.01$), for both the BMI < 22 and BMI > 22 groups.

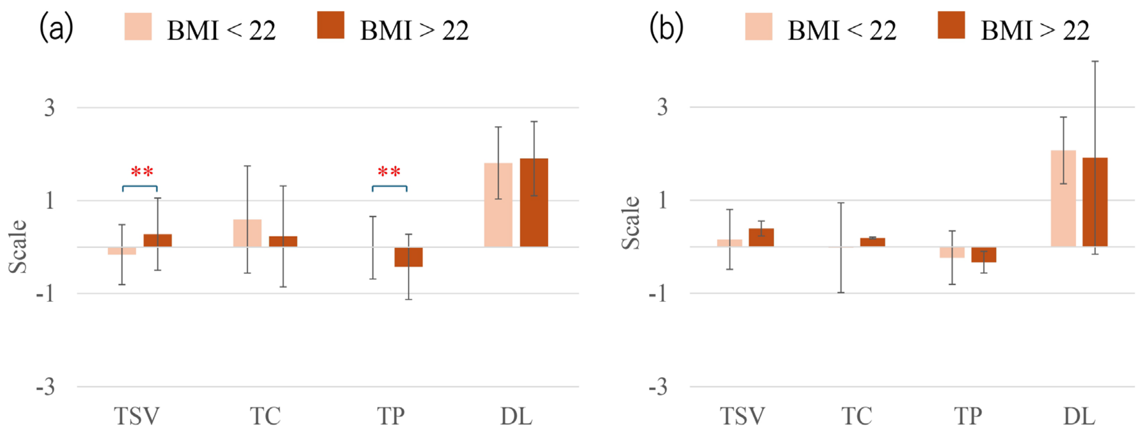

Fig. 4.3. Comparison of thermal sensation vote: TSV; thermal comfort: TC; thermal preference: TP; dissatisfaction level: DL, between BMI < 22 and BMI > 22 groups in summer (a) and winter (b).
(Summer, BMI < 22: BMI > 22 = 37:52; Winter, BMI < 22: BMI > 22 = 28:47)
Values are mean ± standard deviation. *: $p < 0.05$ between BMI groups.

4.4.1.4 Comparison of *M*

Fig. 4.5 shows the comparison of M between the BMI < 22 and BMI > 22 groups. The BMI > 22 group showed significantly higher MET compared to the BMI < 22 group in both seasons ($p < 0.01$).

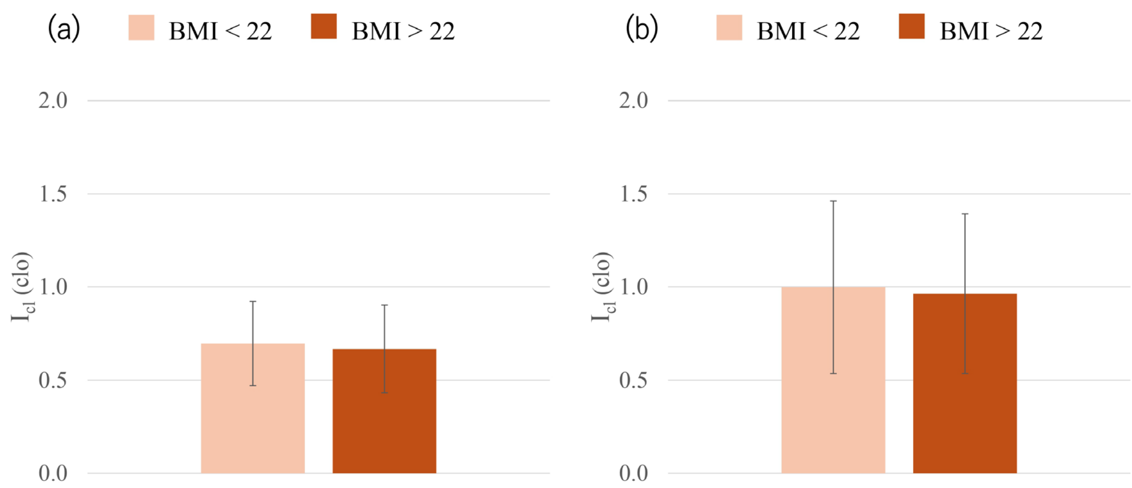

Fig. 4.4. Comparison of clothing insulation (I_{cl}) between BMI < 22 and BMI > 22 groups in summer (a) and winter (b).

(Summer, BMI < 22: BMI > 22 = 37:52; Winter, BMI < 22: BMI > 22 = 28:47)

Values are mean ± standard deviation.

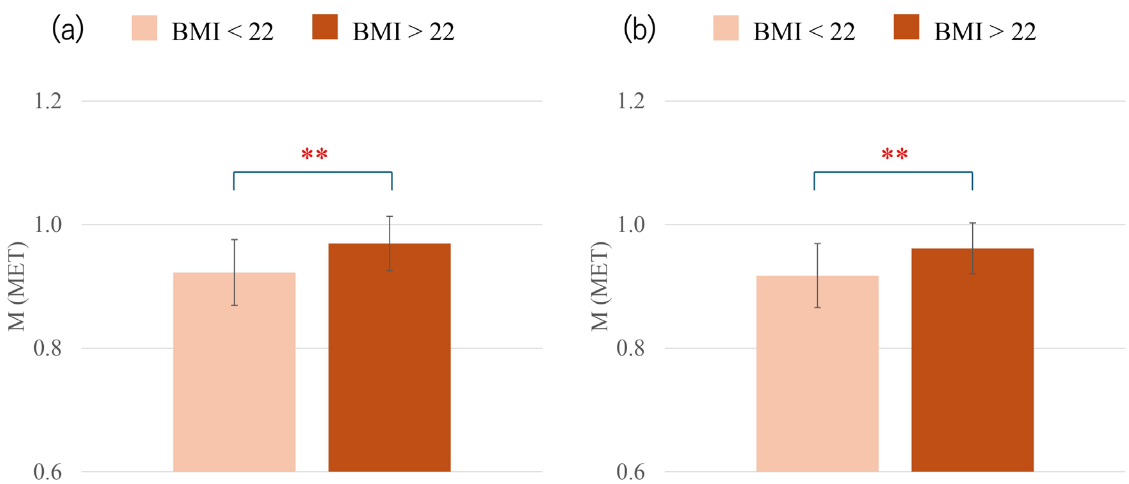

Fig. 4.5. Comparison of metabolic rate (M) between BMI < 22 and BMI > 22 groups in summer (a) and winter (b).

(Summer, BMI < 22: BMI > 22 = 37:52; Winter, BMI < 22: BMI > 22 = 28:47)

Values are mean ± standard deviation. **: $p < 0.01$ between BMI groups.

4.4.1.5 Comparison of *PMV* and *PPD*

Fig. 4.6 shows the *PMV* comparisons between the BMI < 22 and BMI > 22 groups. In both seasons, there were no significant differences in *PMV* between these groups. Additionally, in the *PPD* comparison, there were no significant differences observed between the two groups in both seasons (Fig. 4.7).

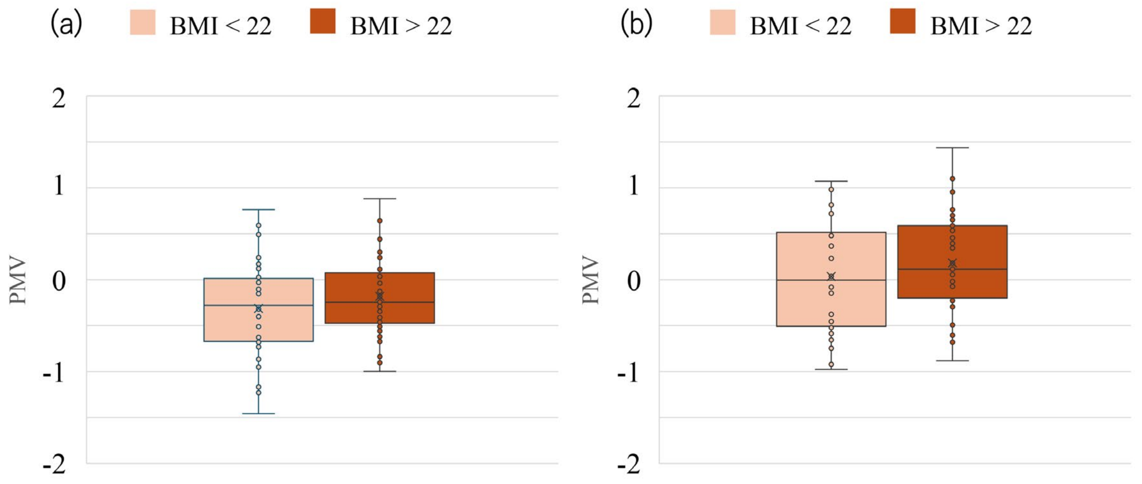

Fig. 4.6. Comparison of predicted mean vote (*PMV*) between BMI < 22 and BMI > 22 groups in summer (a) and winter (b).

(Summer, BMI < 22: BMI > 22 = 37:52; Winter, BMI < 22: BMI > 22 = 28:47)

Values are mean ± standard deviation.

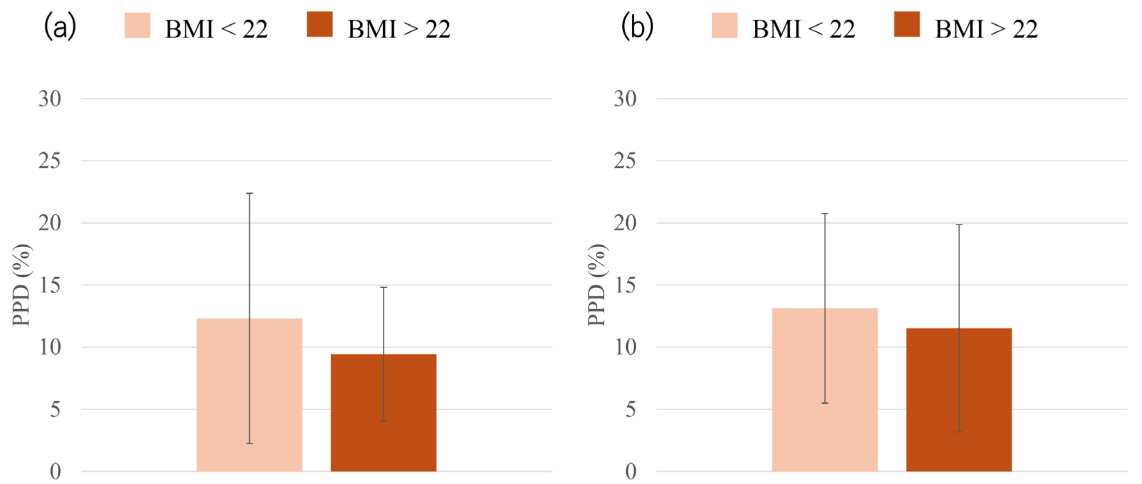

Fig. 4.7. Comparison of predicted percentage of dissatisfied (*PPD*) between BMI < 22 and BMI > 22 groups in summer (a) and winter (b).

(Summer, BMI < 22: BMI > 22 = 37:52; Winter, BMI < 22: BMI > 22 = 28:47)

Values are mean ± standard deviation.

4.4.1.6 Comparison between TSV and *PMV*

Comparing the TSV and *PMV* prediction, the BMI > 22 group showed significantly higher TSV than *PMV* prediction in summer ($p < 0.01$). However, in winter, there was no significant difference (Fig. 4.8). For the BMI < 22 group, there were no significant differences between the TSV and *PMV*.

Additionally, Table 4.4 shows the *PMV* and TSV comparison with the absolute mean values differences with SD, RMSE value and correlation between TSV and *PMV*. There was no significant correlation observed between TSV and *PMV* in all comparisons for *BMI* groups.

4.4.1.7 Comparison of t_{sk}

Local skin temperature comparison between the BMI < 22 and BMI > 22 groups are shown in Fig. 4.9. The BMI > 22 group showed significantly higher t_{nose} temperatures compared to the BMI < 22 group in both seasons ($p < 0.01$). Similarly, the BMI > 22 group showed significantly higher temperatures in the t_{cheek} and $t_{dorsal\ finger}$ in both seasons ($p < 0.05$). In addition, in summer, the BMI > 22 group showed significantly higher temperatures in the $t_{palmar\ finger}$ ($p < 0.05$) and dorsal hand ($p < 0.01$) compared to the BMI < 22 group.

Table 4.5 shows the correlation coefficient (ρ) between TSV and local skin temperature. In summer, for the BMI < 22 group, the temperatures of the t_{cheek} and $t_{eye\ canthus}$ were significantly corelated with TSV ($p < 0.05$ for each). For the BMI > 22 group, the temperatures of the $t_{palmar\ finger}$ and $t_{dorsal\ finger}$ were significant corelated with TSV ($p < 0.05$ for each). In winter, the BMI < 22 group showed significant correlation between TSV and the temperatures of the t_{nose}, $t_{palmar\ finger}$ and $t_{dorsal\ finger}$ ($p < 0.05$ for each). However, no significance correlations found between TSV and local skin temperatures for the BMI > 22 group.

Table 4.4. *PMV* and TSV comparison with absolute mean difference ± SD, RMSE and correlation coefficient "r" value in *BMI* groups.

	Absolute mean difference ± SD	RMSE	r value
Summer			
BMI < 22	0.59 ± 0.51	0.78	0.18
BMI > 22	0.70 ± 0.63	0.94	0.15
Winter			
BMI < 22	0.85 ± 0.67	1.08	-0.14
BMI > 22	0.60 ± 0.48	0.76	0.28

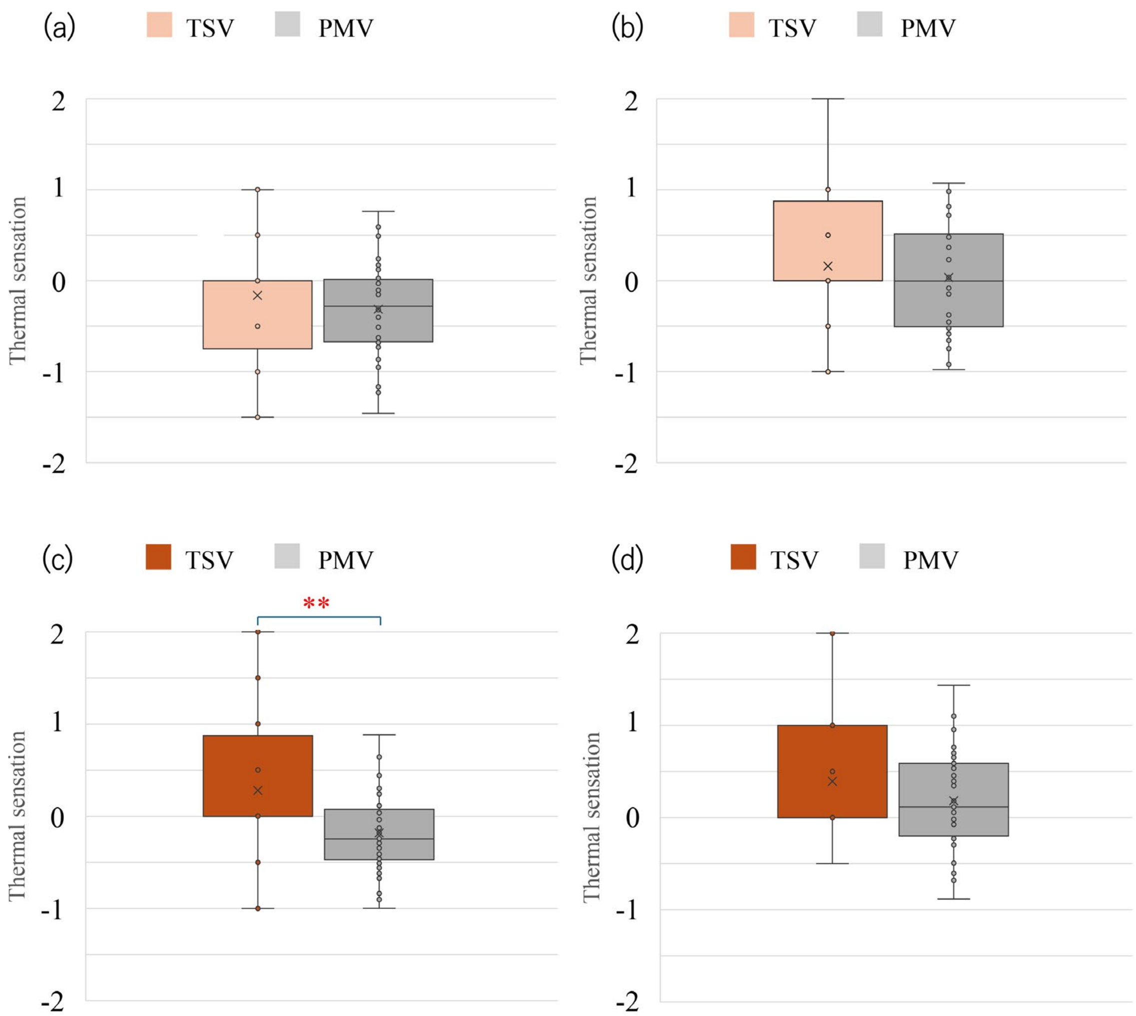

Fig. 4.8. Comparison of thermal sensation vote (TSV) and predicted mean vote (*PMV*) for BMI < 22: summer (a) and winter (b); for BMI > 22: Summer (c) and Winter (d).

(Summer, BMI < 22: BMI > 22 = 37:52; Winter, BMI < 22: BMI > 22 = 28:47)

Values are mean ± standard deviation. **: p < 0.01 between TSV and *PMV*.

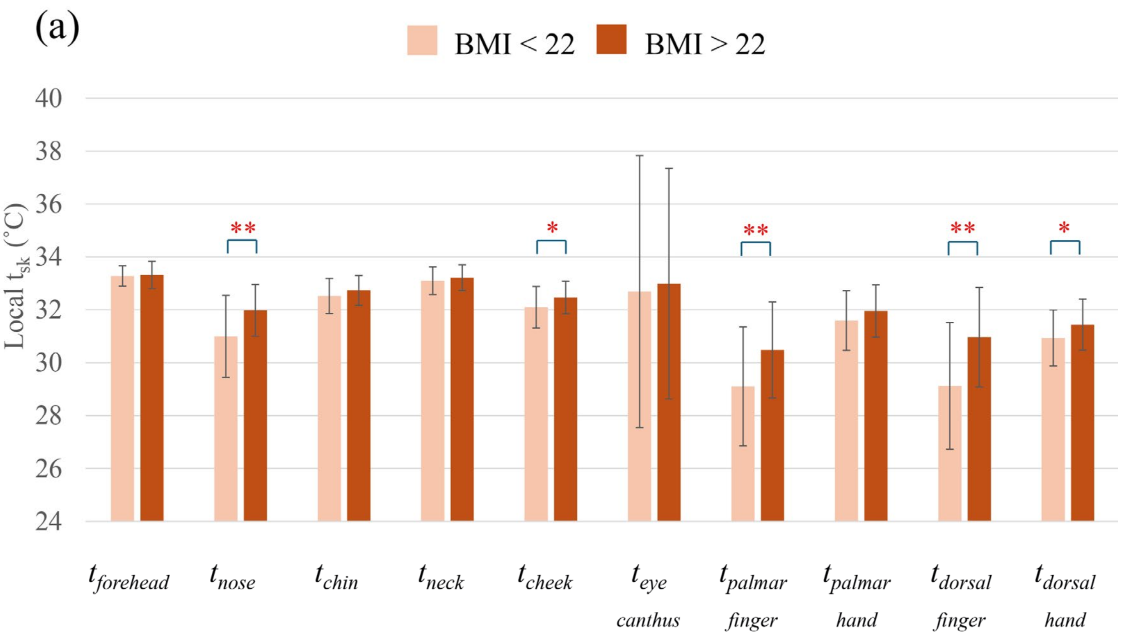

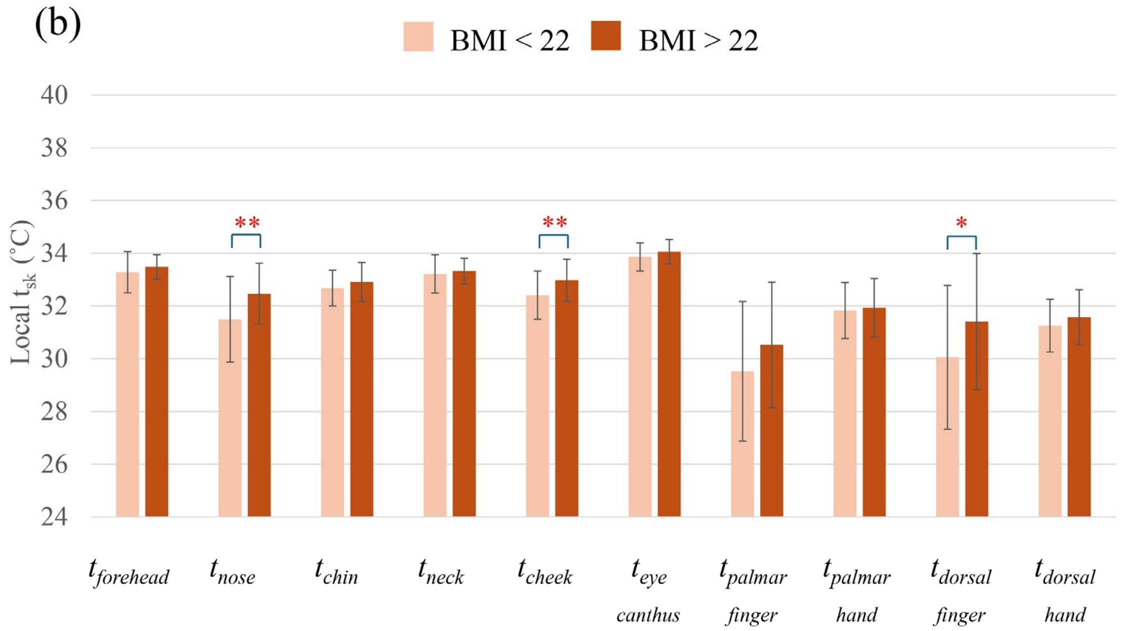

Fig. 4.9. Comparison of local skin temperature (t_{sk}) between BMI < 22 and BMI > 22 groups in summer (a) and winter (b).

(Summer, BMI < 22: BMI > 22 = 37:52; Winter, BMI < 22: BMI > 22 = 28:47)

Values are mean ± standard deviation. *: $p < 0.05$, **: $p < 0.01$ between BMI groups.

Table 4.5. Local skin temperature (t_{sk}) and TSV comparison with Spearman's rank corelation test in *BMI* groups.

		$t_{forehead}$	t_{nose}	t_{chin}	t_{neck}	t_{cheek}	$t_{eye\ canthus}$	$t_{palmar\ finger}$	$t_{palmr\ hand}$	$t_{dorsal\ finger}$	$t_{dorsal\ hand}$
Summer											
BMI < 22	ρ value	0.25	0.32	0.22	0.20	0.46*	0.34*	0.16	0.15	0.11	0.15
BMI > 22	ρ value	-0.07	0.17	-0.05	-0.05	0.09	-0.04	0.31*	0.24	0.27*	0.22
Winter											
BMI < 22	ρ value	0.26	0.39*	0.31	0.27	0.10	0.16	0.40*	0.27	0.43*	0.18
BMI > 22	ρ value	-0.02	-0.09	-0.16	-0.08	-0.07	0.01	-0.18	-0.19	-0.06	-0.04

Values are corelation coefficient (ρ value). * Significant correlation ($p < 0.05$).

4.4.1.8 Comparison of $\Delta t_{proximal - distal}$

Fig. 4.10. Comparison of $\Delta t_{proximal - distal}$ between the BMI < 22 and BMI > 22 groups. It was observed that BMI < 22 group had higher $\Delta t_{forehead - nose}$ and $\Delta t_{palmar\ hand - palmar\ finger}$ comparing with BMI > 22 groups in both summer and winter ($p < 0.05$).

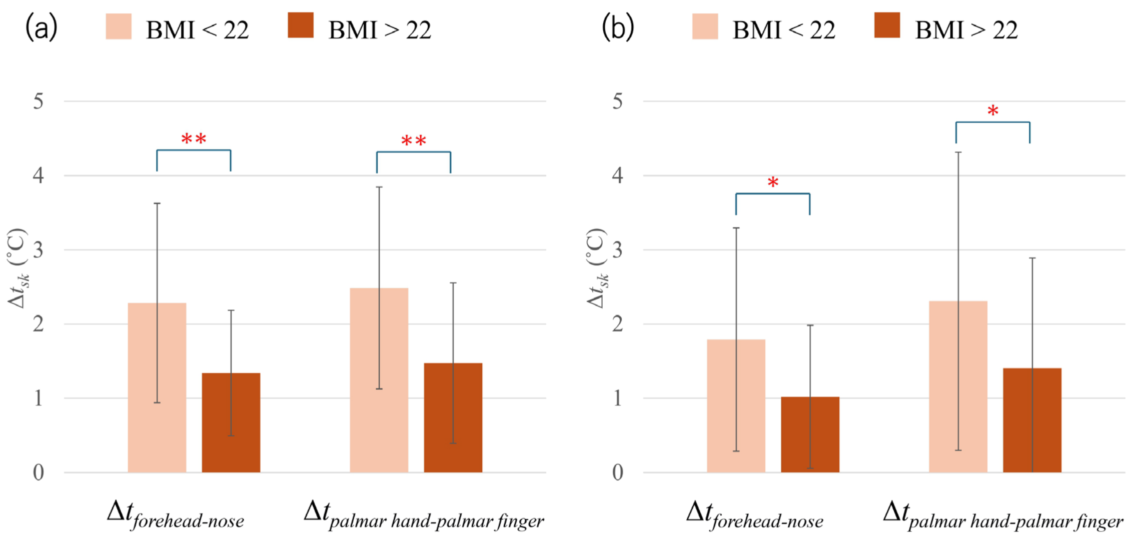

Fig. 4.10. Comparison of $\Delta t_{proximal\text{-}distal}$ between BMI < 22 and BMI > 22 groups in summer (a) and winter (b).

(Summer, BMI < 22: BMI > 22 = 37:52; Winter, BMI < 22: BMI > 22 = 28:47)

Values are mean ± standard deviation. *: $p < 0.05$, **: $p < 0.01$ between BMI groups.

4.4.1.9 Correlation analysis with *BMI*

Table 4.6 represents the relationships between *BMI* and various factors, including gender, CC, I_{cl}, *M,* TSV, TC, TP, DL, *PMV* and *PPD*. Furthermore, partial correlations among these factors were analyzed to assess their relationships with *BMI*. In summer, gender, CC, *M*, TSV, TP, *PMV* and *PPD* had significant moderate correlations with *BMI* (ρ = -0.47, r = -0.64, ρ = 0.63, 0.36, -0.41, r = 0.29 and 22, respectively, $p < 0.05$). In addition, in partial correlation analysis, when gender was controlled, correlation with CC, *M,* TSV, TP and *PMV* become slightly lower (ρ = -0.27, 0.53, 0.26, -0.27 and 0.26, respectively, $p < 0.05$). When CC was controlled, gender, *M,* TP and *PMV* were significantly correlated, though it was little weaker (ρ = -0.36, 0.58, -0.23 and 0.23, respectively, $p < 0.05$). When I_{cl} was controlled, mostly all the correlations remained same and significant correlations observed for gender, CC, *M,* TSV, TP, *PMV* and *PPD* (ρ = -0.47, -0.37, 0.65, 0.34, -0.31, 0.48 and -0.22, respectively, $p < 0.05$). When *M* was controlled, no significant correlation was observed. While gender and CC were controlled together, *M* and *PMV* were significantly correlated with *BMI* (ρ = 0.51 and 0.23, respectively, $p < 0.05$).

In winter, gender, CC and *M* showed significant correlation with *BMI* (ρ = -0.38, -0.42 and r = 0.56, respectively, $p < 0.01$). In partial correlation, while gender was controlled, reduced correlation was observed and CC, *M* and TSV showed significant correlation with *BMI* (ρ = -0.29, 0.42 and 0.31, respectively, $p < 0.05$). Reduced correlation found while CC was controlled and then gender and *M* showed significant correlation with *BMI* (ρ = -0.25 and 0.45, respectively, $p < 0.05$). When I_{cl} was controlled, mostly all the correlations remained same and gender, CC, *M,* TSV, and *PMV* showed significant correlation (ρ = -0.44, -0.42, 0.57, 0.24 and 0.33, respectively, $p < 0.05$). When *M* was controlled, reduced correlation observed, only CC and TSV showed significant correlation (ρ = -0.23 and 0.27, respectively, $p < 0.05$). While gender and CC were controlled together, *M* and TSV showed significantly correlated with *BMI* (ρ = 0.41 and 0.27, respectively, $p < 0.05$).

In Table 4.7, the correlations between *BMI* and local t_{sk} as well as $\Delta t_{proximal\text{ - }distal}$ are shown. In summer, several significant correlations were noted. Significant correlations were figured out for t_{nose}, t_{chin}, t_{cheek}, $t_{palmr\ finger}$, $t_{palmr\ hand,}$ $t_{dorsal\ finger}$ and $t_{dorsal\ hand}$ with *BMI* (r = 0.40, 0.21, 0.23, 0.38, 0.23, 0.43 and 0.24, respectively, $p < 0.05$). Significant negative correlations were observed for $\Delta t_{forehead\text{ - }nose}$ and $\Delta t_{palmar\ hand\text{ - }palmar\ finger}$ with the *BMI* (r = -0.44 and -0.47, respectively, $p < 0.01$). In the partial correlation analysis while gender was controlled, correlation level became little weaker, however t_{nose}, $t_{palmr\ finger}$, $t_{dorsal\ finger}$, $\Delta t_{forehead\text{ - }nose}$ and $\Delta t_{palmar\ hand\text{ - }palmar\ finger}$ were significantly correlated with the *BMI* (ρ = 0.25, 0.24, 0.30, -0.32 and -0.28, respectively, $p < 0.05$). Similarities found while CC was controlled, little bit weaker correlation observed for t_{nose}, $t_{palmr\ finger}$, $t_{dorsal\ finger}$, $\Delta t_{forehead\text{ - }nose}$ and $\Delta t_{palmar\ hand\text{ - }palmar\ finger}$ with the *BMI* (ρ = 0.31, 0.30, 0.36, -0.37 and -0.35, respectively, $p < 0.01$). However, while I_{cl} was controlled mostly all the correlations remained same and significant correlations with the *BMI* were observed at t_{nose}, $t_{palmar\ finger}$, $t_{dorsal\ finger}$, $\Delta t_{forehead\text{ - }nose}$ and $\Delta t_{palmar\ hand\text{ - }palmar\ finger}$ (ρ = 0.40, 0.36, 0.42, -0.45 and -0.41, respectively, p <

0.01). While M was controlled, correlation became weaker, though $t_{palmar\ finger}$, $t_{dorsal\ finger}$, $\Delta t_{forehead\ -\ nose}$ and $\Delta t_{palmar\ hand\ -\ palmar\ finger}$ were significantly correlated (ρ = 0.25, 0.31, -0.28 and -0.27, respectively, $p < 0.05$). When gender and CC controlled together only $t_{dorsal\ finger}$, $\Delta t_{forehead\ -\ nose}$ and $\Delta t_{palmar\ hand\ -\ palmar\ finger}$ were significantly correlated with *BMI* (ρ = 0.28, -0.27 and -0.24, respectively, $p < 0.05$).

In the winter, there were hardly any significant correlation found with *BMI*, though $t_{nose,}$ t_{cheek} and $\Delta t_{palmar\ hand\ -\ palmar\ finger}$ had significant correlation (r = 0.26, 0.36 and 0.23 $p < 0.01$). Controlling CC, I_{cl}, gender and CC together, t_{cheek} was still significantly correlated with *BMI* (ρ = 0.29, 0.36 and 0.29, respectively, $p < 0.05$). Beside that I_{cl} controlled condition $\Delta t_{palmr\ hand\ -\ palmar\ finger}$ was significantly correlated with *BMI* (ρ = -0.23, $p < 0.05$). While M was controlled, no significant correlation was observed.

Fig. 4.11 shows the Correlation between *BMI* and $\Delta t_{proximal\ -\ distal}$ in summer and winter. It was observed that lower *BMI* individuals tend to have greater $\Delta t_{proximal\ –\ distal}$. Comparing the summer and winter $\Delta t_{proximal\ –\ distal}$, in winter $\Delta t_{proximal\ –\ distal}$ was lower for the smaller *BMI* participants.

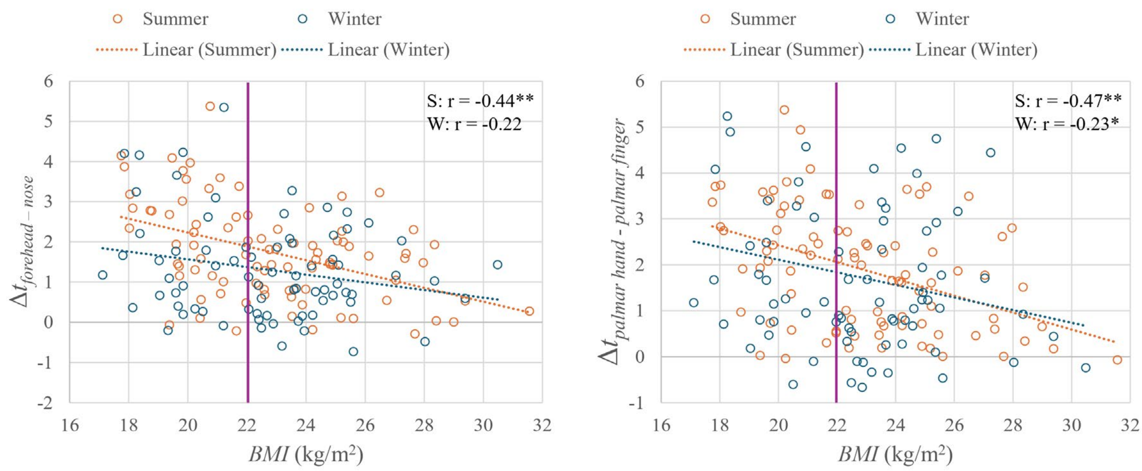

Fig. 4.11. Correlation between *BMI* and $\Delta t_{proximal\ -\ distal}$ in summer and winter.

(S : Summer, W : Winter)

**: $p < 0.01$ between *BMI* and $\Delta t_{proximal\ –\ distal}$, *: $p < 0.05$ between *BMI* and $\Delta t_{proximal\ -\ distal}$.

Table 4.6. Correlations of the *BMI* with gender, CC, I_{cl}, *M,* thermal perceptions, *PMV* and *PPD*.

	Gender	CC	I_{cl}	M	TSV	TC	TP	DL	PMV	PPD
Summer										
r or ρ value	-0.47**	-0.38**	-0.02	0.64**	0.36**	-0.17	-0.41**	0.01	0.29**	-0.22*
Partial ρ (controlled: gender)	-	-0.27*	0.19	0.53**	0.26*	-0.17	-0.27*	0.13	0.26*	-0.12
Partial ρ (controlled: CC)	-0.36**	-	-0.01	0.58**	0.22	-0.21	-0.23*	0.03	0.23*	-0.14
Partial ρ (controlled: I_{cl})	-0.47**	-0.37**	-	0.65**	0.34**	-0.17	-0.31**	0.04	0.48**	-0.22*
Partial ρ (controlled: M)	0.14	-0.20	0.19	-	0.15	-0.12	-0.15	0.11	0.10	0.03
Partial ρ (controlled: gender, CC)	-	-	0.16	0.51**	0.18	-0.20	-0.21	0.11	0.23*	-0.08
Winter										
r or ρ value	-0.38**	-0.42**	-0.03	0.56**	0.22	0.01	-0.17	0.00	0.14	-0.06
Partial ρ (controlled: gender)	-	-0.29*	0.20	0.42**	0.31**	0.03	-0.12	0.00	0.22	0.11
Partial ρ (controlled: CC)	-0.25*	-	0.02	0.45**	0.21	0.01	-0.13	0.01	0.12	-0.01
Partial ρ (controlled: I_{cl})	-0.44**	-0.42**	-	0.57**	0.24*	0.02	-0.12	-0.03	0.33**	-0.06
Partial ρ (controlled: M)	0.06	-0.23*	0.17	-	0.27*	0.12	-0.03	-0.11	0.11	0.05
Partial ρ (controlled: gender, CC)	-	-	0.17	0.41**	0.27*	0.02	-0.12	0.02	0.18	0.09

BMI: body mass index, I_{cl}: clothing insulation, *M*: metabolic rate, TSV: thermal sensation vote, TC: thermal comfort, TP: thermal preference, DL: dissatisfaction level, *PMV*: predicted mean vote, *PPD*: predicted percentage of dissatisfied. Values are correlation coefficient (ρ value).

**: Significant correlation ($p < 0.01$), *: Significant correlation ($p < 0.05$).

Table 4.7. Correlation of the *BMI* with local t_{sk} and Δt_{sk} differences.

	$t_{forehead}$	t_{nose}	t_{chin}	t_{neck}	t_{cheek}	$t_{eye\ canthus}$	$t_{palmar\ finger}$	$t_{palmr\ hand}$	$t_{dorsal\ finger}$	$t_{dorsal\ hand}$	$\Delta t_{forehead\ -\ nose}$	$\Delta t_{palmar\ hand\ -\ palmar\ finger}$
Summer												
r value	0.01	0.40**	0.21*	0.05	0.23*	0.04	0.38**	0.23*	0.43**	0.24*	-0.44**	-0.47**
Partial ρ (controlled: gender)	-0.10	0.25*	0.11	-0.05	0.05	0.07	0.24*	0.13	0.30**	0.15	-0.32**	-0.28**
Partial ρ (controlled: CC)	-0.04	0.31**	0.13	-0.06	0.12	0.02	0.30**	0.16	0.36**	0.18	-0.37**	-0.35**
Partial ρ (controlled: I_{cl})	-0.03	0.40**	0.18	-0.01	0.20	0.04	0.36**	0.21	0.42**	0.22	-0.45**	-0.41**
Partial ρ (controlled: *M*)	-0.17	0.19	0.12	-0.07	0.00	-0.06	0.25*	0.16	0.31**	0.17	-0.28*	-0.27*
Partial ρ (controlled: gender, CC)	-0.10	0.21	0.08	-0.09	0.01	0.05	0.21	0.11	0.28*	0.13	-0.27*	-0.24*
Winter												
r value	0.14	0.26*	0.16	0.03	0.36**	0.13	0.10	-0.13	0.12	0.00	-0.22	-0.23*
Partial ρ (controlled: gender)	0.05	0.11	0.07	-0.08	0.27*	0.08	0.01	-0.13	0.03	0.02	-0.10	-0.10
Partial ρ (controlled: CC)	0.06	0.14	0.09	-0.10	0.29*	0.05	0.03	-0.14	0.08	-0.04	-0.13	-0.14
Partial ρ (controlled: I_{cl})	0.14	0.26*	0.16	0.02	0.36**	0.13	0.10	-0.13	0.12	0.00	-0.22	-0.23*
Partial ρ (controlled: *M*)	-0.05	0.04	0.05	-0.12	0.22	0.05	0.05	-0.06	0.05	0.07	-0.07	-0.11
Partial ρ (controlled: gender, CC)	0.02	0.07	0.05	-0.14	0.25*	0.04	-0.01	-0.14	0.03	-0.01	-0.07	-0.08

BMI: body mass index, I_{cl}: clothing insulation, *M*: metabolic rate, $t_{forehead}$: forehead skin temperature, t_{nose}: nose skin temperature, t_{chin}: chin skin temperature, t_{neck}: neck skin temperature, t_{cheek}: cheek skin temperature, $t_{eye\ canthus}$: eye canthus skin temperature, $t_{dorsal\ hand}$: dorsal hand skin temperature, $t_{palmar\ hand}$: palmar hand skin temperature, $t_{dorsal\ finger}$: dorsal finger skin temperature, and $t_{palmar\ finger}$: palmar finger skin temperature. Values are correlation coefficient (ρ value).

**: Significant correlation ($p < 0.01$), *: Significant correlation ($p < 0.05$).

4.4.2 Gender differences

4.4.2.1 Morphological differences

It was observed that in the female group, percentage of BMI > 22 individuals were lower comparing with BMI < 22 individuals. Additionally, it was observed that in the female group, percentage of non-cold constitution individuals were lower comparing with cold constitution individuals. Additionally, females hight, weight and *BMI* were significantly lower comparing with males ($p < 0.05$) (Table 4.1).

4.4.2.2 Comparison of thermal perceptions

Fig. 4.12 shows the comparison of TSV, TC, TP and DL between the two gender groups. In summer, the male group showed higher TSV compared to the female group with a statistically significant difference ($p < 0.05$). In that season, TC, TP and DL showed no significant gender differences. In winter, there were no significant gender differences observed in TSV, TC, TP, and DL. However, the female group showed a wider range in DL during winter compared to the male group.

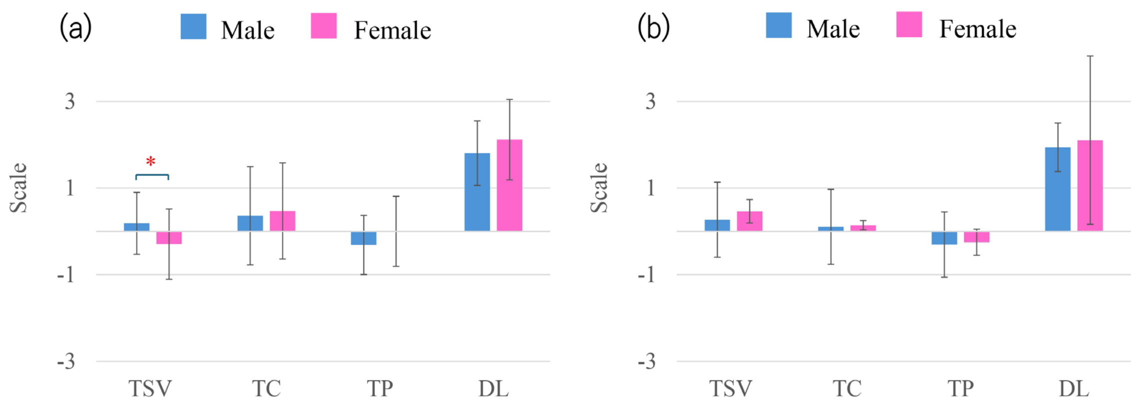

Fig. 4.12. Comparison of thermal sensation vote (TSV), thermal comfort (TC), thermal preference (TP) and dissatisfaction level (DL), between male and female groups in summer (a) and winter (b). (Summer, M:F = 72:17; Winter, M:F = 61:14)
Values are mean ± standard deviation. *: $p < 0.05$ between gender groups.

4.4.2.3 Comparison of I_{cl}

Fig. 4.13 shows the comparison of clothing insulation predicted by IRT. I_{cl} was significantly higher ($p < 0.01$) in the female group than in the male group in both seasons. Additionally, in winter, I_{cl} was significantly higher ($p < 0.01$) compared to I_{cl} in summer for both male and female groups.

4.4.2.4 Comparison of *M*

Fig. 4.14 shows the comparison of *M* prediction. The male group showed significantly higher MET ($p < 0.01$) than the female group in both seasons.

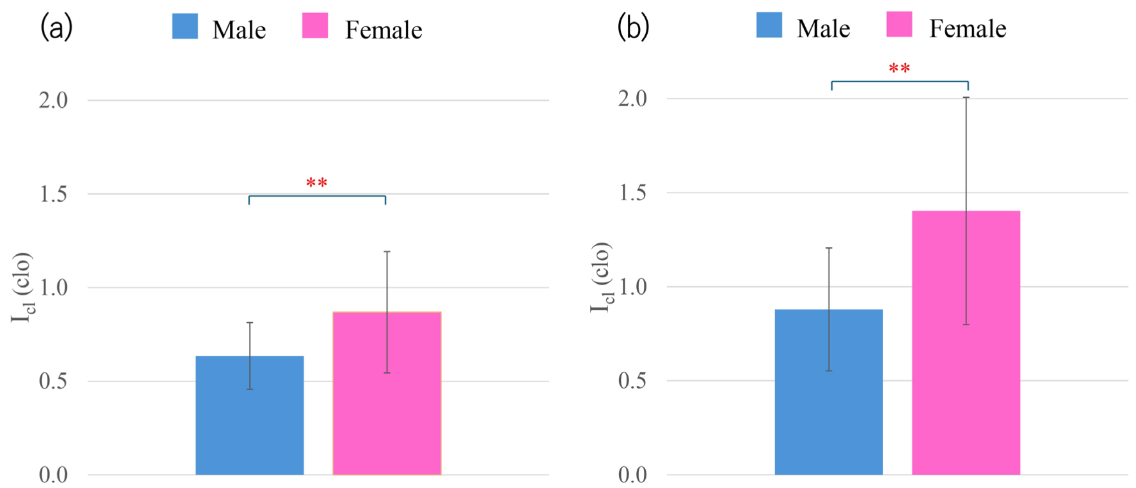

Fig. 4.13. Comparison of clothing insulation (I_{cl}) between male and female groups in summer (a) and winter (b).

(Summer, M:F = 72:17; Winter, M:F = 61:14).

Values are mean ± standard deviation. **: $p < 0.01$ between gender groups.

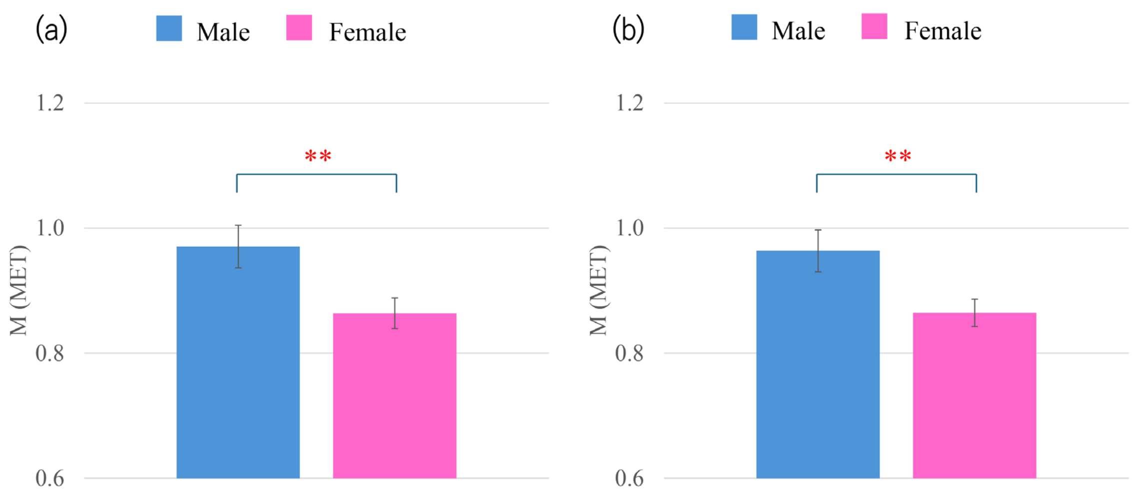

Fig. 4.14. Comparison of metabolic rate (*M*) between male and female groups in summer (a) and winter (b).

(Summer, M:F = 72:17; Winter, M:F = 61:14)

Values are mean ± standard deviation. **: $p < 0.01$ between gender groups.

4.4.2.5 Comparison of *PMV* and *PPD*

Fig. 4.15 shows the *PMV* comparisons between the male and female groups. In summer and winter, *PMV* predictions from IRT showed no significant differences between the male and female groups. In the *PPD* comparison in winter (Fig. 4.16), the female group showed significantly higher dissatisfaction than the male group ($p < 0.01$), while there was no significant gender difference in summer.

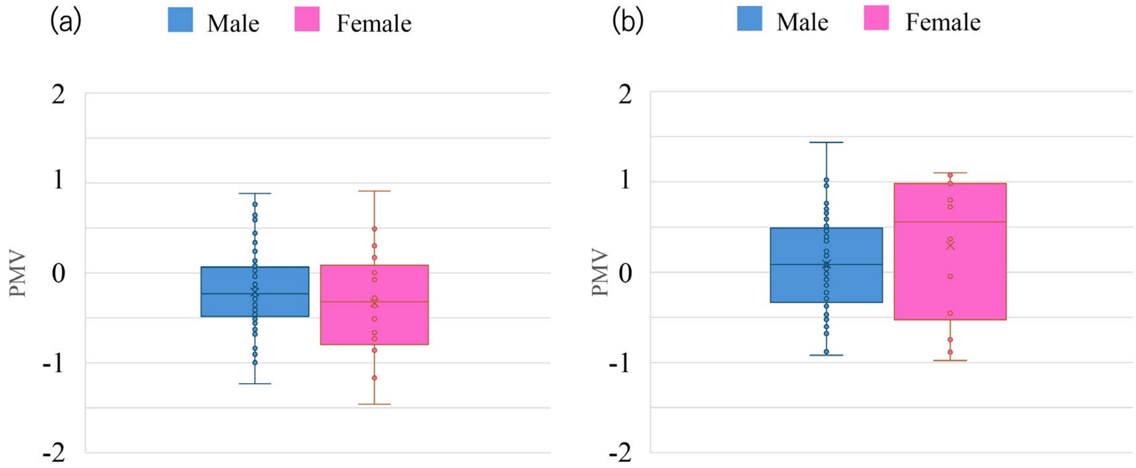

Fig. 4.15. Comparison of predicted mean vote (*PMV*) between male and female groups in summer (a) and winter (b).

(Summer, M:F = 72:17; Winter, M:F = 61:14)

Values are mean ± standard deviation.

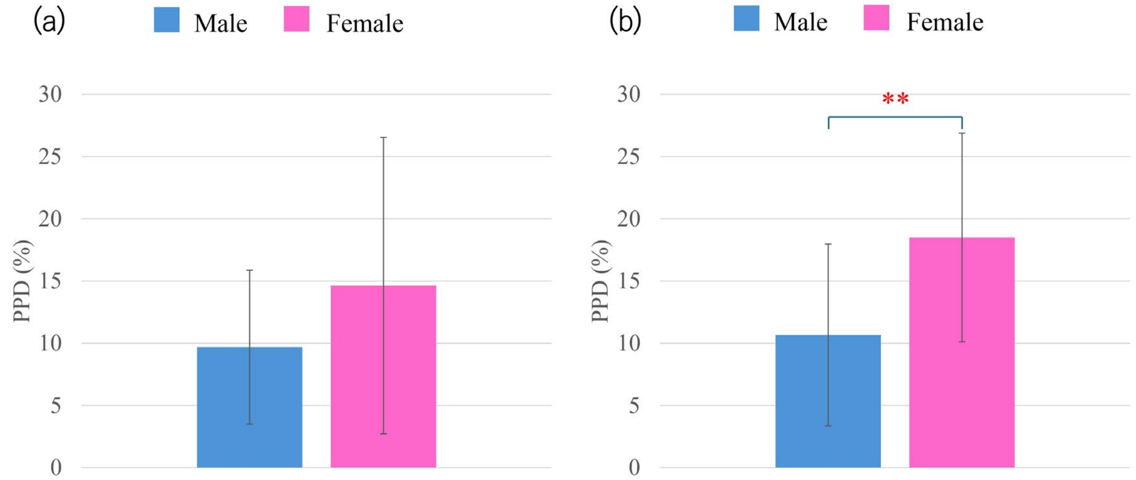

Fig. 4.16. Comparison of predicted percentage of dissatisfied (*PPD*) between male and female groups in summer (a) and winter (b).

(Summer, M:F = 72:17; Winter, M:F = 61:14)

Values are mean ± standard deviation. **: $p < 0.01$ between gender groups.

4.4.2.6 Comparison between TSV and *PMV*

A comparison between TSV (as reference value for prediction) and *PMV* prediction is described in Fig. 4.17. In the male group, TSV was significantly higher than *PMV* ($p < 0.01$) in summer. In other cases, there were no significant differences between *PMV* and TSV.

Comparing the TSV and *PMV* prediction, Table 4.8 shows the absolute mean differences with standard deviation (SD), root mean square error (RMSE) and correlation between TSV and *PMV*. There was no significant correlation observed between *PMV* and TSV in both seasons for both gender groups.

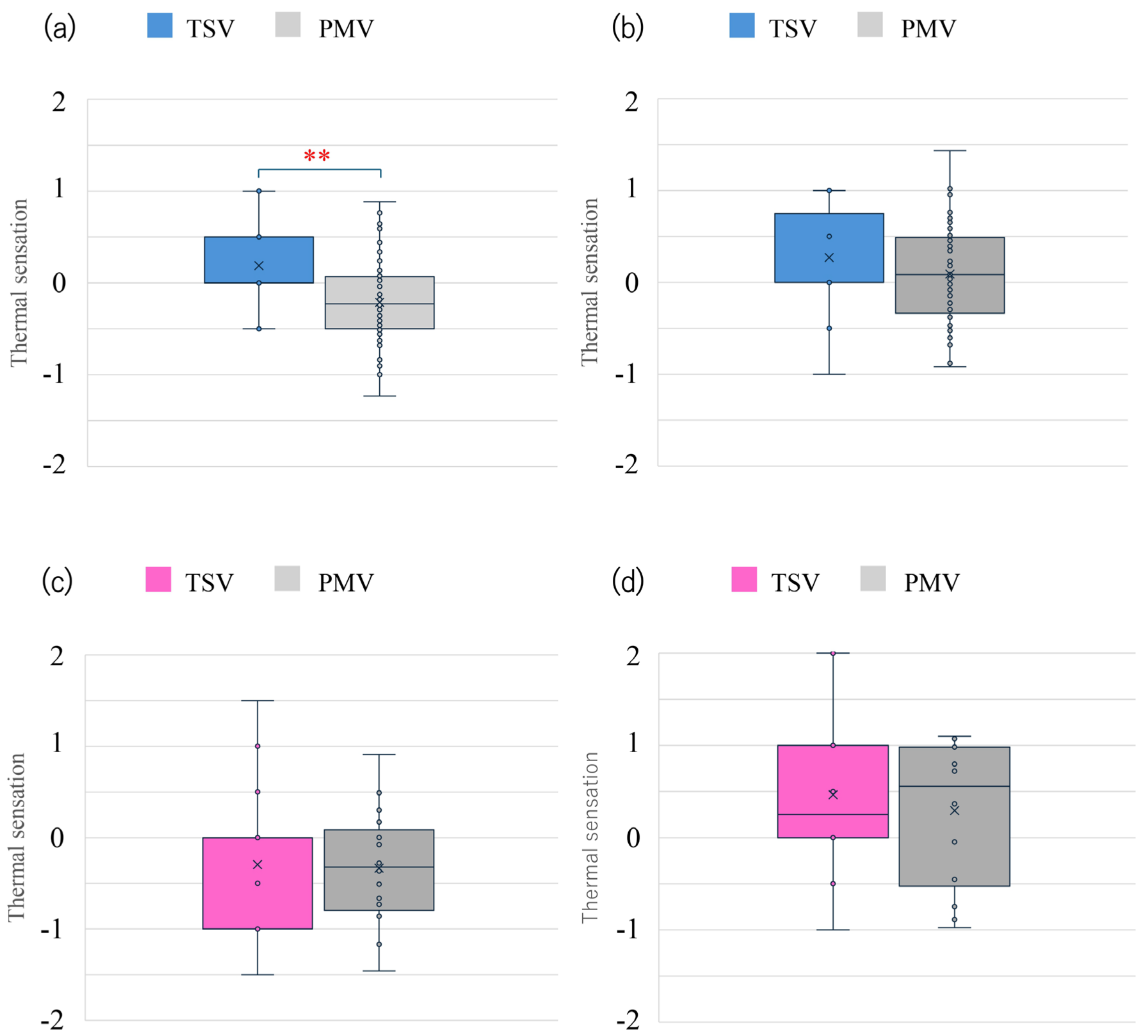

Fig. 4.17. Comparison of thermal sensation vote (TSV) and predicted mean vote (*PMV*) for male in summer (a) and winter (b); for female in summer (c) and winter (d).
(Summer, M:F = 72:17; Winter, M:F = 61:14)
Values are mean ± standard deviation. **: $p < 0.01$ between TSV and *PMV*.

Table 4.8. *PMV* and TSV comparison with absolute mean difference ± SD, RMSE and correlation coefficient "r" value in gender groups.

	Absolute mean difference ± SD	RMSE	r value
Summer			
Male	0.66 ± 0.60	0.89	0.13
Female	0.61 ± 0.55	0.81	0.27
Winter			
Male	0.65 ± 0.57	0.86	0.01
Female	0.87 ± 0.53	1.03	0.20

4.4.2.7 Comparison of t_{sk}

Local skin temperature on the face and hand are shown in Fig. 4.18. The male group showed significantly higher t_{nose} compared to the female group in both seasons ($p < 0.01$). The hand and finger temperatures of the male group were significantly higher compared to the female group in summer ($p < 0.05$). Table 4.9 shows correlation coefficient (ρ) between TSV and local skin temperature. In summer, for the male group, t_{nose}, $t_{palmar\ finger}$, $t_{palmar\ hand}$, $t_{dorsal\ finger}$, and $t_{dorsal\ hand}$ significant correlation with TSV ($p < 0.01$). For the female group, t_{cheek} temperature showed significant correlation with TSV ($p < 0.05$). In winter, however, no significant correlation was found between TSV and t_{sk} for either group.

Table 4.9. Local skin temperature (t_{sk}) and TSV comparison with Spearman's rank corelation test in gender groups.

		$t_{forehead}$	t_{nose}	t_{chin}	t_{neck}	t_{cheek}	$t_{eye\ canthus}$	$t_{palmar\ finger}$	$t_{palmar\ hand}$	$t_{dorsal\ finger}$	$t_{dorsal\ hand}$
Summer											
Male	ρ value	0.05	0.32*	0.07	0.11	0.21	0.05	0.38*	0.31*	0.36*	0.32*
Female	ρ value	0.06	-0.08	0.11	0.04	0.53*	0.27	-0.33	-0.27	-0.37	-0.37
Winter											
Male	ρ value	0.07	0.17	0.10	0.09	-0.01	0.10	0.12	0.05	0.20	0.07
Female	ρ value	0.38	0.39	0.17	0.17	0.52	0.27	-0.04	-0.25	-0.07	0.02

Values are corelation coefficient (ρ value). * Significant correlation ($p < 0.05$).

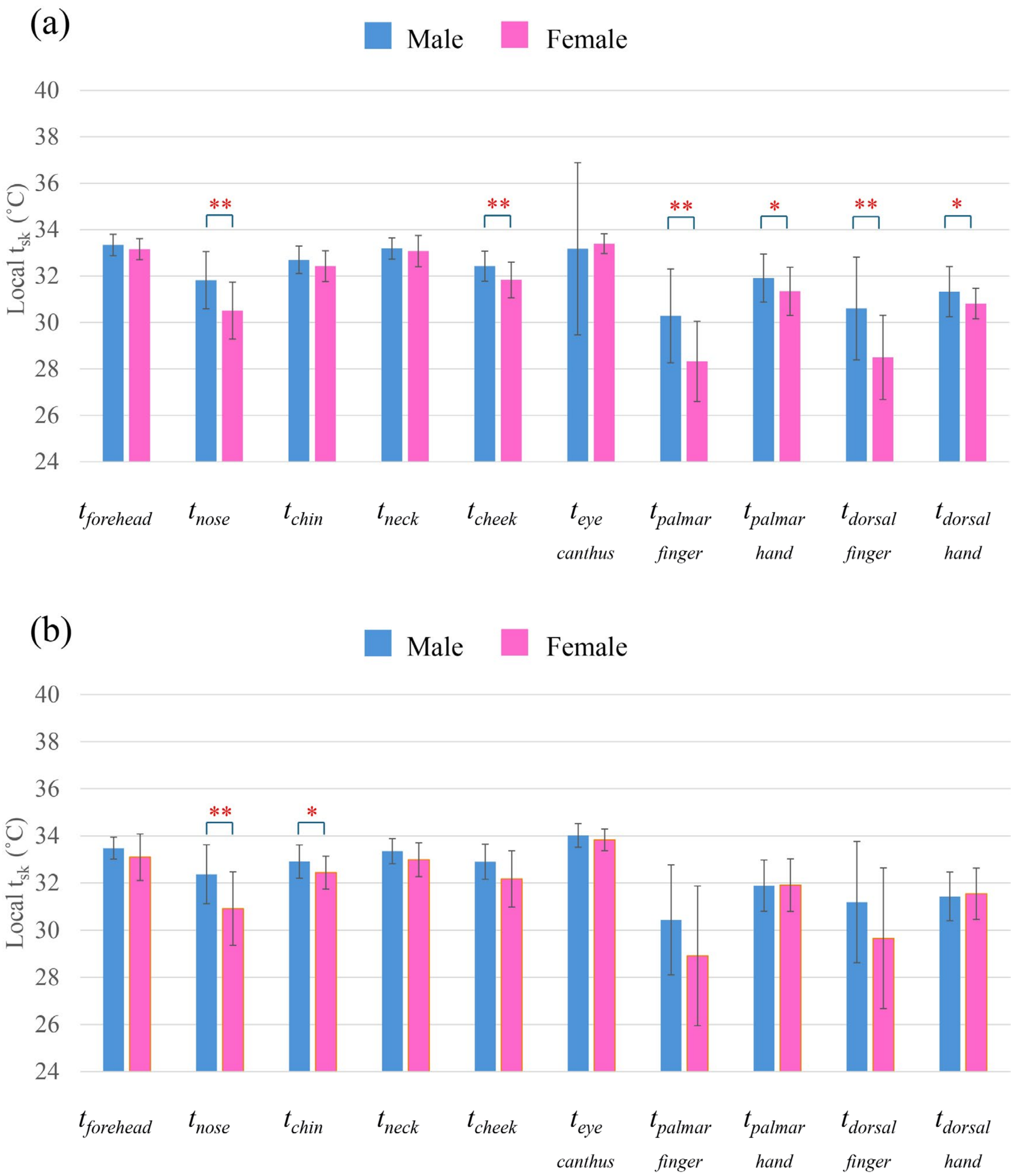

Fig. 4.18. Comparison of local skin temperature (t_{sk}) between male and female groups in summer (a) and winter (b).

(Summer, M:F = 72:17; Winter, M:F = 61:14)

Values are mean ± standard deviation. *: $p < 0.05$, **: $p < 0.01$ between gender groups.

4.4.2.8 Comparison of $\Delta t_{proximal - distal}$

Fig. 4.19. shows the comparison of $\Delta t_{proximal - distal}$ between the male and female groups. It was observed that females had higher $\Delta t_{forehead - nose}$ and $\Delta t_{palmar\ hand - palmar\ finger}$ comparing with male groups in both

summer and winter ($p < 0.01$).

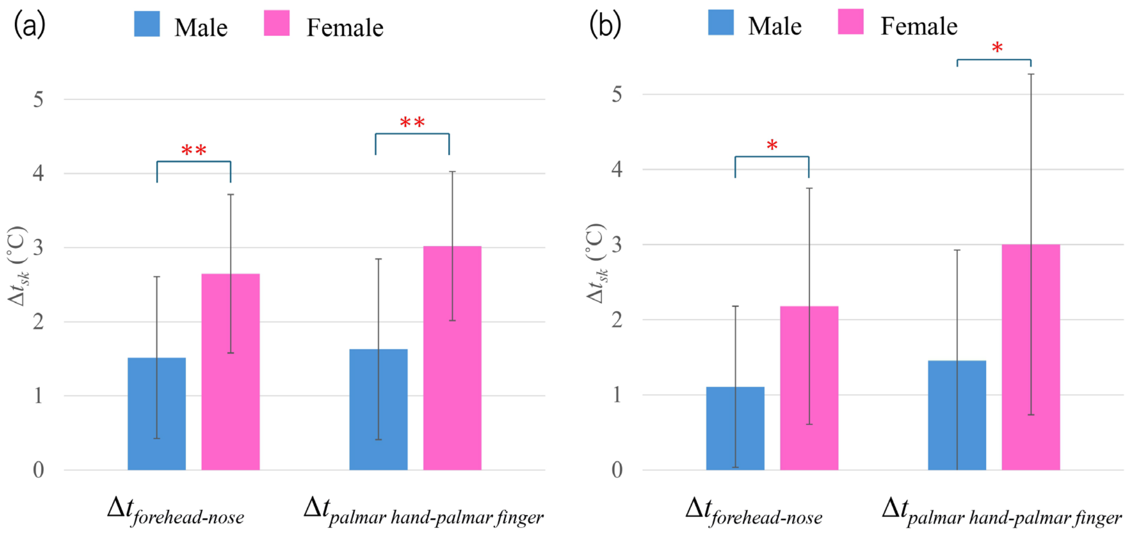

Fig. 4.19. Comparison of $\Delta t_{proximal\text{-}distal}$ between the male and female groups in summer (a) and winter (b).

(Summer, M:F = 72:17; Winter, M:F = 61:14)

Values are mean ± standard deviation. *: $p < 0.05$, **: $p < 0.01$ between gender groups.

4.4.2.9 Correlation analysis with gender

Table 4.10 represents the relationships between gender and various factors, including *BMI*, CC, I_{cl}, *M,* TSV, TC, TP, DL, *PMV* and *PPD*. In addition, the partial correlations among these factors were examined to see their relationships with the gender, and the results are shown in Table 4.6. In summer, *BMI*, CC, I_{cl}, *M* and TSV had significant moderate correlations with the gender (ρ = -0.47, 0.33, 0.34, -0.68 and -0.26, respectively, $p < 0.05$). In addition, in partial correlation analysis, when *BMI* was controlled, correlation of the I_{cl} and *M* became stronger with gender (ρ = 0.43, -0.74, $p < 0.01$). When CC was controlled, *BMI*, I_{cl} and *M* were significantly correlated with gender (ρ = -0.36, 0.41 and -0.77, respectively, $p < 0.01$). When I_{cl} was controlled, significant correlations with the gender were observed for *BMI*, CC, *M*, TSV, DL, *PMV* and *PPD* (ρ = -0.47, 0.34, -0.78, -0.27, 0.24, -0.74 and 0.35, respectively, $p < 0.05$). When *M* was controlled, the correlation weakened and only for I_{cl} and *PMV* were significantly correlated with gender (ρ = 0.34 and 0.27, respectively, $p < 0.05$). When *BMI* and CC were controlled together, most of the correlation disappeared. Even though, I_{cl} and *M* were still significantly correlated with the gender (ρ = 0.44 and -0.73, respectively, $p < 0.01$).

In winter, *BMI*, CC, I_{cl}, *M* and *PPD* showed significant correlation with gender (ρ = -0.38, 0.48, 0.35, -0.68 and 0.37, respectively, $p < 0.01$). In partial correlation, when *BMI* was controlled, it did not affect too much on the correlations and CC, I_{cl}, *M*, TSV and *PPD* showed significant correlation (ρ = 0.37, 0.50, -0.73, 0.23 and 0.39, respectively, $p < 0.05$). When CC was controlled, *BMI*, I_{cl}, *M* and *PPD* still showed significant correlations (ρ = -0.25, 0.48, -0.72 and 0.37, respectively, $p < 0.05$). When I_{cl} was controlled, it had little impact on most of the correlations and *BMI*, CC and *PMV* were significantly correlated (ρ = -0.44, 0.49, -0.76 and -0.63, respectively, $p < 0.01$). When *M* was controlled, I_{cl}, *PMV* and *PPD* were significantly correlated (ρ = 0.41, 0.32 and 0.38, respectively, $p < 0.01$). When *BMI* and CC were controlled together, the correlation were little bit elevated and significant correlation were found in I_{cl}, *M,* TSV, *PMV* and *PPD* (ρ = 0.50, -0.70, 0.27, 0.24 and 0.38, respectively, $p < 0.05$).

In Table 4.11, the correlations between gender and local t_{sk} as well as $\Delta t_{proximal\ -\ distal}$ are summarized. In summer, several significant correlations were noted. Significant negative correlations were figured out for t_{nose}, t_{cheek}, $t_{eye\ canthus}$, $t_{palmr\ finger}$, $t_{palmar\ hand}$, $t_{dorsal\ finger}$ and $t_{dorsal\ hand}$ with cold constitution (ρ = -0.38, -0.31, -0.24, -0.37, -0.22, -0.37 and -0.24, respectively, $p < 0.05$). Significant positive correlations were observed for $\Delta t_{forehead\ -\ nose}$ and $\Delta t_{palmar\ hand\ -\ palmar\ finger}$ with the gender (ρ = 0.36 and 0.43, respectively, $p < 0.01$). In the partial correlation analysis while *BMI*, CC and *M* were controlled separately, the magnitude of most of the correlations reduced. However, $\Delta t_{palmar\ hand\ –\ palmar\ finger}$ was significantly correlated with the gender (ρ = 0.28, 0.37, 0.26, respectively and $p < 0.01$). In addition, $\Delta t_{forehead\ –\ nose}$ was significantly correlated with the gender while CC was controlled (ρ = 0.34, $p < 0.01$). When I_{cl} was controlled, most of the correlation remained same and the t_{nose}, t_{cheek}, $t_{palmar\ finger}$, $t_{dorsal\ finger}$ and $t_{dorsal\ hand}$ were significantly negatively correlated with the gender (ρ = -0.36, 0.25, -0.34, -0.33 and -0.23, respectively, $p < 0.05$). Additionally positive correlations were found for $\Delta t_{forehead\ -\ nose}$ and $\Delta t_{palmar\ hand\ -\ palmar\ finger}$ when I_{cl} was controlled (ρ = 0.38 and 0.39, respectively, $p < 0.01$). While when *BMI* and CC were controlled together, correlation decreased a little, however t_{nose}, t_{cheek}, $t_{palmr\ finger}$, $\Delta t_{forehead\ -\ nose}$ and $\Delta t_{palmar\ hand\ -\ palmar\ finger}$ showed significant correlation with gender (ρ = -0.26, -0.26, -0.22, 0.23 and 0.27, respectively, $p < 0.05$)

In winter, significant negative correlations were found for t_{nose}, t_{chin} and t_{neck} (ρ = -0.36, -0.24 and -0.23, respectively, $p < 0.05$). A significant positive correlation was observed for $\Delta t_{forehead\ -\ nose}$ and $\Delta t_{palmar\ hand\ -\ palmar\ finger}$ with the gender (ρ = 0.27 and 0.28, $p < 0.05$). When *BMI* was controlled, t_{nose}, t_{cheek}, $\Delta t_{forehead\ -\ nose}$ and $\Delta t_{palmar\ hand\ -\ palmar\ finger}$ showed significant correlations (ρ = -0.34, -0.26, 0.28 and 0.29, respectively, $p < 0.05$). When CC was controlled, t_{nose}, t_{cheek}, $\Delta t_{forehead\ -\ nose}$ and $\Delta t_{palmar\ hand\ -\ palmar\ finger}$ showed significant correlations (ρ = -0.30, -0.24, 0.25 and 0.27, respectively, $p < 0.05$). When I_{cl} was controlled, t_{nose}, $\Delta t_{forehead\ -\ nose}$ and $\Delta t_{palmar\ hand\ -\ palmar\ finger}$ showed significant correlation (ρ = -0.39, 0.35 and 0.30, respectively, $p < 0.01$). When *M* was controlled, correlation value reduced and only $t_{palmar\ finger}$ and $\Delta t_{palmar\ hand\ -\ palmar\ finger}$ showed significant correlation (ρ = -0.24 and 0.25, respectively, $p < 0.05$). Interestingly when *BMI* and CC were controlled together, t_{nose}, $\Delta t_{forehead\ -\ nose}$ and $\Delta t_{palmar\ hand\ -\ palmar\ finger}$ showed significant correlation ((ρ = -0.28, -0.23 and 0.25, respectively, $p < 0.05$).

Table 4.10. Correlations of the gender with *BMI*, CC, I_{cl}, *M,* thermal perceptions, *PMV* and *PPD*.

	BMI	CC	I_{cl}	*M*	TSV	TC	TP	DL	*PMV*	*PPD*
Summer										
ρ value	-0.47**	0.33**	0.34**	-0.68**	-0.26*	0.02	0.18	0.15	-0.09	0.18
Partial ρ (controlled: *BMI*)	-	0.20	0.43**	-0.74**	-0.12	-0.04	0.04	0.20	0.02	0.18
Partial ρ (controlled: CC)	-0.36**	-	0.41**	-0.77**	-0.14	0.06	0.08	0.18	-0.04	0.18
Partial ρ (controlled: I_{cl})	-0.47**	0.34**	-	-0.78**	-0.27*	-0.05	0.16	0.24*	-0.74**	0.35**
Partial ρ (controlled: *M*)	0.14	0.08	0.34**	-	-0.05	-0.09	-0.14	0.17	0.27*	-0.07
Partial ρ (controlled: *BMI*, CC)	-	-	0.44**	-0.73**	-0.06	-0.01	-0.01	0.20	0.04	0.15
Winter										
ρ value	-0.38**	0.48**	0.35**	-0.68**	0.09	0.03	0.07	0.10	0.160	0.37**
Partial ρ (controlled: *BMI*)	-	0.37**	0.50**	-0.73**	0.23*	0.03	-0.02	0.08	0.22	0.39**
Partial ρ (controlled: CC)	-0.25*	-	0.48**	-0.72**	0.20	0.04	0.03	0.05	0.20	0.37**
Partial ρ (controlled: I_{cl})	-0.44**	0.49**	-	-0.76**	0.09	-0.00	0.01	0.01	-0.63**	0.12
Partial ρ (controlled: *M*)	0.06	0.23	0.41**	-	0.22	-0.15	-0.17	0.26	0.32*	0.38**
Partial ρ (controlled: *BMI*, CC)	-	-	0.50**	-0.70**	0.27*	0.04	-0.01	0.05	0.24*	0.38**

BMI: body mass index, I_{cl}: clothing insulation, *M*: metabolic rate, TSV: thermal sensation vote, TC: thermal comfort, TP: thermal preference, DL: dissatisfaction level, *PMV*: predicted mean vote, *PPD*: predicted percentage of dissatisfied. Values are correlation coefficient (ρ value).

**: Significant correlation ($p < 0.01$), *: Significant correlation ($p < 0.05$).

Table 4.11. Correlation of the gender with local t_{sk} and Δt_{sk} gradient.

	$t_{forehead}$	t_{nose}	t_{chin}	t_{neck}	t_{cheek}	$t_{eye\ canthus}$	$t_{palmar\ finger}$	$t_{palmar\ hand}$	$t_{dorsal\ finger}$	$t_{dorsal\ hand}$	$\Delta t_{forehead\ -\ nose}$	$\Delta t_{palmar\ hand\ -\ palmar\ finger}$
Summer												
ρ value	-0.16	-0.38**	-0.18	-0.11	-0.31**	-0.24*	-0.37**	-0.22*	-0.37**	-0.24*	0.36**	0.43**
Partial ρ (controlled: BMI)	-0.16	-0.28*	-0.11	-0.09	-0.28*	0.08	-0.24*	-0.12	-0.21	-0.11	0.25	0.28*
Partial ρ (controlled: CC)	-0.14	-0.34**	-0.14	-0.04	-0.28**	0.08	-0.31**	-0.16	-0.31*	-0.16	0.34**	0.37**
Partial ρ (controlled: I_{cl})	-0.05	-0.36**	-0.11	0.03	-0.25*	0.04	-0.34*	-0.19	-0.33*	-0.23*	0.38**	0.39**
Partial ρ (controlled: M)	-0.02	-0.17	-0.13	-0.03	-0.15	0.27*	-0.24*	-0.16	-0.22*	-0.14	0.18	0.26*
Partial ρ (controlled: BMI, CC)	-0.16	-0.26*	-0.10	-0.07	-0.26*	0.09	-0.22*	-0.11	-0.20	-0.10	0.23*	0.27*
Winter												
ρ value	-0.16	-0.36**	-0.24*	-0.20	-0.23*	-0.15	-0.21	0.01	-0.20	0.03	0.27*	0.28*
Partial ρ (controlled: BMI)	-0.21	-0.34**	-0.21	-0.26*	-0.21	-0.11	-0.22	-0.05	-0.19	0.05	0.28*	0.29*
Partial ρ (controlled: CC)	-0.17	-0.30**	-0.19	-0.13	-0.24*	-0.06	-0.18	0.01	-0.19	0.09	0.25*	0.27*
Partial ρ (controlled: I_{cl})	-0.21	-0.39**	-0.17	-0.18	-0.32	-0.07	-0.17	0.08	-0.12	0.05	0.35*	0.30**
Partial ρ (controlled: M)	0.02	-0.16	-0.14	-0.12	-0.11	-0.03	-0.24*	-0.17	-0.19	-0.06	0.18	0.25*
Partial ρ (controlled: BMI, CC)	-0.16	-0.28*	-0.17	-0.16	-0.18	-0.05	-0.18	-0.03	-0.18	0.09	0.23*	0.25*

BMI: body mass index, I_{cl}: clothing insulation, *M*: metabolic rate, $t_{forehead}$: forehead skin temperature, t_{nose}: nose skin temperature, t_{chin}: chin skin temperature, t_{neck}: neck skin temperature, t_{cheek}: cheek skin temperature, $t_{eye\ canthus}$: eye canthus skin temperature, $t_{dorsal\ hand}$: dorsal hand skin temperature, $t_{palmar\ hand}$: palmar hand skin temperature, $t_{dorsal\ finger}$: dorsal finger skin temperature, and $t_{palmar\ finger}$: palmar finger skin temperature. Values are correlation coefficient (ρ value).

**: Significant correlation ($p < 0.01$), *: Significant correlation ($p < 0.05$).

4.4.3 Cold constitution differences

4.4.3.1 Morphological differences

It was observed that in the NC group, number of females were less comparing with males. Additionally in the NC group, body height, weight and *BMI* were significantly higher comparing with the CC group ($P < 0.05$) (Table 4.1).

4.4.3.2 Comparison of thermal perceptions

Fig. 4.20 illustrates the TSV, TC, TP and DL comparisons between the CC group and the NC group. In summer, CC group showed significantly lower TSV comparing with the NC group ($p < 0.01$). Additionally, CC group showed significantly higher TP comparing with the NC group ($p < 0.01$). No significant differences were observed for TC and TP between the CC group and the NC group in summer. On the other hand, in winter, no significant differences were found in TSV , TC, TP and DL between the two groups.

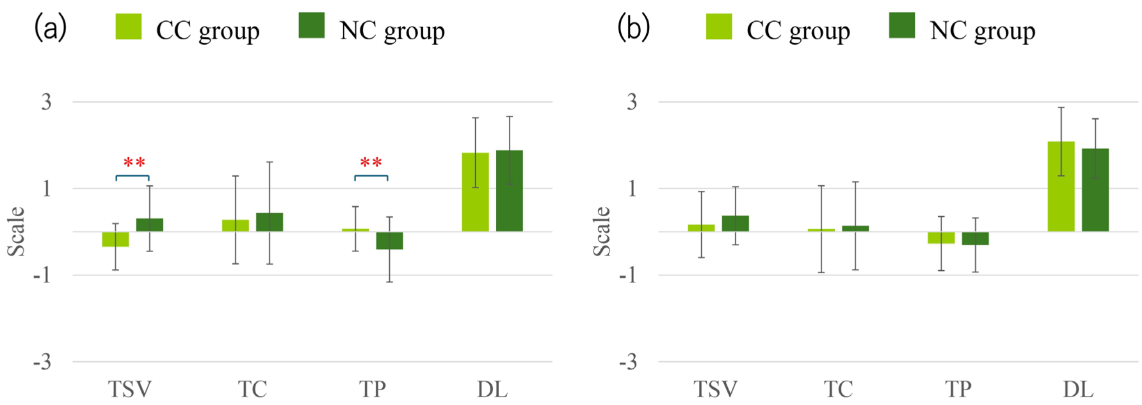

Fig. 4.20. Comparison of thermal sensations between CC group and NC group in summer (a) and winter (b).

(Summer, CC group : NC group = 29:60, Winter, CC group : NC group = 24:51)

Values are mean ± standard deviation. **: $p < 0.01$ between the groups.

4.4.3.3 Comparison of I_{cl}

Fig. 4.21 shows the I_{cl} comparison between the groups. No significant differences were observed for the I_{cl} between the groups in either summer or winter. However, when the summer I_{cl} and the winter I_{cl} were compared, the I_{cl} in winter was significantly greater than that in the summer for both the groups ($p < 0.01$).

4.4.3.4 Comparison of *M*

Fig. 4.22 highlights the *M* comparison between the groups. The results revealed that CC group had a significantly lower *M* in both seasons comparing with the NC group ($p < 0.01$).

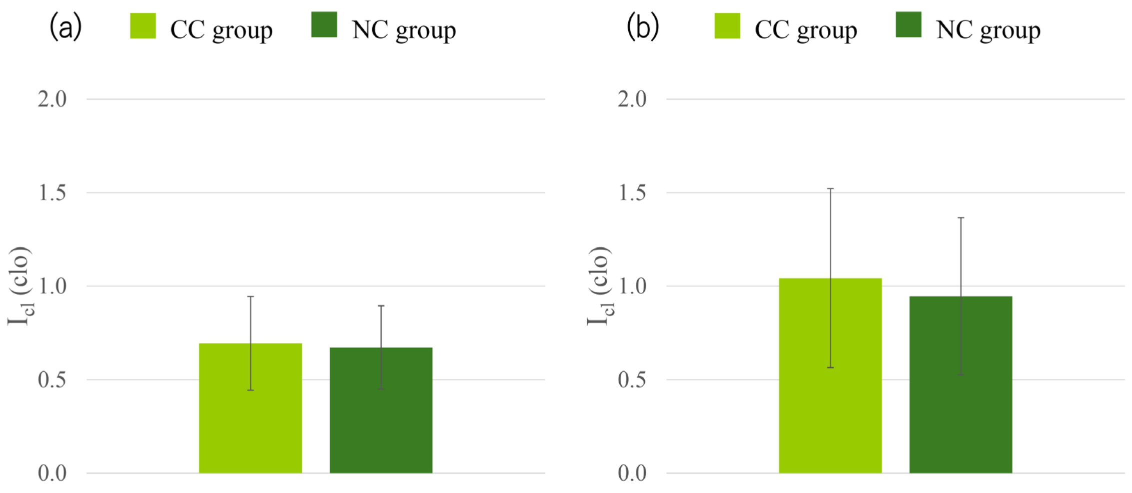

Fig. 4.21. Comparison of clothing insulation (I_{cl}) between CC group and NC group in summer (a) and winter (b).

(Summer, CC group : NC group = 29:60, Winter, CC group : NC group = 24:51)

Values are mean ± standard deviation.

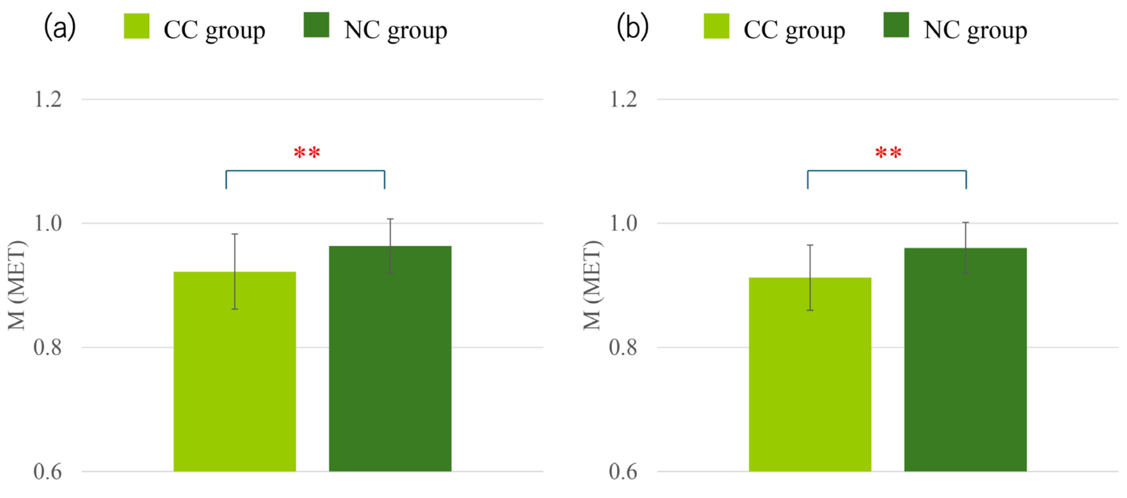

Fig. 4.22. Comparison of metabolic rate (*M*) between CC group and NC group in summer (a) and winter (b).

(Summer, CC group : NC group = 29:60, Winter, CC group : NC group = 24:51)

Values are mean ± standard deviation. **: $p < 0.01$ between the groups.

4.4.3.5 Comparison of *PMV* and *PPD*

As shown in Fig. 4.23, there were no significant differences observed in *PMV* between the CC group and the NC group in either summer or winter. Fig. 4.24 presents *PPD* comparison between the two groups. In summer, CC group showed significantly higher *PPD* comparing with the NC group ($p < 0.05$). However, in winter No significant difference was observed for *PPD* between the groups.

Table 4.12 also shows the *PMV* and TSV comparison including the absolute mean values differences with SD, RMSE values and correlation between TSV and *PMV*. No significant correlation was observed between TSV and *PMV* in all comparisons for the cold constitution groups.

Table 4.12. *PMV* and TSV comparison with absolute mean difference ± SD, RMSE and correlation coefficient "r" value in cold constitution groups.

	Absolute mean difference ± SD	RMSE	r value
Summer			
CC group	0.52 ± 0.38	0.64	0.24
NC group	0.72 ± 0.65	0.83	0.04
Winter			
CC group	0.86 ± 0.59	1.03	-0.12
NC group	0.62 ± 0.54	0.82	0.15

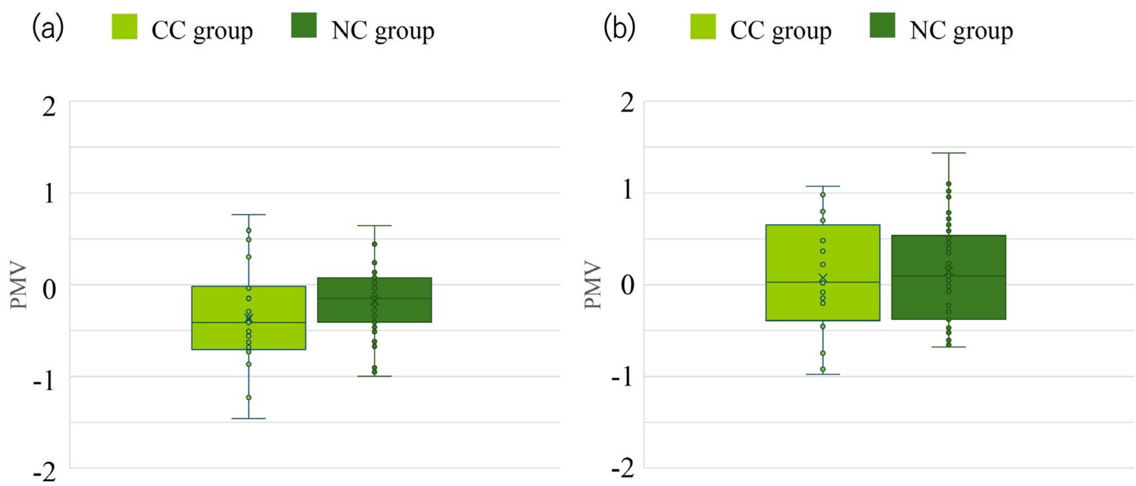

Fig. 4.23. Comparison of predicted mean vote (*PMV*) between CC group and NC group in summer (a) and winter (b).

(Summer, CC group : NC group = 29:60, Winter, CC group : NC group = 24:51)

Values are mean ± standard deviation.

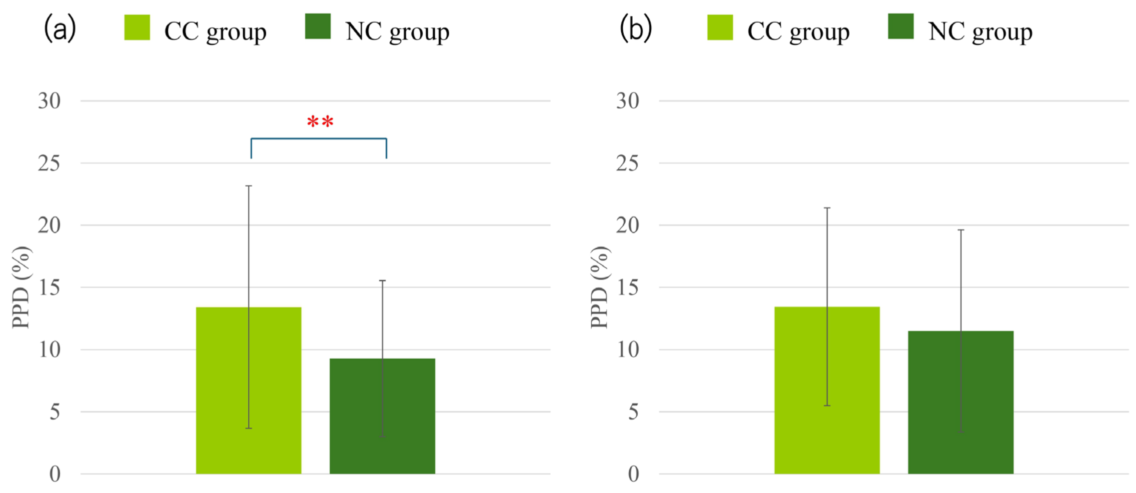

Fig. 4.24. Comparison of predicted percentage of dissatisfied (*PPD*) between CC group and NC group in summer (a) and winter (b).

(Summer, CC group : NC group = 29:60, Winter, CC group : NC group = 24:51)

Values are mean ± standard deviation. **: $p < 0.01$ between the groups.

4.4.3.6 Comparison between TSV and *PMV*

A comparison between TSV (as reference value for prediction) and *PMV* prediction is illustrated in Fig. 4.25. In the NC group, TSV was significantly higher than *PMV* ($p < 0.01$) in summer. In other cases, there were no significant differences between *PMV* and TSV.

4.4.3.7 Comparison of t_{sk}

Fig. 4.26 represents the local skin temperature comparison between the groups. It was observed that CC group have relatively lower skin temperature comparing with the NC group. Especially in the summer, CC group had significantly lower t_{nose}, t_{cheek}, $t_{palmar\ hand}$ and $t_{dorsal\ hand}$ comparing with the NC group ($p < 0.05$). In winter, CC group also showed significantly lower t_{nose}, t_{neck} and t_{cheek} comparing with the NC group ($p < 0.05$).

Table 4.13 shows the correlation coefficient (ρ) between TSV and local skin temperature. No significant correlations were found between TSV and local skin temperatures for the cold constitution groups except CC group's t_{dorsal} was significantly correlated with TSV in summer ($p < 0.05$).

4.4.3.8 Comparison of $\Delta t_{proximal\ -\ distal}$

Fig. 4.27 illustrates the temperature difference between $t_{forehead}$ and t_{nose}, as well as t_{palm} and $t_{palmar\ finger}$. The CC group had significantly greater $\Delta t_{forehead\ -\ nose}$ and $\Delta t_{palmar\ hand\ -\ palmar\ finger}$ comparing with the NC group both in summer ($p < 0.05$) and winter ($p < 0.01$).

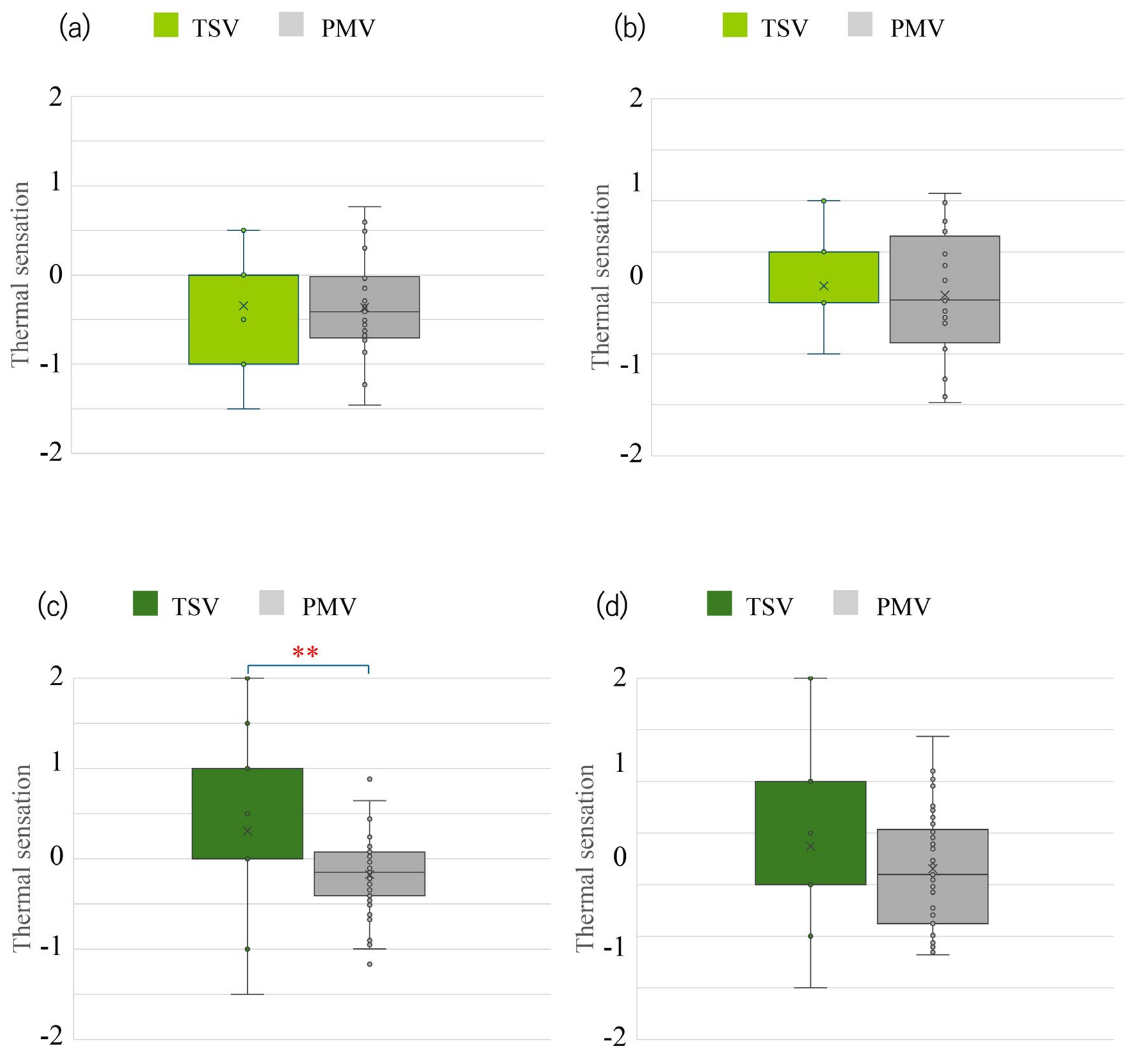

Fig. 4.25. Comparison of thermal sensation vote (TSV) and predicted mean vote (*PMV*) for CC group: summer (a) and winter (b); for NC group: summer (c) and winter (d).

(Summer, CC: NC = 29:60; Winter, CC: NC = 24:51)

Values are mean ± standard deviation. **: $p < 0.01$ between TSV and *PMV*.

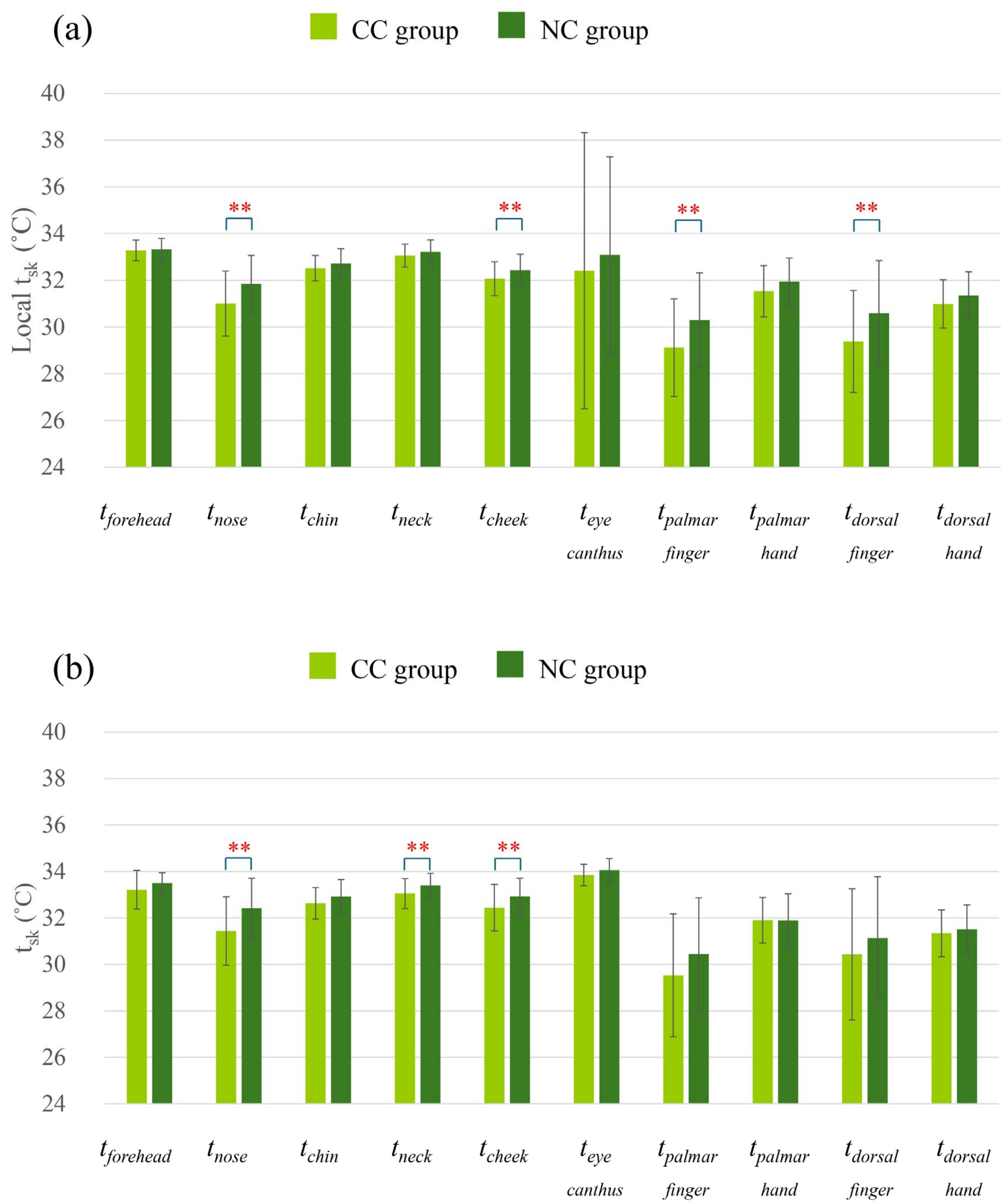

Fig. 4.26. Comparison of local skin temperature (t_{sk}) between CC group and NC group in summer (a) and winter (b).

(Summer, CC group : NC group = 29:60, Winter, CC group : NC group = 24:51)

Values are mean ± standard deviation. **: $p < 0.01$ between groups.

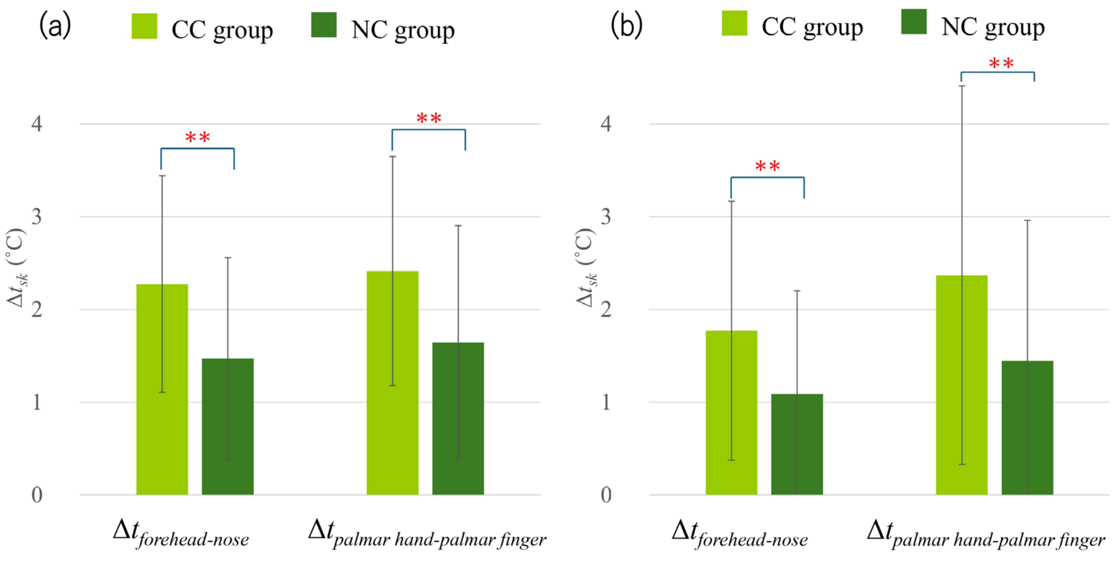

Fig. 4.27. Comparison of $\Delta t_{proximal\text{-}distal}$ between CC group and NC group in summer (a) and winter (b). (Summer, CC group : NC group = 29:60, Winter, CC group : NC group = 24:51) Values are mean ± standard deviation. **: $p < 0.01$ between the groups.

Table 4.13. Local skin temperature (t_{sk}) and TSV comparison with Spearman's rank corelation test in cold constitution groups.

		$t_{forehead}$	t_{nose}	t_{chin}	t_{neck}	t_{cheek}	$t_{eye\ canthus}$	$t_{palmar\ finger}$	$t_{palmar\ hand}$	$t_{dorsal\ finger}$	$t_{dorsal\ hand}$
Summer											
CC group	ρ value	0.11	0.23	0.19	0.12	0.35	0.19	0.18	0.02	0.20	0.14
NC group	ρ value	0.03	0.18	0.03	0.03	0.23	0.21	0.25	0.21	0.19	0.16
Winter											
CC group	ρ value	0.22	0.24	0.23	-0.02	0.16	0.24	0.32	0.23	0.43*	0.33
NC group	ρ value	0.03	0.02	-0.03	0.09	-0.05	0.03	-0.04	-0.10	0.02	-0.05

Values are corelation coefficient (ρ value). * Significant correlation ($p < 0.05$).

Table 4.14. Correlations of the cold constitution with gender, *BMI*, I_{cl}, *M,* thermal perceptions, *PMV* and *PPD*.

	Gender	*BMI*	I_{cl}	*M*	TSV	TC	TP	DL	*PMV*	*PPD*
Summer										
ρ value	0.33**	-0.38**	-0.01	-0.33**	-0.44**	-0.10	0.30**	-0.03	-0.21*	0.27*
Partial ρ (controlled: gender)	_	-0.27*	0.13	-0.18	-0.35**	-0.13	0.27*	-0.07	-0.20	0.20
Partial ρ (controlled: *BMI*)	0.16	_	0.13	-0.16	-0.31*	-0.20	0.21*	0.02	-0.14	0.20
Partial ρ (controlled: I_{cl})	0.30**	-0.37**	_	-0.34*	-0.38**	-0.12	0.29**	-0.00	-0.24*	0.30**
Partial ρ (controlled: *M*)	0.05	-0.21	0.12	_	-0.31*	-0.17	0.21*	-0.04	-0.18	0.14
Partial ρ (controlled: gender, *BMI*)	_	_	-0.06	-0.04	-0.31**	-0.14	0.22*	-0.06	-0.11	0.16
Winter										
ρ value	0.48**	-0.42**	0.13	-0.39**	-0.10	0.01	0.02	0.09	-0.04	0.10
Partial ρ (controlled: gender)	_	-0.29*	-0.15	-0.14	-0.22	-0.05	0.01	0.07	-0.15	-0.09
Partial ρ (controlled: *BMI*)	0.37**	_	0.10	-0.29*	-0.04	-0.03	-0.03	0.10	-0.01	0.10
Partial ρ (controlled: I_{cl})	0.49**	-0.42**	_	-0.44**	-0.15	-0.04	0.02	0.09	-0.32**	0.06
Partial ρ (controlled: *M*)	0.23*	-0.23*	-0.03	_	-0.14	-0.11	-0.06	0.17	-0.03	0.04
Partial ρ (controlled: gender, *BMI*)	_	_	-0.10	-0.02	-0.14	-0.04	-0.03	0.08	-0.10	-0.06

BMI: body mass index, I_{cl}: clothing insulation, *M*: metabolic rate, TSV: thermal sensation vote, TC: thermal comfort, TP: thermal preference, DL: dissatisfaction level, *PMV*: predicted mean vote, *PPD*: predicted percentage of dissatisfied. Values are correlation coefficient (ρ value).

**: Significant correlation ($p < 0.01$), *: Significant correlation ($p < 0.05$).

Table 4.15. Correlation of the cold constitution with local t_{sk} and Δt_{sk} differences.

	$t_{forehead}$	t_{nose}	t_{chin}	t_{neck}	t_{cheek}	$t_{eye\ canthus}$	$t_{palmar\ finger}$	$t_{palmar\ hand}$	$t_{dorsal\ finger}$	$t_{dorsal\ hand}$	$\Delta t_{forehead\ -\ nose}$	$\Delta t_{palmar\ hand\ -\ palmar\ finger}$
Summer												
ρ value	-0.08	-0.27*	-0.14	-0.15	-0.21*	-0.17	-0.17	-0.27*	-0.18*	-0.26*	0.31**	0.30**
Partial ρ (controlled: gender)	0.03	-0.21	-0.09	-0.12	-0.14	-0.09	-0.15	-0.11	-0.14	-0.10	0.24*	0.16
Partial ρ (controlled: *BMI*)	-0.03	-0.19	-0.08	-0.15	-0.17	-0.06	-0.13	-0.09	-0.10	-0.08	0.21	0.13
Partial ρ (controlled: I_{cl})	-0.01	-0.33*	-0.16	-0.13	-0.23*	-0.06	-0.25*	-0.17	-0.25*	-0.15	0.37**	0.27*
Partial ρ (controlled: *M*)	0.04	-0.19	-0.10	-0.12	-0.14	-0.02	-0.16	-0.12	-0.15	-0.12	0.23*	0.16
Partial ρ (controlled: gender, *BMI*)	-0.00	-0.15	-0.07	-0.14	-0.13	-0.07	-0.09	-0.07	-0.06	-0.07	0.17	0.09
Winter												
ρ value	-0.23*	-0.33**	-0.20	-0.27*	-0.23	-0.23*	-0.01	-0.17	-0.09	-0.13	0.25*	0.21
Partial ρ (controlled: gender)	-0.13	-0.16	-0.08	-0.19	-0.12	-0.15	-0.07	-0.00	-0.02	-0.11	0.12	0.10
Partial ρ (controlled: *BMI*)	-0.19	-0.25*	-0.14	-0.30*	-0.12	-0.16	-0.14	-0.06	-0.08	-0.09	0.19	0.17
Partial ρ (controlled: I_{cl})	-0.21	-0.31**	-0.17	-0.27*	-0.25*	-0.18	-0.16	0.02	-0.10	-0.08	0.25*	0.23*
Partial ρ (controlled: *M*)	-0.09	-0.17	-0.11	-0.21	-0.13	-0.14	-0.14	-0.07	-0.07	-0.14	0.15	0.16
Partial ρ (controlled: gender, *BMI*)	-0.11	-0.14	-0.06	-0.22	-0.05	-0.13	-0.07	-0.04	-0.01	-0.11	0.09	0.07

BMI: body mass index, I_{cl}: clothing insulation, *M*: metabolic rate, $t_{forehead}$: forehead skin temperature, t_{nose}: nose skin temperature, t_{chin}: chin skin temperature, t_{neck}: neck skin temperature, t_{cheek}: cheek skin temperature, $t_{eye\ canthus}$: eye canthus skin temperature, $t_{dorsal\ hand}$: dorsal hand skin temperature, $t_{palmar\ hand}$: palmar hand skin temperature, $t_{dorsal\ finger}$: dorsal finger skin temperature, and $t_{palmar\ finger}$: palmar finger skin temperature. Values are correlation coefficient (ρ value).

**: Significant correlation ($p < 0.01$), *: Significant correlation ($p < 0.05$).

4.4.3.9 Correlation analysis with cold constitution

Table 4.14 represents the relationships between cold constitution and various factors, including gender, *BMI*, I_{cl}, *M,* TSV, TC, TP, DL, *PMV* and *PPD*. Additionally, the partial correlations among these factors were analyzed to examine their relationships with the cold constitution, and the results are shown in Table 4.14. In summer gender, *BMI*, *M*, TSV, TP, *PMV* and *PPD* had significant moderate correlations with the cold constitution (ρ = 0.33, -0.38, -0.33, -0.44, 0.30, -0.21 and 0.27, respectively, $p < 0.05$). In addition, in partial correlation analysis, when gender was controlled, correlation of the *BMI* and the cold constitution became weak, although it was significant (ρ = -0.27, $p < 0.05$). The correlation with TSV remains significant (ρ = -0.35, $p < 0.01$) and TP remains a moderate positive correlation (ρ = 0.27, $p < 0.05$). When *BMI* was controlled, only TSV and TP were significantly correlated with cold constitution (ρ = -0.31 and -0.21, respectively, $p < 0.05$). When I_{cl} was controlled, significant correlations were observed for gender, *BMI*, *M*, TSV, TP, *PMV* and *PPD* (ρ = 0.30, -0.37, -0.34, -0.38, 0.29, -0.24 and 0.30, respectively, $p < 0.05$). When *M* was controlled, the correlation weakened and only for TSV and TP were significantly correlated with cold constitution (ρ = -0.31 and 0.21, respectively, $p < 0.05$). When gender and *BMI* were controlled together, most of the correlation disappeared. Even though, TSV and TP were still significantly correlated with the cold constitution (ρ = -0.31 and 0.22, respectively, $p < 0.05$).

In winter, gender, *BMI* and *M* showed significant correlation with cold constitution (ρ = 0.48, -0.42 and -0.39 respectively, $p < 0.01$). In partial correlation, while gender was controlled, it weakened the correlation and only *BMI* was significantly correlated with cold constitution (ρ = -0.29, $p < 0.05$). When *BMI* was controlled, gender and *M* still showed significant but weaker correlations (ρ = 0.37 and -0.29, respectively, $p < 0.05$). When I_{cl} was controlled, it had little impact on most of the correlations and gender, *BMI*, *M* and *PMV* were significantly correlated (ρ = 0.49, -0.42, -0.44 and -0.32 respectively, $p < 0.01$). When *M* was controlled, most correlations weakened, although gender and *BMI* were significantly correlated (ρ = 0.23 and -0.23, respectively, $p < 0.05$). When gender and *BMI* were controlled together, the correlation disappeared.

In Table 4.15, the correlations between cold constitution and local t_{sk} as well as $\Delta t_{proximal\ -\ distal}$ are summarized. In summer, several significant correlations were noted. Significant negative correlations were figured out for t_{nose}, t_{cheek}, $t_{palmar\ hand}$ and $t_{dorsal\ finger}$ with cold constitution (ρ = -0.27, -0.21, -0.27 and -0.18, respectively, $p < 0.05$). Significant positive correlations were observed for $\Delta t_{forehead\ -\ nose}$ and $\Delta t_{palmar\ hand\ -\ palmar\ finger}$ with the cold constitution (ρ = 0.31 and 0.30, respectively, $p < 0.05$). In the partial correlation analysis while gender, *BMI* and *M* controlled separately, the magnitude of most of the correlations reduced. However, while gender and *M* were controlled, in both cases $\Delta t_{forehead\ –\ nose}$ was significantly correlated with the cold constitution (ρ = 0.24 and 0.23, respectively, $p < 0.05$). When I_{cl} was controlled, most of the correlation elevated slightly and the t_{nose}, t_{cheek}, $t_{palmar\ finger}$ and $t_{dorsal\ finger}$ were significantly negatively correlated with the cold constitution (ρ = -0.33, 0.23, -0.25 and -0.25, respectively,

$p < 0.05$). Additionally positive correlations were identified for $\Delta t_{forehead\ -\ nose}$ and $\Delta t_{palmar\ hand\ -\ palmar\ finger}$ (ρ = 0.37 and 0.27, respectively, $p < 0.05$). While gender and *BMI* were controlled together, no significant correlation was observed with cold constitution.

In winter, significant negative correlations were observed for $t_{forehead}$, t_{nose}, t_{neck} and $t_{eyecanthus}$ (ρ = -0.23, -0.33, -0.27 and -0.23, respectively, $p < 0.05$). A significant positive correlation was observed for $\Delta t_{forehead\ -\ nose}$ with the cold constitution (ρ = 0.25, $p < 0.05$). When *BMI* was controlled, it reduced correlation levels, and statistical significance was found for t_{nose} and t_{neck} (ρ = -0.25 and -0.30 respectively, $p < 0.05$). When gender, *M* and gender combined with *BMI* were controlled together, no significant correlations was observed. However, while I_{cl} was controlled, the correlations slightly increased, and significant negative correlations were found for t_{nose}, t_{neck} and t_{cheek} (ρ = -0.31, -0.27 and -0.25, respectively, $p < 0.05$). Additionally positive correlations were observed for $\Delta t_{forehead\ -\ nose}$ and $\Delta t_{palmar\ hand\ -\ palmar\ finger}$ with the cold constitution (ρ = 0.25 and 0.23, respectively, $p < 0.05$).

4.5 Discussion

4.5.1 Thermal sensations and morphological characteristics

This research was conducted in office environment where thermal environment was in the range of thermoneutral both in summer and winter. This likely explains why most participants responded with “neutral” for TSV, “neither” for TC and “no change” for TP (Fig. 4.3, Fig. 4.11, Fig 4.19). However, the mean DL was near to “slightly satisfied”, probably due to the human expectation of better conditions, which guide the participants to engage in some adaptive activities [34, 59].

From the TSV results, it appears that the BMI < 22 group had marginally higher cold sensitivity compared to the BMI > 22 group (Fig. 4.3), which is in line with prior research findings [117]. Individuals with higher *BMI* generally have a higher metabolic rate because larger bodies require more energy to maintain basic physiological functions. Additionally, they have lower surface area to volume ratio, which results in less heat loss per unit heat production [216, 217]. This is likely why the BMI > 22 group had lower cold sensitivity compared to the BMI < 22 group.

It was also observed that the female participants were slightly more sensitive to cold compared to the male participants. Previous study also demonstrated similar findings [129]. They also found that females have significantly lower TSV compared to males. Another study also mentioned the higher dissatisfaction of females compared to that of males under the same thermal environments [202]. Males typically have higher metabolic rates than females, resulting in more heat production [218]. This might be explained by higher percentage of muscle mass in the male body [123]. Some studies have reported greater cutaneous thermal sensitivity in females than in males, which was assessed by the magnitude and threshold of the local thermal sensation to the peltier plate attached on the skin surface [219, 220]. In addition, there have been studies reporting that females showed lower skin temperature and reduced skin blood flow during or after cold exposure compared to males [221]. This might be explained in part by the greater sensitivity of adrenergic receptors in cutaneous blood vessel and/or the lower bioavailability of nitric oxide, which is known as vasodilator, in females with cold constitution [151]. Moreover, higher surface area to mass ratio might be one another reason for lower cold tolerance in females [222]. Additionally, typically, males have higher *BMI* than females [223, 224], and the BMI > 22 group in this study had a higher ratio of male participants (Table 4.1). This result indicates the influence of physiological and morphological characteristics on TSV [34, 59, 196].

From the morphological characteristics analysis of cold constitution group (Table 4.1) it was observed that mostly in the NC group, the female participants were less than males, which is consistent with the findings of some prior studies [150, 225]. Notably, the body height, weight and *BMI* of the individuals in the NC group were significantly higher than those in the CC group. This aligns with some previous research, where researchers also mentioned the association of thinness with cold constitution [226]. Previous researches had shown that individuals with lower *BMI* have less insulation due to lower fat mass, and that individuals with lower *BMI* feels colder than those with higher *BMI* do [199]. Possibly due to this leanness, cold constitution individuals tend to feel colder compared to others, and this aligns with the findings in this research on TSV, TC, TP and DL differences between the CC group and the NC group (Fig. 4.20). The findings showed that in summer, TSV and TP had significant differences between the CC group and the NC group. The CC group reported colder than did the NC group. Additionally, the CC group voted their thermal preference warmer compared to the NC group. This result supports the basic principle of cold constitution where, cold constitution individuals feel colder than the other individuals do [227]. However, in winter, there were no significant differences observed between the groups. Possibly higher clothing insulation in winter comparing summer helped to elevate the thermal sensation in CC group ($p < 0.01$). Another possible reason can be seasonal acclimatization in thermoregulation [228]. In this experiment, the indoor environmental conditions were similar in both summer and winter, maintained at approximately 25.0 ~25.5°C. However, the outdoor conditions differed significantly, hot in summer and cold in winter. Which may explain why participants felt slightly cool indoors during summer but warm during winter.

From the correlation and partial correlation analysis it was observed that in most cases TSV was significantly correlated with *BMI,* gender and cold constitution (Table 4.6, Table 4.10, 4.14). Strikingly in partial correlation analysis, while controlling for gender, *BMI* and cold constitution vice versa, the correlation weakened, which clearly signify the association of these individual variations with thermal sensation.

4.5.2 Clothing insulation

It was observed that across both *BMI* groups and cold constitution groups, there were no significant differences in clothing insulation, except winter I_{cl} were higher than summer I_{cl} for all groups, although the indoor environmental conditions were mostly similar. This likely indicates that one's psychological state depending on seasonal variation can affect their clothing selection as a behavioural adaptation [202, 229].

When, comparing gender differences, females showed significantly higher I_{cl} than males both in summer and winter. Most likely due to higher cold sensitivity, females had significantly higher clothing insulation (Fig. 4.13) as their behavioural thermoregulation compared to males [34, 202]. The difference in I_{cl} between them is especially pronounced in winter. This indicates the seasonal acclimatization might be induced in behavioural thermoregulation [230]. The higher I_{cl} in winter probably elevated the TSV for females, which is why no significant difference in TSV was observed between males and females during winter. In these regards, it can be illustrated that I_{cl} likely influences TSV. Significant correlation between gender and I_{cl} (Table 4.10) also indicates the importance of clothing insulation as an adaptive behavioural thermoregulation across gender.

Notably, the significant I_{cl} difference between gender groups but not between *BMI* groups indicates that morphological differences between males and females are not the major reason for the behavioural clothing selection. Instead, higher skin cold sensitiveness of females [219, 220], as well as clothing norms, may influence them to wear more cloths than males.

In addition, between CC group and NC group there were no I_{cl} difference observed either in summer or winter. However, significantly higher I_{cl} in winter than in summer for both CC group and NC group demonstrates the behavioural adaptation of thermoregulation. It was observed that in summer, the CC group reported feeling significantly colder than the NC group did, despite both groups having nearly the same clothing insulation. Most likely, clothing culture and norms suppressed behavioural adaptation and likely led to wearing lighter clothing for the CC group in summer, even though they felt cold. That can be the reason for the lack of significant correlation observed for I_{cl} with the cold constitution. However, in winter, higher clothing insulation enabled cold constitution individuals to adapt comfortably to the thermal environment.

There was significant correlation observed between I_{cl} and gender (Table 4.10) only, though no significant direct correlation observed between I_{cl} and *BMI* as well I_{cl} and the cold constitution, suggesting that I_{cl} was not significantly associated with the *BMI* and cold constitution (Table 4.6, Table 4.14). In addition, when I_{cl} was controlled in partial correlation with cold constitution, the general correlation coefficient of gender, *BMI* and *M* with cold constitution did not have a substantial effect, which also indicates the minimum influence of cold constitution on I_{cl}. Similarities also observed while controlling I_{cl} in correlation analysis with *BMI.* Most likely, clothing culture and norms are the reason of significant correlation between I_{cl} and gender. Using the I_{cl} is a type of behavioral thermoregulation. However, the results suggested that people with cold constitution or BMI < 22 did not have enough behavioral adaptations to cold.

4.5.3 Metabolic heat production

While *M* prediction, the BMI > 22 group had significantly higher *M* prediction compared to the BMI < 22 group (Fig. 4.3), males had significantly higher *M* prediction compared to females (Fig. 4.14), and NC group had significantly higher *M* prediction compared to CC group (Fig. 4.22). This result is consistent with previous studies [14, 151, 215]. It was observed that higher *BMI* individuals produce higher metabolic heat and mostly males have higher *BMI* [202, 203]. This can be related with presence of female individuals in the CC group as well as lower *BMI* individuals in the CC group, that's why CC group had lower metabolic heat production (Table 4.1).

This result are related with TSV results, especially in summer, where lower *M* indicates lower TSV for the BMI < 22 group, female group and CC group. However, in winter, higher I_{cl} might reduce the effect of *M*, which is likely why there were no significant differences observed in TSV between BMI < 22 and BMI > 22 groups, between males and females, as well as CC group and NC group.

Interestingly, in the correlation analysis, it was observed that *M* was significantly correlated with *BMI*, gender and cold constitution (Table 4.6, Table 4.10 and Table 4.14). Controlling for *M* in partial correlation analysis significantly weaken the correlation among gender, *BMI*, cold constitution and other thermal sensations, both in summer and winter. This result signifies the close relationship of *M*, and highlights the differences of *M* among *BMI*, gender and cold constitution groups. Therefore, these findings suggest that higher *BMI* is a key determinant of increased metabolic rate, which significantly affects TSV.

4.5.4 *PMV - PPD* and TSV

PMV predictions (Fig. 4.6, Fig. 4.15, Fig. 4.23) displays no significant differences between groups of *BMI*, gender and cold constitution. Even *PMV* predictions mostly showed a similar tendency like TSV (Fig. 4.8, Fig. 4.17, Fig. 4.25). However, in summer, it was observed that TSV in BMI > 22 group was significantly higher than the *PMV*.

It can be said that *PMV* just predicts the thermal sensation based on mathematical calculation, whereas TSV is a complex individual thermal perception. TSV relies on many personal factors including psychological state, acclimatization, acclimation and most importantly morphological characteristics [231-234].

Individuals with higher *BMI* often have greater body fat [235], which can reduce heat dissipation due to its insulating properties and it can effect on TSV. This physiological limitation in thermoregulation may cause them to feel warmer in hot environments. However, such individual thermoregulatory responses are not directly accounted for in the *PMV* model. Additionally, seasonal acclimation and individual desire can be other reasons behind the differences between TSV and *PMV*. Notably, in BMI > 22 group the percentage of males and NC group's individuals are higher. Interestingly in summer, males and NC groups' TSV were also significantly higher than *PMV*.

Furthermore, *PPD* comparison between *BMI* groups, there were no significant differences, though BMI < 22 tends to have slightly higher *PPD*. In gender, females tended to be higher compared to male participants (Fig. 4.7), especially in winter females showed significantly higher *PPD* compared to males. This might be similar characteristics to the greater DL observed in females compared to males. Therefore, for females, behavioural thermoregulation such as higher clothing insulation [236] induces less heat loss. In a thermoneutral condition, especially in winter, this may be why females showed significantly higher *PPD* compared to males. Similar results were observed while comparing *PPD* in CC and NC group (Fig. 4.24). During summer CC group showed significantly higher *PPD* comparing with NC group. This is likely due to the higher proportion of females and the lower *BMI* individuals observed in that CC group.

In addition, considering the *PMV* prediction method in this study, it is mentionable that several studies have argued that *PMV* often predicts a higher thermal sensation compared to actual human perception [237, 238], whereas model in this study predicts *PMV* mostly without any significant differences with TSV (except in summer for the males, BMI > 22 group and NC group). One potential justification for the elevated *PMV* estimation could be flaws in predicting I_{cl} due to the diverse range of clothing ensembles, whereas IRT solely depends on thermal status. On the other hand, ISO 8996 [15] suggested metabolic rate calculations are probably biased by gender and ethnic differences [182], which might lead to overestimation of the *M*. However, the *M* prediction model based on the *BMR* and *PAR* in this study is lower than the ISO generalized *M* according to the MET chart. This might be one of the reasons for better *PMV* prediction in this study.

4.5.5 Local skin temperature

Skin temperature is one of the parameters reflecting physiological response to the thermal environment. Several studies have suggested that local skin temperatures can provide closer and more sensitive indicators of thermal sensation [239, 240].

Some studies have shown that distal body parts are the earliest to feel cold [241] and individuals with cold sensation tends to have lower t_{sk} in those areas [242]. It can be described as the association of vasoconstriction with the cold sensation along with the tendency to perceive a thermoneutral environment as cold [150]. In cold environment sympathetic nervous system releases noradrenaline (NA) from the nerve ending and binds to adrenergic receptors to the vascular smooth muscle cell membrane to induce vasoconstriction [243]. It has also been reported that long-term local cold exposure reduces endothelial nitric oxide (NO) synthase activity, which suppresses NO-mediated vasodilation [244]. It modulates vasoconstriction by activating intracellular signalling pathways that regulate smooth muscle contraction [244]. It reduces blood flow to the distal part of the body caused by vasoconstriction [124]. That's the important aspect to address how the human body physiologically responds to varying thermal conditions.

In the case of *BMI* groups, the BMI > 22 group had significantly higher t_{nose} and t_{cheek} temperatures compared to the BMI < 22 group in both seasons (Fig. 4.9). This might be due to the presence of high

AVAs in nose and finger regions [43, 45, 245]. In those areas vasoconstriction to sympathetic activation seems to be greater comparing with other skin regions, because of AVAs presence. Remarkably only in summer, BMI < 22 group had significantly lower hand skin temperature compared to the BMI > 22 group, not in winter. This indicates that in summer in the air-conditioned office environment, peripheral vasoconstriction probably occurs to reduce heat loss in lower *BMI* group compared to higher *BMI* group. In winter, although indoor conditions were comparable with summer, participants adapted by wearing higher clothing insulation. This likely reduced heat loss and minimized vasoconstriction at hand region in the BMI < 22 group. This result also represents greater cold sensitivity in the BMI < 22 group.

From the correlation analysis (Table 4.7), it was also observed that distal body local skin temperatures have significant correlation with *BMI*. In addition, when controlling M in partial correlation, the significance level between *BMI* and local t_{sk} weakened, indicating that M is strongly associated with *BMI* in terms of heat production and heat distribution. Individuals with higher *BMI* tend to have higher metabolic heat generation, and it is linked to more evenly distributed skin temperatures t_{sk} across the body and less cold sensitivity.

From the local t_{sk} comparison (Fig. 4.18), females showed significantly lower t_{nose} in both seasons and significantly lower temperature in hand region only in summer. Lower temperature at distal body part again remarks the presence of AVAs at that nose and hand area, and indicates vasoconstriction. While no significant gender difference observed in hand skin temperature in winter, possibly indicates the behavioural adaptation. Higher I_{cl} in winter might be the fact behind it. And this could affect the TSV results also. That's why in summer, females had significantly lower TSV than females, whereas no significant gender difference was observed in winter. Possibly higher I_{cl} in winter elevated distal body parts t_{sk} and eventually increased warm feelings for females.

In cold constitution difference groups, it was observed that r t_{nose}, t_{cheek}, $t_{palmar\ finger}$ and $t_{dorsal\ finger}$ were significantly lower in the CC group comparing the NC group in summer (Fig. 4.26). In winter only t_{nose}, t_{neck} and t_{cheek} showed significantly lower in the CC group than in the NC group (Fig. 4.26). There were no significant differences observed at the hand region in winter. One possible reason again can be highlighted as higher I_{cl} in winter than in summer for both groups like it happened in *BMI* and gender groups. Mostly it was observed that, the extra clothing was used to cover the trunk body, and particularly in winter people used to wear full sleeve clothing. It is possible that this kind of clothing could increase the hand region temperature for people with cold constitution. However, in the face area, there was no effect of clothing. This may explain the consistent local skin temperature difference in the face region between the CC group and the NC group, even in winter. Therefore, it can be presumed that no correlation was found between I_{cl} and the cold constitution, however a higher I_{cl} may serve as a behavioural adaptation to reduce body heat loss and enhance comfort for cold constitution people.

From the correlation analysis it was also noticed that distal body skin temperature such as t_{nose}, $t_{palmar\ finger}$ and $t_{dorsal\ finger}$ were mostly correlated with *BMI*, gender and cold constitution, even while controlling the other factors, they remained significant, which explain the substantial association of distal body parts skin temperature with g *BMI*, gender and cold constitution.

In analysis of temperature difference between proximal and distal body part, it was observed that $\Delta t_{forehead-nose}$ and $\Delta t_{palmar\ hand\ -\ palmar\ finger}$ were significantly higher for the BMI < 22, females, and CC group in both summer and winter (Fig. 4.10, Fig. 4.19, Fig. 4.27). It was also observed that $\Delta t_{forehead-nose}$ and $\Delta t_{palmar\ hand\ -\ palmar\ finger}$ were mostly significantly correlated with *BMI*, gender, and cold constitution. This result clearly indicates that the vasoconstriction phenomenon occurred at the distal part of the body to suppress heat dissipation from the skin surface, especially for BMI < 22, females, and CC group. This event also matches the findings of previous studies [23, 244, 246, 247]. A lower skin temperature at the distal part of the body may lead to a cold sensation in individuals. However, it was observed that comparing with summer, correlation of $\Delta t_{forehead-nose}$ and $\Delta t_{palmar\ hand\ -\ palmar\ finger}$ with *BMI*, gender, and cold constitution were little bit weaker in winter. Probably higher I_{cl} in winter compared with summer I_{cl} was the basic reason behind the weaker correlation.

In Fig. 4.11, it was observed that with the decrease of *BMI* the $\Delta t_{forehead-nose}$ and $\Delta t_{palmar\ hand\ -\ palmar\ finger}$ became greater, which clearly indicates the association of strong vasoconstriction at distal body parts and *BMI*. It also reveals that lower *BMI* have less heat production, that's why to reduce heat loss, distal body parts t_{sk} became lower in cold condition, whereas mostly proximal body parts t_{sk} remained constant. Interestingly in winter it seems to have lower vasoconstriction (because of less $\Delta t_{forehead-nose}$ and $\Delta t_{palmar\ hand\ -\ palmar\ finger}$) in lower *BMI* individuals. Possibly higher I_{cl} in winter and seasonal acclimation were the reason behind it.

4.6 Limitations

This research was conducted solely in a thermoneutral office environment. Future studies should explore a broader range of thermal environments to provide a more comprehensive understanding of IRT's applications and better quantify individual differences. In this research, limited data loggers were used to collect sample environmental condition. As a result, microclimatic variations were not captured and treated each zone as having uniform environmental conditions. Additionally, the unequal gender ratio suggests that including more female participants in future studies could offer a clearer representation of gender differences. In this research because of small number of female participants, it can limit the power to detect the significant gender differences.

4.7 Summary

This study was carried out to investigate the individual differences in thermal perceptions and physiological responses. Individual differences were investigated based on differences between *BMI* above 22 kg/m^2 and lower than 22 kg/m^2, male and female, and individuals having cold constitution or not. From the research work the following outcomes can be drawn.

a) Even in thermoneutral environment, BMI < 22 group, females and CC group reported feeling colder than BMI > 22, males and NC group, respectively in summer, while in winter, no significant difference was observed between these groups.

b) *M* was higher in BMI > 22, males and NC group comparing BMI > 22, males and NC groups, respectively in both seasons.

c) Female participants had higher clothing insulation in both seasons comparing with males. No differences observed for *BMI* or cold constitution differences. Though, all groups I_{cl} was significantly higher in winter than in summer, indicates behavioural adaptation by season.

d) Higer TSV than *PMV* for BMI > 22, males and NC group, indicating physiological, psychological, and behavioural adaptations can affect TSV, but are not captured by the *PMV* model.

e) Differences between groups were observed in local t_{sk}, where males, BMI > 22 and NC group had higher skin temperature compared to females, BMI < 22 group and CC group, respectively.

f) $t_{forehead\ -\ nose}$ and $\Delta t_{palmar\ hand\ -\ palmar\ finger}$ were significantly higher in the BMI < 22 group, females and CC group comparing BMI > 22, males and NC group, respectively, indicating stronger vasoconstriction at the distal body parts for BMI < 22 group, females and CC group.

In conclusion, the results suggest that individual differences such as *BMI*, gender, and cold constitution have strong influence in thermal perceptions. In thermoneutral condition metabolic heat production (*M*) and behavioural thermoregulation (I_{cl}) also have significant impact on individual thermal perceptions. It was also observed that thermoregulatory responses, such as skin temperature and proximal-to-distal skin temperature differences helps to shape individual thermal perceptions.

CHAPTER 5: Assessing physiological responses to develop a real-time thermal sensation prediction model

5.1 Introduction

In the modern lifestyle, humans spend the majority of their time in built environments. Most of that environments are designed to maintain a uniform thermal condition. However, individuals often perceive thermal environments differently. As a result, prolonged exposure to such conditions may pose potential discomfort to some occupants.

Generally, people act as active participants rather than passive recipients of environmental conditions. This perspective defines that in thermally discomfort situation, individuals respond by taking necessary actions aimed at regaining comfort [34]. While the thermal environment changes, cutaneous thermal receptors detect and transmit this information to support autonomic thermoregulation [248, 249]. This also contributes to the perception of thermal comfort through the integration of thermal sensations [198]. The resulting thermal sensations drive behavioral thermoregulation, such as adjusting air conditioning, changing clothing or posture, drinking fluids, or seeking more comfortable environments [44]. In addition, physiological thermoregulation also takes place as an involuntary process that operates autonomously and independently. Physiological responses like regulating vasomotor control and blood flow to distal body parts for enhancing or suppressing heat loss. In addition, metabolic heat production is a fundamental component of the human thermoregulatory process, playing a crucial role in maintaining thermal balance and ensuring comfort.

From the previous studies it was observed that *PMV* model can predict TSV moderately (Chapter 3), even though it considers personal factors like I_{cl} and M, combining with environmental factors. Also, the reliance of *PMV* on multiple variables makes it complex to calculate. On the other hand, studies on individual differences (Chapter 4) have shown that physiological responses such as skin temperature and proximal to distal skin temperature gradients are prominent indicators of group differences and they are associated with thermal sensations. Furthermore, it was also observed that these physiological differences among groups vary with seasonal climatic changes. It was also noticed that these physiological responses can be easily detected using only infrared thermography.

Therefore, considering these factors from the viewpoint of human physiological responses, individual differences and simplistic approach to predict TSV, it was presumed that temperature gradient between proximal and distal body parts may serve as an alternative approach to estimate thermal perception. Specially $\Delta t_{proximal-distal}$, indicates the level of vasoconstriction in thermoneutral zone, which was also found correlated with thermal sensation [36].

5.2 Aim of the study

To clarify the effect of the wide range of the ambient condition, here 3 seasons data were combined to analyse. This part of the research aims to investigate behavioural adaptations and physiological responses across different climatic conditions and their association with thermal sensation. In addition, this study aimed to evaluate the potential of using $\Delta t_{proximal-distal}$ to predict TSV. Furthermore, this section proposes a novel model for predicting TSV based on physiological responses like $\Delta t_{forehead-nose}$.

5. 3 Methods

The analyses in this section are based on the dataset described in Chapter 3, with some modifications.

5.3.1 Participants

In this study, 88 students from Hokkaido University participated in summer, 100 in autumn, and 68 in winter. Though, some participants took part in multiple seasons. To ensure the independence of the dataset, data were screened, and only one record per participant was retained. As a result, the final dataset included 65 participants for summer, 62 for autumn, and 63 for winter. Table 5.1 shows the morphological characteristics of the 190 participants.

Table 5.1. Morphological characteristics of the participants.

Morphology	Average ± SD
Number of participants	190
Gender (Male : Female)	100: 90
Age (year)	21.5 ± 2.0
Height (cm)	165.5 ± 8.6
Weight (kg)	56.6 ± 10.2
BMI (kg/m^2)	20.6 ± 2.4
BSA (m^2)	1.6 ± 0.2

BMI: body mass index, *BSA*: body surface area.

5.3.2 Research protocol

Morphological data were collected at the beginning of the session, followed by a 60-minute stabilization period to allow participants to acclimate to the indoor environment. After stabilization, participants provided their thermal sensation vote, and thermal image was taken to predict t_{cl}, t_{sk} and eventually *PMV*.

5.3.3 Environmental data

Four fundamental environmental data were collected (t_a, t_g, *RH*, and v_a). The data collection process was described at Section 3.3.3.

5.3.4 Thermal sensation vote (TSV)

Thermal sensation voting was carried out through a questionnaire survey. The process was described at Section 3.3.4. Participants answered their thermal sensation in a 7-point scale ranging -3 to 0 to 3 representing cold to neutral to hot.

5.3.5 Prediction of t_{sk} and calculation of *PMV*

IRT camera was used to measure t_{sk} for assessing vasomotor response. IRT was also used to predict t_{cl}, and the results of t_{cl} and t_{sk} were used for predicting I_{cl} to calculate *PMV*. The process and other details were explained at Section 3.3.5 and Section 3.3.6. For the calculation of *PMV*, four environmental factors and two individual factors (M and I_{cl}) were used. Here M was calculated from *BMR*, which was estimated considering the morphological characteristics and physical activity ratio (*PAR*), as explained in the previous chapters.

5.3.6 Statistical analysis

In this study correlations between t_a and other factors were analyzed by Pearson correlation test (considering parametric data sets). Correlation of TSV with other values were analyzed using Spearman's rank correlation test (considering TSV as non-parametric data). Linear regression analysis was conducted to develop the prediction model. For all statistical analyses, differences were considered significant at $p < 0.05$. The analyses were performed using IBM SPSS Statistics version 20 software.

5.4 Results

This research was conducted in summer, autumn, and winter seasons, with air temperature ranging approximately from 20°C ~ 28°C. This temperature range provided an opportunity to analyse TSV, behavioural adaptations, and physiological responses across varying environmental conditions.

To evaluate this I_{cl}, M, t_{sk} and $\Delta t_{proximal-distal}$ were analysed in relation to t_a and TSV (Table 5.2). Based on the analysis, this study proposed a new TSV prediction model by linear regression analysis.

Table 5.2. Correlation of different parameters with t_a and TSV.

	Correlation coefficient	t_a	t_r	RH	v_a	PMV	I_{cl}	M	$t_{forehead}$	t_{nose}	$t_{palmar\ finger}$	$\Delta t_{forehead-nose}$	$\Delta t_{forhead-palmar\ finger}$
t_a	r value	-	0.98 **	0.70 **	0.64 **	0.75 **	0.15 *	-0.03	0.73 **	0.84 **	0.86 **	-0.77 **	-0.81 **
TSV	ρ value	0.64 **	0.63 **	0.42 **	0.36 **	0.57 **	0.09	0.13	0.55 **	0.63 **	0.57 **	-0.58 **	-0.52 **

5.4.1 Correlation between t_a and TSV

Fig. 5.1 shows the correlation between TSV and t_a. Significant positive correlation observed between them ($\rho = 0.64$, $p < 0.01$) (Table 5.2). With the rise of t_a it was observed that TSV also shifted to the warmer side, which indicates strong association between these two parameters.

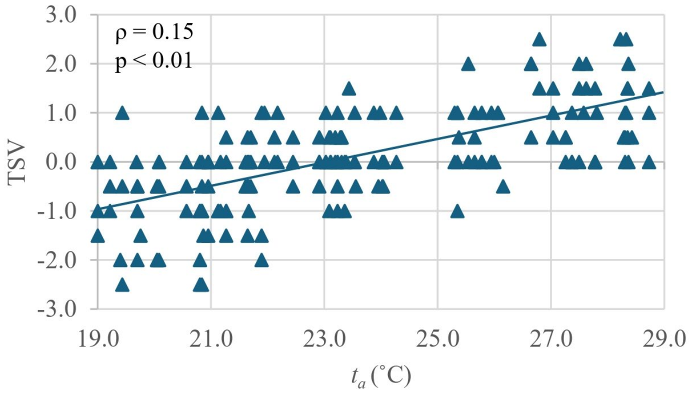

Fig. 5.1 Correlation between TSV and t_a.

**: $p < 0.01$ between TSV and t_a.

5.4.2 Correlation of I_{cl} with t_a and TSV

From Table 5.2 it was observed that there was a significant, though very weak, correlation between I_{cl} and t_a ($r = 0.15$, $p < 0.05$). No correlation was observed between I_{cl} and TSV. Fig. 5.2 (a) presents the relationship between I_{cl} and t_a. Fig. 5.2 (b) shows the relationship between I_{cl} and TSV. No distinct patterns or significant correlations were observed between I_{cl} and TSV.

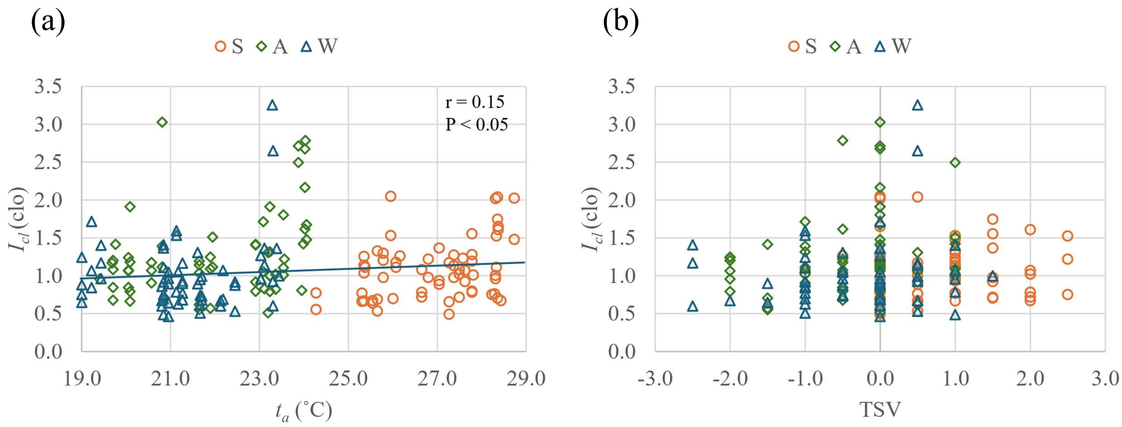

Fig. 5.2 Correlation between I_{cl} and t_a (a), I_{cl} and TSV (b), in summer, autumn and winter.

(S : Summer, A : Autumn, W : Winter)

*: $p < 0.05$ between I_{cl} and t_a prediction.

5.4.3 Correlation of *M* with t_a and TSV

There was no significant correlation observed between *M* and t_a, as well as *M* and TSV (Table 1, Fig. 5.3). However, two distinct patterns in *M* were observed consistently across variations in environmental conditions and TSV, attributable to gender differences.

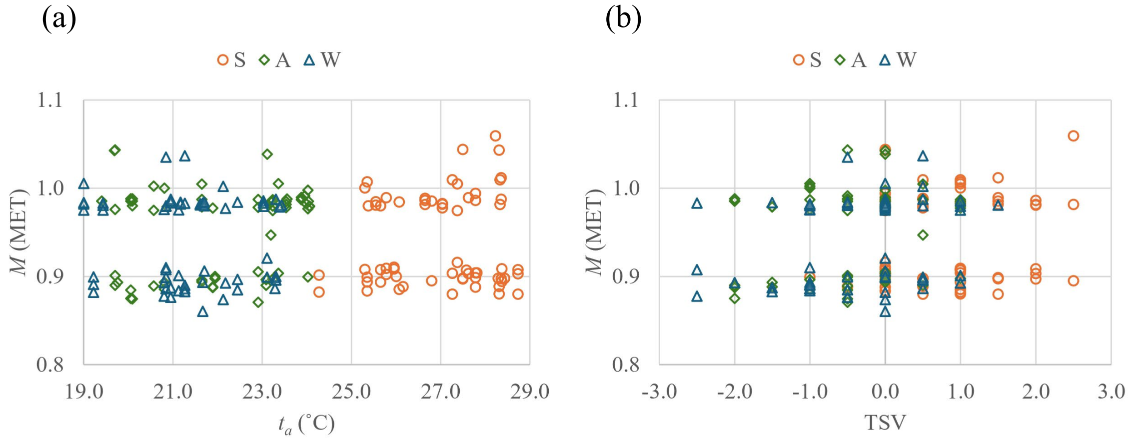

Fig. 5. 3 Correlation between *M* and t_a (a), *M* and TSV (b), in summer, autumn and winter.
(S : Summer, A : Autumn, W : Winter)

5.4.4 Correlation of t_{sk} with t_a and TSV

From Table 5.2, the significant correlation of t_a with $t_{forehead}$, t_{nose} and $t_{palmar\ finger}$ were observed (r = 0.73, 0.84 and 0.86, $p < 0.01$). Significant correlations between TSV and $t_{forehead}$, t_{nose} and $t_{palmar\ finger}$, were also observed (ρ = 0.55, 0.63, 0.57 and 0.60, $p < 0.01$).

Fig 5.4 shows the correlation of $t_{forehead}$ with t_a and TSV, t_{nose} with t_a and TSV, and $t_{palmar\ finger}$ with t_a and TSV. It was observed that the $t_{forehead}$ was mostly in a narrow range in all environmental conditions and different thermal sensations. Whereas t_{nose} and $t_{palmar\ finger}$ data distribution was wider in the lower temperature, however with the increase of t_a, they became narrower. It was also observed that at neutral TSV, the data distribution of t_{nose} and $t_{palmar\ finger}$ were very wider, whereas in warmer sensation and the cooler sensation side it became narrower.

5.4.5 Correlation of $\Delta t_{proximal-distal}$ with t_a and TSV

Here, $\Delta t_{proximal-distal}$ were analysed as a thermoregulatory response to the environmental conditions. Significant negative correlation was observed between t_a and $\Delta t_{forehead-nose}$ and $\Delta t_{forhead-palmar\ finger}$ (r = -0.77 and -0.81, $p < 0.01$). TSV and $\Delta t_{forehead-nose}$ and $\Delta t_{forhead-palmar\ finger}$ were also significantly correlated (r = -0.58 and -0.52, $p < 0.01$) (Table 5.2).

Form the scatter plot illustration between $\Delta t_{forehead-nose}$ and t_a, it was observed that in warmer condition the $\Delta t_{forehead-nose}$ data were in a narrow range comparing the cooler condition (Fig. 5.5 (a)). Similarities also observed for $\Delta t_{forhead-palmar\ finger}$ data sets (Fig. 5.5 (c)).

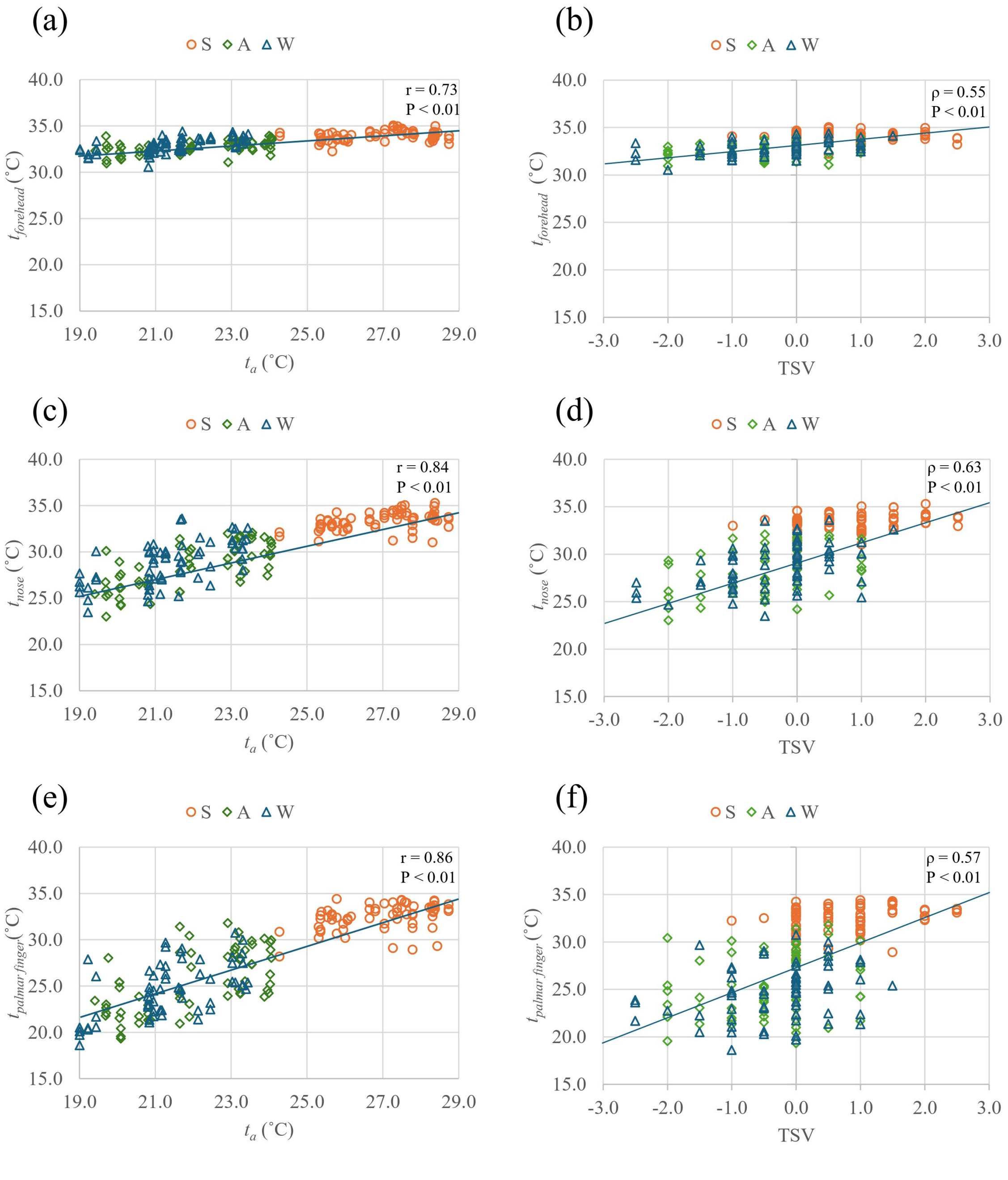

Fig. 5.4 Correlation between $t_{forehead}$ and t_a (a), $t_{forehead}$ and TSV (b), t_{nose} and t_a (c), t_{nose} and TSV (d), $t_{palmar\ finger}$ and t_a (e), $t_{palmar\ finger}$ and TSV (f), in summer, autumn and winter.

(S : Summer, A : Autumn, W : Winter)

**: $p < 0.01$.

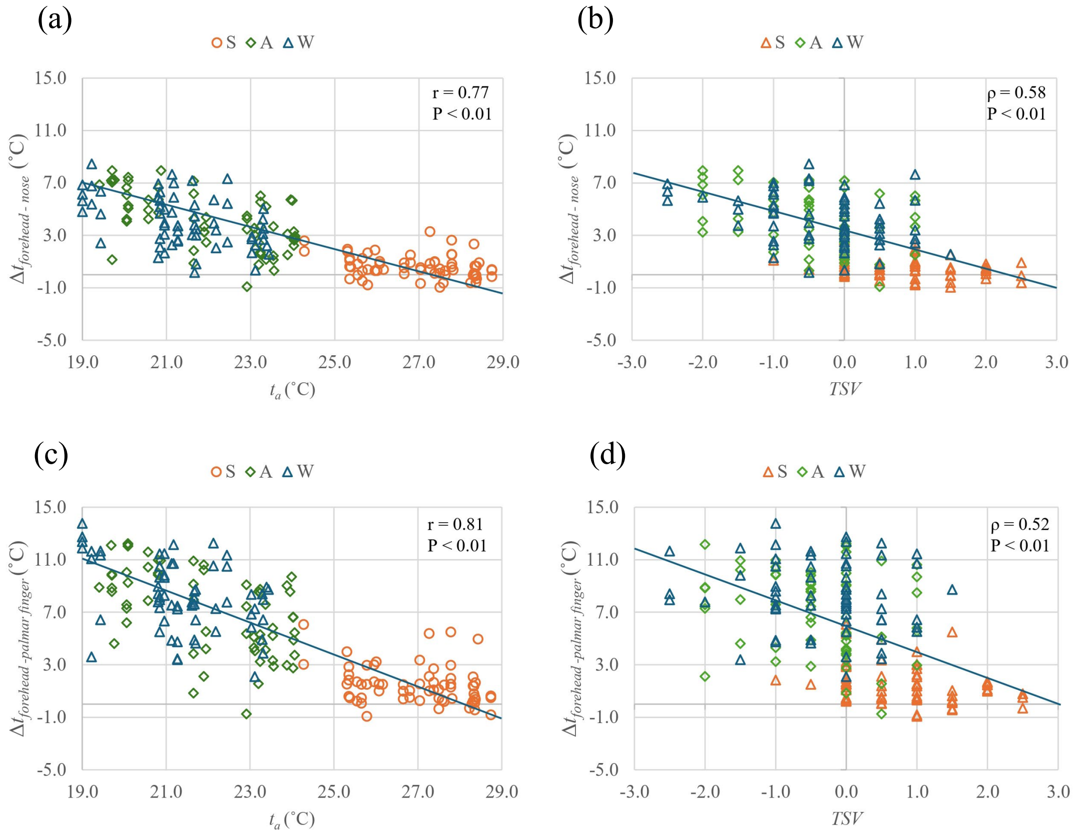

Fig. 5.5 Correlation between $\Delta t_{forehead - nose}$ and t_a (a), $\Delta t_{forehead - nose}$ and TSV (b), $\Delta t_{forhead - palmar\ finger}$ and t_a (c), $\Delta t_{forhead - palmar\ finger}$ and TSV (d), in summer, autumn and winter.

(S : Summer, A : Autumn, W : Winter)

**: $p < 0.01$

5.4.6 Developing TSV prediction model based on physiological responses

In this research by linear regression analysis a new predictive equation was developed to predict thermal sensation and named as "thermal sensation prediction" (*TSP*). Considering the skin temperature gradient from proximal to distal body part as a parameter reflecting vasoconstriction [27, 28], the equation for the *TSP* was developed from $\Delta t_{forehead - nose}$.

$$TSP = 0.737 - 0.238 \times \Delta t_{forehead - nose} \quad \text{(Equation 5.1)}$$

$r = 0.58$, $N = 190$, $p < 0.01$

5.5 Discussion

It is assumed that occupants adapt thermal environment by some behavioural adaptations, metabolic heat production and thermoregulatory responses [250-252]. In this study, participants were free to choose their clothing, though other behavioural adaptation such as opening windows, controlling heating or cooling system was not practiced by any individuals.

From the analysis, both clothing insulation and metabolic rate didn't show any impactful contribution to TSV. Even with the wide range of t_a, I_{cl} and M were not affected so much by the change of t_a. Considering these fact, only physiological thermoregulation, such as local skin temperatures and temperature gradient between proximal to distal body parts, were found to significantly predict TSV.

It is important to note that body regions rich in AVAs exhibit greater sensitivity to sympathetic nervous system activity [43, 51]. In response to changes in ambient temperature, these areas undergo pronounced vasoconstriction, resulting in reduced skin blood flow and lower skin temperature at the distal extremities. While keeping the core body temperature, proximal body parts t_{sk} remain relatively constant across different environmental conditions, showing minimal variation in response to external temperature changes. From the previous chapters it was observed that t_{sk} at distal body parts fluctuate more significantly due to vasomotor control, which is highly influenced by environmental changes [211]. Considering the physiological perspective, in this section, $t_{forehead,}$ was analyzed as proximal body part's t_{sk} and t_{nose}, $t_{palmar\ finger}$ were analyzed as distal body parts' t_{sk} to observe the temperature gradient between proximal and distal body parts.

In addition, considering the potential for non-invasive data collection via IRT, temperatures at the $t_{forehead,}$ t_{nose} and $t_{palmar\ finger}$ are easily obtainable, as these body parts are typically uncovered by clothing throughout all seasons. That was another consideration to considering the local skin temperatures and temperature gradients to analyze with t_a and TSV.

It was observed that in the lower temperature condition, t_{nose} , $t_{palmar\ finger}$ data were widely distributed while with the increase of t_a, the ranges became narrower. The results indicate that under lower air temperature conditions, vasoconstriction occurred in distal body parts, as a thermoregulatory response. However, the degree of vasoconstriction varied among participants, potentially due to differences in physical characteristics, as well as influences of M and I_{cl}. In contrast, under warmer conditions, the thermoregulatory response shifts toward heat dissipation rather than retention. Consequently, vasoconstrictive response at distal body regions is attenuated. It increases skin temperatures of distal areas approaching those of proximal regions. Since core body temperature is generally maintained around 37°C in all individuals, skin temperatures of the nose and palmar fingers tend to stabilize within a normal range under warmer conditions. This physiological responses at warmer condition limits the possibility to predict TSV in warmer environments. This phenomenon also observed in data distribution between t_a with $t_{forhead-nose}$ and $\Delta t_{forhead-palmar\ finger}$.

While developing the prediction model, several physiological indicators were considered. It was observed that single local skin temperature such as $t_{forehead}$, t_{nose} and $t_{palmar\ finger}$ were correlated with TSV. Although single-point local skin temperature is influenced by environmental conditions and may not accurately reflect true vasomotor thermoregulation, proximal-distal temperature differences were used in developing the prediction model. This approach reduces the impact of environmental factors and provides a more reliable representation of vasomotor thermoregulatory responses.

The temperature difference between the forehead and nose ($\Delta t_{forhead - nose}$) was selected due to its physiological importance, particularly within the thermoneutral zone, as it reflects changes in vasomotor activity and peripheral blood flow regulation. Physiologically, due to the higher density of AVAs at the nose region, the nose as a distal region responds rapidly to environmental changes, while the forehead as a proximal region remains more stable [27-29]. This dynamic difference enhances predictivity of thermal sensation, across different conditions. In addition, both measurement sites are located within the same body region, making the analysis of temperature differences more physiologically relevant compared to measurements taken from two spots from two distinct body regions (such as $\Delta t_{forhead - palmar\ finger}$).

As well as practical advantages such as it enables easy data collection using IRT focused solely on the face. Sometimes IRT used to have measurement error however, applying the same sensor error to both points helps minimize the error.

Finally, the developed TSP model demonstrated a strong positive correlation with TSV, indicating that the model is sufficiently reliable for estimating thermal sensation, particularly within the thermoneutral zone.

5.6 Limitations

Despite these promising findings, this study has limitations. The environmental conditions were mostly within thermoneutral ranges, even during summer and winter, what can limit the generalizability of the results.

5.7 Summary

This part of the research investigates behavioural adaptations, metabolic heat production and physiological responses under different climatic conditions and their relationship with TSV. The major findings can be listed as follows,

a) I_{cl} and M were mostly similar when t_a is ranged around 20°C ~ 28°C.

b) Distal body skin temperature such as t_{nose} and $t_{palmar\ finger}$ changes rapidly with t_a changes, while proximal body skin temperature such as t_{head} was mostly stable.

c) Temperature gradient between proximal and distal body parts such as $\Delta t_{forhead - nose}$ and $\Delta t_{forhead - palmar\ finger}$ were significantly correlated with t_a and TSV.

d) The new predictive model, *TSP* can estimate TSV based on the skin temperature gradient between proximal and distal body regions.

In conclusion, the newly developed model (*TSP*) based on the temperature gradient between proximal and distal body regions ($\Delta t_{forhead - nose}$) demonstrates strong potential as a reliable predictor of thermal sensation, particularly within the thermoneutral zone. This physiologically grounded approach reflects underlying vasomotor responses and offers a promising, non-invasive assessment method when integrated with infrared thermography technology. Its application could significantly enhance real-time thermal comfort evaluation in practical indoor environmental monitoring contexts.

CHAPTER 6: Summary and future perspective

This research aimed to develop a consistent, simple, and non-invasive method for real-time thermal sensation prediction using infrared thermography, with the ultimate objective of dynamically regulating the thermal environment based on individual comfort demand. In contrast to traditional static comfort models, this study comprised the complexity of human thermal perceptions by emphasizing the individual differences in behavioral adaptation, metabolic heat production and physiological responses, under identical thermoneutral conditions accepted by international standards.

The central premise of this research lies in the recognition that thermal comfort, thermal perceptions and physiological thermoregulations are highly individualized. Even within similar thermoneutral conditions, thermal sensation and physiological responses vary significantly among individuals due to differences in morphological characteristics, metabolic heat production, choice of clothing, various personal adaptation strategies and physiological thermoregulation.

The results of this study confirm that IRT can be efficiently utilized to predict thermal sensation in real time as a non-invasive manner, by estimating *PMV* using individual I_{cl} estimated from the clothing surface and skin temperature. Alongside, *M* can be estimated from morphological characteristics. When these morphological predictions and thermographic predictions are integrated into *PMV* estimation, they significantly enhance the accuracy of thermal sensation assessment. This enables real-time feedback on occupant comfort, thereby providing opportunities for immediate thermal environmental adjustments.

Advancing into physiological determinants, certain local skin temperatures and proximal-distal temperature gradients were observed to be substantially indicative of individual thermal sensation. Remarkably, proximal-distal temperature gradients can serve as a reliable indicator of peripheral vasoconstriction, which is closely associated with thermal sensation and thermoregulatory responses.

Importantly, temperature gradients between proximal and distal skin regions could provide a more reliable indicator of vasomotor activity than single-point skin temperature measurements. While skin temperature is influenced by both ambient conditions and thermoregulatory responses, the proximal-to-distal skin temperature gradient is considered to reflect thermoregulatory vasomotor activity more specifically. This is because both proximal and distal skin sites are similarly affected by the environment, whereas the distal regions show greater temperature reductions due to vasoconstriction. In addition, two-point IRT-based temperature gradient measurements minimize sensor inaccuracy and distance-induced variability compared to single-site readings.

In this context, distal regions such as the fingers or nose are more sensitive to thermoregulatory vasomotor responses than proximal sites like the forehead, making them more effective indicators of thermal state. Thus, the proximal-distal temperature gradient provides a robust and physiologically meaningful predictor of individual thermal comfort.

This process is also advantageous due to the ease of capturing these temperatures from the body areas that are typically uncovered by clothing insulation. Based on this, a new model was proposed for predicting thermal sensation and it found strongly correlated with actual TSV data collected across all seasons.

Moving forward, the next step will be to incorporating real time tracking of robust morphological variations and behavioral adaptations as indicators alongside vasomotor control could enhance the accuracy of thermal sensation predictions.

Following the research outcomes, in future in indoor environment air conditioning systems could be evolved by incorporating real-time, individualized thermal comfort assessment technique. By predicting skin temperature and proximal-distal skin temperature gradients through IRT, predicting morphological characteristics such as body mass, height, sex, and age. Through commonly installed webcam-based imaging, integrating AI and machine learning algorithms could estimate each occupant's thermal sensation without the need for intrusive sensors or manual input. These systems will automatically detect morphological features and enabling accurate consideration of individual physiological differences to predict thermal sensation. This approach will replace traditional thermal assessment methods, allowing for dynamic, personalized temperature control at personal level. Beyond comfort, this innovation will contribute to significant energy savings by minimizing over-conditioning in heating, ventilation, and air conditioning system. Ultimately, such technology has the potential to define a new global standard for thermal environment design, contributing to the modification of ISO standards to reflect individual variability. This direction aligns with flexible working styles by providing thermal environments tailored to individual needs in activity-based work environments. It's a great possibility that personalized thermal control systems informed by real-time comfort assessments could replace conventional heating, ventilation, and air conditioning system operations with adaptive solutions that simultaneously improve comfort and well-being. Fig 6.1 shows a conceptual diagram of automated indoor air conditioning system with personal heating/cooling system based on individual physiological responses, morphological characteristics and behavioral adaptations.

Looking ahead, future research should explore the integration of real time thermal assessment considering occupant movement analysis and machine learning algorithms. By embedding AI-driven systems into thermal comfort prediction, indoor environment as well built spaces can become more responsive. Such advancements would support the creation of intelligent comfort systems that autonomously adapt to occupants' thermal requirements over time. Adaptive thermal environments that continuously learn from occupant feedback and behavior can be more efficient for overall well-being and elevated human performance. This study, therefore, opens a new pathway toward the realization of modern, sustainable, and human-centric built environments.

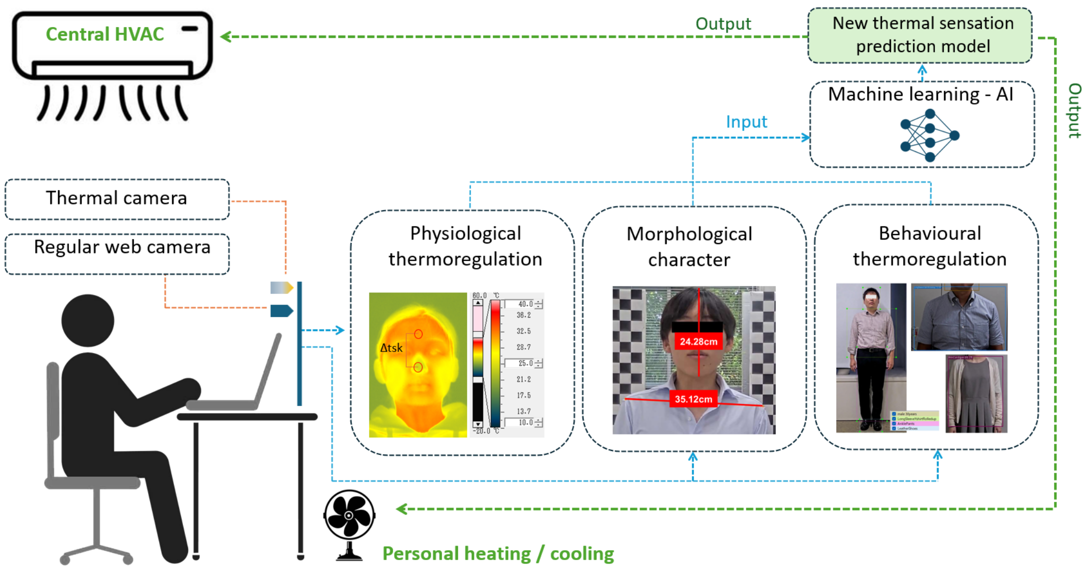

Fig. 6.1. Conceptual diagram of automated indoor air conditioning system with personal heating/ cooling system based on individual physiological responses, morphological characteristics and behavioral adaptations.

REFERENCES

[1] ASHRAE, ASHRAE Handbook-Fundamentals. American Society of Heating, Refrigerating, and Air-Conditioning Engineers, Atlanta, 2021.

[2] R. De Dear, G.S. Brager, Developing an adaptive model of thermal comfort and preference, Indoor environmental Quality, UC Berkeley (1998).

[3] P.O. Fanger, Thermal Comfort: Analysis and Applications in Environmental Engineering, McGraw Hill Book Company, United States, 1970.

[4] A.S. Ali, S.J.L. Chua, M.E.L. Lim, Physical environment comfort towards Malaysian universities office employers' performance and productivity, Facilities 37(11/12) (2019) 686-703.

[5] B. Herbig, A. Schneider, D. Nowak, Does office space occupation matter? The role of the number of persons per enclosed office space, psychosocial work characteristics, and environmental satisfaction in the physical and mental health of employees, Indoor Air 26(5) (2016) 755-67.

[6] J. Van Hoof, Forty years of Fanger's model of thermal comfort: comfort for all?, Indoor air 18(3) (2008).

[7] L. Taylor, S.L. Watkins, H. Marshall, B.J. Dascombe, J. Foster, The Impact of Different Environmental Conditions on Cognitive Function: A Focused Review, Front Physiol 6 (2016).

[8] ASHRAE-55, Thermal Environmental Conditions for Human Occupancy, Atlanta, GA, 2010.

[9] K. Vimalanathan, T. Ramesh Babu, The effect of indoor office environment on the work performance, health and well-being of office workers, Journal of environmental health science and engineering 12 (2014) 1-8.

[10] Y. Al Horr, M. Arif, A. Kaushik, A. Mazroei, M. Katafygiotou, E. Elsarrag, Occupant productivity and office indoor environment quality: A review of the literature, Building and environment 105 (2016) 369-389.

[11] ISO 7730, Ergonomics of the thermal environment — Analytical determination and interpretation of thermal comfort using calculation of the PMV and PPD indices and local thermal comfort criteria, Geneva, Switzerland, 2005.

[12] A. Lipczynska, S. Schiavon, L.T. Graham, Thermal comfort and self-reported productivity in an office with ceiling fans in the tropics, Building and Environment 135 (2018) 202-212.

[13] K.C. Parsons, Human thermal environments: the effects of hot, moderate, and cold environments on human health, comfort and performance, CRC press2007.

[14] J.R. Speakman, C. Selman, Physical activity and resting metabolic rate, Proceedings of the Nutrition Society 62(3) (2003) 621-634.

[15] ISO 8996, Ergonomics of the thermal environment — Determination of metabolic rate, Geneva, Switzerland, 2004.

[16] S. Gao, R. Ooka, W. Oh, Experimental investigation of the effect of clothing insulation on thermal comfort indices, Building and Environment 187 (2021) 107393.

[17] J. Huang, D. Shi, Z. Fang, Y. Gao, C. Zhuang, J. Zhai, Impact of short-term thermal experience on thermal sensation: A case study of Chongqing, China, Building and Environment 179 (2020) 106921.

[18] N. Umemiya, Seasonal variations of physiological characteristics and thermal sensation under identical thermal conditions, J Physiol Anthropol 25(1) (2006) 29-39.

[19] Y. Zhu, Q. Ouyang, B. Cao, X. Zhou, J. Yu, Dynamic thermal environment and thermal comfort, Indoor air 26(1) (2016) 125-137.

[20] H. Zhang, E. Arens, C. Huizenga, T. Han, Thermal sensation and comfort models for non-uniform and transient environments: Part I: Local sensation of individual body parts, Building and Environment 45(2) (2010) 380-388.

[21] L. Zhuang, J. Huang, F. Li, K. Zhong, Psychological adaptation to thermal environments and its effects on thermal sensation, Physiology & Behavior 247 (2022) 113724.

[22] B.K. Biswas, K. Ishii, Y. Watanabe, J. Li, Y. Tan, A. Dempoya, S.-i. Lee, T. Iwamura, S. Konoshita, H. Wakabayashi, Predicting individual variability in thermal sensation, PMV predictions, and local skin temperature differences using infrared thermography, Building and Environment 269 (2025) 112477.

[23] Z. Wang, R. de Dear, M. Luo, B. Lin, Y. He, A. Ghahramani, Y. Zhu, Individual difference in thermal comfort: A literature review, Building and Environment 138 (2018) 181-193.

[24] T. Yamato, M. Aomine, Relationships between cold constitution and accelerated plethysmogram in young females, Health Evaluation and Promotion 32(6) (2005) 493-499.

[25] N. Hashiguchi, Y. Tochihara, T. Ohnaka, C. Tsuchida, T. Otsuki, Physiological and subjective responses in the elderly when using floor heating and air conditioning systems, Journal of physiological anthropology and applied human science 23(6) (2004) 205-213.

[26] J.M. Johnson, C.T. Minson, D.L. Kellogg Jr, Cutaneous vasodilator and vasoconstrictor mechanisms in temperature regulation, Comprehensive physiology 4(1) (2014) 33-89.

[27] I.B. Mekjavic, M.J. Tipton, Myths and methodologies: Degrees of freedom–limitations of infrared thermographic screening for Covid-19 and other infections, Experimental Physiology 107(7) (2022) 733-742.

[28] J.R. House, M.J. Tipton, Using skin temperature gradients or skin heat flux measurements to determine thresholds of vasoconstriction and vasodilatation, European journal of applied physiology 88 (2002) 141-145.

[29] K. Kräuchi, C. Cajochen, E. Werth, A. Wirz-Justice, Functional link between distal vasodilation and sleep-onset latency?, American Journal of Physiology-Regulatory, Integrative and Comparative Physiology (2000).

[30] M. Nakamura, T. Yoda, L.I. Crawshaw, S. Yasuhara, Y. Saito, M. Kasuga, K. Nagashima, K. Kanosue, Regional differences in temperature sensation and thermal comfort in humans, Journal of applied physiology 105(6) (2008) 1897-1906.
[31] L.G. Berglund, Comfort and humidity, ASHRAE journal 40(8) (1998) 35.
[32] A.P. Gagge, A new physiological variable associated with sensible and insensible perspiration, American Journal of Physiology-Legacy Content 120(2) (1937) 277-287.
[33] ISO 28802, Ergonomics of the physical environment — Assessment of environments by means of an environmental survey involving physical measurements of the environment and subjective responses of people, Geneva, Switzerland, 2012.
[34] J.F. Nicol, M.A. Humphreys, Adaptive thermal comfort and sustainable thermal standards for buildings, Energy and Buildings 34(6) (2002) 563-572.
[35] A.P. Gagge, J.A. Stolwijk, J.D. Hardy, Comfort and thermal sensations and associated physiological responses at various ambient temperatures, Environmental research 1(1) (1967) 1-20.
[36] D. Wang, H. Zhang, E. Arens, C. Huizenga, Observations of upper-extremity skin temperature and corresponding overall-body thermal sensations and comfort, Building and Environment 42(12) (2007) 3933-3943.
[37] Y.Y. Wu, B. Cao, Recognition and prediction of individual thermal comfort requirement based on local skin temperature, J Build Eng 49 (2022).
[38] S.-Y. Son, Thermoregulation, in: Y. Tochihara (Ed.), The Thermal Environment: From Viewpoints of Physiological Anthropology and Environmental Ergonomics, Srringer, Singapore, 2025.
[39] T. Edition, Glossary of terms for thermal physiology, The Japanese Journal of Physiology 51(2) (2001) 245.
[40] N. Taylor, A. S. , N. Kondo, W.L. Kenney, The physiology of acute heat exposure, with implications for human performance in the heat, Physiological Bases of Human Performance During Work and Exercise, Elsevier Health Sciences2008.
[41] W.L. Kenney, J.M. Johnson, Control of skin blood flow during exercise, Med Sci Sports Exerc 24(3) (1992) 303-12.
[42] J.M. Johnson, D.L. Kellogg Jr, Thermoregulatory and thermal control in the human cutaneous circulation, Front Biosci (Schol Ed) 2(3) (2010) 825-53.
[43] L. Walloe, Arterio-venous anastomoses in the human skin and their role in temperature control. Temperature (austin) 3 (1): 92–103, 2016.
[44] T. Wijayanto, Physiological responses and performance in hot environments, in: Y. Tochihara (Ed.), The Thermal Environment: From Viewpoints of Physiological Anthropology and Environmental Ergonomics, Springer2025.
[45] L. Walløe, Arterio-venous anastomoses in the human skin and their role in temperature control, Temperature 3(1) (2016) 92-103.

[46] T. Fukazawa, Cold, hot and health, Apparel and health: from the basics to evolving clothing, Tokyo: Inoueshin (2012) 20.

[47] N.A. Taylor, M.J. Tipton, G.P. Kenny, Considerations for the measurement of core, skin and mean body temperatures, Journal of thermal biology 46 (2014) 72-101.

[48] M.J. Thompson, N. Ninis, R. Perera, R. Mayon-White, C. Phillips, L. Bailey, A. Harnden, D. Mant, M. Levin, Clinical recognition of meningococcal disease in children and adolescents, The lancet 367(9508) (2006) 397-403.

[49] M. Zhang, Computational modeling and simulation of hand-specific heat transfer and thermoregulation during cold stress, Iowa State University, 2021.

[50] H. Wakabayashi, H. Sakaue, T. Nishimura, Recent updates on cold adaptation in population and laboratory studies, including cross-adaptation with nonthermal factors, J Physiol Anthropol 44(1) (2025) 1-29.

[51] H. Wakabayashi, Physiological responses and performance in cold environments, in: Y. Tochihara (Ed.), The Thermal Environment: From Viewpoints of Physiological Anthropology and Environmental Ergonomics, Springer, Singapore, 2025, pp. 101-138.

[52] I. Campbell, Body temperature and its regulation, Anaesthesia & Intensive Care Medicine 9(6) (2008) 259-263.

[53] C. Bergmann, Ueber die Verhaltnisse der Warmeokonomie der Thierezuihrer Grosse, Gottinger Studien 3 (1847) 595-708. .

[54] G.A. Selkirk, T.M. McLellan, Influence of aerobic fitness and body fatness on tolerance to uncompensable heat stress, Journal of Applied Physiology 91(5) (2001) 2055-2063.

[55] F. Fantozzi, M. Rocca, An extensive collection of evaluation indicators to assess occupants' health and comfort in indoor environment, Atmosphere 11(1) (2020) 90.

[56] G. Brager, G. Paliaga, R. De Dear, Operable windows, personal control and occupant comfort, (2004).

[57] J.F. Nicol, Characterising occupant behaviour in buildings: towards a stochastic model of occupant use of windows, lights, blinds, heaters and fans, Proceedings of the seventh international IBPSA conference, Rio, 2001, pp. 1073-1078.

[58] S. Herkel, U. Knapp, J. Pfafferott, A preliminary model of user behaviour regarding the manual control of windows in office buildings, Proc. 9th Int. IBPSA Conf. BS2005, Montréal, 2005, pp. 403-410.

[59] G.S. Brager, R.J. De Dear, Thermal adaptation in the built environment: a literature review, Energy and buildings 27(1) (1998) 83-96.

[60] N.A. Taylor, Ethnic differences in thermoregulation: genotypic versus phenotypic heat adaptation, Journal of Thermal Biology 31(1-2) (2006) 90-104.

[61] J.-Y. Lee, M. Saat, C. Chou, N. Hashiguchi, T. Wijayanto, H. Wakabayashi, Y. Tochihara, Cutaneous warm and cool sensation thresholds and the inter-threshold zone in Malaysian and Japanese males, Journal of Thermal Biology 35(2) (2010) 70-76.
[62] H. Wakabayashi, H. Sakaue, T. Nishimura, Recent updates on cold adaptation in population and laboratory studies, including cross-adaptation with non-thermal factors., Journal of Physiological Anthropology 44 (2025).
[63] M. Nikolopoulou, K. Steemers, Thermal comfort and psychological adaptation as a guide for designing urban spaces, Energy and buildings 35(1) (2003) 95-101.
[64] S. Kaplan, R. Kaplan, Cognition and environment: Functioning in an uncertain world, (No Title) (1982).
[65] J. Liu, R. Yao, J. Wang, B. Li, Occupants' behavioural adaptation in workplaces with non-central heating and cooling systems, Applied Thermal Engineering 35 (2012) 40-54.
[66] Y. Tochihara, J.-Y. Lee, H. Wakabayashi, T. Wijayanto, I. Bakri, K. Parsons, The use of language to express thermal sensation suggests heat acclimatization by Indonesian people, International journal of biometeorology 56 (2012) 1055-1064.
[67] Y. Lin, L. Yang, W. Zheng, Y. Ren, Study on human physiological adaptation of thermal comfort under building environment, Procedia Engineering 121 (2015) 1780-1787.
[68] S. Itoh, K. Doi, A. Kuroshima, Enhanced sensitivity to noradrenaline of the Ainu, International Journal of Biometeorology 14 (1970) 195-200.
[69] K. Pandolf, Time course of heat acclimation and its decay, International journal of sports medicine 19(S 2) (1998) S157-S160.
[70] F. Yamazaki, K. Hamasaki, Heat acclimation increases skin vasodilation and sweating but not cardiac baroreflex responses in heat-stressed humans, Journal of Applied Physiology 95(4) (2003) 1567-1574.
[71] J.-Y. Lee, H. Wakabayashi, T. Wijayanto, N. Hashiguchi, M. Saat, Y. Tochihara, Ethnic differences in thermoregulatory responses during resting, passive and active heating: application of Werner's adaptation model, European journal of applied physiology 111 (2011) 2895-2905.
[72] Y. Tochihara, H. Wakabayashi, J.-Y. Lee, T. Wijayanto, N. Hashiguchi, M. Saat, How humans adapt to hot climates learned from the recent research on tropical indigenes, J Physiol Anthropol 41(1) (2022) 27.
[73] T. Wijayanto, H. Wakabayashi, J.-Y. Lee, N. Hashiguchi, M. Saat, Y. Tochihara, Comparison of thermoregulatory responses to heat between Malaysian and Japanese males during leg immersion, International journal of biometeorology 55 (2011) 491-500.
[74] S. Carlucci, L. Pagliano, A review of indices for the long-term evaluation of the general thermal comfort conditions in buildings, Energy and Buildings 53 (2012) 194-205.

[75] S. Zare, N. Hasheminejad, H.E. Shirvan, R. Hemmatjo, K. Sarebanzadeh, S. Ahmadi, Comparing Universal Thermal Climate Index (UTCI) with selected thermal indices/environmental parameters during 12 months of the year, Weather and climate extremes 19 (2018) 49-57.
[76] F.R.d.A. Alfano, B.I. Palella, G. Riccio, J. Toftum, Fifty years of Fanger's equation: Is there anything to discover yet?, International Journal of Industrial Ergonomics 66 (2018) 157-160.
[77] ISO 9920, Ergonomics of the thermal environment — Estimation of the thermal insulation and evaporative resistance of a clothing ensemble, Geneva, Switzerland, 2007.
[78] A. Ganpule, S. Tanaka, K. Ishikawa-Takata, I. Tabata, Interindividual variability in sleeping metabolic rate in Japanese subjects, European journal of clinical nutrition 61(11) (2007) 1256-1261.
[79] W.N. Schofield, Predicting basal metabolic rate, new standards and review of previous work, Hum Nutr Clin Nutr 39 Suppl 1 (1985) 5-41.
[80] W.P.T. James, E.C. Schofield, Human Energy Requirements, Oxford University Press, Oxford, 1990.
[81] R. Kuriyan, P.P. Easwaran, A.V. Kurpad, Physical activity ratio of selected activities in Indian male and female subjects and its relationship with body mass index, British Journal of Nutrition 96 (2006) 71-79.
[82] S. Fujimoto, T. Watanabe, A. Sakamoto, K. Yukawa, K. Morimoto, Studies on the physical surface area of Japanese part 18 calculation formulas in three stages over all age, Nippon Eiseigaku Zasshi (Japanese Journal of Hygiene) 23(5) (1968) 443-450.
[83] R. Hisayama, A. Nomoto, H. Yoda, M. Akimoto, S. Ogata, S. Tanabe, H. Tsutsumi, Y. Ozeki, Proceedings of the Reiwa 2nd Annual Meeting (Online) Vol. 6 Thermal Environmental Assessment, Reiwa 2nd Annual Meeting of the Society of Air Conditioning and Sanitary Engineers, 2020.
[84] R. Hisayama, A. Nomoto, H. Yoda, M. Akimoto, S. Ogata, S. Tanabe, H. Tsutsumi, H. Ozeki, Proceedings of the Reiwa 2nd Annual Meeting (Online) Vol. 6 Thermal Environmental Assessment, Reiwa 2nd Annual Meeting of the Society of Air Conditioning and Sanitary Engineers, 2020.
[85] K. Blazejczyk, Y. Epstein, G. Jendritzky, H. Staiger, B. Tinz, Comparison of UTCI to selected thermal indices, International journal of biometeorology 56 (2012) 515-535.
[86] A.P. Gagge, A. Fobelets, L. Berglund, A standard predictive index of human response to the thermal environment, Build. Eng.92 (2B) (1986) 709-731.
[87] P. Höppe, The physiological equivalent temperature–a universal index for the biometeorological assessment of the thermal environment, International journal of Biometeorology 43 (1999) 71-75.
[88] P. Bröde, D. Fiala, K. Błażejczyk, I. Holmér, G. Jendritzky, B. Kampmann, B. Tinz, G. Havenith, Deriving the operational procedure for the Universal Thermal Climate Index (UTCI), International journal of biometeorology 56 (2012) 481-494.
[89] D. Fiala, K.J. Lomas, M. Stohrer, A computer model of human thermoregulation for a wide range of environmental conditions: the passive system, Journal of applied physiology 87(5) (1999) 1957-1972.
[90] C. Yaglou, D. Minaed, Control of heat casualties at military training centers, (1957).

[91] W. Ji, Y. Zhu, H. Du, B. Cao, Z. Lian, Y. Geng, S. Liu, J. Xiong, C. Yang, Interpretation of standard effective temperature (SET) and explorations on its modification and development, Building and Environment 210 (2022) 108714.
[92] Z. Fang, Y. Zhang, Y. Yang, X. Zhou, Z. Zheng, Experimental investigation of standard effective temperature (SET*) adapted for human walking in an indoor and transitional thermal environment, Science of The Total Environment 793 (2021) 148421.
[93] P. Cohen, O. Potchter, A. Matzarakis, Daily and seasonal climatic conditions of green urban open spaces in the Mediterranean climate and their impact on human comfort, Building and environment 51 (2012) 285-295.
[94] A. Costantino, M. Ferrara, M. Arnesano, E. Fabrizio, Off-the-shelf wearable sensing devices for personalized thermal comfort models: A systematic review on their use in scientific research, J Build Eng 70 (2023) 106379.
[95] Z. Wang, R. Matsuhashi, H. Onodera, Towards wearable thermal comfort assessment framework by analysis of heart rate variability, Building and Environment 223 (2022) 109504.
[96] W. Handouzi, C. Maaoui, A. Pruski, A. Moussaoui, Objective model assessment for short-term anxiety recognition from blood volume pulse signal, Biomedical Signal Processing and Control 14 (2014) 217-227.
[97] H. Kim, D. Jung, H. Choi, T. Hong, Advanced prediction model for individual thermal comfort considering blood glucose and salivary cortisol, Building and Environment 224 (2022) 109551.
[98] S.A. Mansi, G. Barone, C. Forzano, I. Pigliautile, M. Ferrara, A.L. Pisello, M. Arnesano, Measuring human physiological indices for thermal comfort assessment through wearable devices: A review, Measurement 183 (2021) 109872.
[99] M.J. Hasselberg, J. McMahon, K. Parker, The validity, reliability, and utility of the iButton® for measurement of body temperature circadian rhythms in sleep/wake research, Sleep medicine 14(1) (2013) 5-11.
[100] B. Yang, X. Li, Y. Hou, A. Meier, C. Xiaogang, J.-H. Choi, F. Wang, H. Wang, A. Wangner, D. Tyan, A. Li, T. Olofsson, H. Li, Non-invasive human thermal comfort assessment based on multiple angle/distance facial key-region temperatures recognition, Energy and Buildings 224(110261) (2020).
[101] F. De Oliveira, S. Moreau, C. Gehin, A. Dittmar, Infrared imaging analysis for thermal comfort assessment, 2007 29th Annual international conference of the IEEE engineering in medicine and biology society, IEEE, 2007, pp. 3373-3376.
[102] J.R. Speakman, S. Ward, Infrared thermography: principles and applications, Zoology-Jena- 101 (1998) 224-232.
[103] D.G. Moreira, J.T. Costello, C.J. Brito, J.G. Adamczyk, K. Ammer, A.J. Bach, C.M. Costa, C. Eglin, A.A. Fernandes, I. Fernández-Cuevas, Thermographic imaging in sports and exercise medicine: A

Delphi study and consensus statement on the measurement of human skin temperature, Journal of thermal biology 69 (2017) 155-162.

[104] J. Foster, A.B. Lloyd, G. Havenith, Non-contact infrared assessment of human body temperature: The journal Temperature toolbox, Temperature 8(4) (2021) 306-319.

[105] E. Ring, K. Ammer, Infrared thermal imaging in medicine, Physiological measurement 33(3) (2012) R33.

[106] H.-Y. Wu, M. Rubinstein, E. Shih, J. Guttag, F. Durand, W. Freeman, Eulerian video magnification for revealing subtle changes in the world, ACM transactions on graphics (TOG) 31(4) (2012) 1-8.

[107] S.-E. Wei, V. Ramakrishna, T. Kanade, Y. Sheikh, Convolutional pose machines, Proceedings of the IEEE conference on Computer Vision and Pattern Recognition, 2016, pp. 4724-4732.

[108] H. Na, J.-H. Choi, H. Kim, T. Kim, Development of a human metabolic rate prediction model based on the use of Kinect-camera generated visual data-driven approaches, Building and Environment 160 (2019) 106216.

[109] R.F. Rupp, N.G. Vásquez, R. Lamberts, A review of human thermal comfort in the built environment, Energy and Buildings 105 (2015) 178-205.

[110] G.T. Leites, G.S. Cunha, J. Obeid, B. Wilk, F. Meyer, B.W. Timmons, Thermoregulation in boys and men exercising at the same heat production per unit body mass, European journal of applied physiology 116 (2016) 1411-1419.

[111] Z. Wang, Z. Ying, A. Bosy-Westphal, J. Zhang, M. Heller, W. Later, S.B. Heymsfield, M.J. Müller, Evaluation of specific metabolic rates of major organs and tissues: comparison between nonobese and obese women, Obesity 20(1) (2012) 95-100.

[112] L. Wang, X. Ren, X. Zhu, W. Li, J. Yang, H. Zhang, J. Yang, H. Yin, Effects of body muscle and fat on differences in thermal preference, Building and Environment 243 (2023) 110643.

[113] A. Lipczynska, A. Mishra, S. Schiavon, Experimental evaluation of the effect of body mass on thermal comfort perception, (2020).

[114] T. Yoshida, K. Nagashima, S. Nakai, A. Yorimoto, T. Kawabata, T. Morimoto, Nonshivering thermoregulatory responses in trained athletes: effects of physical fitness and body fat, The Japanese journal of physiology 48(2) (1998) 143-148.

[115] W.H. Organization, Body Mass Index – BMI, https://www.who.int/news-room/fact-sheets/detail/obesity-and-overweight, 2020.

[116] K. Tan, Appropriate body-mass index for Asian populations and its implications for policy and intervention strategies, The lancet (2004).

[117] M. Mozaffarieh, P. Fontana Gasio, A. Schötzau, S. Orgül, J. Flammer, K. Kräuchi, Thermal discomfort with cold extremities in relation to age, gender, and body mass index in a random sample of a Swiss urban population, Population Health Metrics 8 (2010) 1-5.

[118] M. Indraganti, R. Ooka, H.B. Rijal, Thermal comfort in offices in India: Behavioral adaptation and the effect of age and gender, Energy and Buildings 103 (2015) 284-295.
[119] M. He, J. Guo, H. Liu, F. Xiong, S. Zhou, Y. Wu, B. Li, R. Kosonen, Does BMI affect thermal comfort in young people in warm indoor environments? Evidence from a climate chamber experiment in non-normal BMIs, J Build Eng 106 (2025) 112618.
[120] D. Jung, D. Kim, J. Park, J.Y. Lee, Greater body mass index is related to greater self-identified cold tolerance and greater insensible body mass loss, J Physiol Anthropol 35 (2016) 1-5.
[121] K. Rewitz, D. Müller, Influence of gender, age and BMI on human physiological response and thermal sensation for transient indoor environments with displacement ventilation, Building and Environment 219 (2022) 109045.
[122] L.G. Kraemer-Aguiar, M.L.d. Miranda, D.A. Bottino, R.d.A. Lima, M.d.G.C.d. Souza, M.d.M. Balarini, N.R. Villela, E. Bouskela, Increment of body mass index is positively correlated with worsening of endothelium-dependent and independent changes in forearm blood flow, Front Physiol 6 (2015) 223.
[123] I. Janssen, S.B. Heymsfield, Z. Wang, R. Ross, Skeletal muscle mass and distribution in 468 men and women aged 18–88 yr, Journal of applied physiology (2000).
[124] N. Charkoudian, Mechanisms and modifiers of reflex induced cutaneous vasodilation and vasoconstriction in humans, Journal of applied physiology 109(4) (2010) 1221-1228.
[125] P. Fanger, J. Højbjerre, J. Thomsen, Thermal comfort conditions in the morning and in the evening, International journal of biometeorology 18 (1974) 16-22.
[126] L. Yang, S. Zhao, S. Gao, H. Zhang, E. Arens, Y. Zhai, Gender differences in metabolic rates and thermal comfort in sedentary young males and females at various temperatures, Energy and Buildings 251 (2021) 111360.
[127] L. Schellen, M.G. Loomans, M.H. de Wit, B.W. Olesen, W. van Marken Lichtenbelt, The influence of local effects on thermal sensation under non-uniform environmental conditions—Gender differences in thermophysiology, thermal comfort and productivity during convective and radiant cooling, Physiology & behavior 107(2) (2012) 252-261.
[128] W. McArdle, J. Magel, T. Gergley, R. Spina, M. Toner, Thermal adjustment to cold-water exposure in resting men and women, Journal of Applied Physiology 56(6) (1984) 1565-1571.
[129] H. Liu, Y. Wu, D. Lei, B. Li, Gender differences in physiological and psychological responses to the thermal environment with varying clothing ensembles, Building and Environment 141 (2018) 45-54.
[130] L. Lan, Z. Lian, W. Liu, Y. Liu, Investigation of gender difference in thermal comfort for Chinese people, European journal of applied physiology 102 (2008) 471-480.
[131] L. Schellen, M. Loomans, M. de Wit, W. van Marken Lichtenbelt, The influence of different cooling techniques and gender on thermal perception, Building Research & Information 41(3) (2013) 330-341.

[132] J.A. Wagner, S.M. Horvath, Influences of age and gender on human thermoregulatory responses to cold exposures, Journal of Applied Physiology 58(1) (1985) 180-186.
[133] J.P. Cooke, M.A. Creager, P.J. Osmundson, J.T. Shepherd, Sex differences in control of cutaneous blood flow, Circulation 82(5) (1990) 1607-1615.
[134] J.-Y. Lee, J.-W. Choi, Influences of clothing types on metabolic, thermal and subjective responses in a cool environment, Journal of Thermal Biology 29(4-5) (2004) 221-229.
[135] K. Kaikaew, J.C. van den Beukel, S.J. Neggers, A.P. Themmen, J.A. Visser, A. Grefhorst, Sex difference in cold perception and shivering onset upon gradual cold exposure, Journal of thermal biology 77 (2018) 137-144.
[136] T. Ichinose-Kuwahara, Y. Inoue, Y. Iseki, S. Hara, Y. Ogura, N. Kondo, Sex differences in the effects of physical training on sweat gland responses during a graded exercise, Exp Physiol 95(10) (2010) 1026-32.
[137] Y. Inoue, Y. Tanaka, K. Omori, T. Kuwahara, Y. Ogura, H. Ueda, Sex-and menstrual cycle-related differences in sweating and cutaneous blood flow in response to passive heat exposure, European journal of applied physiology 94 (2005) 323-332.
[138] A. Kawahata, Sex differences in sweating. , Essential Problems in Climatic Physiology, (1960) 169–184.
[139] B. Kingma, A. Frijns, W. van Marken Lichtenbelt, The thermoneutral zone: implications for metabolic studies, Frontiers in Bioscience-Elite 4(5) (2012) 1975-1985.
[140] M.Y. Beshir, J.D. Ramsey, Comparison between male and female subjective estimates of thermal effects and sensations, Applied Ergonomics 12(1) (1981) 29-33.
[141] J. Choi, A. Aziz, V. Loftness, Investigation on the impacts of different genders and ages on satisfaction with thermal environments in office buildings, Building and Environment 45(6) (2010) 1529-1535.
[142] F. Grivel, V. Candas, Ambient temperatures preferred by young European males and females at rest, Ergonomics 34(3) (1991) 365-378.
[143] C. Peng, Survey of thermal comfort in residential buildings under natural conditions in hot humid and cold wet seasons in Nanjing, Frontiers of Architecture and Civil Engineering in China 4 (2010) 503-511.
[144] W. Liu, Z. Lian, Q. Deng, Y. Liu, Evaluation of calculation methods of mean skin temperature for use in thermal comfort study, Building and Environment 46(2) (2011) 478-488.
[145] K. Cena, R. De Dear, Thermal comfort and behavioural strategies in office buildings located in a hot-arid climate, Journal of Thermal Biology 26(4-5) (2001) 409-414.
[146] I. Fato, F. Martellotta, C. Chiancarella, Thermal comfort in the climatic conditions of Southern Italy, Transactions-American Society of Heating Refrigerating and Air Conditioning Engineers 110(2) (2004) 578-593.

[147] R.F. Rupp, J. Kim, R. de Dear, E. Ghisi, Associations of occupant demographics, thermal history and obesity variables with their thermal comfort in air-conditioned and mixed-mode ventilation office buildings, Building and Environment 135 (2018) 1-9.

[148] Z. Wang, A field study of the thermal comfort in residential buildings in Harbin, Building and Environment 41(8) (2006) 1034-1039.

[149] N. Dawes, Fukushin and Kampo: Abdominal Diagnosis in Traditional Japanese and Chinese Medicine, Singing Dragon2020.

[150] Y. Uchida, K. Ueshima, K. Kano, M. Minami, Y. Mizukami, K. Morimoto, Correlations between "hie-sho" interview score and progesterone, fat intake, and Kupperman index in pre-and post-menopausal women: a pilot study, The journal of physiological sciences 69 (2019) 673-681.

[151] F. Yamazaki, The cutaneous vasoconstrictor response in lower extremities during whole-body and local skin cooling in young women with a cold constitution, The journal of physiological sciences 65 (2015) 397-405.

[152] M. Suzuki, T. Tsuchida, A. Ibe, Cold sensitivity among female clinical nurses in Japan: A nationwide study, International Journal of Nursing Studies Advances 6 (2024) 100208.

[153] Y. Ogata, K. Kaneko, K. Goto, K. Kono, M. Yamamoto, Physiological mechanism of Hiesho - Evaluation by
cardiovascular and autonomic dynamics, Jpn J Nurs Art Sci 15 (2017) 227-234.

[154] F. Yamazaki, Physiological characteristics of women's cold constitution and effects of exercise, The Journal of Physical Fitness and Sports Medicine 13(5) (2024) 139-144.

[155] K. Nagashima, T. Yoda, T. Yagishita, A. Taniguchi, T. Hosono, K. Kanosue, Thermal regulation and comfort during a mild-cold exposure in young Japanese women complaining of unusual coldness, Journal of applied physiology 92(3) (2002) 1029-1035.

[156] N. Yamada, H. Yoshimura, Determinants of chilliness among young women and their application to psychopharmacological trials, Nihon Shinkei Seishin Yakurigaku Zasshi= Japanese Journal of Psychopharmacology 29(5-6) (2009) 171-179.

[157] T. Ikeda, Y. Suzuki, T. Maeda, Relationships between Menstrual symptoms, lifestyle habit, and cold sensitivity in High School students, 2013.

[158] M. Jin, S. Liu, S. Schiavon, C. Spanos, Automated mobile sensing: Towards high-granularity agile indoor environmental quality monitoring, Building and Environment 127 (2018) 268-276.

[159] M. Arif, M. Katafygiotou, A. Mazroei, A. Kaushik, E. Elsarrag, Impact of indoor environmental quality on occupant well-being and comfort: A review of the literature, International Journal of Sustainable Built Environment 5(1) (2016) 1-11.

[160] L. Lan, P. Wargocki, D.P. Wyon, Z. Lian, Effects of thermal discomfort in an office on perceived air quality, SBS symptoms, physiological responses, and human performance, Indoor air 21(5) (2011) 376-390.

[161] L. Smith, S. Karvonen, Mental health, stress and office work: Examining the relationship between workplace environment and well-being, Journal of Occupational Health Psychology 23(1) (2018) 32-44.

[162] M. Frontczak, P. Wargocki, Literature survey on how different factors influence human comfort in indoor environments, Building and environment 46(4) (2011) 922-937.

[163] Y. Zhang, R. Zhao, Overall thermal sensation, acceptability and comfort, Building and environment 43(1) (2008) 44-50.

[164] J. Kim, Y. Zhou, S. Schiavon, P. Raftery, G. Brager, Personal comfort models: Predicting individuals' thermal preference using occupant heating and cooling behavior and machine learning, Building and environment 129 (2018) 96-106.

[165] B.W. Olesen, International standards for the indoor environment, Indoor air 14 (2004).

[166] L. Lan, Z. Lian, L. Pan, The effects of air temperature on office workers' well-being, workload and productivity-evaluated with subjective ratings, Applied ergonomics 42(1) (2010) 29-36.

[167] D. Enescu, A review of thermal comfort models and indicators for indoor environments, Renewable and Sustainable Energy Reviews 79 (2017) 1353-1379.

[168] E.E. Broday, J.A. Moreto, A.A. de Paula Xavier, R. de Oliveira, The approximation between thermal sensation votes (TSV) and predicted mean vote (PMV): A comparative analysis, International Journal of Industrial Ergonomics 69 (2019) 1-8.

[169] S. Zhang, Z. Lin, Extending predicted mean vote using adaptive approach, Building and Environment 171 (2020) 106665.

[170] H. Feriadi, N.H. Wong, Thermal comfort for naturally ventilated houses in Indonesia, Energy and buildings 36(7) (2004) 614-626.

[171] R. Maiti, PMV model is insufficient to capture subjective thermal response from Indians, International Journal of Industrial Ergonomics 44(3) (2014) 349-361.

[172] A. Youssef, A. Youssef Ali Amer, N. Caballero, J.-M. Aerts, Towards online personalized-monitoring of human thermal sensation using machine learning approach, Applied Sciences 9(16) (2019) 3303.

[173] O. Gocer, C. Candido, K. Gocer, A. Brambilla, L. Thomas, N. Billoria, M. Mackey, T. Alizadeh, S. Sarkar, Overlaps in space utilisation patterns and IEQ conditions observed in Activity-Based Working supportive office, Building and Environment 220 (2022) 109273.

[174] J.-H. Lee, Y.-K. Kim, K.-S. Kim, S. Kim, Estimating clothing thermal insulation using an infrared camera, Sensors 16(3) (2016) 341.

[175] P. Zheng, Y. Liu, H. Wu, H. Wang, Non-invasive infrared thermography technology for thermal comfort: A review, Building and Environment (2023) 111079.

[176] ISO 7726, Ergonomics of the Thermal Environment — Instruments for Measuring Physical Quantities, Geneva, Switzerland, 1998.

[177] X. Tian, L. Fang, W. Liu, The influencing factors and an error correction method of the use of infrared thermography in human facial skin temperature, Building and Environment 244 (2023) 110736.
[178] K. Lee, H. Choi, H. Kim, D.D. Kim, T. Kim, Assessment of a real-time prediction method for high clothing thermal insulation using a thermoregulation model and an infrared camera, Atmosphere 11(1) (2020) 106.
[179] Q. Wang, Y. Zhou, P. Ghassemi, D. McBride, J.P. Casamento, T.J. Pfefer, Infrared thermography for measuring elevated body temperature: clinical accuracy, calibration, and evaluation, Sensors 22(1) (2021) 215.
[180] ASHRAE, Thermal comfort, ASHRAE Handbook-Fundamentals. American Society of Heating, Refrigerating, and Air-Conditioning Engineers, Atlanta, 2021.
[181] R. Passmore, J.V.G. Durnin, Energy, Work and Leisure, Heinemann Educational Books,, London, 1967.
[182] G. Havenith, I. Holmér, K. Parsons, Personal factors in thermal comfort assessment: clothing properties and metabolic heat production, Energy and buildings 34(6) (2002) 581-591.
[183] N.M. Byrne, A.P. Hills, G.R. Hunter, R.L. Weinsier, Y. Schutz, Metabolic equivalent: one size does not fit all, Journal of Applied physiology (2005).
[184] E.T. Poehlman, M.J. Toth, Mathematical ratios lead to spurious conclusions regarding age-and sex-related differences in resting metabolic rate, The American journal of clinical nutrition 61(3) (1995) 482-485.
[185] A. Sparti, J.P. DeLany, J.A. de la Bretonne, G.E. Sander, G.A. Bray, Relationship between resting metabolic rate and the composition of the fat-free mass, Metabolism 46(10) (1997) 1225-1230.
[186] Y. Zhai, M. Li, S. Gao, L. Yang, H. Zhang, E. Arens, Y. Gao, Indirect calorimetry on the metabolic rate of sitting, standing and walking office activities, Building and Environment 145 (2018) 77-84.
[187] R. Kuriyan, P.P. Easwaran, A.V. Kurpad, Physical activity ratio of selected activities in Indian male and female subjects and its relationship with body mass index, British journal of nutrition 96(1) (2006) 71-79.
[188] K. Kuklane, R. Toma, Validation of ISO 9920 clothing item insulation summation method based on an ambulance personnel clothing system, Industrial health 59(1) (2021) 27-33.
[189] R. De Dear, G.S. Brager, Developing an adaptive model of thermal comfort and preference, (1998).
[190] W. Kempton, L.L. Layne, The consumer's energy analysis environment, Energy Policy 22(10) (1994) 857-866.
[191] J. Han, W. Yang, J. Zhou, G. Zhang, Q. Zhang, D.J. Moschandreas, A comparative analysis of urban and rural residential thermal comfort under natural ventilation environment, Energy and Buildings 41(2) (2009) 139-145.

[192] G. Liu, S. Jiang, Y. Ji, Y. Zhang, G. Wang, S. Liang, S. Liang, Research on the calculation method of dressing thermal resistance based on infrared thermal imaging technology, E3S Web of Conferences, EDP Sciences, 2022, p. 03005.
[193] J.D. Hardy, E.F. Du Bois, The technic of measuring radiation and convection, J. Nutr 15 (1938) 461.
[194] N. Ramanathan, A new weighting system for mean surface temperature of the human body, Journal of applied physiology 19(3) (1964) 531-533.
[195] K.C. Parsons, The effects of gender, acclimation state, the opportunity to adjust clothing and physical disability on requirements for thermal comfort, Energy and Buildings 34(6) (2002) 593-599.
[196] F. Nicol, M. Humphreys, S. Roaf, Adaptive thermal comfort: principles and practice, Routledge2012.
[197] K. Chen, M. Rys, E.S. Lee, Modeling of thermal comfort in air conditioned rooms by fuzzy regression analysis, Mathematical and computer modelling 43(7-8) (2006) 809-819.
[198] H. Hensel, K. Schafer, Thermoreception and temperature regulation in man, Recent advances in medical thermology, Springer1984, pp. 51-64.
[199] K. Rewitz, D. Mueller, Influence of gender, age and BMI on human physiological response and thermal sensation for transient indoor environments with displacement ventilation, Building and Environment 219 (2022).
[200] T. Mills, D. Gallagher, J. Wang, S. Heshka, Modelling the relationship between body fat and the BMI, International journal of body composition research 5(2) (2007) 73.
[201] C.J. Smith, J.M. Johnson, Body mass index and gender influence temperature regulation during exercise, Physiology & Behavior 164 (2016) 141-146.
[202] S. Karjalainen, Thermal comfort and gender: a literature review, Indoor air 22(2) (2012) 96-109.
[203] E.B. Neves, A.C.C. Salamunes, R.M. de Oliveira, A.M.W. Stadnik, Effect of body fat and gender on body temperature distribution, Journal of thermal biology 70 (2017) 1-8.
[204] A. Nakagawa, T. Nakaya, A survey of clothing insulation for university students in Japan: Effect of clothing insulation distribution between the upper and lower body in the winter, J Build Eng 44 (2021) 103287.
[205] Q. Zhao, J. Lyu, H. Du, Z. Lian, Z. Zhao, Gender differences in thermal sensation and skin temperature sensitivity under local cooling, Journal of Thermal Biology 111 (2023) 103401.
[206] H.N. Mayrovitz, M.B. Regan, Gender differences in facial skin blood perfusion during basal and heated conditions determined by laser Doppler flowmetry, microvascular research 45(2) (1993) 211-218.
[207] A. Takatori, Assessment of diagnostic criterion of coldness in women with thermography, Nihon Sanka Fujinka Gakkai Zasshi 44(5) (1992) 559-565.
[208] M. Sadakata, Characteristics of peripheral dermovascular in the subjects regarded as the cold constitution, J Jap Society of Nursing Research 27 (2004) 106.

[209] L. Yang, H.Y. Yan, J.C. Lam, Thermal comfort and building energy consumption implications - A review, Appl Energ 115 (2014) 164-173.

[210] WHO, Obesity: Preventing and managing the global epidemic, World Health Organization (WHO)2000.

[211] C. Huizenga, H. Zhang, E. Arens, D. Wang, Skin and core temperature response to partial-and whole-body heating and cooling, Journal of thermal biology 29(7-8) (2004) 549-558.

[212] R.J. De Dear, J.W. Ring, P.O. Fanger, Thermal sensations resulting from sudden ambient temperature changes, Indoor air 3(3) (1993) 181-192.

[213] K. Terasawa, On the recognition and treatment of, Hie-sho"(chillphobia) in the traditional Kampoh medicine," Shoyakugaku Zasshi 41(2) (1987) 85-96.

[214] S. Sakaguchi, Effects of acupuncture on cold sensitivity, Journal of the Japan Society of Acupuncture and Moxibustion 53(1) (2003) 49-54.

[215] A.A. Ganpule, S. Tanaka, K. Ishikawa-Takata, I. Tabata, Interindividual variability in sleeping metabolic rate in Japanese subjects, European journal of clinical nutrition 61(11) (2007) 1256-1261.

[216] I. Janssen, A.E. Mark, Elevated body mass index and mortality risk in the elderly, Obesity reviews 8(1) (2007) 41-59.

[217] J.L. Kuk, S. Lee, S.B. Heymsfield, R. Robert, Waist circumference and abdominal adipose tissue distribution: influence of age and sex, The American Journal of Clinical Nutrition 81(6) (2005) 1330-1334.

[218] R. Ferraro, S. Lillioja, A.-M. Fontvieille, R. Rising, C. Bogardus, E. Ravussin, Lower sedentary metabolic rate in women compared with men, The Journal of clinical investigation 90(3) (1992) 780-784.

[219] N. Gerrett, Y. Ouzzahra, S. Coleby, S. Hobbs, B. Redortier, T. Voelcker, G. Havenith, Thermal sensitivity to warmth during rest and exercise: a sex comparison, European journal of applied physiology 114 (2014) 1451-1462.

[220] Y. Inoue, N. Gerrett, T. Ichinose-Kuwahara, Y. Umino, S. Kiuchi, T. Amano, H. Ueda, G. Havenith, N. Kondo, Sex differences in age-related changes on peripheral warm and cold innocuous thermal sensitivity, Physiology & behavior 164 (2016) 86-92.

[221] V. Candas, A. Dufour, Hand skin temperatures associated with local hand discomfort under whole-body cold exposure, Journal of the Human-Environment System 10(1) (2007) 31-37.

[222] H. Kaciuba-Uscilko, R. Grucza, Gender differences in thermoregulation, Current Opinion in Clinical Nutrition & Metabolic Care 4(6) (2001) 533-536.

[223] I. Janssen, S.B. Heymsfield, D.B. Allison, D.P. Kotler, R. Ross, Body mass index and waist circumference independently contribute to the prediction of non-abdominal, abdominal subcutaneous, and visceral fat, The American Journal of Clinical Nutrition 75(4) (2002) 683-688.

[224] J.C. Wells, M.S. Fewtrell, Measuring body composition, Archives of Disease in Childhood 91(7) (2006) 612-617.

[225] S. Sakaguchi, H. Kuge, H. Mori, J. Miyazaki, T.H. Tanaka, K. Hanyu, T. Takeda, K. Sasaki, Extraction of items identifying hiesho (cold disorder) and their utility in young males and females, Journal of Integrative Medicine 14(1) (2016) 36-43.
[226] T. Yamato, M. Aomine, Physical characteristics and living environment in female students with cold constitution, Health Evaluation and Promotion 29(5) (2002) 878-884.
[227] T. Yoshino, K. Katayama, K. Munakata, Y. Horiba, R. Yamaguchi, S. Imoto, S. Miyano, K. Watanabe, Statistical analysis of hie (cold sensation) and hiesho (cold disorder) in kampo clinic, Evidence-Based Complementary and Alternative Medicine 2013(1) (2013) 398458.
[228] H.A. Brown, T.H. Topham, B. Clark, J.W. Smallcombe, A.D. Flouris, L.G. Ioannou, R.D. Telford, O. Jay, J.D. Periard, Seasonal heat acclimatisation in healthy adults: a systematic review, Sports Medicine 52(9) (2022) 2111-2128.
[229] R. De Dear, G. Schiller Brager, The adaptive model of thermal comfort and energy conservation in the built environment, International journal of biometeorology 45 (2001) 100-108.
[230] J. Kwon, J. Choi, The relationship between environmental temperature and clothing insulation across a year, International journal of biometeorology 56 (2012) 887-893.
[231] S.S. Cheung, T.M. McLellan, Heat acclimation, aerobic fitness, and hydration effects on tolerance during uncompensable heat stress, Journal of applied physiology 84(5) (1998) 1731-1739.
[232] R. McGinn, M.B. Ducharme, Effects of exercise and thermal stress on regional instantaneous heat exchange by core and skin temperatures, European Journal of Applied Physiology 106(2) (2009) 291-307.
[233] I.B. Mekjavic, O. Eiken, Contribution of thermal and nonthermal factors to the regulation of body temperature in humans, Journal of applied physiology 100(6) (2006) 2065-2072.
[234] N.A. Taylor, M.J. Tipton, Habituation, acclimatization and conditioning to heat and cold, Comprehensive Physiology 4(1) (2014) 439-468.
[235] W.J. Hannan, R.M. Wrate, S.J. Cowen, C.P. Freeman, Body mass index as an estimate of body fat, International Journal of Eating Disorders 18(1) (1995) 91-97.
[236] D. Du Bois, E.F. Du Bois, A formula to estimate the approximate surface area if height and weight be known, Archives of Internal Medicine 17(6) (1916) 863-871.
[237] M.A. Humphreys, J.F. Nicol, The validity of ISO-PMV for predicting comfort votes in every-day thermal environments, Energy and buildings 34(6) (2002) 667-684.
[238] Z. Wang, R. de Dear, M.H. Luo, B.R. Lin, Y.D. He, A. Ghahramani, Y.X. Zhu, Individual difference in thermal comfort: A literature review, Building and Environment 138 (2018) 181-193.
[239] E.A. Arens, H. Zhang, The skin's role in human thermoregulation and comfort, Indoor environmental Quality, UC Berkeley (2006).
[240] J.-H. Choi, D. Yeom, Study of data-driven thermal sensation prediction model as a function of local body skin temperatures in a built environment, Building and Environment 121 (2017) 130-147.

[241] M. Kondo, Y. Okamura, Cold constitution: analysis of the questionnaire, Nihon Sanka Fujinka Gakkai Zasshi 39(11) (1987) 2000-2004.
[242] M. Sadakata, Y. Yamada, Perception of foot temperature in young women with cold constitution: analysis of skin temperature and warm and cold sensation thresholds, J Physiol Anthropol 26(4) (2007) 449-457.
[243] B.K. Alba, J.W. Castellani, N. Charkoudian, Cold-induced cutaneous vasoconstriction in humans: Function, dysfunction and the distinctly counterproductive, Experimental physiology 104(8) (2019) 1202-1214.
[244] G.J. Hodges, J.A. Traeger III, T. Tang, W.A. Kosiba, K. Zhao, J.M. Johnson, Role of sensory nerves in the cutaneous vasoconstrictor response to local cooling in humans, American Journal of Physiology-Heart and Circulatory Physiology 293(1) (2007) H784-H789.
[245] T. Bergersen, A search for arteriovenous anastomoses in human skin using ultrasound Doppler, Acta physiologica scandinavica 147(2) (1993) 195-201.
[246] X. Xu, H. Zhang, G. Wu, Z. Lian, H. Xu, Sex differences in body temperature and thermal perception under stable and transient thermal environments: A comparative study, Science of The Total Environment 951 (2024) 175323.
[247] H.H.T. Reis, C.J. Brito, M. Sillero-Quintana, A.G. da Silva, I. Fernández-Cuevas, M.S. Cerqueira, F.Z. Werneck, J.C.B. Marins, Can the body mass index influence the skin temperature of adolescents assessed by infrared thermography?, Journal of Thermal Biology 111 (2023) 103424.
[248] R.J. Schepers, M. Ringkamp, Thermoreceptors and thermosensitive afferents, Neuroscience & Biobehavioral Reviews 34(2) (2010) 177-184.
[249] A.A. Romanovsky, Skin temperature: its role in thermoregulation, Acta physiologica 210(3) (2014) 498-507.
[250] R. Rawal, S. Manu, Y. Shukla, L.E. Thomas, R. de Dear, Clothing insulation as a behavioural adaptation for thermal comfort in Indian office buildings, Proceedings of the 9th Windsor Conference: Making Comfort Relevant, Windsor, UK, 2016, pp. 7-10.
[251] P. Webb, Temperatures of skin, subcutaneous tissue, muscle and core in resting men in cold, comfortable and hot conditions, European journal of applied physiology and occupational physiology 64 (1992) 471-476.
[252] N.A. Taylor, Human heat adaptation, Comprehensive Physiology 4(1) (2014) 325-365.

Acknowledgements

First and foremost, I would like to express my deepest gratitude to my supervisor, Associate Professor Hitoshi Wakabayashi, for his exceptional guidance, mentorship, and unwavering support throughout the course of my research and the preparation of this dissertation. His insightful advice and continuous encouragement have been instrumental in shaping both the direction and outcome of this work.

I am also sincerely thankful to Assistant Professor Sang-il Lee for his guidance in various research activities, which significantly broadened my academic perspective and skills.

My sincere appreciation extends to Research Associate Dr. Ayano Dempoya for her dedicated support and assistance throughout my research activities.

I would also like to express my heartfelt thanks to Ms. Akiko Yanagisawa for her consistent and efficient administrative support, which greatly facilitated the smooth progress of my research.

I am sincerely grateful to the E-Program office staff at Hokkaido university and the Ministry of Education, Culture, Sports, Science and Technology (MEXT) of Japan for generous support and continuous assistance throughout my studies.

I am truly grateful to Professor Katsunori Nagano and Professor Taro Mori for their ongoing guidance and support throughout the course of my research.

I would like to acknowledge my laboratory colleagues—Mr. Koichi Ishii, Mr. Kaisei Okamoto, Mr. Yu Watanabe, Ms. Maho Kameda, Ms. Jiating Li, Ms. Yumiko Tan, and Mr. So Takeuchi—for their valuable contributions and continued support.

This work was partially supported by Taisei Corporation. I would like to thank Dr. Takuji Iwamura and Mr. Shingo Konoshita for their consistent support and collaboration.

I would also like to extend my appreciation to all the participants who took part in the experiments, whose involvement made this study possible.

I am deeply grateful to my parents and my family for their enduring support, patience, and encouragement throughout this academic journey.

Finally, I would like to express my sincere and heartfelt gratitude to the late Professor Yasuhiro Hamada. His kindness and support were instrumental in initiating my doctoral journey. His encouragement and guidance will always be remembered with deep respect and appreciation.